Title	Characterising the geochemistry of the natural environment using compositional data analysis
Author(s)	Wheeler, Seán
Publication Date	2021-05-31
Publisher	NUI Galway
Item record	http://hdl.handle.net/10379/16916

NUI GALWAY

DOCTORAL THESIS

Characterising the geochemistry of the natural environment using Compositional Data Analysis

Author:

Seán Wheeler

Supervisors:

Dr. Tiernan Henry

Dr. John Murray

A thesis submitted in fulfilment of the requirements

for the degree of Doctor of Philosophy

May 2021

Contents

Declaration of Authorship

I declare that this thesis has not been submitted, in whole or in part, to this, or any other University for any degree. Except where otherwise started, this work is the original work of the author.

Signed: _Seán Wheeler_

Date: _31ˢᵗ May 2021_

Abstract

The geochemistry of the natural environment (e.g. soils, streams, sediments and groundwater) is representative of the source(s) from which these materials are derived. In fact, a geochemical dataset is essentially a breakdown of the parts that together form the composition of materials. As pointed out by Pearson (1897), spurious correlation can occur when attempting multivariate analysis on a dataset that is compositional in nature (i.e. the variables are measured as parts of some whole e.g. mg/l). Compositional Data Analysis (CoDA) was developed by John Aitchison (1982) and others to solve this issue, and is therefore the correct mathematical framework by which to statistically analyse these types of data. CoDA also allows for a unique interrogation of compositional data primarily through the use of the multi-dimensional compositional bi-plot.

CoDA methods have been used extensively here, and in some cases compared to traditional multivariate statistical methods, in order to better understand the relationship between geochemistry and the natural environment on a variety of temporal and spatial scales. Specifically, two studies were undertaken; i) the geochemistry of groundwater in the area surrounding Lisheen Mine in Co. Tipperary, Ireland, and ii) the geochemistry of soils, stream sediments and stream waters in the border region of Ireland.

Geochemistry datasets from Lisheen Mine offer a unique opportunity to investigate the chemical nature groundwater in an area prior to, during and following significant mining activity. Overall it would appear that the local groundwater was relatively un-impacted by the excavation of lead/zinc massive sulphides over a 16 year period (1999 – 2015). This may be in part thanks to the buffering effect of the host Carboniferous Limestone reducing the potential for acid mine drainage. Groundwater chemistry in the area appears to be more influenced by nitrogen from peat bogs, local agricultural practices and in some places redox reactions.

The border region (composed of the six counties that border Northern Ireland) was the subject of an extensive geochemical examination by the Tellus Survey completed in 2013. The resulting freely available datasets were analysed here using CoDA. The primary, secondary and tertiary factors controlling soil, sediment and stream water geochemistry were determined. The dominant control on each of these materials is bedrock geology. However, soil type, land-use practices and topography also influence geochemistry.

Keywords: CoDA, Geochemistry, Lisheen Mine, Tellus Border Project

Acknowledgements

Firstly, to my supervisor, Dr. Tiernan Henry; I owe you an enormous debt of gratitude for offering me this incredible opportunity and supporting my work completely throughout the past four years. I have learned so much from you and I appreciate everything you have done for me.

To my other supervisor, Dr. John Murray; I am extremely grateful for your continued support throughout my research, and the invaluable training you have given me since I started as an undergraduate at NUI Galway.

Additionally I am immensely grateful to the following;

Dr. Liam Morrison and Prof. Frank McDermott who, in addition to my supervisors, helped me with the publication of some of the work within this thesis.

The team at Lisheen Mine, in particular Stephen Wheston, for sharing invaluable knowledge about the geology and hydrogeology of the area.

Martin Nauton-Fourteu and David O'Leary for assisting me with field work at Lisheen.

Dr. Sarah Blake for her guidance and expertise regarding the application of CoDA to groundwater geochemistry.

Ana Mendes, Nessa Golden and Ellen McGrory for taking time out of their own work to give me clean-room and sample preparation training.

The CoDA Group, in particular Juan Jose Egozcue and Vera Pawlowsky-Glahn, for support with the statistical methods used for compositional data.

All of my friends and colleagues, past and present, within Earth and Ocean Science NUI Galway and iCRAG for their continued support and friendship.

Finally to my parents, Siobhán and Steve, for always believing in me – this is for you.

"When one tugs at a single thing in nature, he finds it attached to the rest of the world."

– John Muir

Chapter One: *Introduction*

1.1 Overview

The spatial distribution of chemical elements on Earth has constantly changed since the planet's formation (e.g. Ringwood, 1966; Wetherill, 1990; Schaefer and Fegley, 2010), as a consequence of geological, hydrological, atmospheric, biological and, more recently, anthropogenic processes (e.g. Lewis and Maslin, 2015), all of which are intrinsically inter-related. The variation in the geochemical composition of the Earth's crust is reflected in the heterogeneity of the geology generally. Rocks can often be categorised by their unique chemical signatures, which, in continental settings, is usually the primary control for the geochemistry of what lies directly above (e.g. soils, flora, rivers, lakes etc.). Another major control is weathering: this can depend on geographical setting (including latitudinal and topographic considerations), which in turn influences the prevailing climate regime. More recently, humans have significantly modified the geochemistry of land surface environments, particularly since the onset of the industrial revolution (~250 years ago) which brought about greater demands on agriculture, due to a rising global population, and concentrated particular chemical elements and compounds in growing urban and industrial settings (e.g. Janzen, 2004; Amundson *et al.*, 2015; Goudie, 2018).

Many industries require detailed knowledge of how the chemical makeup of natural materials is distributed throughout the physical environment. For example, the exploration for potential mining/quarrying sites is reliant on a robust understanding of how the target minerals vary spatially over the area being investigated (e.g. Rose and Gundlach, 1981; Govett, 2013; Kyser *et al.*, 2015). In agriculture, the geochemistry of soils can inform best land-use practices as well as areas requiring an artificially altered chemistry in order to make the land more fertile for certain crops (e.g. Kronberg and Nesbitt, 1981; Liao *et al.*, 2007; Fu *et al.*, 2010; da Silva *et al.*, 2017). Environmental monitoring, to maintain a healthy ecosystem and track the influence of human activities, also relies on significant geochemical datasets that include both spatial and temporal information (e.g. Fortescue, 2012; Lyons and Harmon, 2012; Marques *et al.*, 2019). Advances in analytical methods, and wider availability of sophisticated instrumentation, means that the scale of geochemical datasets has increased quite significantly. The ability to collect large amounts of time series datasets has improved too; this makes processing and

interpretation of the data more complex too. Silver (2012) has described this as separating the signal from the noise: we can collect large datasets over long time intervals, but this means we might have to work harder to prise out the "meaning" or signal from these data.

Three sequential processes are required to successfully utilise and interpret the geochemical distribution of elements and compounds in the natural environment: (1) sample material recovery; (2) laboratory analysis of the recovered sample(s); *and*, (3) statistical analysis of the resulting data. This study focuses on the third and final part of this process, with the primary objective being to evaluate the use of statistical methods for geochemical analysis, with a particular focus on water geochemistry, on a variety of spatial and temporal scales. However, the importance of understanding methods of sample recovery and laboratory analysis should not be overlooked or understated, as these greatly inform how the subsequent data can be analysed and how reliable or unreliable the outcomes are.

As described in the following section, Compositional Data Analysis (CoDA) is proposed as the most optimum mathematical framework for the statistical analysis of geochemical data. In addition, CoDA offers a unique graphical representation that facilitates analysis of a large number of variables simultaneously. This is particularly useful in the field of geochemistry where ever more advanced methods of laboratory analysis (e.g. inductively coupled plasma mass spectrometry [ICP-MS]) provide increasingly more detailed chemical information on any given sample. The benefits and drawbacks of CoDA are highlighted in this thesis through a detailed study of groundwater geochemistry from Lisheen Mine in south-central Ireland. These datasets are approached from both a mineral exploration and environmental monitoring perspectives.

CoDA can also be utilised for geochemical spatial mapping studies, where a particular combination of elements and compounds, that are indicative of variation between material types (e.g. soil types or rock types), can be mapped. The spatial extent of the Lisheen Mine datasets are not sufficiently large enough to demonstrate this particular CoDA application. Therefore, a large regional- to national-scale geochemical (soil, sediment and stream water) dataset is utilised in this report instead. This dataset was sourced from the Tellus Survey, which is a national geochemical and geophysical acquisition programme in Ireland and Northern Ireland, specifically geochemistry datasets from a geographic area termed the *Border Region* are used herein.

1.2 Background to Compositional Data Analysis (CoDA)

The compositional geochemistry of any sample is reflective of the source of the material being sampled (e.g. Ottesen *et al*., 1989; Újvári *et al*., 2008; White, 2020). For example, the chemical composition of rock is primarily indicative of the conditions in which it formed (e.g. Nockolds, 1954; Bhatia, 1985; Govett, 2013) and it also reflects, to varying degrees, subsequent weathering (e.g. Formoso, 2006; Moses *et al.,* 2014). The geochemical alteration of rocks generally occurs over protracted (geological) time-scales and therefore their composition does not usually change in the time-frame of the single human lifetime (there are exceptions, of course!). However, this is not the case with soils which are more readily chemically altered over considerably shorter time periods by climatic and anthropogenic affects (i.e. <1000 years). In comparison to rocks and soils, surface water and groundwater are extremely susceptible to geochemical alteration on even shorter time-scales (e.g. within minutes). However, the variation of components (i.e. chemical elements and compounds) between two or more water samples is generally very slight, in comparison to soils and rocks, as more than 99% of any sample is typically H_2O. This highlights the necessity for methods of statistical analysis that can identify subtle variations between the components (e.g. Van Den Brink *et al.,* 2007; Cloutier *et al*., 2008; Blake *et al*., 2016).

Geochemical sampling and analysis traditionally focuses on the major elemental components. For example, groundwater samples are routinely analysed for, and characterised by, the concentrations of major anions and cations (e.g. HCO_3^{2-}, Cl^-, SO_4^{2-}, Ca^{2+}, Mg^{2+}, Na^+, K^+) as these typically make up more than 90% of dissolved mass in groundwater. However, improvements in analytical technologies in geochemistry (including ICP-MS) have allowed for routine measurement of a wide range of elements with greater accuracy. Elements that were not traditionally considered as important for groundwater characterisation studies (e.g. Conti *et al.,* 2000; Younger, 2000 etc.) may actually be valuable for evaluating the primary controls on water chemistry. Relatively newer methods of statistical analysis (e.g. Principal Component Analysis [PCA] and CoDA) can be used to assess which elemental relationships are particularly important in defining the chemistry of groundwater (e.g. Gallo and Buccianti, 2013; Engle and Blondes, 2014; Blake *et al.,* 2016), at specific locations within relatively uniform or homogenous broader geological contexts, and also within relatively small areas (e.g. Lisheen Mine, which is <30km^2). These methods of data analysis provide an efficient way to explore variance in large datasets and unlike some conventional approaches to geochemical data (e.g.

Piper and also Harker diagrams), do not rely on *a-priori* expectations about inter-element behaviour.

Appropriate datasets for PCA are generally in the form of a data table consisting of variables (e.g. chemical parameters) and observations (e.g. a particular sample for which that variable was measured) that are in some way inter-correlated. PCA works by extracting the important and pertinent information and expressing it as new set of orthogonal variables called principal components (Machiwal *et al.*, 2018). Displaying the resulting data as point co-ordinates on maps provides a representation of the pattern of similarity between observations and variables (Jolliffe, 2002; Jackson, 2005; Saporta and Niang, 2009; Abdi and Williams, 2010). However, using any correlative technique (e.g. ternary diagram, PCA, cluster analysis) on raw compositional data can lead to spurious correlations as a result of the 'closure problem' (e.g. Chayes and Trochimczyk, 1978) or the 'negative bias problem' (*see below*).

'Standard' multivariate analysis methods do not account for the relative nature of compositional datasets and may lead to spurious and inaccurate results. The reason for this is described as the 'negative bias problem' and has been alluded to by Chayes (1960, 1962, 1971), Krumbein (1962) and Mosimann (1962, 1963). As pointed out by Aitchison (2003), the problem can be described as follows: for a D-part composition $[X_1, . . ., X_D]$ with the component sum $X_1 + . . . + X_D = 1$, since:

$$cov(X_1, X_2 + \ldots + X_D) = 0 \text{ [Equation 1.1]}$$

we have:

$$cov(X_1, X_2) + \cdots + cov(X_1, X_D) = -var(X_1) \text{ [Equation 1.2]}$$

The right hand side of Equation 1.2 is negative, implying that at least one of the covariances on the left must be negative and therefore the correlations are not free to range over the usual (-1 to 1) interval.

Early attempts to solve this problem focused on corrective treatments to 'standard' methods (e.g. Darroch and James, 1974; Chayes and Trochimezyk, 1978). The necessity for a method that takes into account the special nature of the compositional sample space was first recognised and developed by Aitchison and Shen (1980), and subsequently by Aitchison (1982, 1983, 1985, 1986). Key to this new approach was the recognition that compositional data provide information only about the *relative magnitudes* of the parts, and *not their absolute values*. Therefore, this information essentially concerns ratios of the components. In general,

ratios do not show exact relationships in terms of variation (e.g. no exact relationship between var(X_i/X_j) and var(X_j/X_i)). However, log ratios are different:

$$\text{var}\{\log(X_i/X_j)\} = \text{var}\{\log(X_j/X_i)\} \quad \text{[Equation 1.3]}$$

There is also a one-to-one correspondence between compositions and a full set of log ratios:

$$[Y_1 \ldots, Y_{D-1}] = [\log(X_1/X_D) \ldots \log(X_{D-1}/X_D)] \quad \text{[Equation 1.4]}$$

with inverse:

$$[X_1, X_2 \ldots, X_D] = [\exp(Y_1) \ldots \exp(Y_{D-1})1]/\{\exp(Y_1) + \ldots + \exp(Y_{D-1}) + 1\} \quad \text{[Equation 1.5]}$$

Therefore, any problem or hypothesis concerning compositions can be fully expressed in terms of log ratios and vice versa. Because log-ratio transformation takes the log-ratio vector onto the whole of the real space, it is possible to then use all methods of unconstrained multivariate analyses on the result (with caution). Recently, significant advancements have been made in CoDA theory and its applications (e.g. Egozcue and Pawlowsky-Glahn, 2011; Tolosana-Delgado and van den Boogaart, 2011; van den Boogaart and Tolosana-Delgado, 2013; McKinley *et al.,* 2016).

The only information in a geochemical dataset processed using CoDA is given by the ratios between components which are preserved under multiplication by a positive constant. This implies that the geometric sample space of compositional data is always a standard 'simplex' (Equation 1.6; Fig. 1.1) that sums to a constant (e.g. k = 1):

$$S^D = \{X = [x_1, x_2, \ldots, x_D] \in \mathbb{R}^D \mid x_i > 0, i = 1,2, \ldots, D; \sum_{i=1}^{D} x_i = k \} \quad \text{[Equation 1.6]}$$

Normalisation to the simplex is called 'closure' and is denoted by $\mathsf{C}[\cdot]$:

$$\mathsf{C}[x_1, x_2, \ldots, x_D] = \left[\frac{x_1}{\sum_{i=1}^{D} x_i}, \frac{x_2}{\sum_{i=1}^{D} x_i}, \ldots, \frac{x_D}{\sum_{i=1}^{D} x_i} \right], \quad \text{[Equation 1.7]}$$

where D is the number of parts (components) and [·] denotes a row vector.
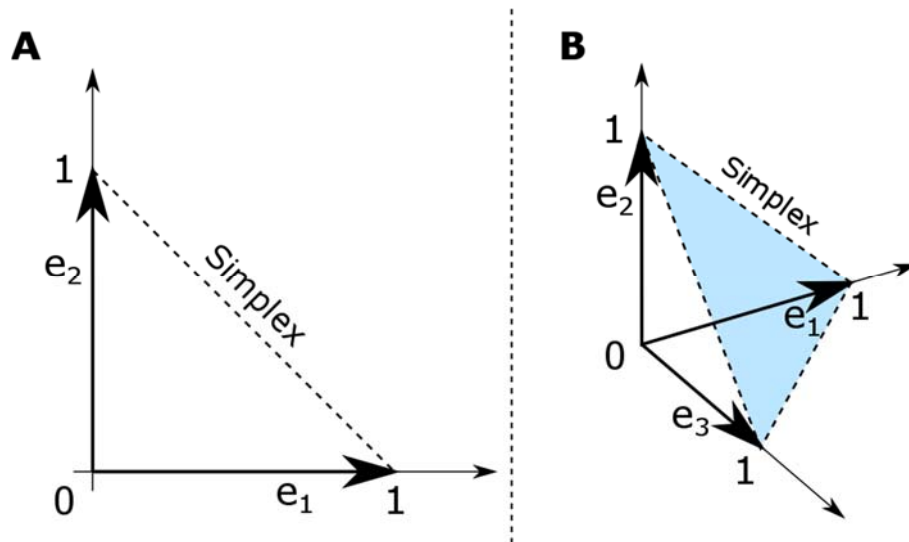
***Fig. 1.1: A)** 1-standard simplex in R^2. **B)** 2-standard simplex in R^3 (Modified from Filzmoser et al., 2018).*

Although the log-ratio method avoids the negative bias problem by maintaining positive values, the question remaining is what divisor should be used for the transformation. Three methods have been suggested:

(1) additive log-ratio;

(2) centre-log ratio; *and*

(3) isometric log-ratio.

The use of the additive log-ratio (alr) method, whereby an arbitrary component was chosen as the divisor, was common initially in the literature (e.g. Pawlowsky and Burger, 1992; Pawlowsky *et al.*, 1994; Walvoort and Gruijter, 2001). However, the distances in the transformed space following alr, are not the same for different divisors. This is more of a conceptual problem, however, as Aitchison (1986) and Aitchison *et al.* (2000) demonstrated that dependant variables are invariant to the choice of divisor. The centre-log ratio (clr) transformation entirely avoids the necessity for choosing a component as the divisor by instead using the geometric mean. However, the clr covariance matrix is singular and therefore requires adaption to be used with some multivariate techniques.

The isometric log-ratio (ilr) method uses a suitable orthonormal basis to represent compositions as coordinates in the simplex (Egozcue *et al.*, 2003). This avoids both the choice of arbitrary component (i.e. alr) and the singularity issue (i.e. clr). As there is no canonical basis in the simplex (S^D), sequential binary partition (SBP) of the components is suggested by Egozcue and

Pawlowsky-Glahn (2005) to acquire 'balances'. Choosing the basis for the SBP should be informed by the statistical question. For example, in aqueous geochemistry, the basis would be separated based on *a priori* knowledge of chemical interactions. The application of these transformation methods is described in the methods section.

1.2.1 Key Principles of CoDA

As pointed out by some mathematically-focussed geoscientists (e.g. Rehder and Zier, 2001), distance metrics following log-ratio transformation make traditional operations (e.g. multiplication and addition) inappropriate and, therefore, statistical methods that require these operators cannot be used in a traditional way. However, by considering a few key principles, an entire mathematical framework can be derived which includes appropriate distance metrics.

1.2.1.1 Scale Invariance

Scale invariance is essentially the concept that CoDA can only make meaningful statements about the ratios of components (Aitchison *et al.*, 2000). If a composition is scaled by a constant (e.g. ppm) then vectors of proportional positive components form an equivalence class. It is therefore intuitive to select a representative of this equivalence class to facilitate analysis and interpretation. Traditionally this would be done by normalising the vector in such a way that the components sum to a constant, *k*. As discussed previously, compositional closure on the simplex is accomplished by Equation 1.7.

1.2.1.2 Subcompositional Coherence

The second key principal is subcompositional coherence (e.g. Aitchison, 1992), which implies that any inferences made about the full composition must be the same for any sub-compositional unit. Firstly, scale invariance, as described above, must hold for any subcomposition. Additionally the idea of *subcompositional dominance* implies that any distances measured between two full compositions must be larger than (or at least equal to) the distance measured between any subcomposition.

1.2.1.3 Permutation Invariance

Permutation invariance is simply the inference that any conclusion made about a given composition should not depend on the order of the parts. This key principal is intuitive in most cases, in particular with regards geochemistry, where elements and compounds can be rearranged without affecting the interpretations.

1.2.2 Aitchison Geometry

Based upon the maintaining of the principles of scale invariance and sub-compositional coherence, Aitchison (1986) and later Aitchison and Ng (2005) developed perturbation (i.e. addition) and powering (i.e. multiplication). As described by Bacon-Shone (2011), a perturbation $\boldsymbol{p} = (p_1, \ldots, p_D)$ is a differential scaling operator that when applied to the composition $\boldsymbol{x} = (x_1, \ldots, x_D)$ yields the composition:

$$X = p \ \oplus x = C(p_1 x_1, \ldots, p_D x_D), \text{ [Equation 1.8]}$$

where C is the closure operator that scales elements to ensure that we remain in the unit simplex. Similarly powering can be described by:

$$X = a \ \odot x = C(x_1^a, \ldots, x_D^a) \text{ [Equation 1.9]}$$

The Aitchison distance is given by:

$$d_a(x, y) = \left\{ \sum_{i=1}^{D} \left[\log \frac{x_i}{g_m(x)} - \log \frac{y_i}{g_m(y)} \right]^2 \right\}^{\frac{1}{2}}, \text{ [Equation 1.10]}$$

where $g_m(\cdot)$ is the geometric mean of the components. The centre for a composition distribution is:

$$Cen[x] = \ C(\exp\{E[\log(x)]\}), \text{ [Equation 1.11]}$$

with the variation matrix, **T**, as the most convenient measure of variability.

These mathematical operations mimic those used on non-compositional data and allow for the full range of traditional statistical methods (e.g. PCA) to be used within the 'simplex' (the compositional sample space). The specific log-ratio transformations used are described in more detail in Chapter 2: Methods. The advantages of CoDA are then demonstrated in the context of mineral exploration and environmental remediation at Lisheen Mine in south-central Ireland

and, on a much larger scale, in the context of material (e.g. geology, soils etc.) mapping on the Irish side of the border between Ireland and Northern Ireland. These study areas are introduced in the next section.

1.3 Introduction to Lisheen Mine

Geochemistry is a major component of mining generally (e.g. Large and McGoldrick, 1998; Brand, 1999; Ghasemzadeh *et al.*, 2019). From the outset (at initial prospecting and exploration stage) soil, sediment, solid bedrock, surface water and groundwater samples are regularly analysed with the intention of discovering anomalies indicative of the possible presence of economic deposits in the subsurface. In cases where mining commences, and also following mine closure, the primary focus of further geochemical sampling is for the purposes of environmental monitoring, particularly in areas where drinking water supplies could be affected (e.g. Banks *et al.*, 1997; Prommer *et al.*, 2000; Neiva *et al.*, 2015).

Groundwater monitoring, in particular, has become standard practice in locations where mining has taken place (e.g. Lisheen Mine), or is currently taking place (e.g. Eang, 2018; Zeng *et al.*, 2018). Raw material extraction can often result in geochemical changes in soil, surface water and groundwater (e.g. Aslibekian *et al.*, 1999; Olsen *et al.*, 2012; Connelly *et al.*, 2005), primarily as a consequence of exposing minerals to oxygenated conditions (and pre-present water). Given suitable pH levels, a variety of oxides may form, as minerals (e.g. sulphides) as the host rocks dissolve, thereby mobilising potentially harmful elements into permeating groundwater. In extreme cases this effect is termed 'acid mine drainage' and is the focus of significant research (e.g. Colmer and Hinkle, 1947; Johnson and Hallberg, 2005; Akcil and Koldas, 2006; Simate and Ndlovu, 2014; Tabelin *et al.*, 2020). This effect can be reduced in cases where the ore deposit host rock acts as a 'pH buffer' (e.g. limestone). However, the potential for contamination of both surface and groundwater remains and therefore the groundwater geochemistry is routinely monitored in the area surrounding mining operations.

Lisheen Mine is of particular interest in this context as, at the time of writing, it is the most recently discovered (1997) and most recently closed large mine in Ireland (2015; Courtney, 2018). This site thus affords an opportunity to analyse groundwater geochemical data from the initial exploration phase, through the active mining phase to the monitoring and remediation phase post-closure. As of 2021, only one lead and zinc mine (Tara in Navan) is still in operation

in Ireland, but Ireland has a long mining history (e.g. Gillmor, 1965; Aldwell, 1990; O'Brien, 1994; see next section below), and exploration continues to uncover new resources.

1.3.1 Mining History in Ireland

Ireland's mining history stretches back to Bronze Age copper extraction (c. 2400 – 1800 B.C.) in the southwest of the country (O'Brien, 2013). These primitive copper mines are present in the form of shallow workings (rarely deeper than 10m) that targeted mineralised quartz veins and near-surface copper enriched horizons within sedimentary rock sequences. Copper was particularly valuable at this time given it is a necessary component in the manufacture of bronze, when combined with tin, which was generally sourced from Cornwall in southwest England. One of the earliest known copper mines in Ireland is found at Ross Island near Killarney in County Kerry (Fig. 1.2 [location 22]). Radiocarbon dating has estimated that metalworking was taking place between 2400 and 2000 B.C. at this particular site (Herity and Eogan, 1996). Following careful modern excavation at Ross Island, O'Brien (1995) reported evidence that the copper ore was mined, hand-picked, crushed and smelted in shallow pit furnaces; all at the one location. Another important example of an ancient copper mine is seen at Mount Gabriel in County Cork (also in the southwest of Ireland) where a significant amount of ore was mined between 1700 and 1500 B.C. (O'Brien, 1994, 2003). Excavation work at this site indicates that Ireland was a major exporter of copper around this time.

Following Bronze Age extraction, very little mining activity was recorded on the island of Ireland for over three millennia. Commercial metal mining resumed in the 18th and 19th centuries, with examples of activity at Allihies in County Cork (Fig. 1.2 [location 2]), Bunmahon in County Waterford on the south coast (Fig. 1.2 [location 6]) and Avoca on the eastern coast in County Wicklow (Fig. 1.2 [location 3]). In particular, iron sulphide (pyrite) mining at Avoca was a significant operation for the time (mid-19th century), with one of the largest open pits in world being developed there in the 1850s (Gallagher and O'Connor, 1999). The operation at Avoca can also be seen as Ireland's first experience of major environmental impacts to the local hydrological system caused by large-scale mining activity, primarily as a result of acid-mine drainage (AMD). The contamination of local land and the Avoca watershed is still an issue today. A joint project of the Environmental Protection Agency (EPA) and Geological Survey Ireland (GSI) has classified the Avoca Mine site as '*Grade I*', indicating

the presence of '*large volumes of metal-rich waste that potentially pose risks to human and animal health and safety as well as to the environment*' (Stanley *et al.*, 2010).

Global demand for raw materials, including metals, increased exponentially throughout the 20th century (e.g. Krausmann *et al.*, 2009; Stuermer, 2017). At that time, it was rapidly realised that if Ireland was to utilise its mineral resources, the country would need an appropriate taxation and regulatory framework for this sector of the economy. An early attempt at this was made in 1931 with the *Mines and Minerals Act*. However, this act did not consider the rights of access to land for prospecting and did not clearly distinguish between minerals and the solid or unconsolidated matrix of the ground. The more thorough *Minerals Development Act* (Government of Ireland, 1940) was later introduced to address these issues.

Following the signing into law of important mining legislation in the 1930s and 1940s, the Irish government were now able to encourage mineral exploration by issuing exploration and prospecting licences. Crucially, these licences did not require the permission of local land owners, whose concerns were handled by the newly formed Mining Board. In certain circumstances, these licences even allowed the State to acquire the resultant mineral rights. A change in approach then occurred in the 1950s with the realisation that the capital cost of exploration and mine development was significant for a country with little mining experience. *The Finance (Profits of Certain Mines) (Temporary Relief From Taxation) Act* of 1956 can be viewed as evidence that the government at the time intended to move away from a State-controlled mineral extraction industry in favour of an internationally funded and resourced commercial alternative. Interest in mineral exploration in Ireland increased significantly following the passing of this particular act.
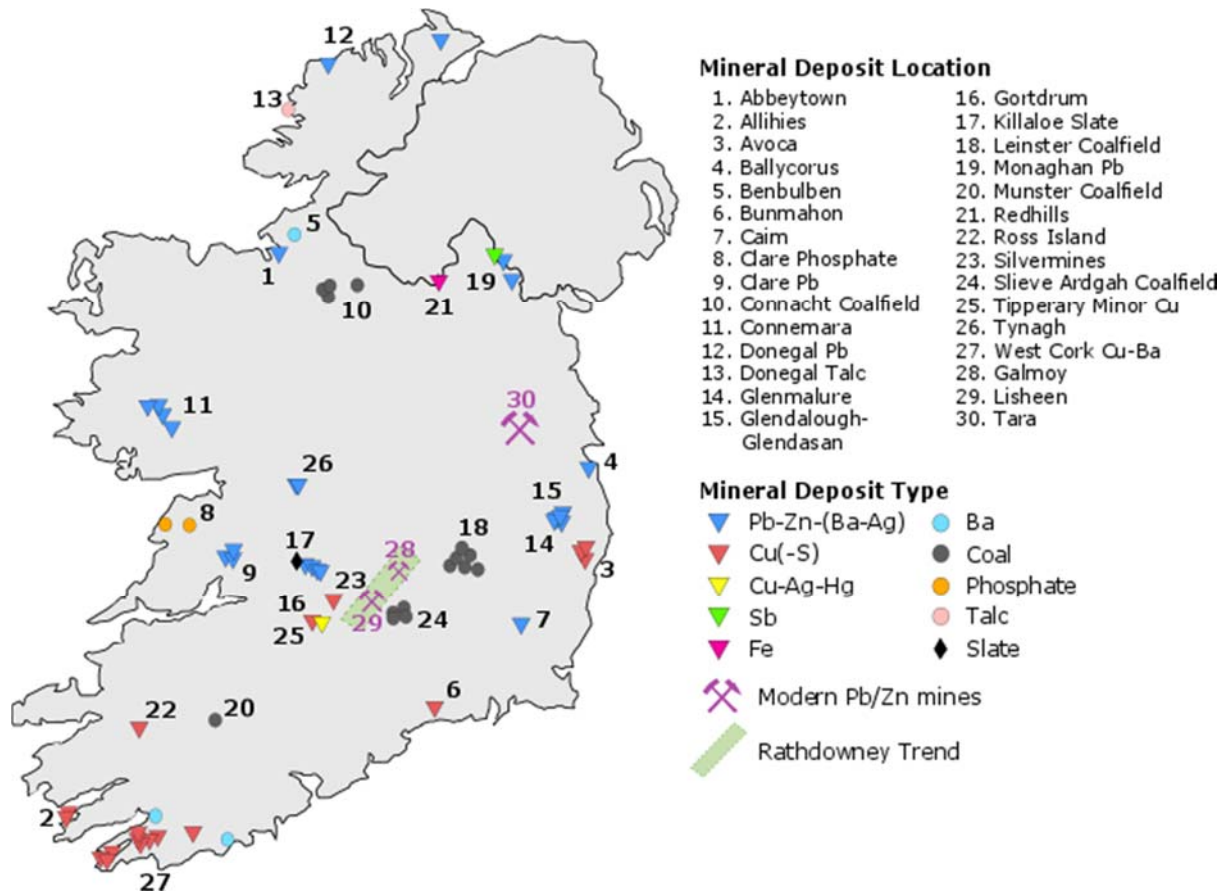
Mineral Deposit Location

1. Abbeytown	16. Gortdrum
2. Allihies	17. Killaloe Slate
3. Avoca	18. Leinster Coalfield
4. Ballycorus	19. Monaghan Pb
5. Benbulben	20. Munster Coalfield
6. Bunmahon	21. Redhills
7. Caim	22. Ross Island
8. Clare Phosphate	23. Silvermines
9. Clare Pb	24. Slieve Ardgah Coalfield
10. Connacht Coalfield	25. Tipperary Minor Cu
11. Connemara	26. Tynagh
12. Donegal Pb	27. West Cork Cu-Ba
13. Donegal Talc	28. Galmoy
14. Glenmalure	29. Lisheen
15. Glendalough-Glendasan	30. Tara

Mineral Deposit Type

Pb-Zn-(Ba-Ag) Ba
Cu(-S) Coal
Cu-Ag-Hg Phosphate
Sb Talc
Fe Slate

Modern Pb/Zn mines

Rathdowney Trend

Fig. 1.2: Map of Ireland showing the general location of selected historic and active mines and mineral deposits (modified from Stanley et al., 2010).

In 1950, the South African mining and investment company *Johannesburg Consolidated Investments (JCI),* purchased the *Abbeytown Mining Company* and began developing the Abbeytown deposit in county Sligo on the west coast (Fig. 1.2 [location 1]), which had been worked for lead, zinc, silver and nickel since the 18th century. Metal grades were low (1%Pb and 2.5% Zn), but very high metal prices at the time (£180/t Pb and £190/t Zn) made the project commercially viable. Following the discovery of higher grade ore below the index bed workings, JCI further developed the mine using the room and pillar method, which was made less expensive by the introduction of trackless mining at the site in 1953 (Kelly, 2007) – a first for an Irish mine. An important feature of the mineralisation at Abbeytown was its location within the Mississippian (Carboniferous) stratigraphy. The main ore target was hosted within the early Viséan Ballyshannon Limestone Formation, a transgressive sequence of limestones (typically calcarenite-grade), shales and calcareous sandstones (Persellin *et al.,* 2010; Stanley *et al*., 2010). The Abbeytown orebody itself was compared to the hugely economically important Mississippi Valley-Type (MVT) deposits in the United States. During the period of

operation (up to closure in 1961) it is estimated that a total of 9,685 tons of lead and 14,350 tons of zinc were shipped as concentrates out of Sligo (Kelly, 2007).

The first time a previously unmined significant economic mineral deposit was found in Ireland was in 1961 at Tynagh in County Galway (Fig. 1.2 [location 26]). With almost 10 million tonnes of economic-grade zinc and lead, Tynagh is described as the first major discovery of a metalliferous mineral deposit in Ireland (Kearns, 1976). It is also the first example in Ireland of a discovery of a major ore deposit by means of modern (at that time) exploration methods. Historical records noting the presence of lead and copper from a number of sources (e.g. Cole, 1922) helped to pinpoint the target area for a soil sampling and geochemical analysis survey. Anomalous values of approximately 1000 ppm lead and 8000 ppm zinc to the north of a major fault structure ('*North Tynagh Fault*') encouraged further investigation. An electromagnetic geophysical survey detected a large conductive body beneath the surface which was interpreted to be a mass of strongly mineralised rock. A large drilling programme (160 diamond drill holes) then refined the knowledge of the deposit which, again, lay within Carboniferous (Mississippian) limestone, not dissimilar to the situation at Abbeytown. Between 1965 and 1982 approximately 8 million tonnes of ore was extracted (Johnson, 1999). However, limited remediation and no groundwater monitoring was completed following the closure of the mine in 1982 (Henry, 2011, 2014).

The Silvermines Mine in County Tipperary (Fig. 1.2 [location 23]) has a similar geology to Tynagh and was mined over a similar interval of time with the main Pb/Zn mine operating between 1963 and 1982. An additional open-cast barite mine at the same location was briefly excavated in 1993. The main mine area contained approximately 17.7 million tonnes of ore at 6.4% Zn, 2.5% Pb, and 23.0 g/t Ag (Andrew, 1986), of which 11 million tonnes was mined at 10% Zn + Pb. The additional barite deposit produced 5.0 million tonnes of 85% $BaSO_4$ (Torremans *et al.*, 2018).

A number of significant mineral discoveries since Tynagh and Silvermines have all been subject to more modern environmental assessments and remediation plans, including groundwater monitoring. The deposit at Tara Mines at Navan in County Meath was first discovered in 1970 and is still operational today as the largest zinc mine in Europe (e.g. Fitch Solutions, 2018). The Tara orebody is much larger in terms of scale than any other deposit discovered to date in Ireland; it lies between 50-100m below ground level and is present over a spatial area of 6.5 by 1.5 km (Ashton *et al.*, 2016). The total pre-mining resource is believed

to be in excess of 112 million tonnes of ore, with an average of 7.9% Zinc and 1.9% ore (Ashton *et al.*, 2016). As with both Tynagh and Abbeytown, this Pb/Zn mineralisation is found within Mississippian (Carboniferous) limestone.

In the mid-1990s several significant Pb/Zn mineral deposits were discovered in south-central Ireland, again within Mississippian limestone, along the Rathdowney Trend (Fig. 1.2), a northeast-southwest zone of carbonates which are commonly diagenetically altered (dolomitised). Two of these deposits were economically significant: Galmoy Mine in County Kilkenny, which opened in 1997, and the larger Lisheen Mine (approximately 7.5 kilometres to the southwest) in County Tipperary, which began production in 1999. When considered together, all of these broadly similar Pb/Zn deposits (Tara, Lisheen, Galmoy, Silvermines, Tynagh) serve to rank Ireland as first in the world for zinc discoveries per square kilometre and they have accounted for approximately 1.5% of global zinc mined to date. As Tara Mine is still operational, Galmoy and particularly Lisheen offer the most recent examples of modern mine closure and remediation in Ireland.

1.3.2 History of Lisheen Mine

The Lisheen deposit was originally discovered by Chevron Mineral Corporation of Ireland (CMCI) who were encouraged by the discovery at Galmoy to take out prospecting licences in the area (Hitzman *et al.,* 1992; see also Hitzman *et al.,* 2002). A weak soil geochemical anomaly led to the commencement of drilling in 1990. Several diamond drill holes found encouraging results, including one particular hole (3262-1), which intersected Pb/Zn mineralisation with grades in excess of 35% Zn and 6% Pb (Quaid and Wheston, 2017). CMCI and Ivernia West then entered a joint venture to fully delineate the orebody; however, in 1993 CMCI sold its share in the project to Minorco (a subsidiary of Anglo American). Continued exploration together with Environmental Impact Studies (EISs) and planning applications occurred throughout the mid-1990s. The first ground was broken at the mine site in 1998. At this stage three ore zones (150-200 metres below ground level) had been identified: Derryville, Main and Main North.

At this point a contract mining firm (Cementation) were employed to develop the underground operation. This started with the building of a 15° decline that allowed for heavy machinery and equipment to be driven to the underground mine workings. A 1.5km conveyor belt for ore

transport was also installed in the decline. Vertical shafts were also driven directly above the orebodies for circulation of fresh air and emergency egress. The development process was setback when a major water-bearing geological structure (F2/F3) was intercepted by the main decline. This fault structure is discussed further in Sections 1.3.5.2 and 1.3.5.4.

The first ore was mined in the Derryville Zone in September 1999, followed shortly by ore from the Main Zone. As anticipated by the exploration team, some common issues with underground mines slowed progress at Lisheen (Quaid and Wheston, 2017). These included: the rolling nature of the orebody, poor ground conditions and significant groundwater ingress. The major milestone of the first million tonnes of ore mined was reached in 2001. All ore from underground was delivered to the mine concentrator on the surface site where it was milled and separated into zinc and lead concentrate. This concentrate was then transported to the Port of Cork on the south coast for shipment to international smelters. Lead and zinc from Lisheen was sold to buyers in Europe, America and Asia.

Following a decision by Anglo American to divest its zinc and lead operations, Lisheen Mine was bought by the Indian multinational, Vedanta in 2010. Underground operations were expanded under the new ownership. This expansion included accessing the Island Pod via a 1km adit driven through the limestone bedrock. A combination of this new reserve and the purchasing of ore from Galmoy Mine, extended the life of the Lisheen Mine from 2013 to 2015.

Tailings from the mining and ore processing operation were stored in an on-site Tailings Management Facility (TMF). The TMF is an artificial impoundment with a continuous gravity dam wall that is 8 to 22 metres height containing approximately 6.6 Mt of tailings that are high in pyrite/marcasite (Smart *et al.*, 2015). At its base, the TMF has a geosynthetic clay liner (GCL) and a linear low density polyethylene liner (LLDPE) in combination with other geotextiles. To prevent acid mine drainage (AMD) by exposing sulphides to the atmosphere, the tailings have been covered with a capping layer and local soils (Smart *et al.*, 2015).

Plans for mine closure had already begun by the time mining had ceased in late 2015. By this time approximately 60% of the TMF had already been rehabilitated to pasture farmland. At this stage the entrances and underground workings including the main decline were backfilled and capped with concrete. The concentrator building and the stockpile structure ("tepee") were dismantled and all foundations and associated materials were removed. Underground pumps

were removed in December 2015, initiating the rebound of the water table to its natural state (see Wheeler *et al.,* 2021).

1.3.3 Geographic location and setting of Lisheen Mine

Lisheen Mine is located c.10km north-east of the town of Thurles in County Tipperary, Ireland (Fig. 1.3). The local topographic high is Devils Bit Mountain (478m AOD) in the north-west of the study area, which is chiefly composed of Silurian siliciclastic sedimentary rocks (Cope, 1959; Archer, 1981; Holland, 2009). Surface water generally flows from north to south (principally through the rivers Suir, Drish and Goul). The majority of the land in County Tipperary is used for a variety of agricultural activities, particularly pasture for the production of dairy. The land immediately north and east of Lisheen Mine, including directly above some parts of the underground mine workings, is peat bog which had been traditionally harvested but now serves as the site for a wind farm. To the south and west of the mine site is primarily agricultural land. With the exception of the peats, the soil is generally composed of low-permeability glacial till.
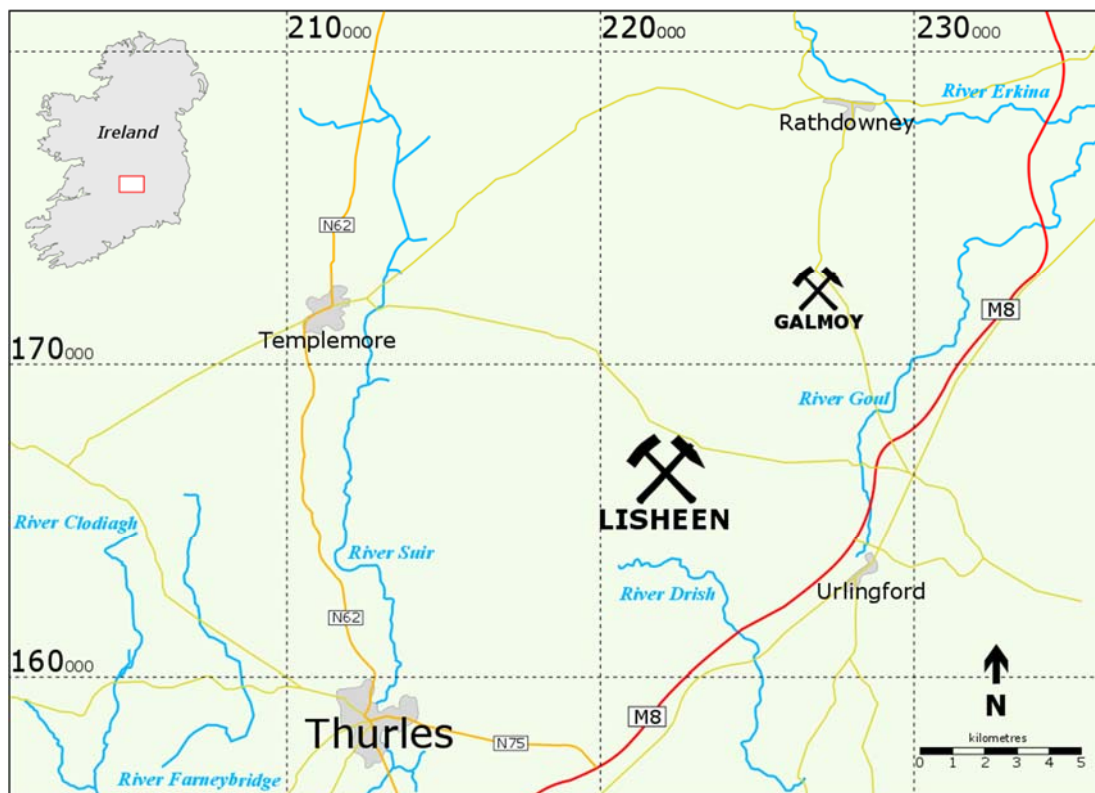

Fig. 1.3: *Geographic map of the Lisheen study area showing the locations of Lisheen and Galmoy mines relative to rivers, main roads and towns (coordinates in Irish National Grid).*

1.3.4 Meteorology

The climate in Ireland is heavily influenced by proximity to the North Atlantic Ocean. In particular, warm water from the Iberian Peninsula south of Ireland and warm winds associated with the North Atlantic Current (NAC) (supplying warm water from the Gulf of Mexico driven by thermohaline circulation) aids in maintaining a temperate climate in Ireland in comparison to similar latitudes (e.g. Eastern Canada; e.g. Ottersen *et al.*, 2001). The NAC is the driver of Ireland's prevailing south-westerly winds which bring temperate air and significant amounts rain to the island. Generally summers are mild and winters are cool and wet.

Atmospheric circulation in Ireland is controlled by the polar front, which is defined as the transition zone between the warm and moist air moving with the NAC northwards and colder, drier and denser air moving southwards from the Arctic (Rohan, 1975). In the North Atlantic, the polar front can be traced for thousands of kilometres from the eastern United States north eastward across the Atlantic Ocean. Disturbances often amplify and deepen along this front, forming large scale depressions in mid-latitudes. A continuous sequence of depressions bring warm, moist air, causing significant levels of precipitation across the whole of Ireland. Intense storms regularly recorded off the northwest coast of Ireland are predicted to move further south in the period of 2041 to 2060 (Nolan, 2008), potentially altering Ireland's climate regime.

One of the closest weather stations to Lisheen is Littleton (Fig. 1.4). A 20-year annual average rainfall (arithmetic mean) from 1998 to 2018 was calculated to be 939 mm/year based on daily rainfall data acquired from Met Éireann (the Irish meteorological service). This is lower than the national average (~1200 mm/year) but representative of precipitation conditions in south central Ireland. Figure 1.5 provides a detailed graphical representation of rainfall data in the Lisheen area from December 2015 to October 2016. This time frame is of direct interest to the geochemical samples discussed in chapters 3 and 4.
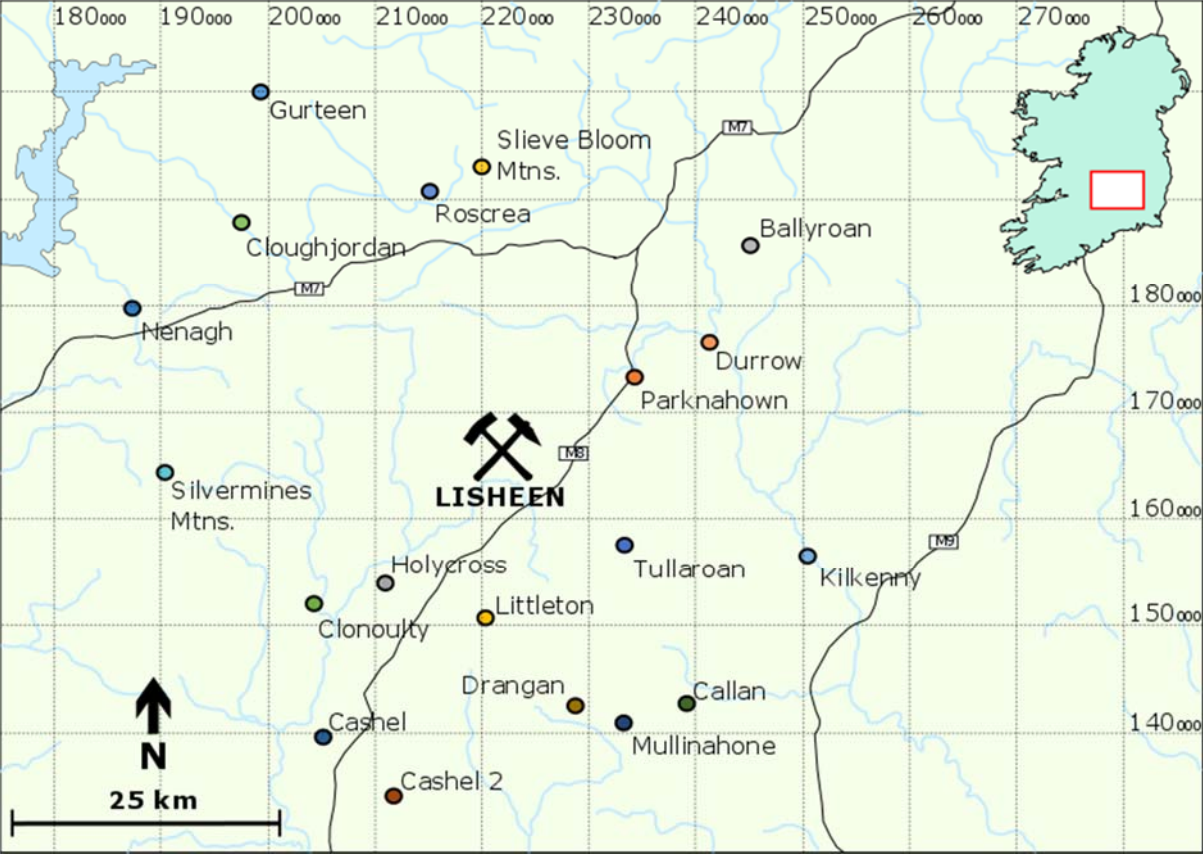
Fig. 1.4*: Rainfall locations for the data displayed in Figure 1.5 (coordinates in Irish National Grid).*
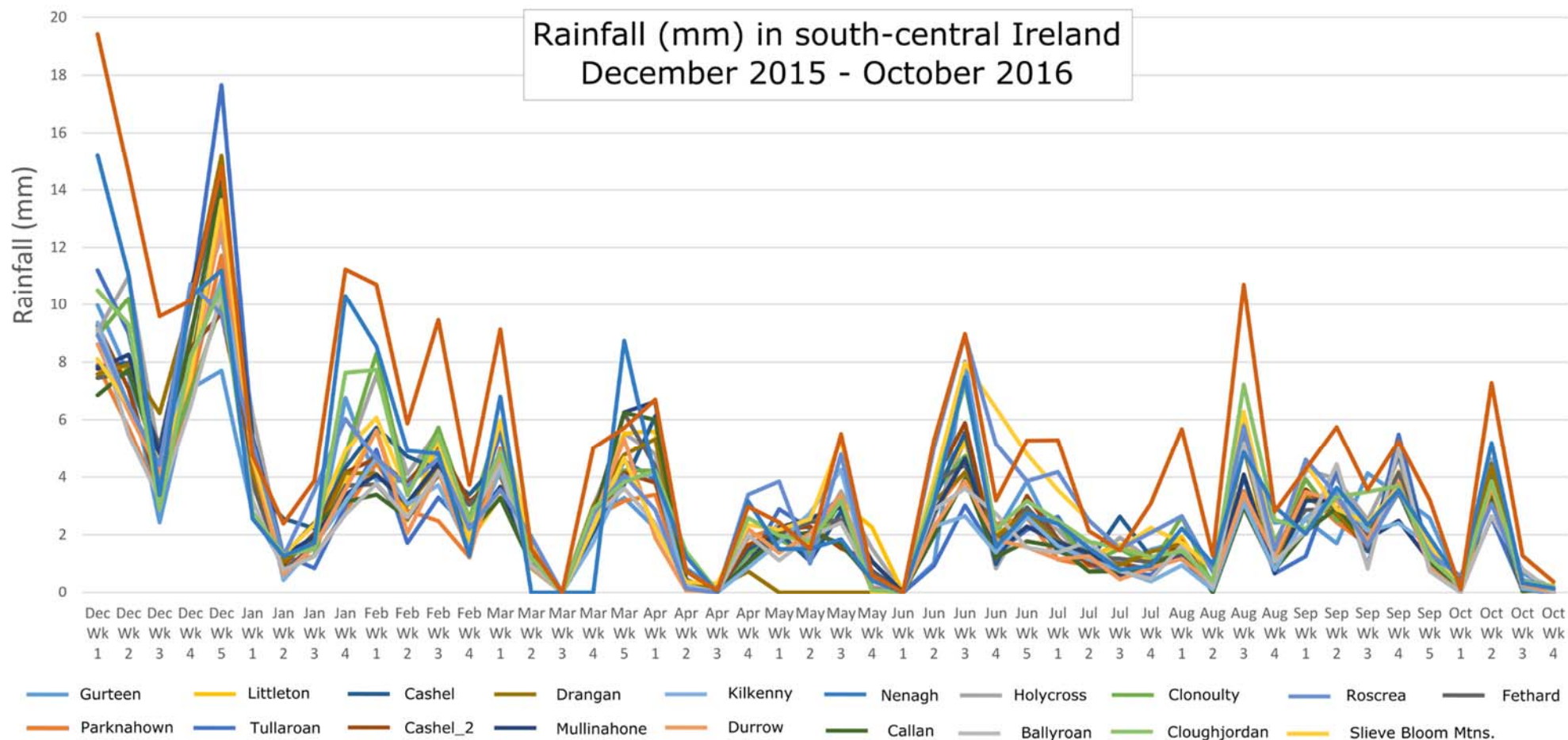
Fig. 1.5: Regional rainfall data in the area around Lisheen Mine during a period of interest discussed in Section 4.3.1.

1.3.5 Geological/Hydrogeological Context

1.3.5.1 Geological Overview

Lisheen was the most significant of a number of base-metal (Zn-Pb) ore deposits that lie along the NE-SW Rathdowney Trend in south-central Ireland (Fig. 1.6; Hitzman 1995; Hitzman *et al.,* 2002; Fusciardi *et al.,* 2004; Wilkinson and Hitzman, 2015). These mineral deposits are believed to have developed in this part of Ireland as a result of extensive Carboniferous deep-seated normal faulting that provided conduits for mineral-rich ore forming hydrothermal fluids, depositing the highest concentrations of Zn mineralisation ($130,000km^3$) discovered to date (e.g. Johnston *et al*., 1996; Hitzman *et al*., 1998; Hitzman, 1999; O'Reilly *et al*., 1999; Wilkinson *et al*., 2005; Kyne *et al*., 2019).

The structural fabric at Lisheen is broadly ENE-NE trending, which mirrors underlying reactivated Lower Paleozoic (Caledonian) structures (Kyne *et al.,* 2019). This broad trend reflects proximity to the Iapetus Suture Zone, which represents the area of convergence between the continents of Laurentia and Avalonia during the latter stages of what has been termed the Caledonian Orogenic Cycle (e.g., Chew, 2009, 2012; Chew and Strachan, 2014). The Lower Paleozoic basement rocks are rarely intercepted by modern exploration as they lie at significant depth in the Irish Midlands (Fig. 1.7). Where they crop out or are closer to the surface in the northeast they do not contain economic deposits and are believed to consist primarily of low-grade metasedimentary rocks (Morris, 1983); but the presence of major buried intrusive bodies across the Irish midlands has also been implied by geophysical surveys (e.g. Jacob *et al.,* 1985; Morris and Max, 1995; Readman *et al.,* 1997).

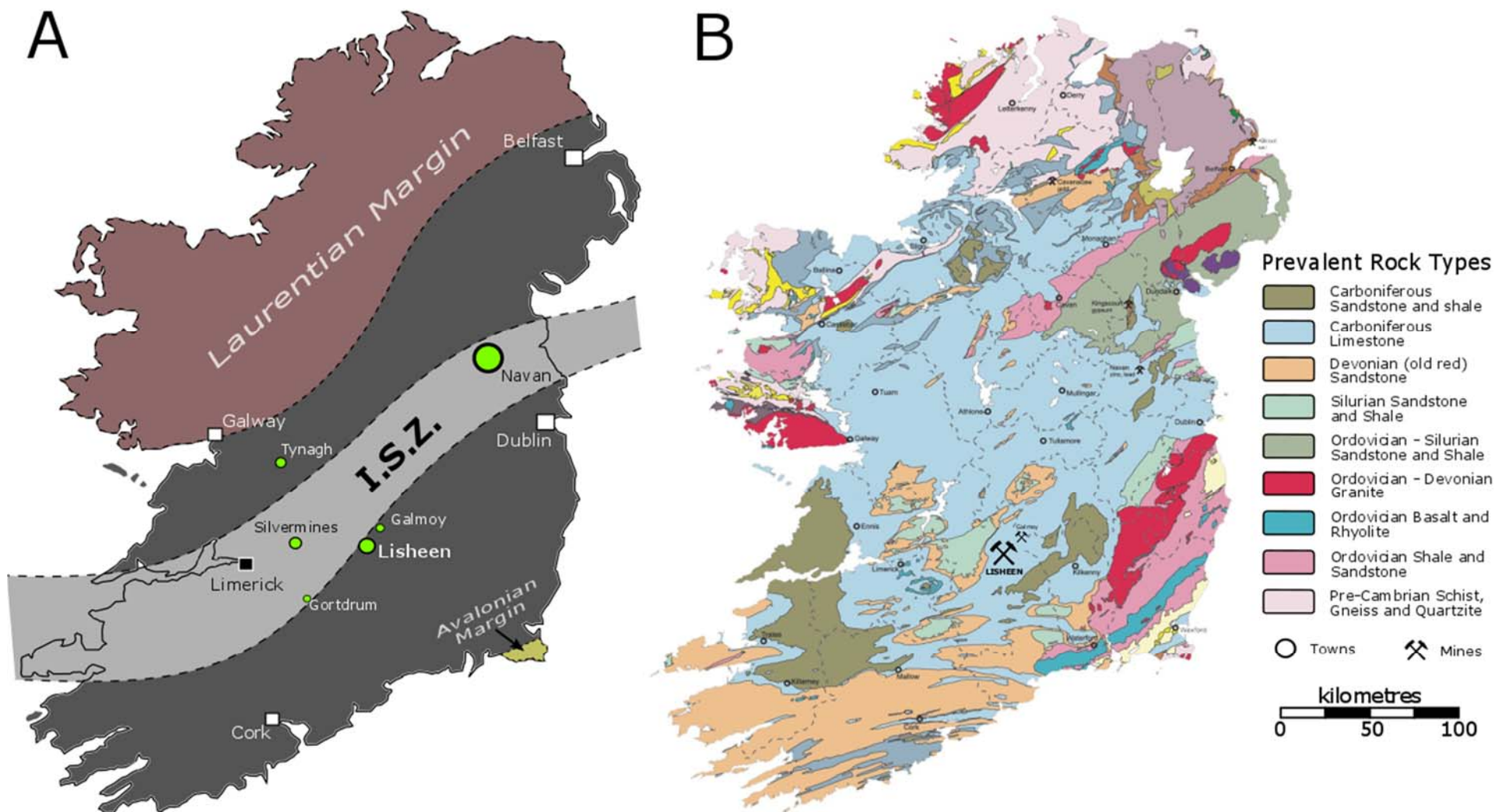**Fig. 1.6: A)** *Map of Ireland showing the locations of economic Pb/Zn mineral deposits (green-filled circles) relative to the Iapetus Suture Zone (ISZ) and the Avalonian and Laurentian margins between which are rocks formed within the Iapetus Ocean (modified after Blake et al., 2016).* **B)** *Geological bedrock map of Ireland showing the general location if Lisheen Mine (modified after GSI, 2004).*
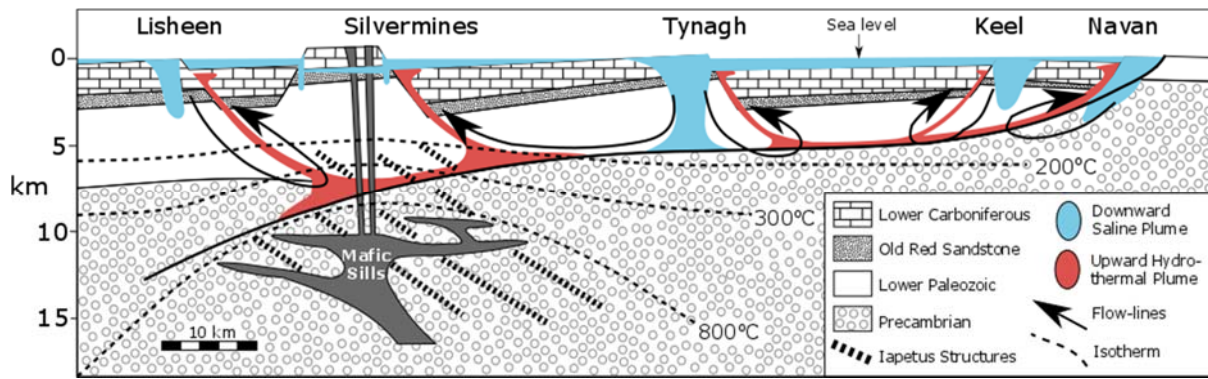
Fig. 1.7: *Broadly north-south cross-section profile through the Irish lithospheric crust, modelling the genesis of major mineral deposits (modified from Wilkinson and Hitzman, 2015).*

In Ireland, the Lower Paleozoic basement is unconformably overlain by a late Devonian to Carboniferous (Mississippian) transgressive sequence, initially beginning in terrestrial (red-bed) siliciclastic facies and progressing stratigraphically upwards into marine carbonates (e.g., MacDermot and Sevastopulo, 1972; Clayton *et al.,* 1986; Graham, 2009; Graham and Sevastopulo, 2020). During the Tournaisian, these carbonate sediments were produced largely in ramp environments; however, later during the Viséan, extensional re-activation of faults led to a more complex palaeogeography, with the formation of several intracratonic basins and adjacent carbonate platform highs (e.g. Leeder, 1982, 1987; Somerville 2008; Sevastopulo and Wyse Jackson, 2009; Murray, 2010). Later, during the Serpukhovian and Bashkirian, carbonate production ceased and was replaced by non-calcareous facies (Sevastopulo, 2009; Barham *et al.,* 2014; Fallon and Murray, 2015).

The Mississippian stratigraphy of the Lisheen mine area is described by Hitzman *et al.* (2002) and is summarised in Figures 1.8 and 1.9. The Ballymartin and Ballysteen Limestone formations are predominantly composed of argillaceous limestones and interbedded shales, reflecting the initial ramp phase of sedimentation. Subsequently, in late Tournaisian times, a regionally widespread series of carbonate mudbanks developed, termed Waulsortian Limestone (Lees and Miller, 1995). Base-metal mineralisation is associated primarily with the base of this relatively pure carbonate facies, particularly where it has been regionally dolomitised along the Rathdowney Trend (Wilkinson and Hitzman, 2015). The ore deposits at Lisheen occurred at an average depth of c. 170m (EIS, 2013). The generally low permeability of the bedrock (Murray and Henry, 2018), together with significant faulting along the Rathdowney Trend and karstification of the upper 30m of the bedrock, means that regional

groundwater flow is primarily propagated through fractures, and is broadly directed from NNW towards SSE (Lisheen mine closure plan, 2016).

Most groundwater flow at the mine site, and in the broader east Thurles region, occurs in the upper 30–50m of epi-karst. This horizon at the top of the vadose zone of the karst aquifer is primarily characterised by enhanced storage capacity (Williams, 1983). Due to the nature of the base of the epi-karstic zone (i.e. reduced fracture frequency, a capillary barrier in the narrowing fissures and/or clay residues from dissolution blocking the fissures), the majority of flow occurs laterally across the base (Bauer *et al*., 2005). Therefore, a reduced connection exists between shallow groundwater in epi-karst and deeper groundwater in these limestone aquifers. The bulk of the bedrock in the region is classed as *'Locally important aquifers'* by the GSI, while the Waulsortian Limestone Formation is classed as *'Regionally important (karstified – diffuse)'*. The bedrock sequence is overlain by low permeability glacial till and peaty soils. In particular, a large area to the east of the mine is covered in extensive saturated peat deposits (up to 14m deep).

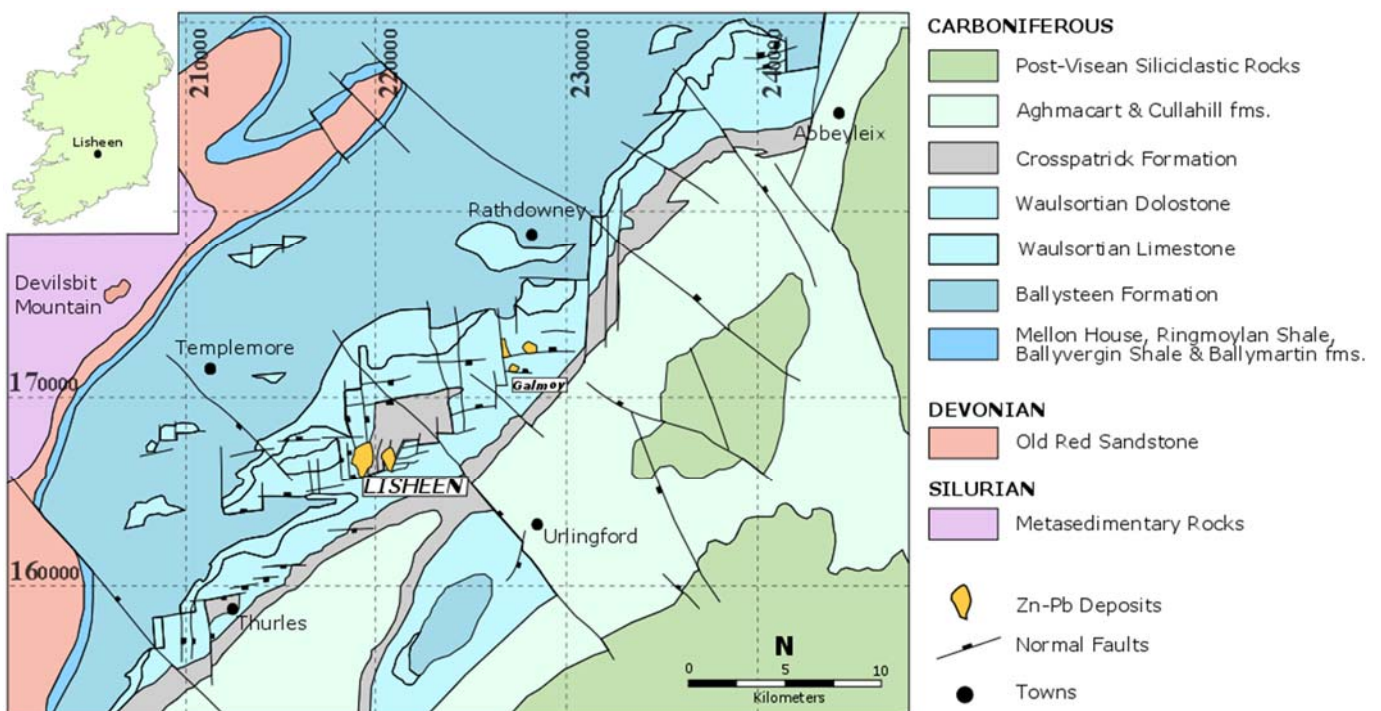*Fig. 1.8: Paleozoic bedrock geology of the area surrounding Lisheen Mine in County Tipperary (modified after Hitzman et al., 2002).*
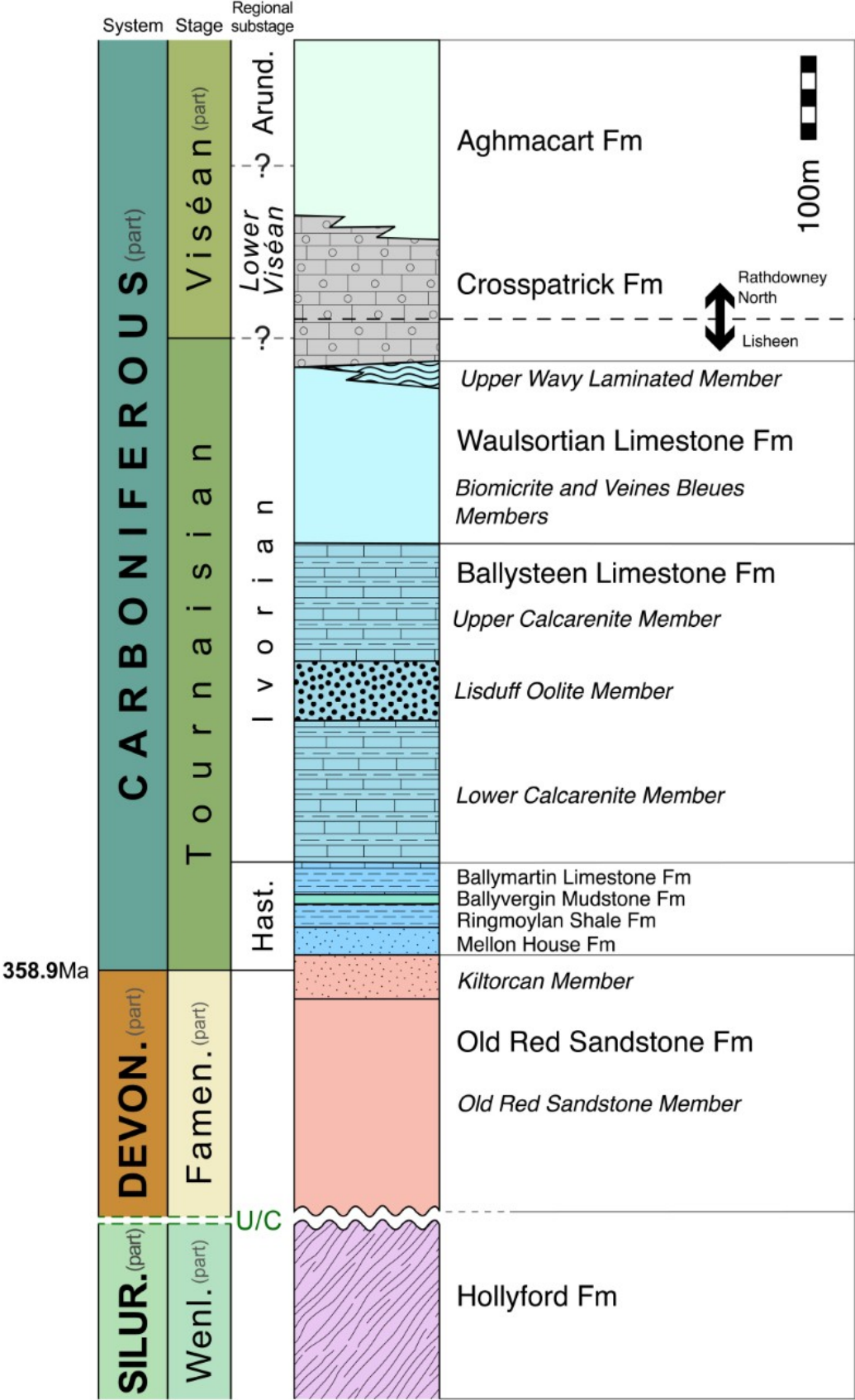
Fig. 1.9: *Chrono- and lithostratigraphy summary of the Lisheen area (modified after Hitzman et al., 2002). Colour coding for formally defined international chronostratigraphic units is according to the Commission for the Geological Map of the World, Paris, France.*

1.3.5.2 Structural Geology

Given the economic importance and significance of the Lisheen mineral deposit, the local structural trends have been extensively studied (e.g. Eyre, 1998; Hitzman, 1999; Fusciardi *et al.*, 2004; Wilkinson *et al.*, 2005; Kyne *et al.*, 2017). On a larger structural scale, the deposit lies on the southern limb of the Littleton regional syncline. A variety of structures can be grouped into a number of 'families' as per Torremans *et al.*, 2018:

1. <u>E-ENE trending normal fault segments</u>

   The most important structure in terms of mineralisation at Lisheen, is an array of east to east-north-east left-stepping normal fault segments (red sub-horizontal lines in Fig. 1.10). These faults are characteristic of the Rathdowney Trend and similar structures are developed at Galmoy, the other major known deposit along the Rathdowney Trend (Hitzman, 1999). Defining the southern extent of the Waulsortian-hosted ore bodies, the five major normal faults have a displacement on the order of 160-220m, with north-west dipping relay ramps transferring displacement from one segment to another. Minor normal faults with displacements of up to 15m strike parallel to the major faults.

2. <u>NW trending relatively minor structures</u>

   Low displacement (< 10m) north-west trending normal faults (thicker black lines in Fig. 1.10), monoclines, and fault bend folds are regular occurrences within the ore body.

3. <u>NE trending reverse faults</u>

   North-east trending dextral oblique-slip reverse faults crosscut the segmented normal faults (blue lines in Fig. 1.10). Associated fault bend folds and overfolds occur in the hanging wall of these structures within the Ballysteen Limestone Formation. This group of structures are believed to have formed in a transpressive regime during north-south oriented shortening during the Variscan orogeny, later in the Carboniferous (Coller, 1984; Hitzman, 1999).

4. <u>NW trending strike-slip faulting</u>

   Generally dextral north-west trending sub-vertical strike-slip faults cross-cut all of the previous structural groups (thin black lines labelled F in Fig. 1.10). These faults have displacements up to 75m (F7 fault) and are associated with higher rates of groundwater flow. Identified as post-Variscan, these structure may be related to north-south Alpine compression during the Cenozoic (during either the Paleocene or Oligocene; Carboni *et al.*, 2003; Fusciardi *et al.*, 2004; Cooper *et al.*, 2012).
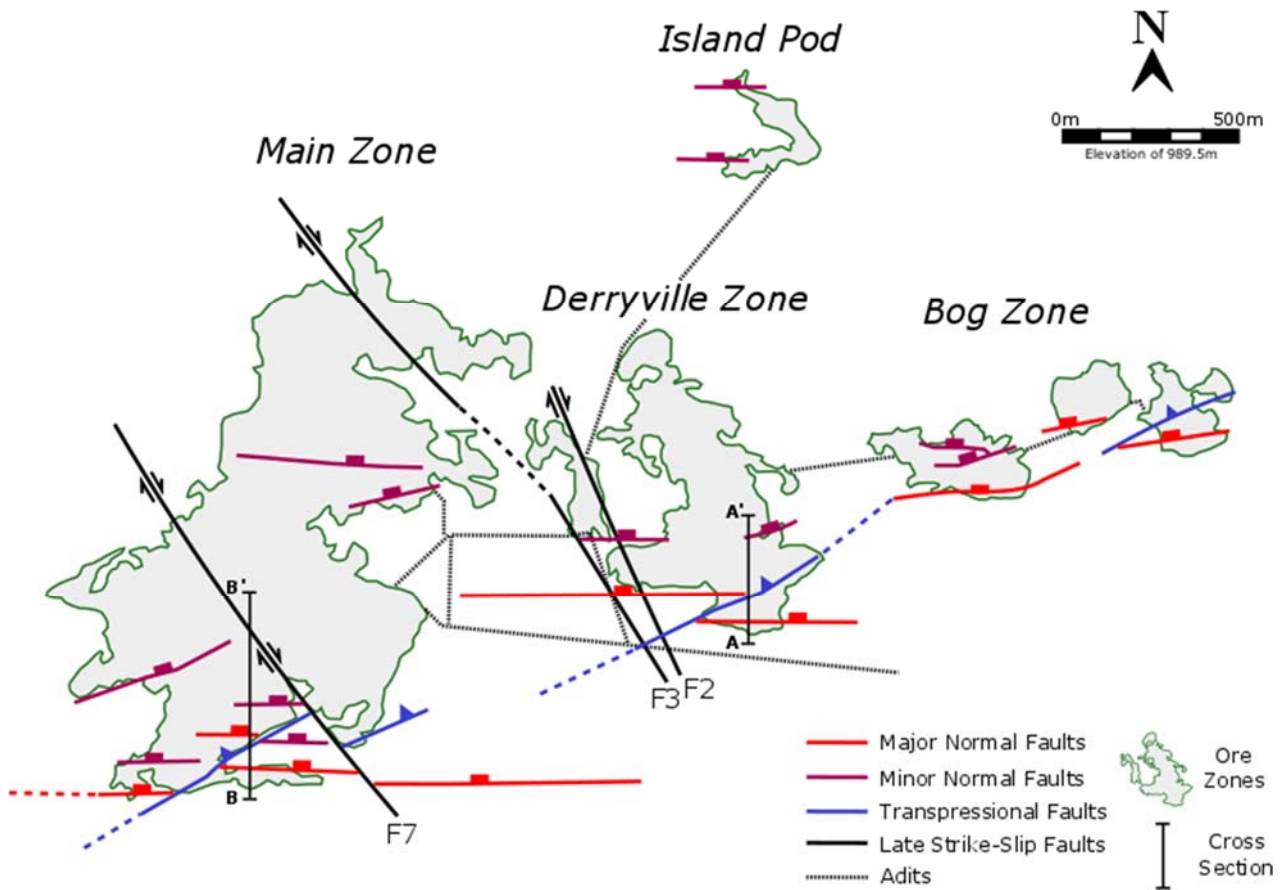
Fig. 1.10: *Underground workings and main geological (brittle) structures at Lisheen Mine (modified after Torremans et al., 2018). Location of cross-sections A-A' and B-B' in Figure 1.11 are shown.*

1.3.5.3 Mineralisation

Many of the large Pb/Zn mineral deposits in Ireland (e.g. Tynagh, Silvermines, Galmoy, Lisheen, Tara) display a number of similarities in terms of the style of mineralisation. All share characteristics of both Mississippi Valley-Type (MVT) and Sedimentary Exhalative (SedEx) deposits (e.g. Duane *et al.*, 1986; LeHuray *et al*., 1987). Similarities to MVT deposits include: carbonate hosting, epigenetic-style textures, association with significant dolomitisation and a relatively simple mineralogy. Additional similarities with SedEx deposits include: proximity to major faults that are interpreted to act as feeders for mineralisation, relatively hot hydrothermal fluids postulated during mineral deposition (100-280°C) and the presence of stratified sulphide textures in some locations. This duality has led to the adoption of the term 'Irish-Type Deposits' to describe the hybrid ore deposit type at Lisheen and elsewhere (e.g. Everett *et al*., 1999; Wilkinson *et al*., 2005).

The first mineral alteration to occur at Lisheen was the regional dolomitisation of the Waulsortian Limestone Formation, which is common along the south-eastern margin of the Rathdowney Trend (Shearley *et al.*, 1996; Hitzman *et al.*, 1998; Sevastopulo and Redmond, 1999; Wilkinson *et al.*, 2005a). Minor dolomitisation is also seen in non-argillaceous carbonate horizons of the overlying Crosspatrick Formation (Sevastopulo and Redmond, 1999; Fig. 1.9). This regional dolomitisation was then followed by gradually evolving stages of sulphide mineralisation described in detail in Torremans *et al.*, 2018. The earliest stage was the mineralisation of iron sulphides which form much of the pyrite cap to the Zn-Pb orebodies throughout the ore deposit. These appear as disseminated to massive Fe sulphides (pyrite and marcasite [both FeS_2]). Highly fractionated $\delta^{34}S$ signatures, also seen in minor non- to weakly colloform pink-brown sphalerite [$(Zn,Fe)S$] and galena [PbS] that infill the intergranular dolomite porosity, are interpreted to be the result of bacteriogenic sulphate reduction (e.g. Hitzman *et al.,* 2002; Wilkinson *et al.*, 2005b).

Colloform pyrite and marcasite are followed by more course-grained varieties that are associated with early minor sphalertie and galena (Fuscardi *et al.*, 2004; Wilkinson *et al.*, 2005b). A change from predominantly Fe sulphides to Zn/Pb sulphides can be identified by the appearance of bravoite [$(Fe,Ni)S_2$] rims on early pyrite, which is interpreted to have occurred concomitant with an influx of hot Zn-Pb metal bearing hydrothermal fluids into the host rocks (Eyre, 1998; Fuscardi *et al.*, 2004; Wilkinson *et al.*, 2005b, 2011).

The main Zn-Pb sulphide stage occurs as predominantly sphalerite and galena which progressively replaced and overprinted breccia matrix dolomite clasts of regional dolomite and early Fe sulphides (Hitzman *et al.*, 2002). These main ore stage sulphides have higher $\delta^{34}S$ values as a consequence of thermal sulphate reduction at increasingly higher temperatures at the time of formation (Eyre, 1998; Wilkinson *et al.*, 2005b).

Nickel-bearing phases of mineralisation are also evident by the presence of niccolite [$NiAs$] and bravoite as well as trace nickel in pyrite and sphalerite (Wilkinson *et al.*, 2005b, 2011). In addition, copper is present in chalcopyrite [$CuFeS_2$] and tennantite [$(Cu,Fe)_{12}As_4S_{13}$] with accessory bornite [Cu_5FeS_4] and, again, as a trace element in sphalerite (Wilkinson *et al.*, 2005b). Arsenic can be found in arsenian pyrite [FeS_2], tennantite [$Cu_6[Cu_4(Fe,Zn)_2]As_4S_{13}$] and arsenopyrite [$FeAsS$], and barium in barite [$BaSO_4$] and barium feldspar [$\underline{BaAl_2Si_2O_8}$] (Hitzman *et al.*, 2002; Wilkinson *et al.*, 2005b).

High iron ore tonnages were seen in the hanging wall of major and minor normal faults at Lisheen. These structures also control the distribution of the thick pyrite caps that sit above the Zn-Pb mineralisation in the hanging wall rocks of the faults. In contrast, Cu, Ni, Co, Cd and Ag are concentrated proximal to distinct points (interpreted as feeders) along the normal fault segments (Kyne *et al*., 2019). These concentrations decrease over a relatively short distance (~10 to 100m) along the base of the Waulsortian Limestone Formation in the hanging wall and also within the Lisduff Oolite Member (of the underlying Ballysteen Limestone Formation) in the footwall of the normal faults (Fig. 1.11; see also Fig. 1.9). The orebodies in the footwall and hanging wall align when the lithological units are restored to position prior to Variscan dextral oblique-slip movement on reverse faults (Kyne *et al*., 2017). Lower concentrations of Ni, Ag, Cd, Co, As and Cu occur locally on other minor ENE trending normal faults in the Waulsortian Limestone Formation, most notably in the Main Zone East and North. Elevated Ni, Cu and Co are not seen in other parts of the mine (Torremans *et al*., 2018).

Arsenic concentration within mine rocks correlate well with the distribution of iron and with copper, nickel, cobalt and silver, due to the presence of arsenian pyrite and arsenopyrite within iron-sulphide rich areas (Hitzman *et al*., 2002; Wilkinson *et al*., 2005b). High zinc and lead concentrations are present within the hanging wall of the major normal fault segments proximal to the Ni-Cu-As-Ag-Co-Cd rich points, and Zn/Pb and Zn/(Zn+Pb+Fe) ratios increase in a north-northeast direction away from the normal faults and feeders (Torremans *et al*., 2018). The Island Pod and Bog Zone Central orebodies have very high Zn/Pb and significant Zn+Pb contents but lack elevated Cu, Co and Ag values (Doran *et al*., 2017).

Significant cadmium at Lisheen is found within dark-red sphalerite which varies strongly as a result of texture, paragenetic timing and location (Wilkinson *et al*., 2005b, 2011). Sphalerites with elevated Cd occur paragenetically late or within the Lisduff Oolite Member ore samples (Wilkinson *et al*., 2005b). Areas with low Zn/Cd and high Cd contents (e.g. the base of the Main Zone-Derryville Ramp) are interpreted as a product of late pulses of Cd-rich sphalerite mineralisation (Torremans *et al*., 2018).

The orebody is also zoned vertically with Zn/Cu, Zn/Pb and Fe/Zn increasing from bottom to top. Vertical Fe/Zn zoning is reflective of the pyrite cap generally found on top of the sphalerite and galena rich massive-sulphides (Torremans *et al*., 2018). The highest Zn, Pb, Ni, Cu, Co, Cd, Ag and As values occur at or near the base of the Waulsortian Limestone Formation. The

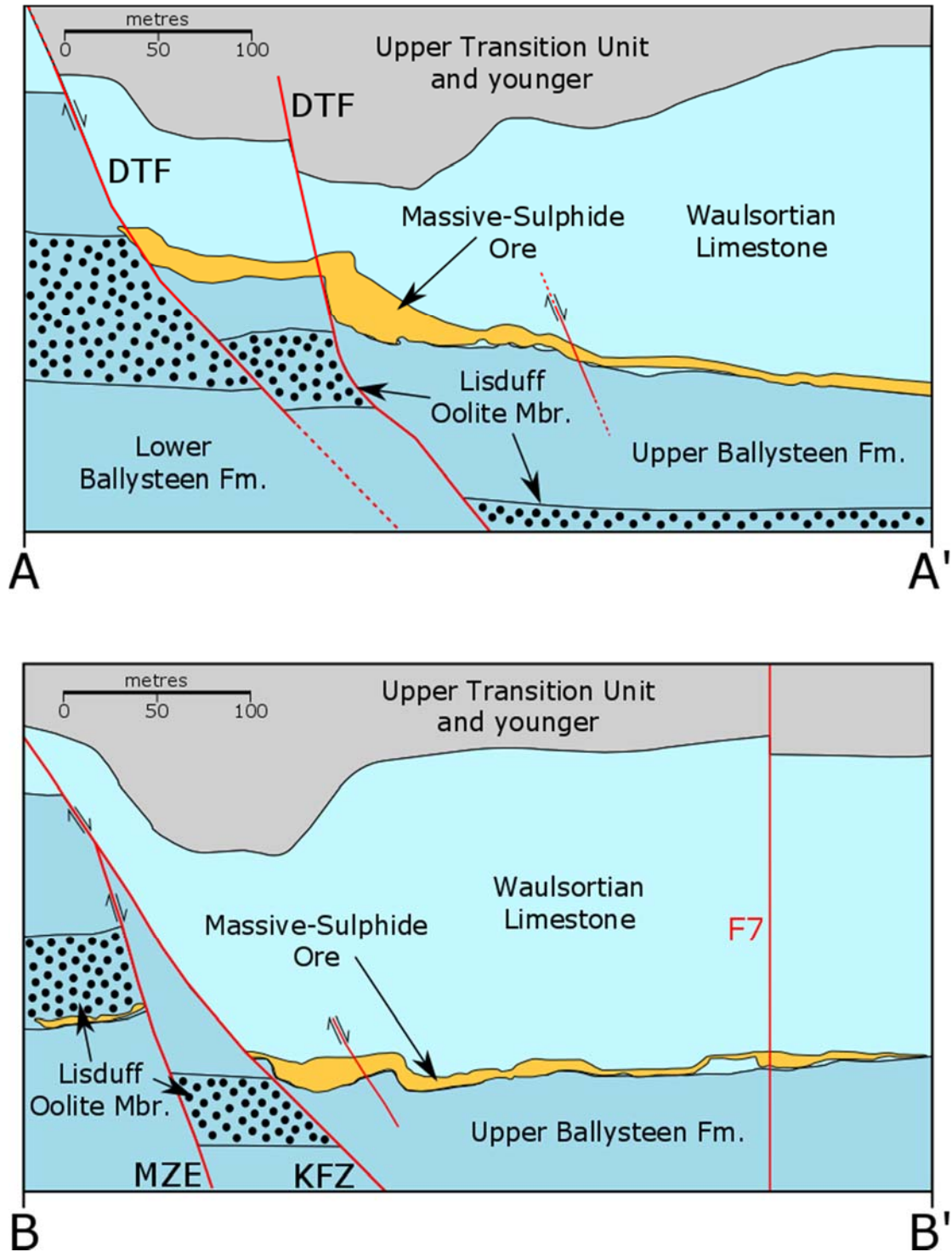Island Pod is an exception, where the highest values occur ~20m above the base (Doran *et al.*, 2017).

Fig. 1.11: *Cross-section profiles A-A' and B-B' highlighting the location of ore relative to the principal lithostratigraphic units and major geological structural features at Lisheen (modified after Torremans et al., 2018). Both of these profiles are oriented south (on left) to north (on right) - see Figure 1.10 for location details.*

1.3.5.4 Groundwater Management during mining operations at Lisheen

From the outset of the active phase of mining at Lisheen (1997), it was apparent that continuous dewatering would be required to maintain safe underground working conditions. The pre-mining groundwater table in the area was between one and three metres below ground level and therefore the planned mine workings would be under some 200m of head, which required the use of surface wells for initial dewatering. Prior to the construction of the main decline connecting to the orebodies in the subsurface, a number of dewatering wells were installed to lower the local groundwater heads within the Waulsortian Limestone Formation. The decline was cut through the relatively low-permeability argillaceous limestones and shales of the Ballysteen Limestone Formation in the footwall (i.e. to the south) of the Killoran Fault (Fig. 1.11 – see profile B-B'). It was then split and enters the Main Zone and the Derryville Zone (in the fractured permeable Waulsortian Limestone Formation) in the hanging wall at the mining horizon. As ore was removed and more void space was created, direct underground water management became progressively more important and it subsequently superseded the surface wells.

As construction of the main decline advanced, commensurate with mine development, in 1997, a significant volume of water unexpectedly became an issue when a group of major regional geological structures were intercepted (F1, followed by F2 and F3 described above). These fault structures were met at a depth of approximately 120-140m below ground level. At this point the Lisduff Oolite Member is offset upwards and the associated fractures were therefore connected to the decline. As a result the short-term water management strategy had to be modified with the installation of a pumping station at ~140m below ground level (immediately below the F2/F3 feature). This was designed to intercept the water before it had a chance to flow into the mine workings and pump it to the surface as clean, non-contact water, thereby reducing the necessity for water treatment prior to discharge to the natural environment.

In the six months that proceeded the interception of the F2/F3 feature, approximately 33 megalitres per day (MLD) had to be pumped to surface. In the subsequent years, as the aquifer reserve was drained, this amount dropped to an average of 22-24 MLD with a 2-4 MLD seasonal variation depending on the level of rainfall and impact of recharge to the regional groundwater system. The water which emanated from the F2/F3 feature can be thought of as unique in the context of Lisheen Mine as it derived from the Lisduff Oolite Member, whereas the rest of the water managed underground was sourced from the (stratigraphically overlying)

Waulsortian Limestone Formation (Figs. 1.9-1.10). As a result of a different behaviour compared to other waters in Lisheen Mine, the F2/F3 feature was managed separately during the life of the mine and subsequent closure.

Following the early identification of the F1, F2 and F3 fault features, a further seven similar geological fracture structures were identified in the Lisheen area. The importance of these structures in terms of their effect on regional drawdown is realised by the NNW-SSE elongation of the groundwater-level cone of depression (Fig. 1.12), which was present during active pumping from underground.

As is the case with most underground mining operations, groundwater management was projected based on two types of inflow:

i)   Storage removal from the local aquifer (in this case the Waulsortian Limestone Formation and the Lisduff Oolite Member) and

ii)   Recharge from rainfall over the area of drawdown.

For this reason it was anticipated that inflows would be 100-140 MLD in the early years of operation at Lisheen Mine, falling to approximately 72 MLD once the storage within the local aquifers had been essentially drained. These conditions were considered to be met in 2006 when the hydrological system was almost in steady state (Water Management Consultants, 2009).

Local and regional groundwater wells were routinely water-depth measured to check the influence of the cone of depression on local supply. Outside of the immediate vicinity of the mine, these wells showed that water level variation due to drawdown at Lisheen was less than 1m, which is within the variation caused by seasonal variation. Therefore, it can be said that active pumping operations at the mine had a fairly minimal impact on the regional groundwater system.
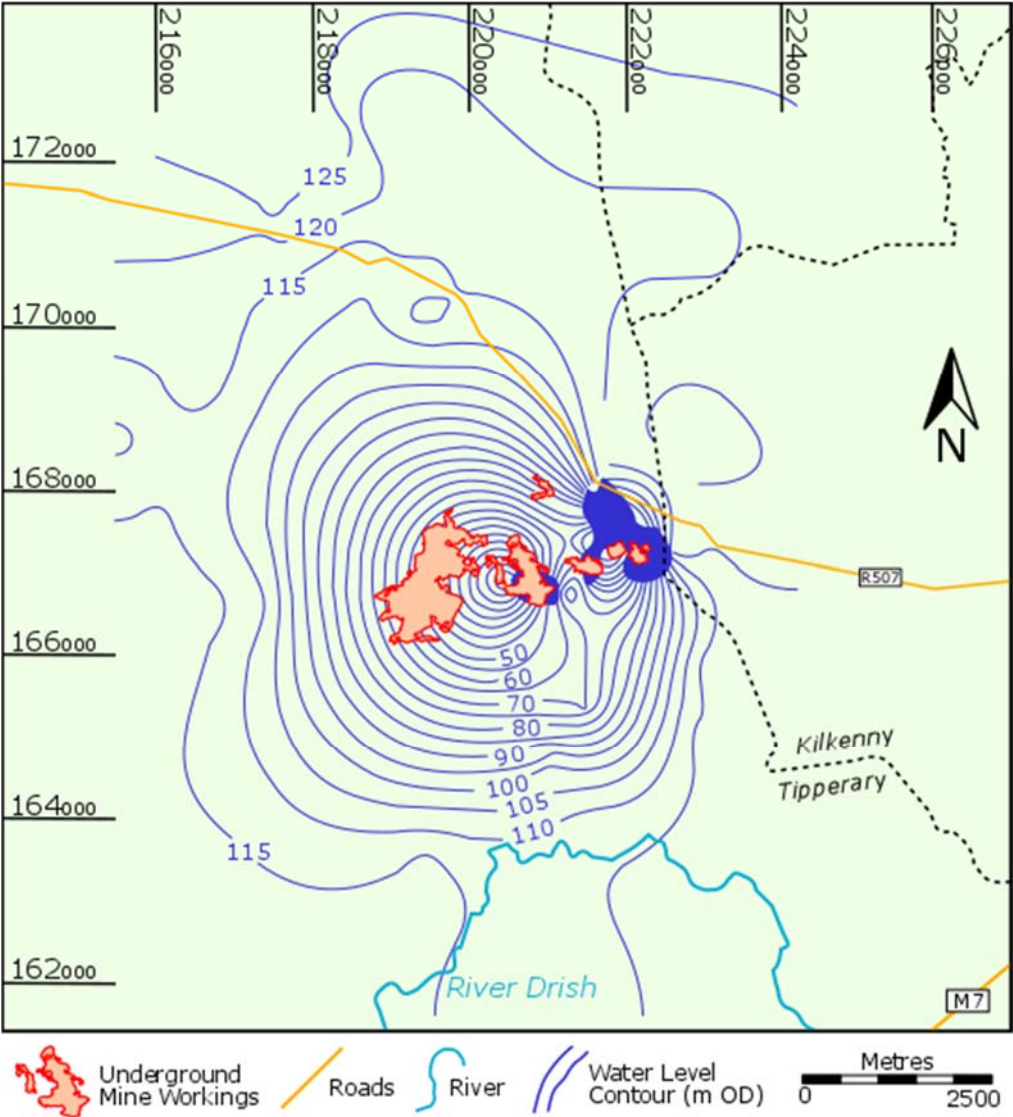
Fig.1.12: *Contour map of groundwater drawdown in the area of Lisheen Mine due to underground pumping during the time the mine was in operation. Note: the NNW-SSE orientation and slight elongation of the cone of depression of the water table (modified after Water Management Consultants, 2009).*

1.4 The Tellus Survey

Geochemical datasets are invariably growing in complexity and scale due to continued sampling for a variety of purposes (e.g. environmental studies, mineral exploration and water resource management). Depending on the motive, these data acquisition programmes can occur at quite different scales (e.g. local, regional or national) and resolutions (e.g. 1:25,000m, 1:200m etc.). Less practically complex methods of analysis (e.g. ICP-MS) allow for a greater spectrum of elements to be detected and accounted for, at relatively low cost. All of this leads to sizeable datasets that require newer, more efficient, methods of statistical analysis than is typically traditional in geochemistry. Geochemistry data (soil, water and sediment) from the border region of Ireland are used to demonstrate the value of CoDA on a much larger scale than that seen at Lisheen Mine, for evaluating relationships between material chemical composition and surrounding geo-environmental and land-use conditions.

1.4.1 Background to the Tellus Survey

The Tellus Survey (named after the Roman goddess of the Earth), was conceived by the Geological Survey of Northern Ireland (GSNI) in the 1990s as a major geoscience project that would benefit the whole island of Ireland (e.g. Young *et al.,* 2016). The main objectives of this very considerable undertaking were to:

i)   Provide a modern geophysical and geochemical dataset which would allow for geological maps to be updated,

ii)   Stimulate investment in mineral exploration, *and*

iii)   Generate an environmental baseline for Ireland (Cowan and Verbruggen, 2016).

The data collection that provides the basis for the completion of these objectives was planned on a regional-scale to industry standards, ensuring exploration and development could be managed in-line with environmental regulation.

As discussed previously (Section 1.3.1), Ireland is an important location for metallic ores and is the major source of European zinc. Modern exploration, particularly in the north of Ireland, has focused on the discovery of gold (e.g. Wilkinson *et al*., 1999; Parnell *et al*., 2000; Lusty *et al*., 2012). The Tellus Project will undoubtedly aid this search and also provide a scope for

finding other significant base metal deposits. The recognition that Ireland should, as much as possible, provide a domestic supply of minerals under well controlled environmental regulations, was a primary motivation for the formation of the project.

The first phase of the Tellus programme in Northern Ireland was funded by the Northern Ireland Government and later retrospectively by the European Union. Between 2004 and 2013 €15 million was spent on the collection of geophysical and geochemical samples (Young, 2016). In addition to discovering natural resources, it was anticipated that the project would benefit agriculture, health, land-use planning and environmental monitoring. The successful application of newly acquired information to each of these sectors prompted further investment from the European Union for a second phase involving the six border counties in the Republic of Ireland (Fig. 1.13).

The Tellus Border Project was managed jointly by the Geological Survey of Northern Ireland (GSNI) and Geological Survey Ireland (GSI) with academic partnerships in Queen's University Belfast and Dundalk Institute of Technology. Together these institutions successfully applied for a €6 million grant from the INTERREG IVA programme of the European Development Fund (Young, 2016). The second phase (i.e. the Tellus Border Project) was completed on time and within budget (Cowan and Verbruggen, 2016).

Today the Tellus initiative continues in the Republic of Ireland with more than half the country surveyed to date and the remainder planned to be completed by the end of 2023. An equivalent project is also taking place in the UK mainland, beginning with surveys in south-west England which were completed in 2013.

1.4.2 Tellus Data Acquisition

1.4.2.1 Airborne Geophysics

Airborne geophysical surveys can cover vast areas relatively quickly when compared with ground geophysics (e.g. Thomson *et al.,* 2007). However, the properties which can be measured from the air are limited to:

i)   The Earth's magnetic field,

ii)   Electrical conductivity of the upper crust, *and*

iii)   Gamma radiation from rocks and soils at the surface.

Spatial changes in the intensities of these parameters are interpreted as variability within the underlying geological structures. These methods are particularly useful in areas where bedrock is obscured by a covering of superficial deposits, such as glacial till, alluvium or peat (e.g. Ireland). Readings are taken at close regular intervals as the aircraft flies in a network of parallel lines. Positioning and height of the aircraft is measured using on-board GPS and radar altimeter systems respectively. All of the data is recorded digitally before correction, standardisation and ultimately contouring. Although incorporating geophysical data into ever complex methods of data analysis (e.g. machine learning) may aid in better understanding the natural environment (e.g. Rodriguez-Galiano *et al.*, 2015; Zuo, 2017; Kirkwood *et al.*, 2020), these data were not used here as the primary focus is on the relationship between geochemistry and variation in terrain.

1.4.2.2 Geochemistry

Geochemical sampling and analysis of soils, streams and rocks is used routinely in mineral exploration (e.g. Hawkes and Webb, 1963; Govett, 2013; Kyser *et al.*, 2015) but also has wide applications to environmental monitoring and agriculture (e.g. mapping concentrations of both essential nutrients and potentially harmful elements; e.g. White & Zasoski, 1999; Hengl *et al.*, 2017; Russell *et al.*, 2021). A regularly-spaced dataset to an exacting protocol provides a baseline for the current chemical composition of the natural environment against which spatial and temporal changes may be measured (e.g. Young, 2016). Data from the Tellus Border Project (Knights and Glennon, 2013) are utilised here, which includes approximately 7,000 soil, stream water and stream sediment samples from the six Irish counties (Donegal, Sligo, Leitrim, Cavan, Monaghan and Louth) that border Northern Ireland. These samples were taken at a nominal interval of one per every $4km^2$ and were analysed for the concentrations of up to 60 elements and compounds (depending on the material sampled).

1.4.3 Study Area

The bedrock geology of the Border Region is primarily composed of Paleozoic siliciclastic and carbonate sedimentary rocks in low lying areas, and more resistant Caledonian felsic igneous intrusives and Precambrian metamorphic rocks in areas of higher elevation (e.g. County Donegal in the north-west) (Fig. 1.13A/B). Just as elevation and lithology are sometimes related as a result of the relative resistance to weathering of the rocks, together they are also associated with soil type.

Generally, in the border region, upland areas where the dominant geology is igneous or metamorphic, are more concomitant with peaty soils whereas lower lying areas are more closely related to mineral soils (Fig. 1.13C). Ultimately, all of these natural environmental factors inform land-use practices in the border region. Recent maps of such practices shows how closely they are related to the natural ground conditions (Fig. 1.13D). Upland areas are maintained as peatland whereas the mineral soils found overlying sedimentary rocks in the lowland areas, are generally used for agricultural practices (predominantly pastures). The inter-relationships between elevation, bedrock geology, soil type and land-use are reflected in the geochemistry of the soil and water in the region.

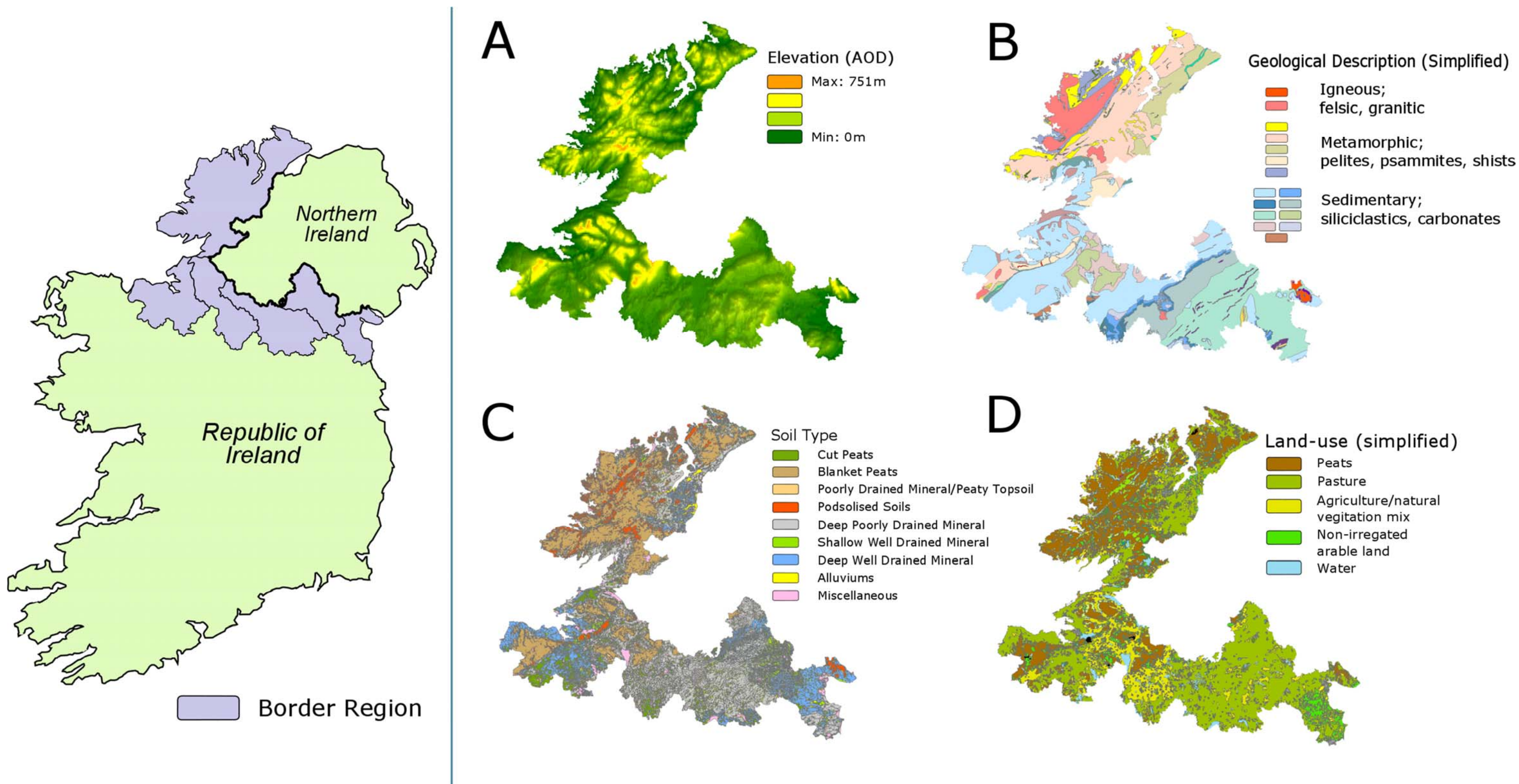**Fig. 1.13:** *(Left) Map showing the location of the Tellus Border Region in Ireland, as defined by Geological Survey Ireland and various State Agencies.(Right) More detailed maps of the Tellus Border Region showing **A)** Elevation (Arc GIS Pro), **B)** Bedrock Geology (Geological Survey Ireland, 2018), **C)** Soil Type (Teagasc, 2014) and **D)** Land-use (Environmental Protection Agency, 2012).*

1.5 Aims and Objectives

The specific aims and objectives of this project are to:

1) Describe and appraise the mathematical importance of Compositional Data Analysis (CoDA) and demonstrate the advantages and disadvantages of a variety of methods within its statistical framework in the context of its application to geochemistry.

2) Assess and determine the optimum procedure for the collection, laboratory analysis and subsequent data analysis of geochemistry samples, particularly water samples.

3) Evaluate the usefulness of CoDA to mineral exploration, environmental monitoring and geochemical mapping, using examples from both Lisheen Mine in County Tipperary and the Tellus Border Region in the northern part of Ireland.

4) Assess the influence of massive-sulphide deposits hosted within Carboniferous (Mississippian) limestone of the Irish midlands on groundwater geochemistry.

5) [With respect to aim/objective (3) above] to take advantage of a unique opportunity to analyse groundwater geochemistry in the area surrounding a significant economic mineral deposit prior to, during and following mining activity.

6) Assess the influence of the physical composition of the natural environmental on the geochemistry of water and soils.

7) [With respect to aim/objective (3) above] to provide primary interpretations of the national geochemical baseline provided by the GSI Tellus Border Region survey.

1.6 Thesis structure

Chapter 2, which follows directly after this, describes some of the methods that are regularly and routinely used for geochemical sample recovery and laboratory analysis. Understanding the limitations of these various methods is essential to informing assumptions when employing the subsequent data analysis which are described in later chapters.

As mentioned previously, the focus of this work is the application of CoDA to a variety of geochemical datasets, particularly groundwater chemistry data. This is highlighted in chapters 3 and 4, wherein CoDA methods are used to better understand the spatial and temporal variation of geochemistry in the area of Lisheen Mine, south-central Ireland. Chapter 3 concerns analysis of water geochemistry data collected before and during mining operations, and Chapter 4 is focussed on post-mine closure datasets.

Chapter 5 concentrates on the capacity of CoDA to inform geochemical mapping over a regionally widespread area (which is not possible with the Lisheen dataset investigated in chapters 3 and 4). To do this, a number of large geochemical datasets from the Tellus border region were analysed and spatially mapped using ArcGIS. Finally, the benefits and drawbacks of applying CoDA to hydrogeochemistry datasets are then discussed in Chapter 6, in the context of the Lisheen and Tellus examples.

Chapter Two: *Methods*

2.1 Overview

The general approaches and methods adopted in geochemistry studies typically consist of three sequential component parts:

i)   Recovery of sample material(s),

ii)   Laboratory analysis, *and*

iii)   Statistical analysis and interpretation of the resulting data

The primary focus of this study is on the third part of this process (iii) – development of strategies for efficiently extracting as much information as possible from any given geochemical dataset. However, when considering data analysis it is essential to understand the assumptions and limitations that have been imposed from the prior sampling and laboratory analysis stages (i-ii), particularly if these have been carried out by a third party. Therefore, all three phases will be discussed here briefly, but the overriding emphasis is on data analysis. This chapter is intended to provide an overview of some of the most common methods in geochemistry and therefore many specific sample recovery, laboratory and data analysis methods are absent as they are beyond the scope of this work.

Approaches to sample recovery are considered, followed by laboratory analysis, and finally, making sense of the results in context is dealt with.

2.2 Sample Material Recovery

The method used to recover a given sample is informed by:

i)   The nature of the material being sampled,

ii)   The properties within the sample that require analysis, *and*

iii)   The specific purpose of the sampling

Various standard procedures can be followed for different material types. For example, the recovery of soil samples may be guided by ISO/TC 190[1] and water samples by ISO/TC 147[2]. Within each of these broad procedures are more specific guidelines depending on the properties of interest. For example, ISO 5664:1984[3] describes the procedure for the determination of ammonia by a distillation and titration method. The purpose of sampling also has a bearing on the methods used. Water sampling, for example, may be approached differently depending on whether the primary interest is ensuring concentrations of elements are below a compliance level or to identify faults within a water treatment process (e.g. European Communities (Drinking Water) (No. 2) Regulations 2007[4]). In any case, understanding safety procedures, quality control and survey design is crucial to preparation prior to field sampling

2.2.1 Safety Procedures

It is essential to note that the first consideration, prior to any sample recovery, is adherence to health and safety procedures. Generally institutions and companies have strict guidelines in this regard. It is considered good practice to complete an appropriate health and safety assessment before embarking on any form of lab or field work. These assessments will cover personal safety equipment, insuring the safety of third parties such as the general public, detailed descriptions of potential hazards and emergency information such as contact details of all involved and distance to nearest hospital (e.g. Gochfeld *et al.,* 2006; Maskall and Stockes, 2008; Tolonen, 2016). Once complete and satisfactory, field and lab work can then commence.

2.2.2 Quality Control

Quality control measures are common to all procedures during sample collection and processing. Selected control samples, separate from those that will inform the resulting dataset, are co-analysed with the intention of assessing the magnitude of errors in the general process of obtaining chemical or physical data. These errors may be systematic and inherent in a method or measurement system, or may randomly occur in independent measurements

---

[1] https://www.iso.org/committee/54328.html

[2] https://www.iso.org/committee/52834.html

[3] https://www.iso.org/standard/11757.html

[4] http://www.irishstatutebook.ie/eli/2007/si/278/made/en/print

(Mueller *et al.*, 2015). In aqueous geochemistry, systematic biases caused by contamination are generally identified through the analysis of *blanks*. These are samples that are prepared with water that is free of measurable constituents. *Spikes* are used to determine the performance of analytical methods and estimate the potential bias due to matrix interference or analyte degradation. Random errors can be identified by using *replicates*. These are two or more additional samples considered identical in composition that are analysed together for comparison.

2.2.3 Survey Design

The design of a geochemical survey will depend on many factors including; geographical area of study site, time and budgetary limitations, spatial variation of ground conditions, avoidance of obvious anthropogenic contamination (unless targeted) and access issues (e.g. Miesch and Barnett, 1976; Fletcher, 1986; Hosseini-Dinani *et al.*, 2019). However, the greatest number of samples at the highest level of spatial consistency possible, under the given constraints, is optimal. Once on site, GPS coordinates for each sample location should be taken and, if possible, accurate elevation readings also. All of these factors will have a direct impact on the spatial analysis of the resulting geochemistry data (e.g. Zhang *et al.*, 2005; Gleeson and Manning, 2008).

2.2.4 Soil and Stream Sediment Sampling

The recovery of soil and stream sediment samples should follow established international standards (e.g. ISO 18400-105:2017[5]; US EPA, 2020a). Some of the geochemistry data used in this research comes from samples collected by Geological Survey Ireland's (GSI) Tellus programme (see Chapter Five), which closely followed these guidelines. Appropriate sample containers often require pre-washing to remove contaminants associated with the manufacturing process. In some cases soil and sediment containers may be reused provided they were not originally used to collect highly contaminated samples and have undergone decontamination cleaning using a sequence of detergents, deionised water and acids (e.g. US EPA, 2020b). New non-powdered disposable gloves should be worn at each sampling location

---

[5] https://www.iso.org/standard/62364.html

or station. Detailed notes about the conditions at the sample site are essential and are generally confirmed by supporting documentary photographic evidence. Samples from different sites are stored separately (e.g. in individual sample bags) and at temperatures that will have a minimal effect in terms of altering the primary geochemical composition.

Soil samples from the GSI Tellus Border Project were collected using hand augers whereas stream sediment samples were wet-sieved. The sampled material was then put into Kraft® paper bags for initial air-drying prior to being transferred to warming cabinets at 30°C to evaporate any remaining moisture. For transport, each sample was placed in a clear outer polybag and stored upright, folded but not sealed. Upon arrival at a trace-level facility which uses no metallic or potentially contaminating apparatus, the samples were freeze-dried and disaggregated by hand using a ceramic mortar and pestle. Subsamples (c. 40g ± 2g) were then taken and agate ball milled so that the final product particle size was <32μm. Cone-and-quartered milled sample splits for the different analytical methods (e.g. XRFS and FA ICPMS for stream sediments and LOI at 450°C, pH by $CaCl_2$, XRFS and ICP_{ar} for soil).

2.2.5 Water Sampling

The geochemistry of water can provide valuable information about the consistency and condition of the natural environment surrounding the sample location (e.g. Benedetti *et al*., 2003; Han and Liu, 2004). However, water samples can be more immediately susceptible than other material (e.g. soil and rock) to contamination as the primary constituent (H_2O) is a 'universal solvent' (Franks, 1973; see also Pohorille and Pratt, 2012). In practice this means that sampling equipment and method must be as close to contaminant-free as possible. This is particularly important when statistically analysing the resulting data, as some methods (e.g. PCA) amplify the effect of small variations in concentration as a result of relative correlation between the various elements and compounds measured. Reducing the potential for contamination begins with selecting an appropriate sample container (generally low density polyethylene) and pre-washing the bottles in acid solutions to remove trace contaminants within the plastic.

2.2.5.1 Bottle Washing Procedure

To ensure that sample containers are as contaminant-free as possible, the following procedure is recommended. It was used in preparation for sample collection in the area surrounding Lisheen Mine (Section 4.3.2). However, this process should be modified depending on the particular nature and requirements of the study in question. Most broader-scale geochemical investigations might not require such a high level of cleaning preparation.

Note: when working with corrosive chemicals such as acids, always ensure appropriate safety precautions are followed.

1. Rinse 60ml low density polyethylene (LDPE) three times with ultrapure water (18.2 MΩ).

2. Fill bottles with ultrapure water and a 1% detergent solution. Shake vigorously and leave to soak for 24 hours.

3. Empty bottle and rinse several times with ultrapure water to remove all traces of detergent.

4. Fill bottles to the lower neck with 40% hydrochloric acid (trace metal grade) solution and leave to soak for one week.

5. Carefully empty the acid solution into an appropriate container for disposal (or recycling if there is another potential laboratory use). Rinse bottles with ultrapure water to remove all traces of acid.

6. Fill bottles to the lower neck with 40% nitric acid (trace metal grade) solution and leave to soak for one week.

7. Carefully empty the acid solution into an appropriate container for safe disposal. Rinse bottles with ultrapure water to remove all traces of acid.

8. Fill bottles to the lower neck with 2% nitric acid (ultra-trace metal grade) solution and leave to soak for 48 hours.

9. Carefully empty the acid solution into an appropriate container for disposal. Rinse the bottles with ultrapure water to remove all traces of acid.

10. Fill the bottles with ultrapure water and store in preparation for sampling.

2.2.5.2 Water Sample Collection Procedure

A highly detailed description of ambient water sampling procedure is given by the US Environmental Protection Agency 'Method 1669' (US EPA, 1996)[6]. In particular this method describes a 'clean hands, dirty hands' procedure whereby one person is responsible for setting up and holding equipment, while another person is solely responsible for making contact with the sample container. This may not be needed in some cases, such as stream water sample collection, as the sampling does not require any additional equipment. However, in the case of recovering groundwater samples, this procedure is recommended.

Stream water samples from the GSI Tellus Border Project were sampled directly using a variety of LDPE bottle sizes. 250ml bottles were used to collect samples for field-based laboratory SEC, pH and total alkalinity analyses. 0.45µm filtered samples were taken into two LDPE bottle sizes; 30ml for NPOC and IC analyses, and 60ml for ICP-MS analysis. The 60ml samples were acidified on the evening of the sampling day with 1% v/v super purity concentrated nitric acid and further acidified with 0.5% v/v super purity hydrochloric acid upon arrival at the laboratory.

Samples taken from groundwater wells in the area around Lisheen Mine (Section 4.3.2) followed this method using the equipment in the schematic below (Fig. 2.1). A peristaltic pump was chosen over other means of recovery as it allows for the 'Low-Flow' method (US EPA, 1996) to be employed. This is based on a theory of minimising hydraulic stress on the aquifer during purging. Water is pumped through at low flow rates to large bottles that hold a multi-parameter probe (YSI in this case). Sampling is initiated, by turning the three-way cell so that flow moves towards collection bottles, once a variety of indicator values (e.g. electrical conductivity, pH, temperature, dissolved oxygen, etc.) stabilise. A second three-way cell can also be installed to take both filtered and unfiltered samples (Fig. 2.1). It is at this point that the samples being recovered are indicative of the characteristics of the local groundwater. This method has the additional benefit of using a 'non-metallic' pumping method as no metal components are ever in contact with the water, which can be the case with other pump types.

However, use of the peristaltic pump method is often limited by the depth to water. At Lisheen it was found that the pump struggled to pull water from depths greater than 8m. In these cases, a bailer is a suggested alternative as the method for sample recovery as it also eliminates metal contact; however, this particular approach makes it more difficult to ascertain when the

---

[6] https://www.epa.gov/sites/production/files/2015-10/documents/method_1669_1996.pdf

indicator parameters have stabilised. Other methods that can be used, depending on access to equipment, include; bladder pumps, submersible centrifugal pumps and inertial pumps (US EPA, 2017).
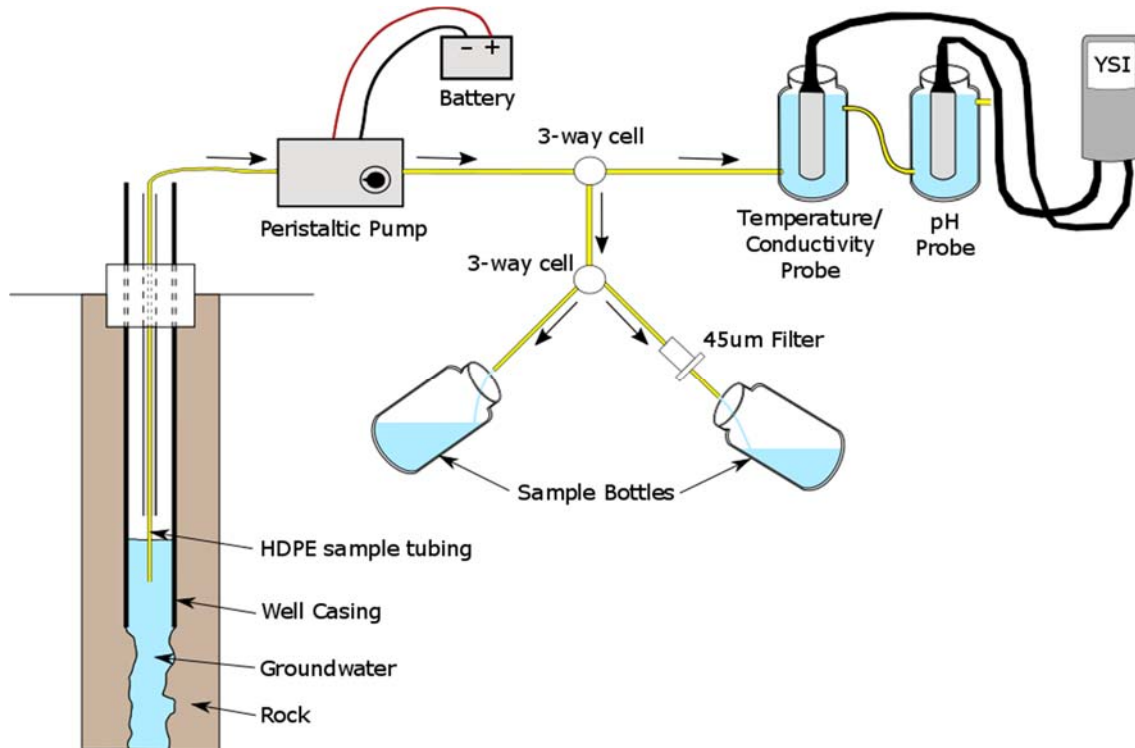

Fig. 2.1: Schematic flow diagram of recommended set-up for groundwater sampling (modified after Henry, 2014). This arrangement was used to acquire samples for the Recent Post-Mining Regional dataset at Lisheen Mine (Section 4.3.2).

2.3 Laboratory Analysis

Laboratory methods of chemical analysis such as Ion Chromatography (IC) and Inductively Coupled Plasma Mass Spectrometry (ICP-MS) are more accurate now than ever (e.g. Guo *et al.*, 2016; Wouters *et al.,* 2017; Meermann and Nischwitz, 2018; Bacon *et al*., 2021). Today ICP-MS is capable of measuring the majority of chemical elements (some by individual isotope) in the periodic table, at accuracies of up to +/- 1 part per trillion (ppt). When ICP-MS is used in combination with IC, to measure various anions (e.g. SO_4^-, Cl^- etc.), and other specialised equipment for some isotopes (e.g. Picarro L2140i for oxygen isotopes), it is possible to get close to a complete set of chemistry data for a given sample. Whether that sample is entirely representative of the particular location where it was taken, however, depends on whether the sampled material has been affected by temporal changes. This is

particularly important with water samples as they are more sensitive to short term environmental changes and therefore require repeated recovery and analysis from the same locations.

Understanding how the methods work, as well as measuring the reliability of the resulting data, can be essential in some studies where small differences in elemental concentrations can greatly alter 'real world' interpretations due to the sensitivity of new data analysis methods (e.g. PCA, machine learning etc.; e.g. see Jolliffe and Cadima, 2016; Zuo, 2017). Therefore, the following is a brief explanation of some of the most common methods used in geochemical sample analysis, some of which were used to obtain the geochemical data for the case studies in this work (detailed in chapters Three and Four).

2.3.1 Inductively Coupled Plasma Mass Spectrometry

Inductively Coupled Plasma Mass Spectrometry (ICP-MS) is the most common and effective method used to detect elements at very low concentrations in a given sample material. The plasma in this process is produced by heating a gas (argon) to high temperature (>6000K) using an electromagnetic coil. This plasma converts the atoms of the elements in the sample to ions, which then enter an electric field and are separated according to their mass/charge (m/z) ratio (Fig. 2.2). The signal intensities are directly proportional to the concentration of the elements in the sample. ICP-MS was used to produce all of the cation concentration data that is statistically analysed in chapters Three and Four.
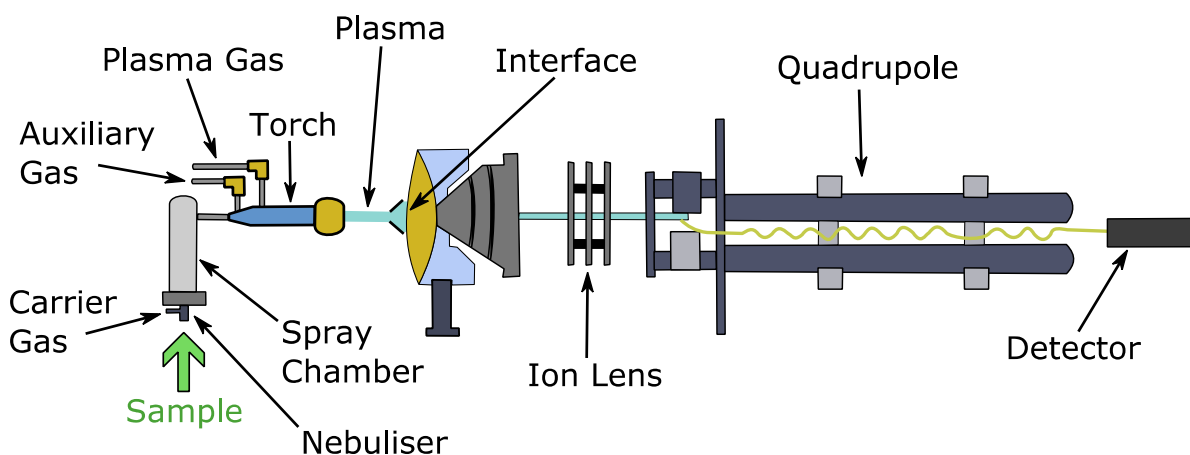

Fig. 2.2: Schematic diagram of a typical Inductively Coupled Plasma Mass Spectrometry (ICP-MS) set-up (modified after http://icpms.ucdavis.edu/ [last accessed 03/05/2021]).

It is recommended that US EPA Method 200.8 (US EPA, 1994)[7] is followed to ensure the ICP-MS instrument is operating accurately and precisely. Firstly, allow the machine time to heat sufficiently (~ 30 minutes). Use a 'tuning solution' (as described by the device manufacturer) to ensure proper signal responses, lens voltages and mass resolution. The instrument is then calibrated using multi-element Standard Reference Materials (SRMs). These SRMs are also used to calculate; Instrument Detection Limits (IDL), Method Detection Limits (MDL) and Linear Dynamic Ranges (LDR), for each analyte.

IDL is three times the standard deviation of ten replicate measurements of a calibration blank. MDL can be calculated by spiking each analyte into reagent water at a concentration of two to five times the IDL and conducting seven replicate analyses of the solution. From this MDL is calculated as:

$$MDL = t \times S \text{ [Equation 2.1]}$$

where t is the t-distribution for 99% confidence level (3.14 for a sample size of 7) and S is the standard deviation. Finally, LDR is determined by running a series of samples of increasing concentration outside the range of the calibration curve, and identifying which concentrations of those analytes fell outside of ±10% of their expected concentration as extrapolated from the calibration curves. Spiked samples and NIST SRMs (e.g. SRM 1643f – trace elements in water) are included in batches of analysed samples in order to maintain a measure of accuracy as analysis occurs.

2.3.2 Ion Chromatography

Ion Chromatography (IC) is a common method used to determine the concentration of a number of important anions within a given water sample (e.g. data in chapters Three and Four), including; sulphate, nitrate, nitrite, chloride, fluoride, bromide and phosphate, to a parts per billion (ppb) range of accuracy (e.g. Morales *et al*., 2000; Jackson, 2001; Szmagara and Krzyszczak, 2019; Höcker *et al*., 2020). This method can only be applied to water samples; however, solid samples (e.g. soils) can be used by first washing out anions and analysing the resulting filtered water. Alternative methods (e.g. X-ray fluorescence) are preferred for solid

---

[7] https://www.epa.gov/esam/epa-method-2008-determination-trace-elements-waters-and-wastes-inductively-coupled-plasma-mass

samples. The IC process works by separating charged molecules based on their respective charged groups.

An appropriate eluent (e.g. dilute solutions of sodium bicarbonate and sodium carbonate with ultrapure water) is prepared and pumped with the sample through the guard column, ion-exchange column and suppressor column before reaching the detector (Fig. 2.3). The guard column removes any larger particles that may potentially damage the ion-exchange column (although the samples should still be filtered at a minimum of 0.45µm before analysis). The ion-exchange column is tightly packed with a stationary adsorbent composed of tiny polymer beads that have positively charged centres. Carbonate and bicarbonate anions coat these beads as the eluent passes through the column.

When the sample enters the column, anions are attracted to the positive bead centres and exchange with the carbonate and bicarbonate ions on the surface. Anions with greater charge are attracted more readily to the beads and heavier anions are slower to move through the column. This results in anions within the sample being separated into bands based on ion type. Finally the sample (now separated) passes through the suppressor column to remove carbonate and bicarbonate ions, resulting in a 'clean' banded sample for the detector to read (Worden, 2005). A more comprehensive description of the process including adaption methods for specific implementations of IC are given by Srinivasan (2017). As with ICP-MS, ensuring the process is working effectively requires testing of standards and calculating detection limits. EPA Method 300.0 (USA EPA, 1993)[8] describes how to use the IC method accurately.

---

[8] https://www.epa.gov/sites/production/files/2015-08/documents/method_300-0_rev_2-1_1993.pdf
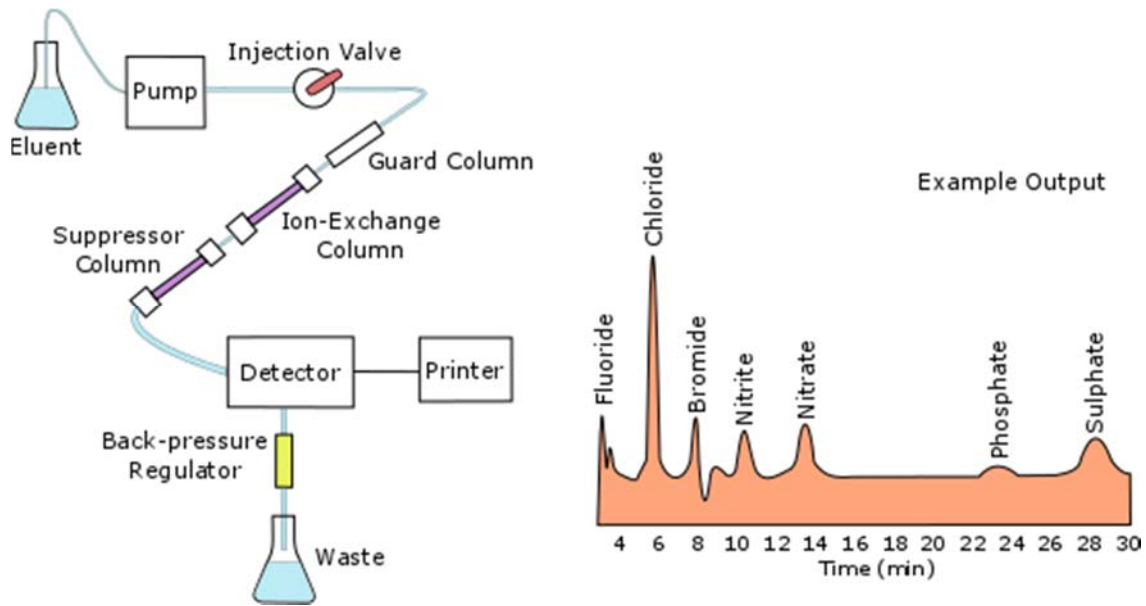
Fig. 2.3: *Schematic diagram of the set-up for Ion Chromatography with an example output (modified after Worden, 2005).*

2.3.3 X-Ray Fluorescence Spectrometry

X-Ray Fluorescence Spectrometry (XRFS) is an established method of geochemical analysis of soil and sediment samples. Exposing these materials to x-rays or gamma-rays causes ionisation as the incoming radiation exceeds the atoms' ionisation energy. This can cause inner electrons to be expelled from the atom, thereby leaving it unstable. Electrons from the outer orbit then fall to fill the gap left by the expelled electron. This falling motion releases energy in the form of a photon with energy equal to the energy difference of the two orbits. Therefore, the difference between the x-ray or gamma-ray energy that is exposed to the sample and the subsequent energy released is characteristic of the atoms present and a measure of the concentration of those atoms.

A common XRFS method is Energy Dispersive Spectrometry (EDS), where a sample is exposed to radiation and the resulting photons are detected and amplified (Fig. 2.4). Wavelength Dispersive Spectrometry (WDS) introduces a crystal into this setup that diffracts the photons before they reach the detector, making it easier to distinguish specific elements of interest. An example of the use of this technology for soil geochemistry analysis is provided by Krishna *et al*., (2007). Both EDS and WDS were used for geochemical analysis of soil and sediment samples from the GSI Tellus Border Region data (Chapter Five).
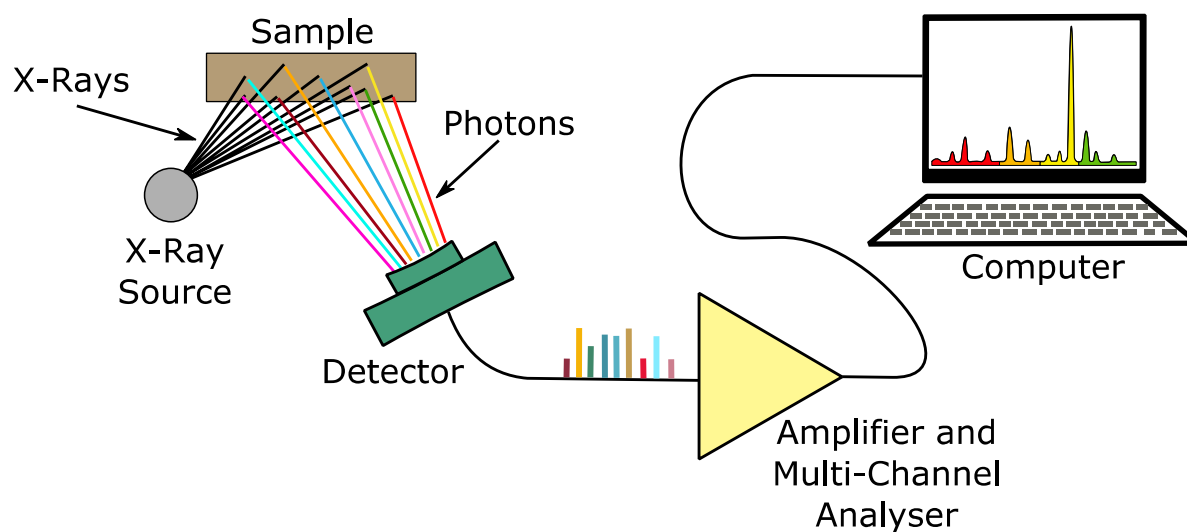
50

2.3.4 Isotope Analysis

Measures of the ratios between individual isotopes of elements can offer additional valuable information to geochemical datasets (e.g. Carucci *et al*., 2012; Birks *et al*., 2019; Newman *et al*., 2021). However, isotopic ratio data is evaluated independently of elemental concentrations as they do not form part of the composition that comprises a given sample. Therefore isotopic data is not investigated as part of this work, but is mentioned here briefly as it can make a significant contribution to the ultimate interpretations of a geochemical study.

Isotopes are atoms of a chemical element with varying numbers of neutrons in their nuclei (and thus have differing atomic masses). They have the same configuration of protons and electrons and the implied mass difference results in small variations in chemical behaviour between different isotopes. The comparative abundance of isotopes from a given element are most easily characterised where difference in isotopic mass is large in proportion to the total atomic mass. Therefore, lighter elements (e.g. hydrogen, carbon, nitrogen, oxygen and sulphur) are traditionally the focus of stable isotope studies (e.g. Hoefs, 1997). Even in these cases, measured variation between isotope concentrations can be subtle and therefore results are reported as deviations from an international standard (e.g. standard mean ocean water [V-SMOW] for hydrogen and oxygen) according to:

$$\delta_{Sample} = (R_{Sample} - R_{Standard})/ R_{Standard} \times 1000‰ \text{ [Equation 2.2]}$$

where R is the isotope ratio (heavy/light) of the sample and standard.

The primary control on hydrogen and oxygen isotopic composition of precipitation is the temperature of the water vapour air mass (e.g. Gat and Gonfiantini, 1981; Araguás-Araguás *et al*., 2000). This can vary with altitude within in a given catchment (Fig. 2.5). Therefore, the isotopic composition of rainfall is indicative of the time and place at which it fell and forms the basis for determining the provenance of natural waters as well as movement and mixing pathways, all of which is the foundation for oxygen isotope hydrology (e.g. Malozewski and Zuber, 1982; Malozewski *et al*., 1983; Clarke and Fritz, 1997; Criss, 1999; Bottrell and Bartlett, 2008).
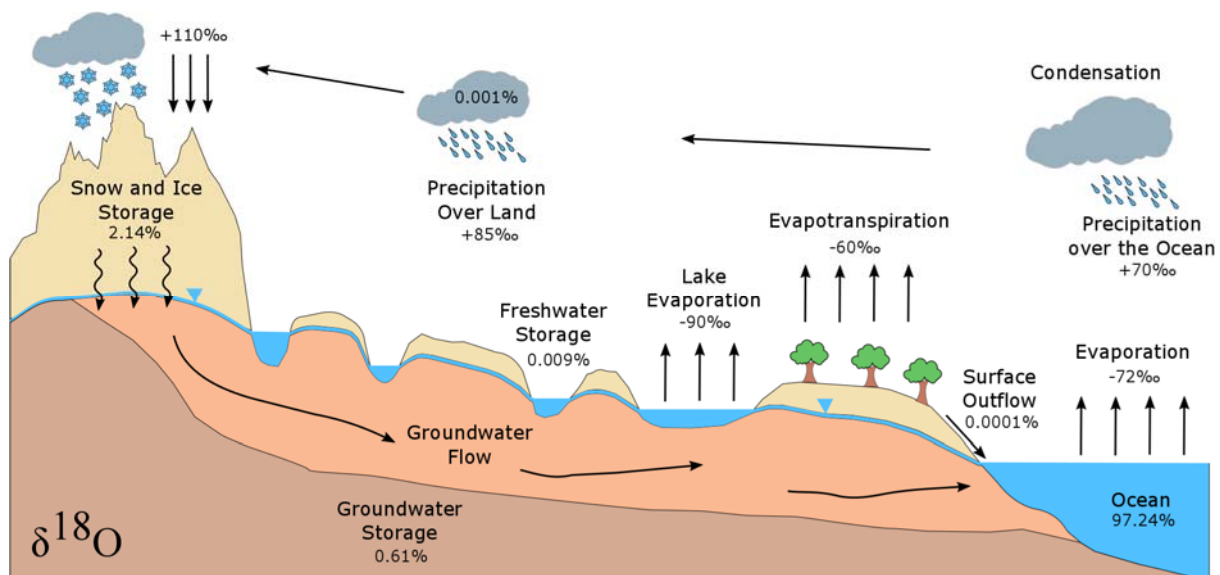
Fig. 2.5: Schematic diagram showing how oxygen isotope ratios can vary in the environment (modified after http://www.hydroisotop.de/areas-of-work/groundwater/ [last accessed 03/05/2021]).

2.3.5 Carbonate and Bicarbonate

Carbonate (CO_3^{2-}) and bicarbonate (HCO_3^-) concentrations in surface water and groundwater samples can provide important data, especially in areas where these anions have a significant influence on ionic balance (e.g. areas with bedrock largely composed of carbonate rocks; e.g. Bruni *et al*., 2002; Lakshmanan *et al*., 2003; Zhi *et al*., 2021). This is also the case at Lisheen Mine and the majority of central Ireland including the central border counties. Traditionally, carbonate and bicarbonate concentrations are calculated in the laboratory by acid-base titration (Fig. 2.6). However, recent technological advances in field-based measuring, such as coupled

ion selective electrodes, have proven to be faster, and as accurate, as titration (Zhan *et al.*, 2016). These methods have the added advantage of instant measurement, therefore avoiding the potential for CO_3^{2-} and HCO_3^- concentration variation during sampling, transport and storage. Titration methods were used to provide carbonate and bicarbonate data for both the Lisheen and Tellus datasets (chapters Three/Four and Five, respectively).
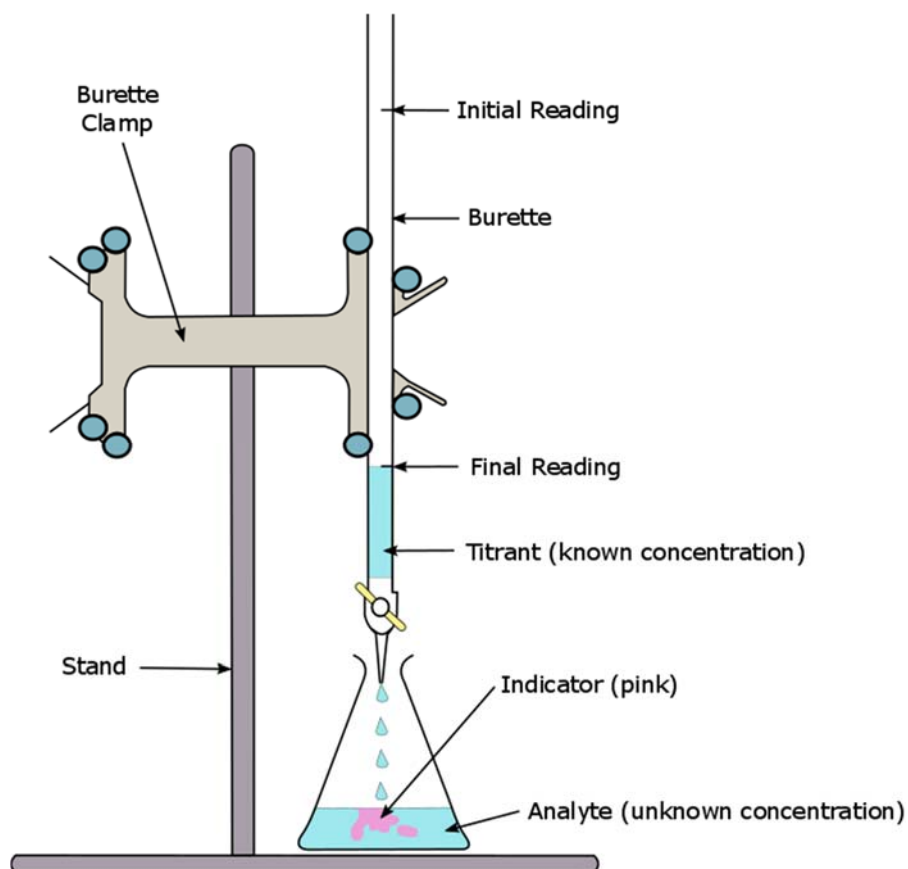
Fig. 2.6: Generic apparatus for acid-base titration (modified after
https://chem.libretexts.org/Courses/University_of_Arkansas_Little_Rock/Chem_1403%3A_General_Chemistry_2/Text/17%
3A_Aqueous_Equilibria/17.03%3A_Acid-Base_Titrations *[last accessed 03/05/2021]).*

2.4 General Data Analysis

While the motivation for the conception of Compositional Data Analysis (CoDA) has been previously introduced in Chapter One, this section offers a more detailed summary of the methods that are used to analyse compositional data. The majority of the methods described herein have been developed from the significant works of John Aitchison (e.g. Aitchison, 1982;

1983; 1985; 1986; 1992), and are considered here in addition to other significant recent developments based upon the summary by Pawlowsky-Glahn and Buccianti (2011). In practice, the theory described below can be implemented on a variety of compositional datasets (e.g. geochemistry datasets) using expert written code packages within the free open-source programming language 'R' and software 'CoDA Pack'.

2.4.1 Log-ratio Transformations

When presented with a compositional dataset (e.g. geochemistry data) the first step of statistical analysis is to log-ratio transform the data. This maintains the important relative information between the variables while also allowing analysis without the constraints of closure (See Section 1.2). There are three methods of transformation, each of which have their own benefits and drawbacks. The first and most computationally simple is the additive log-ratio (*alr*) transformation:

$$alr(x) = \ln\left(\frac{x_1}{x_D}, \frac{x_2}{x_D}, \dots, \frac{x_{D-1}}{x_D}\right)$$ [Equation 2.3]

Although *alr* can work well for analysis where a particular variable is being investigated, it is less effective at exploratory analysis as distances differ depending on the choice of divisor (X_D). It also results in a D-1 matrix (divisor over itself is equal to 1) which is difficult to work with. This issue can be avoided by instead using the geometric mean as the divisor (centre log-ratio transformation, *clr*):

$$clr(z) = \left(\ln\frac{z_1}{\sqrt[D]{\Pi_{j=1}^{D} z_j}}, \dots, \ln\frac{z_D}{\sqrt[D]{\Pi_{j=1}^{D} z_j}}\right)$$ [Equation 2.4]

In order to exploit the well-known properties of Euclidean spaces (e.g. orthonormal basis, coordinate representation, orthogonal projections, definition of angles, ellipses, etc.) for compositional data, the orthonormal bases and corresponding coordinates must first be built for the simplex S^D (see Section 1.2). This is done via the isometric log-ratio transformation (*ilr*) described by Egozcue *et al.* (2003). *Ilr* coordinates can be represented by performing a *Singular Value Decomposition* (SVD) of the *clr*-transformed matrix. However, the resulting log-contrasts are difficult to interpret. Therefore, it is convenient for the analyst to define orthonormal coordinates based on the specifics of the question being asked. For example in

geochemistry, coordinates would be defined on the basis of *a-priori* knowledge of chemical interactions.

A preferred technique of accomplishing this is by using *Sequential Binary Partition* (SBP) of the parts of the composition (Egozcue and Pawlowsky-Glahn, 2005; Thió-Henestrosa *et al.*, 2008). The SBP works by first dividing the variables into two groups indicated by -1 and +1. Each new group is then further subdivided until variables are completely separated. An example of using a SBP to separate a geochemical dataset would be to first begin with grouping anions and cations, followed by further groupings based on known associations (e.g. sodium and chlorine). Using the SBP method the *ilr* coordinates are given by:

$$z_k = \sqrt{\frac{r_k s_k}{r_k + s_k}} \ln \frac{(x_{i_1}, x_{i_1} \dots x_{i_{r_k}})^{\frac{1}{r_k}}}{(x_{j_1}, x_{j_1} \dots x_{j_{s_k}})^{\frac{1}{s_k}}}, \ for \ k = 1, \dots, D-1 \ \text{[Equation 2.5]}$$

where x_i and x_j are constituents coded as + and − and r_k and s_k are the number of constituents coded as + and −, respectively (e.g. Fišerová and Hron, 2011; Shelton *et al.*, 2018).

2.4.2 Dealing with Zeros

Many geochemical datasets contain censored data, of which there are two main types:

i)   Missing data (e.g. due to instrument malfunction) *and*

ii)   Substituted data (i.e. where the detection limit, or some fraction of the detection limit, is replaced, particularly where the concentration of a variable is so low that it exceeds the analytical capabilities of the device)

As a starting point, all censored data should be changed to zero (0), as any other positive value would represent random misinformation. However, one of the problems of the CoDA method is that log transformations fail to operate with zero values. Therefore, any variables or samples with a significant proportion of censored data should be removed entirely (e.g. Blake *et al.*, 2016) and the remaining zeros replaced in some way.

The original approach to this problem was simply to replace all the zeros with a small positive amount less than the detection limit (Aitchison, 1982). Later Fry *et al.* (2000) and Martín-Fernández *et al.* (2003) independently proposed 'in the simplex' approaches. As noted previously, in aqueous geochemistry the presence of zeros is generally as a result of

instrumentation being unable to detect concentrations below a specified detection limit. In these cases, the most appropriate zero replacement technique is using parametric models such as expectation-maximisation (EM) algorithms that are adapted for compositional data.

Palarea-Albaladejo *et al.*, (2007) introduced a modified EM algorithm which first takes an alr-transformed dataset and replaces zeros based on detection limits inputted by the analyst. For example, given a compositional dataset X, the transformed dataset is Y = alr(X). Unknown values within Y can be identified by; $y_{ij} < \ln(\varepsilon_{ij}/x_{iD}) = \psi_{ij}$, where ε_{ij} is the detection limit. Assuming that real random vectors y = alr(x) are distributed according to a (D-1)-dimensional normal distribution with mean $\boldsymbol{\mu}$ and covariance $\boldsymbol{\Sigma}$, then on the tth iteration, the modified E step replaces the values y$_{ij}$ in dataset Y by:

$$y_{ij}^{(t)} = \begin{cases} y_{ij} & if\ y_{ij} \geq \psi_{ij}, \\ E[y_{ij}|y_{i,-j},\ y_{ij} < \psi_{ij}, \mu^{(t)}, \Sigma^{(t)}] & if\ y_{ij} < \psi_{ij}, \end{cases} \text{ [Equation 2.6]}$$

where y$_{i, -j}$ denotes the set of observed variables for the row *i* of the data matrix Y. The expectation here is then given by:

$$E[y_{ij}|y_{i,-j}, y_{ij} < \psi_{ij}] = y_{i,-j}^T \beta_j - \sigma_j \frac{\phi\left(\frac{\psi_{ij} - y_{i,-j}^T \beta_j}{\sigma_j}\right)}{\Phi\left(\frac{\psi_{ij} - y_{i,-j}^T \beta_j}{\sigma_j}\right)}, \text{ [Equation 2.7]}$$

where ϕ and Φ are normal density and distribution functions respectively, σ_j^2 is the conditional variance of variable y$_j$ and β$_j$ denotes the vector of coefficients of the linear regression of y$_{ij}$ on y$_{i,-j}$. The log-ratio EM replacement method described here can be conveniently applied to a compositional dataset using the 'zCompositions' package in R (Palarea-Albaladejo and MartinFernandez, 2015).

2.4.3 Cluster Analysis

2.4.3.1 Hierarchical Clustering

Hierarchical Cluster Analysis (HCA) describes a variety of methods measuring similarity between samples based on a sequence of clustering partitions that can be graphically displayed in a clustering tree called a *dendrogram* (Lance and Williams, 1966). These methods are common for data in Euclidean space and can be adapted to work with compositional data within the simplex by simply first transforming the original data based on the methods described

above (Section 2.4.1). The Lance-Williams algorithm (Equation 2.8) is used to perform HCA with parameters changing depending on the given method. For observations of the ith and j^{th} cluster (which begin with original parts of the composition), clusters are combined via the following:

$$D_{k,i+j} = \alpha_i D_{k,i} + \alpha_j D_{k,j} + \beta D_{i,j} + \gamma |D_{k,i} - D_{k,j}|$$ [Equation 2.8]

The parameters described in the Lance-Williams algorithm (i.e. β and γ) are an efficient way of altering the preferred method of HCA given in the table below (Table 2.1). In particular, Ward's Method is designed to minimise the total within-cluster variance by considering every possible cluster pair at each step and combining the two clusters whose fusion results in a minimum increase of information loss. Therefore, this method is widely used and easily applied to geochemistry data that has been log-ratio transformed. The resulting dendrogram is defined by 'tree cutting' – the number of groups depending on the 'height' of branches as defined by the analyst.

Method	α_i, α_j	β	γ
Single	0.5	0	-0.5
Complete	0.5	0	0.5
Average	0.5	0	0
Centroid	$\dfrac{n_i}{n_i + n_j}$	$\dfrac{n_i n_j}{\left(n_i + n_j\right)^2}$	0
Ward's	$\dfrac{n_i + n_k}{n_i + n_j + n_k}$	$\dfrac{-n_k}{n_i + n_j + n_k}$	0

Table 2.1: *Input parameters for Equation 2.6 depending on the desired clustering method.*

2.4.3.2 K-Means Clustering

One of the most common methods of clustering is via the k-means algorithm. Again, this method can be easily adapted to operate with compositional data by ilr-transforming the original dataset, leaving a D-1 matrix with coordinates; $z_1, . . ., z_n$. At the base of this algorithm

is the calculation of the mean vector, v_k, of a cluster C_k, which is defined as the centroid of the cluster. The components of v_k are calculated by:

$$v_k(\in \mathbb{R}^{D-1}) = \left(\frac{1}{n_{(k)}} \sum_{i=1}^{n_{(k)}} z_{i1}^{(k)}, \ldots, \frac{1}{n_{(k)}} \sum_{i=1}^{n_{(k)}} z_{i,D-1}^{(k)} \right)', \text{ [Equation 2.9]}$$

where $z_i^{(k)} = \left(z_{i1}^{(k)}, \ldots, z_{i,D-1}^{(k)} \right)'$ is the ith observation belonging to the cluster C_k. For each cluster $C_1, \ldots, C_{nc}$ the corresponding cluster means $v_1, \ldots v_{nc}$ are calculated (Filzmoser *et al.*, 2018).

The process of clustering using the k-means algorithm can be summarised in four steps:

1. An initial partition with n_c clusters is selected

2. E-Step: (re)compute the cluster centres using the current cluster membership

3. M-step: Assign each object to the closest cluster centre (i.e. new memberships)

4. Go back to step 2 repeatedly until the cluster memberships and cluster centroids do not change beyond a bound specified by the analyst (termination tolerance)

Essentially the E-step is the fitting step and the M-step is the assignment step. Iterating between the two improves the solution until the cluster assignments stabilise. The algorithm can be found within the base packages in R and can be easily implemented as long as the analyst remembers to first transform the data using the methods described in Section 2.4.1. Some of the conditions of the algorithm can be changed to improve the result depending on the objectives of the given study (e.g. Forgy, 1965; MacQueen, 1967; Hartigan and Wong, 1979).

2.4.3.3 Model-Based Clustering

The primary limitation of the k-means algorithm is that the imputation is based on cluster centres and therefore the resulting clusters tend to be spherically symmetrical, which might not represent the true distribution of the data. Model-based approaches to clustering attempt to solve this issue by adapting the clustering algorithms to take into account the nature of the data. The standard model to do this is multivariate normal distribution representing the distribution of a compositional cluster. As with the other clustering methods described above, model-based clustering can be applied to ilr-transformed compositional data in an R package 'mclust'

(Fraley *et al.*, 2012). A detailed description of model-based clustering can be found in Fraley and Raftery (2002).

2.4.3.4 Fuzzy Clustering

Instead of iteratively separating observations into distinct clusters, fuzzy clustering assigns observations proportionally to all clusters. The primary output sought from fuzzy clustering is the '*membership coefficient*', which is a measure of how related an observation is to a particular cluster. This can be convenient in some studies. For example, in aqueous geochemistry, water is rarely distinctively part of a particular group based on the chemistry but rather a mixture of a number of sources. Like k-means analysis, the results of fuzzy clustering are based on distance to the centre and are therefore spherical which does not take into account the shape of data distribution. Fuzzy clustering can be applied through the R package 'e1071' (Meyer, 2020).

2.4.3.5 Q-Mode Clustering

Q-mode cluster analysis is designed to group sets of variables as opposed to observations that are the focus of the previous clustering methods described here. In geochemistry this would be used to analyse which elements and compounds are likely to be associated in a given sample or across all of the samples. The variation matrix can be used as the basis for measuring dissimilarity between variables of the composition (van den Boogaart and Tolosana-Delgado, 2013; McKinley *et al.*, 2016). The elements of this variation matrix are found via:

$$t_{jk} = var\left[\ln\frac{x_{1j}}{x_{1k}}, \ln\frac{x_{2j}}{x_{2k}}, \ldots, \ln\frac{x_{nj}}{x_{nk}}\right], \text{[Equation 2.10]}$$

where j, k = 1, . . . ,D, and "var" denotes the variance. This method can be applied to a dataset using the R package 'robCompositions' (Templ *et al.*, 2011) and the results displayed on a dendrogam for analysis.

2.4.4 Principal Component Analysis

The primary purpose of Principal Component Analysis (PCA) is to reduce the dimensionality of the input data by constructing new coordinates – principal components (PCs). These PCs

can then either be used to present the data visually, in a way that would be impossible for highly dimensional datasets, or for further statistical analysis. The ultimate aim of PCA is to achieve maximum variability by forming linear combinations of the original variables. There are a number of methods for estimating principal components, however, the discussion here is limited to the Singular Value Decomposition (SVD) method (e.g. Puntanen *et al.*, 2011) and its usefulness for subsequently displaying the resulting components in a '*compositional biplot*'.

Normally Singular Value Decomposition (SVD) is used for reduction of dimensionality. However, when used in conjunction with CoDA, it also provides an ilr-transformation and resulting orthonormal basis. Taking a compositional dataset, the first step is to clr-transform the data (Equation 2.4). The mean value of the clr components are then subtracted. The resulting matrix is then decomposed using SVD:

$$\mathbf{M} = \mathbf{U}\boldsymbol{\Lambda}\mathbf{V}^{\mathbf{T}} \text{ [Equation 2.11]}$$

where $(\cdot)^{\mathrm{T}}$ stands for transpose. The diagonal (D, D)-matrix $\boldsymbol{\Lambda}$ contains the singular values. Starting with the clr data, the last of the singular values must be null. The squares of the singular values add up to the total variance and are variances of the ilr components. Once the column corresponding to the null singular value is removed, two matrices remain:

1. $\mathbf{V}$ (D, D-1) which has columns that are the clr transformation of the elements of an orthonormal basis of the simplex *and*

2. $\mathbf{U}\boldsymbol{\Lambda}$ (n, D-1) which are the ilr coordinates of the centred data with respect to the orthonormal basis of the simplex defined by $\mathbf{V}$ (Pawlowsky-Glahn and Buccianti, 2011)

The Singular Value Decomposition (SVD) biplot (Gabriel, 1971) offers an ideal framework to summarise and display multivariate datasets following adaptation to work within the simplex (Aitchison and Greenacre, 2002). The first orthonormal components, obtained from the process described above, called principal components can be represented in the same plot as the projection of the centred clr-variables. These clr-variables appear as rays from the origin of the plot and are scaled by the singular values so that they have a length proportional to the standard deviation of the variables. The resulting plot offers a graphical display of which combinations of log ratios contain large and small amounts of variability (e.g. see fig. 6 in Blake *et al.*, 2016 and also fig. 5 in Owen *et al.*, 2016).

2.4.5 Independent Component Analysis

Independent Component Analysis (ICA) is a method for maximising the inherent independence of the variables or observations within a given dataset. It is designed for blind source separation, the most common problem of which is often referred to as the '*cocktail party problem*'. This is where the sample (i.e. what someone is hearing at a party) is combined of multiple sound waves from a number of sources (i.e. other people at the party). ICA takes the samples (which are linear combinations of the sources) and utilises the structure of this data to estimate the individual sources (thereby separating each person speaking). In geochemistry the same process can be applied as a sample is a combination of a variety of sources (e.g. Liu *et al.*, 2014; Yang and Cheng, 2015; Kirkwood *et al.,* 2020).

A graphical comparison of the difference between PCA and ICA is provided in Figure 2.7. For gaussian data, PCA (Fig. 2.7A) finds the direction of maximum variability (σ_1) within the data, with the second principal component orthogonal to that (σ_2). In comparison, ICA can be utilised to estimate the maximum variability of each of a number of groups, assuming the data is non-gaussian. In this situation it can be seen that PCA would not provide a good estimation of variability (Fig. 2.7B). As with other statistical methods mentioned in this chapter, there are a number of ways to implement ICA. These methods are well summarised in the context of compositional data in Muehlmann *et al*. (2020).
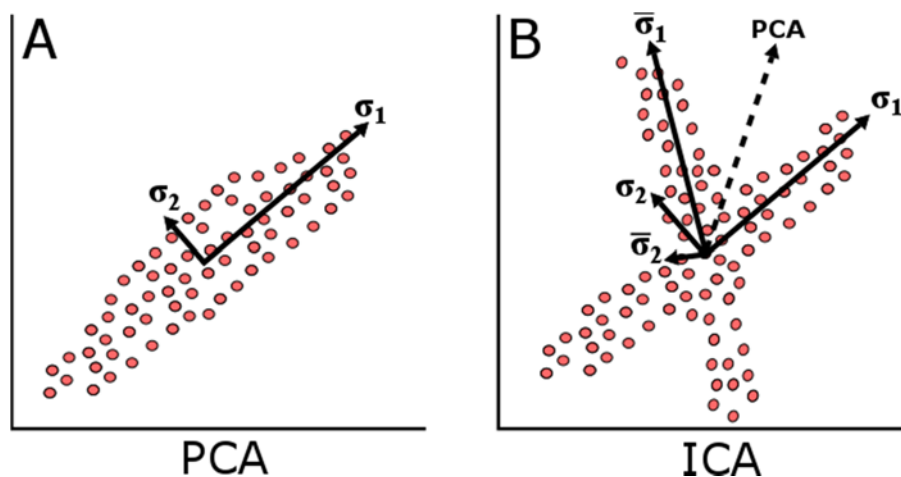

Fig. 2.7: *Simplified graphical comparison of how Principal Component Analysis (PCA) and Independent Component Analysis (ICA) evaluate variability within a dataset.*

2.4.6 Principal/Independent Component Spatial Mapping

The output of the PCA and ICA methods described in the previous two sections (2.3.4 and 2.3.5) are data matrices composed of 'scores' and 'loadings'. The loadings are often the primary focus of both PCA and ICA as they indicate the most important combination of variables within a given dataset. Strong associations between variables can be thought of as groupings and therefore a form of dimension reduction which is described by the loading value of that element for a given component. For example, in geochemistry, if a sample were to have high values (positive or negative non-zero) for sodium and chlorine in the first principal component, then it could be said that this component is representative of the presence of salt in some samples. Scores on the other hand, are values assigned to each sample that indicate the influence of each component. Taking the example mentioned previously of PC1 being influenced by sodium and chloride, if a hypothetical sample then has a relatively high score (this may be positive or negative depending on the transformations) for PC1 then it is likely to be associated with higher variability of salt compared to other samples.

As a score value for each component is assigned to each sample, it is therefore possible to spatially map where a component has most influence. From the example given above, by first looking at the loadings it was possible to deduce that the first component represents the process by which sodium readily offers a free electron to chlorine atoms thereby creating NaCl. By then mapping the scores of the first component, it is possible to see where this process is more prevalent, and therefore negates the need to map the concentrations of sodium and chlorine separately. If the substrate measured for geochemistry was groundwater, it might be the case that high component one values may be closer to the coast where seawater ingress is occurring. This is an example where two variables have been in a sense combined and mapped. Much more complex examples (e.g. the geochemical composition of particular lithologies) can also be mapped in this way (e.g. McKinley *et al.*, 2016; Kirkwood *et al.*, 2020).

2.4.7 Ilr-ion Diagrams

To this point the methods discussed are applicable to most, if not all, geochemistry datasets of sufficient size. However, one particular CoDA method discussed here has been developed specifically for the analysis of water geochemistry data. The Ilr-ion Plot (Shelton *et al.*, 2018) can be thought of as the CoDA equivalent to the ubiquitous Piper diagram. Developed 77 years

ago (at the time of writing), the Piper Diagram (Piper, 1944) has extensively been used for water chemistry type classification (e.g. Jeong, 2001), examining the hydrochemical evolution of natural waters (e.g. Cloutier *et al.*, 2008) and to describe the chemical composition of water in a particular hydrologic setting (e.g. Shekhar and Sarkar, 2013). This plot compares the relative influence of major ions within a sample on a multiple-trilinear diagram (Fig. 2.8A). Here the concentrations are converted to milliequivalents and then normalised to 100%. The three parts of the Piper are aligned in such a way that the ratio of alkali-earths ($Ca^{2+} + Mg^{2+}$) to alkalis ($Na^+ + K^+$) and the ratio of weak acids ($HCO_3^- + CO_3^{2-}$) to strong acids ($Cl^- + SO_4^{2-}$) are projected into the central diamond-shaped field (Fig. 2.8A).

However, the Piper method has some inherent limitations, including difficulty in distinguishing water types when similar chemistries are involved. By applying CoDA methods to the basic principles of the Piper Plot, Shelton *et al.* (2018) has thus strengthened the original classification method. The ilr ion plot is constructed using the same elements converted to milliequivalents (Ca^{2+}, Mg^{2+}, Na^+, K^+, HCO_3^-, CO_3^{2-}, Cl^-, SO_4^{2-}). This data is then isometric log-ratio transformed (Equation 2.5) using the Sequential Binary Partition (SBP) method (Egozcue and Pawlowsky-Glahn, 2005). For the Ilr-ion plot the SBP used is summarised in Table 2.2. The resulting transformed data is then plotted on a four-part bilinear diagram (Fig. 2.8B). The example shown here (Fig. 2.8) is described in greater detail in Section 4.3.1.
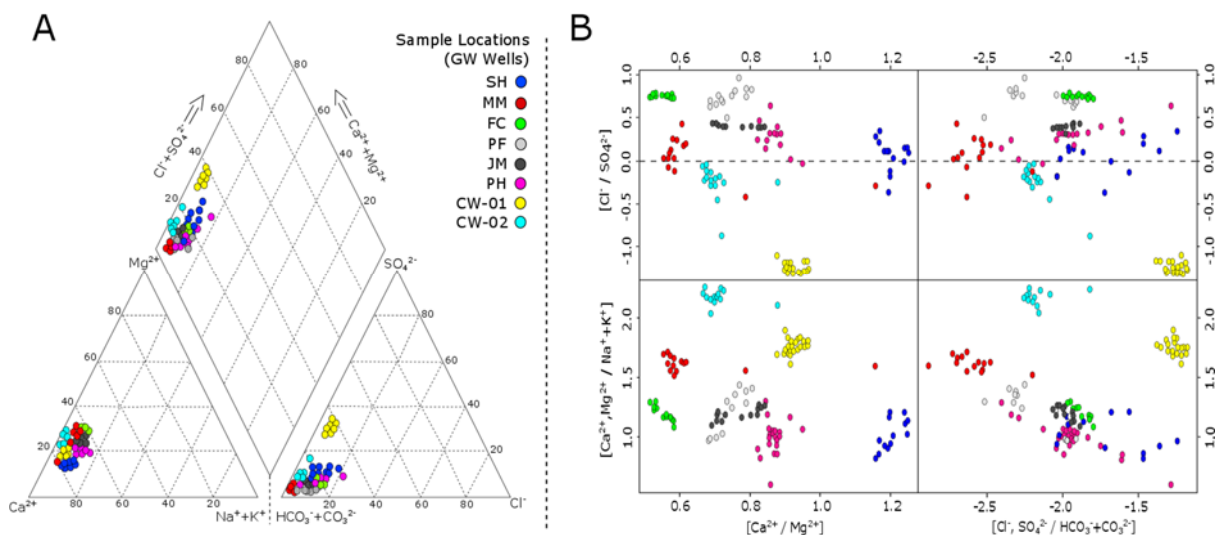

Fig. 2.8: (A) Example dataset plotted on a Piper Diagram. (B) The same dataset plotted using an ilr-ion plot.

	Na + K	Ca	Mg	Cl	HCO$_3$ + CO$_3$	SO$_4$
Z_0	+	+	+	-	-	-
Z_1	-	+	+			
Z_2		+	-			
Z_3				-	+	-
Z_4				+		-

Table 2.2: Sequential Binary Partition (SBP) used by Shelton et al. (2018) for isometric log-ratio transformation (Equation 2.5) to produce the ilr-ion plot (e.g. Fig. 2.8B).

2.5 Specific Data Analysis

Much of the theory involved in the application of compositional data analysis methods are described in the above section (2.4). The specifics of how a variety of these methods were applied to the data in the following 'results' chapters (Three, Four and Five, below) are discussed here. In particular, the data preparation procedures and CoDA methods implemented on the Lisheen and GSI Tellus Border datasets are described in detail.

2.5.1 Data Preparation

The methods of data preparation for all datasets presented in the following chapters were all largely the same. The first step involved amalgamating the available data into a single digital database. This is particularly pertinent for the older Lisheen Mine geochemical data from the 1990s which was provided on paper with individual sample sites on separate pages (Chapter Three). The process of transcribing this data into a digital format may have introduced an element of human error where these datasets are concerned. However, the more recent data from Lisheen and the GSI Tellus Border Project were provided in Microsoft Excel format. While these are an improvement, they are also not impervious to human error.

The next step is to replace the missing data of major anions and cations with an arithmetic average value of that analyte at a particular location. This only applies where multiple samples have been taken from the same location. Replacing major elements with the mean is necessary because these components are the most important for making reasonable interpretations about the broader geochemical system. An alternative is to remove that particular sample from the dataset entirely. However, this also removes a significant amount of 'good data' within the other analytes measured and, as such, should be avoided as much as possible.

Following the replacement of missing data (or removal of samples with missing data), the next phase of data preparation is to deal with values that are recorded as below a certain limit of detection, or *censored* data (see previous Section 2.4.2). This type of data is often recorded for many minor geochemical elements (e.g. rare earth elements) where a given method of analysis (e.g. ICP-MS) cannot accurately measure below a concentration determined by the method (e.g. < 1ppb). In order for many forms of statistical analysis to work, including CoDA, these values need to be converted to real numbers.

Several authors (e.g. Farnham *et al.,* 2002; Güler *et al*., 2002; Raiber *et al.,* 2012) discuss the ways in which censored data can impact multivariate analyses. Güler *et al*. (2002) refer to a number of approaches that can be taken to address censored data (variations on taking a percentage of the lower limit of detection). Raiber *et al.* (2012) suggested that values reported as being below the detection limit should be replaced with a value equal to the detection limit. Two methods were used for the Lisheen datasets:

i)   Replacing these values with half of the detection limit (Güler *et al*., 2012), *and*

ii)   Using the expectation-maximisation (EM) algorithms within the '*zCompositions*' package in R (Palarea-Albaladejo and MartinFernandez, 2015)

Both methods resulted in similar outcomes. This is most likely because CoDA methods rely on the relative comparison of the parts within a composition and the measured values (that did not need to be replaced) were an order of magnitude larger than the replaced value, regardless of replacement method. For consistency, variables that consisted of more than 30% *censored* values were removed entirely and the EM method was used to impute missing data for the remaining variables (as per the recommendations of Blake *et al*., 2018) for all datasets prior to multivariate statistical analyses.

The GSI Tellus Border datasets required the addition of categorical information was not pre-present. Using 'Arc GIS Pro' (version 2.7.3), the geochemistry samples (appearing as three sets of points on a map) were superimposed on soil type (Teagasc, 2014), bedrock geology (Geological Survey Ireland, 2018) and land-use (Environmental Protection Agency, 2012) maps. Using the 'Intersect' tool within the 'Arc Toolbox' the categorical information from each of these maps was added to each dataset so that every sample point had a corresponding soil type, bedrock geology and land-use classification for that specific location.

It should be noted that the inaccuracies included in the categorical maps as a result of mapping methods and data intervals have been inherited by the new dataset and therefore misclassification is possible in some cases. Additionally, in the case of the stream water dataset, it should also be noted that these categories only represent the conditions at the sample point despite the high possibility of water flowing through other terrains prior to sampling.

2.5.2 Undertaking Compositional Data Analysis (CoDA)

Aitchison's (1986) centred log-ratio (*clr*) transformation approach and Egozcue *et al.*'s (2003) isometric log-ratio (*ilr*) approach were both used on the Lisheen datasets (chapters Three and Four), while only the *clr* method was utilised for the Tellus datasets (Chapter Five), following appropriate replacement of non-detect and zero values. The *clr* and *ilr* transformations are defined above by equations 2.4 and 2.5, respectively.

As previously mentioned (Section 2.4.1), data transformed by the isometric log-ratio (ilr) approach first requires a sequential binary partition (SBP) matrix to be defined. In the specific cases where this method was applied to the Lisheen datasets, the SBP described by Table 2.2 (above) was used.

The log-ratio transformations were completed using dedicated R code packages, in particular 'robCompositions' (Templ *et al.*, 2011) and the software package 'CoDA Pack' (Version 2.01). The Piper diagram and ilr-ion plots were created using the methods and R code from Shelton *et al.* (2018). Correlation and cluster analysis (e.g. Pearson correlation, Spearman rank correlation and hierarchical clustering) were completed using a combination of R code (Templ *et al.*, 2011) and methods described by Filzmoser *et al.* (2018).

2.6 Summary

Several methods of geochemical data analysis are sensitive to minor variations between the variables that compose datasets, especially PCA. Therefore, it is important to understand how these datasets are produced and the inherent inaccuracies and assumptions that may affect how representative the resulting data is, in the context of the material being sampled and evaluated. Some common sampling and laboratory analyses methods have been briefly described in this chapter in order to provide a background to where the data originates before the proceeding data analysis methods are described. The fundamental point is that the rigour of the sampling recovery and analysis methods is extremely important given the sensitivity of the data analysis methods to subtle value differences in variable concentrations. The entire recovery, analysis, and statistical investigation of the given sample should be considered as something of a processing continuum. In the following chapter, these methods of data analysis have been applied to a number of groundwater geochemistry datasets from the area around Lisheen Mine in County Tipperary, Ireland.

Chapter Three: *Groundwater Geochemistry at Lisheen A*

[Prior to, and during underground Pb/Zn mining]

3.1 Introduction

This chapter focuses on the application of various statistical analyses to extensive groundwater chemistry datasets from Lisheen Mine in County Tipperary. The data was collected at different phases of initial exploration, mine development and operation, and temporally spans almost two decades (from 1991 to 2009). The mine was a very significant producer of lead and zinc ore when it was operating and a full introduction to the site has already presented in Chapter One. This present chapter provides a broad context to the setting and operation of Lisheen Mine from a hydrogeochemical perspective during the early and middle phases of the life of the mine.

3.2 Data Overview

The geochemistry of groundwater in the Lisheen area has been monitored by a variety of stakeholders, at numerous phases of exploration and mining from the early 1990s up to the present (2021). However, only groundwater sampled and analysed prior to and during active mining operations is examined in this chapter. The methods of data preparation and analysis followed the procedure outlined in Section 2.5. These datasets (see Wheeler, 2021 for data availability) are divided into three chronological groups:

A. Pre-Mining Regional

A number of wells at Lisheen, both locally owned and drilled for exploration purposes, had groundwater sampled and geochemically analysed prior to the discovery of the massive sulphide deposit. An independent contractor (RPS Cairns Ltd.) was tasked with sampling and analysis to establish a regional groundwater geochemistry baseline. Between September 1991 and November 1992 a total of 145 samples were analysed from 77 individual locations. Some of these locations were only sampled once and some

were sampled up to three times. The analytes measured include: suspended solids, colour, pH, electrical conductivity, temperature, hardness, dissolved oxygen, alkalinity, NH_3, NO_2, NO_3, PO_4, SO_4, Cl, Na, K, Ca, Mg, Fe, Mn, As, Pb, Cu, Zn, Cd.

B. Early Mining Regional

Around the time that underground mining commenced in 1999, a number of locations in the Lisheen area were sampled for groundwater geochemistry. Between March and June 1999, 51 individual samples from discrete locations were recovered for analysis. This data set includes the measures of the following analytes: F, Cl, NO_2, NO_3, P, SO_4, Li, Na, NH_4, K, Ca, Mg, Al, As, Ba, Cd, Co, Cr, Cu, Fe, Mn, Ni, Pb, Zn.

C. Mine Workings

During the primary phases of underground mining at Lisheen (1999-2009), approximately 883 individual samples were recovered from a variety of discrete locations where groundwater was inflowing to the mine workings. These samples were analysed at an on-site facility for the following: pH, conductivity, dissolved oxygen, temperature, chemical oxygen demand, suspended solids, turbidity, alkalinity, F, Cl, NO_2, NO_3, P, SO_4, Li, Na, NH_4, Ca, Mg, K, Al, As, Ba, Cd, Co, Cr, Cu, Fe, Mn, Ni, Pb, Zn.

3.3 Results and Discussion

3.3.1 Pre-Mining Regional Dataset (A)

3.3.1.1 Overview

The pre-mining regional groundwater geochemistry dataset (September 1991 to November 1992) from Lisheen consists of 145 individual samples from 77 locations. However, some of these samples were missing coordinate information and therefore had to be removed. For simplicity of analysis, and as a result of limited repeat data, the arithmetic mean was taken for locations that were sampled multiple times. It is assumed that the temporal variation of geochemistry within the groundwater is limited and therefore the average is representative of

the sample site. Following the calculation of arithmetic means and the removal of samples missing coordinate data, a dataset of 69 samples remains (Fig. 3.1).

As this data precedes the discovery of the Pb/Zn massive-sulphide deposit at Lisheen, it has been analysed here from a mineral exploration perspective. In particular, groundwater wells have been grouped based on their distance to (what would subsequently be recognised as) the main ore zone. The specific location these distances are measured to is at 219353166593 in Irish National Grid (TM65), which is directly above the southern margin of the Main Zone (see Fig. 1.10). Of course, there are other considerations besides distance, for example groundwater flow direction, elevation of the well and the depth to groundwater, variation in lithology and structure. However, for a new exploration site much of this information is not known and therefore the aim of this section is to determine whether CoDA can aid in the exploration process by identifying geochemical anomalies associated with economic mineralisation.
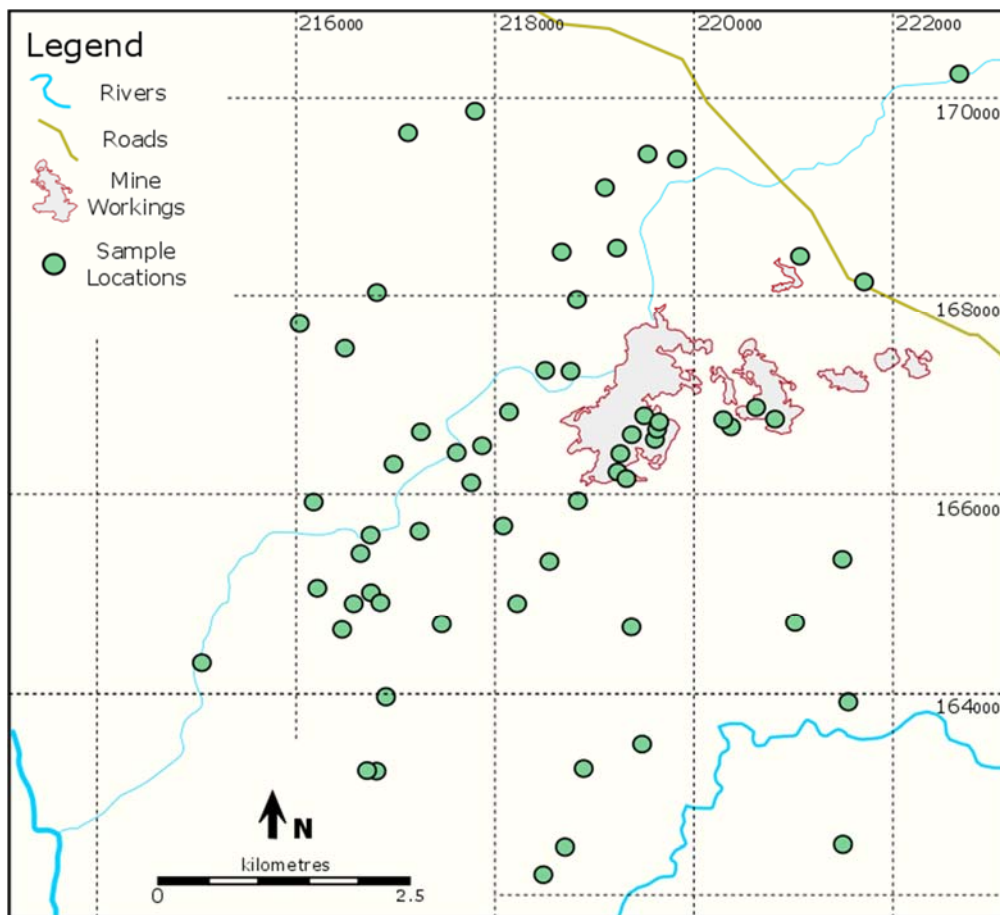

Fig. 3.1: *Geographic map showing the location of sample sites (green filled circles) for the Lisheen Pre-Mining Regional dataset (A) (coordinates are in Irish Grid 1965).*

3.3.1.2 Parameters

The summary statistics table (Table 3.1) provides a general overview of the available data for the Pre-Mining Regional Dataset (A). The maximum values for each analyte highlight cases where variables are significantly higher than the mean, while the standard deviation offers insight as to the extent to which there is variance from the mean. The standard deviation is particularly high for Fe, Mn and Zn (Table 3.1). The Irish/EU groundwater quality threshold values (Irish Statutory Instrument 9 of 2010 - European Communities Environmental Objectives (Groundwater) Regulations 2010)[9] that, when exceeded, indicate a need for further investigation due to the potential effect on drinking water sources, are also provided. Lower threshold values (e.g. arsenic and cadmium) generally indicate higher toxicity. The number of samples (out of a total of 145) that exceed these limits is also given for each relevant variable.

The groundwater threshold limits described in Table 3.1 are based on 75% of the drinking water standards as they are designed to highlight potential contamination that is then investigated under the regulatory framework (S.I. 9/2010)[1]. Samples with variables in excess of the threshold values do not necessarily indicate that groundwater at that location is an unsuitable source of drinking water. Furthermore, some of these samples are taken from exploration wells that, in some cases, make contact with localised mineralisation in the bedrock, thereby providing a chemical signature that is not representative of the majority of groundwater regionally. Some important variables, in the context of groundwater chemistry, are discussed further here:

pH

The majority of samples are slightly alkaline (mean 7.28), which is entirely expected given the Mississippian carbonate host rocks (see Section 1.3.5). However, there are extremes of quite acidic (minimum 5.3) and alkaline (maximum 9.3) water occurrences. Relatively acidic groundwater often occurs close to significant mineral deposits as a result of sulphides (e.g. pyrite) being exposed to water and oxygen (e.g. Akcil and Koldas, 2006). More alkaline water may be sourced from areas that experience less recharge, thereby allowing a greater opportunity for continued ion-exchange reactions between groundwater and carbonate bedrock (e.g. Güler *et al.,* 2017).

---

[9] http://www.irishstatutebook.ie/eli/2010/si/9/made/en/pdf

Variable	Unit	Detection Limit	Max	Mean (arithmetic)	IQR	Standard Deviation	EU Limit (ground-water)	No. of samples above threshold
pH			9.3	7.327586	0	0.438508		
EC	µS/cm		1573	613.9167	299	317.4863	1875	
Temp	°C		15	10.82986	-0.3	1.24491		
NH₃	mg/l	0.01	9.4	0.612844	0	1.0717		
NO₂	mg/l	0.1	1.2	0.232308	0.2	0.181273	0.375	15
NO₃	mg/l	0.1	17	4.784173	-0.3	3.761904	37.5	0
PO₄	mg/l	0.01	11	0.448495	-0.2	1.133442		
HCO₃	mg/l		492	235.269	362	156.0199		
SO₄	mg/l		475	27.97379	25	44.06605	187.5	1
Cl	mg/l		166	34.20833	0	21.38945	187.5	0
Na	mg/l		272	19.68828	23	31.3299		
K	mg/l		193	10.41448	0.3	19.52869		
Ca	mg/l		175	91.30496	57	49.84145		
Mg	mg/l		51	23.09908	-14	9.657767		
Fe	mg/l	0.01	2.419	0.126697	0.21975	0.332629		
Mn	mg/l	0.01	0.942	0.161975	0.12425	0.215799		
As	mg/l	0.001	0.061	0.007397	0.0036	0.01183	0.0075	7
Pb	mg/l	0.0005	0.173	0.023413	0.140173	0.04243	0.01875	15
Cu	mg/l	0.0001	0.076	0.007867	0.0062	0.010657	1.5	0
Zn	mg/l	0.005	0.546	0.050354	0.087	0.081327		
Cd	mg/l	0.0001	0.00138	0.000365	0.00013	0.0003	0.00375	0

Table 3.1 *Data summary table showing the maximum, mean, interquartile range and standard deviation of each analyte for water samples in the Pre-Mining Regional Dataset (A) at Lisheen. European Communities Environmental Objectives (Groundwater) Regulations 2010 Threshold limits (mg/l) are also provided for comparison.*

Temperature (Temp)

In Ireland groundwater temperature generally ranges from 9.5 to 10.5°C (Aldwell and Burdon, 1980). Temperature values within this dataset have a mean of 10.5°C, a minimum value of 7.7°C and a maximum of 15°C. If temperatures above 12°C are considered to be thermal (e.g. Blake *et al*., 2016) then at least some of the groundwater

at Lisheen may be mixing with deeper thermal water, potentially via extensive localised faulting in the bedrock which serves to facilitate fluid movement (see Section 1.3.5.2).

Electrical Conductivity (EC)

The electrical conductivity of water is a measure of its ability to conduct an electrical current. This parameter acts as a generalised proxy for hardness and total dissolved content of water samples. The groundwater threshold value for electrical conductivity is 1875μS/cm and is not exceeded within this dataset, suggesting that the sampled water does not contain high levels of dissolved constituents.

Anions

Bicarbonate (HCO_3^-) is the dominant anion. However, many samples show significantly elevated sulphate (SO_4^{2-}) levels owing to mineral dissolution associated with the Lisheen ore deposit. In almost all cases anions were measured below threshold values (Table 3.1), with the exception of nitrite (NO_2^-) which exceeded the threshold in 15 samples.

Cations

The dominant cations within this dataset are calcium (Ca^{2+}) and to a lesser extent magnesium (Mg^{2+}), due to the dissolution of prevalent limestone and dolostone (see Section 1.3.5). Other cations such as; iron (Fe^{2+}), manganese (Mn^{2+}), zinc (Zn^{2+}), lead (Pb^{2+}) and arsenic (As^{3+}), have particularly high concentrations in some samples. This is most likely explained by the dissolution of sulphide minerals that often contain these components, for example: pyrite [FeS], sphalerite [(Zn,Fe)S], galena [PbS] and arsenopyrite [FeAsS]. A significant number of samples exceed groundwater threshold values for Pb and As (21 and 9 samples, respectively).

3.3.1.3 Piper and ilr-ion Plots

As described previously in Section 2.4.7, one method developed specifically for the analysis of water chemistry data is the Ilr-ion plot (Shelton *et al*., 2018) which is a CoDA version of the Piper diagram (Piper, 1944). The more traditional Piper method is used here for basic characterisation of the water type. With the exception of approximately six outliers, the majority of the samples are clustered in the Ca-HCO$_3$ area with the slight influence of Mg in the bottom-left trilinear plot (Fig. 3.2A). The 'Ca-Mg-HCO$_3$' water type is expected in groundwater extracted from limestone-dolostone aquifers, such as those present in the Mississippian carbonate bedrock at Lisheen (see Section 1.3.5). By isometric log-ratio transforming the same data and plotting it using the methods described in Shelton *et al.* (2018), it is possible to further distinguish between individual samples (Fig. 3.2B). As mentioned above, samples have been grouped based on their distance to the centre of the largest known orebody (which had not been discovered at the time of sampling). It would appear that groundwater samples from closer to the deposit tend to have lower Ca/Mg ratios. However, there is no clear differentiation of water-type groups among the samples.
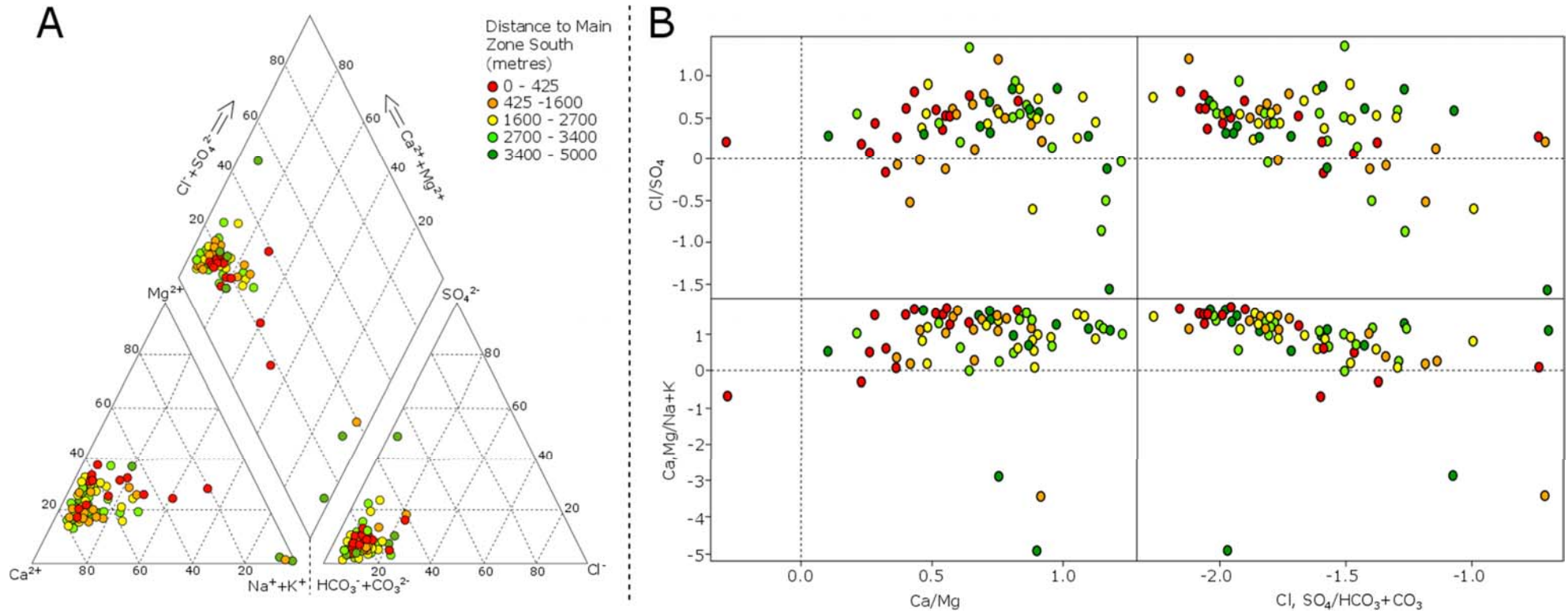
Fig. 3.2: A) *Traditional Piper diagram of the Pre-Mining Regional Dataset (A) from Lisheen, **B)** Ilr-ion plot of the same data in A (method from Shelton et al., 2018).*

3.3.1.4 Cluster Analysis

Cluster analysis affords a deeper insight into the geochemical interrelationships between the full range of elements than is possible with Piper and Ilr-ion plots. The robust CoDA approach of using 'pivot coordinates' (a type of isometric log-ratio transformation), to obtain Pearson/Spearman Rank correlation values and conduct hierarchical cluster analysis dendrograms is described in detail by Filzmoser *et al.* (2018). When these methods are applied to the Pre-Mining Regional Dataset (A) from Lisheen, graphical representations of the relationships between a variety of elements and compounds are revealed (Figs. 3.3 and 3.4).

In the case of Spearman Rank Correlation (Fig. 3.3), some variables displaying apparently strong connections that are of interest are:

- Ca and Mg
- Fe, Mn and As
- Na and Cl
- Pb and Cd

As discussed above with respect to the Ilr-ion plot, the relationship between Ca and Mg is likely the result of the prevalence of dolomitised limestone in the wider Lisheen area. Na and Cl are regularly correlated in water chemistry due to the tendency of sodium atoms providing electrons for chlorine atoms. The connection between Fe and Mn, and to a slightly lesser extent As, may suggest that, in at least some of the wells, the groundwater has experienced anoxic conditions, thereby allowing for the ready dissolution of these elements via redox reactions involving minerals such as pyrite and arsenopyrite. There also appears to be a relatively strong relationship between Pb and Cd. This is most likely as a result of dissolution of minerals associated with the massive-sulphide deposit, in this case galena and cadmium enriched sphalerite (Torremans *et al*., 2018).

Similar connections between particular variables are reflected in a robust Hierarchical Cluster Analysis (Fig. 3.4), again generated using CoDA methods. Small variations of the majority of elements and compounds (NH_3, NO_2, NO_3, SO_4, Mg, HCO_3, Ca, Cl, Na) are reflective of background groundwater geochemistry. PO_4 has been separated from this group because it is not present in the majority of samples and has low variation within the samples where it is actually present. Zn, K and Cu appear to also be grouped, possibly owing to the proportionally higher mobility of these elements in groundwater in comparison to many other variables. The final elemental connections (e.g. Fe, Mn, As and Pb, Cd) are similar to those found from the Spearman Rand correlation discussed above.
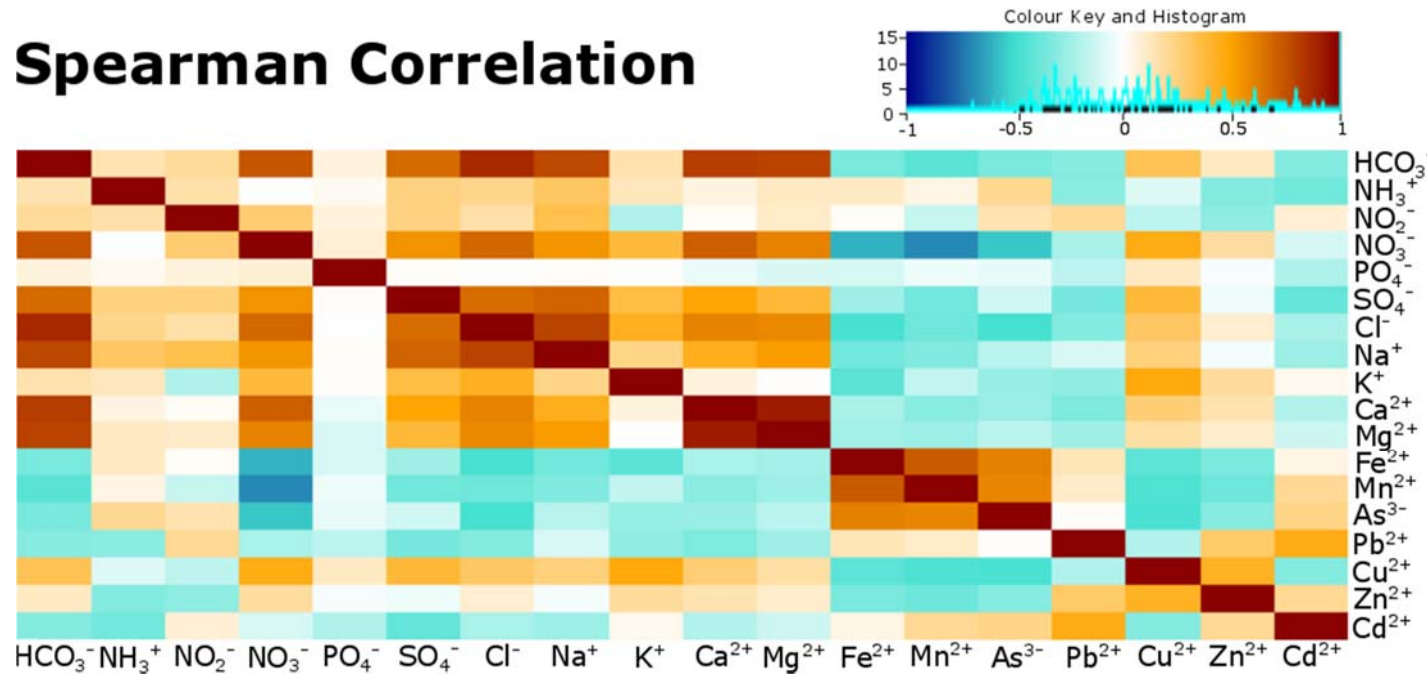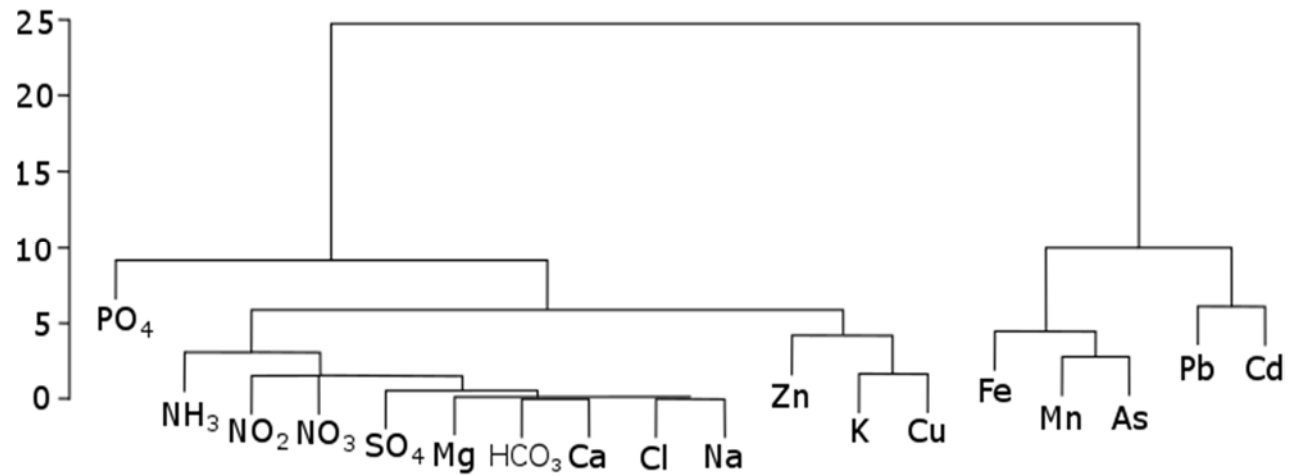
Fig. 3.3: (Left) Visual representation of the results of a Spearman Correlation of Pre-Mining Regional Dataset (A) from Lisheen (darker orange and reds indicate higher correlation).

Fig. 3.4: (Right) Hierarchical cluster analysis dendrogram of Pre-Mining Regional Dataset (A) from Lisheen.

3.3.1.5 CoDA Bi-plot

A variety of terminology is often used when interpreting CoDA bi-plots. As discussed previously in Section 2.4.4, a compositional bi-plot is a multidimensional display of the principal components that define a dataset. When printed, generally only two axes are visible (e.g. the 1st and 2nd principal components are represented by the X- and Y-axis respectively). The coordinate space is populated with data that has resulted from the log-ratio transformation and subsequent Singular Value Decomposition (SVD) of the original dataset. Sample locations appear as discrete points (defined by the values of the principal components displayed). These are often referred to as '*observations*'. The variables (which, in geochemistry, are the elements and compounds), appear as rays from the origin (shown in red throughout this work). These variables can sometimes be referred to as '*rays*' or '*vectors*'. For the sake of simplicity, when interpreting the bi-plot, specific variables are referred to by the name of the element or compound that they represent, despite the fact that they are actually log-ratio transformations of the original concentrations.

The bi-plot (Fig. 3.5) of the Pre-Mining Regional Dataset (A) from Lisheen shows that a large proportion of the samples are positive on the first principal component and located close to the origin, indicating low variability between the components that make up these samples. In particular, the bottom right section of the plot shows that numerous samples are associated with low variability of PO_4, SO_4, HCO_3, Cl, K, Mg, Na, and Ca. Generally, with groundwater geochemistry bi-plots, samples that are associated with low variability of a large number of components are representative of local background groundwater chemistry. Slightly stronger variables on the 1st principal component are NO_3 and Cu, indicating that higher concentrations of nitrate and copper are present in some samples. A number of samples are also defined by higher variations of Zn.

Observations with negative scores for the 1st principal component can be separated into two groups:

i)   Samples associated with Mn, Fe and As, *and*

ii)   Samples associated with Pb and Cd

The first group (bottom left of the bi-plot in Fig. 3.5) are likely to contain samples associated with low oxygen reducing conditions that encourages ion exchange reactions. The other group, with high relative variability of Pb and Cd, are likely indicative of groundwater that has been

in contact with minerals associated with the local massive sulphide deposit (e.g. sphalerite and galena). This is supported by the fact that samples in this group are located closer geographically (red and orange) to the (now) known main lode of the Lisheen ore deposit. When the 1st principal component score values are spatially mapped (Fig. 3.6) it is clear that high negative values are associated with the presence of the Lisheen deposit and that there is likely significant crossover between the two aforementioned groups as a result of samples being characterised by both of these geochemical processes simultaneously.
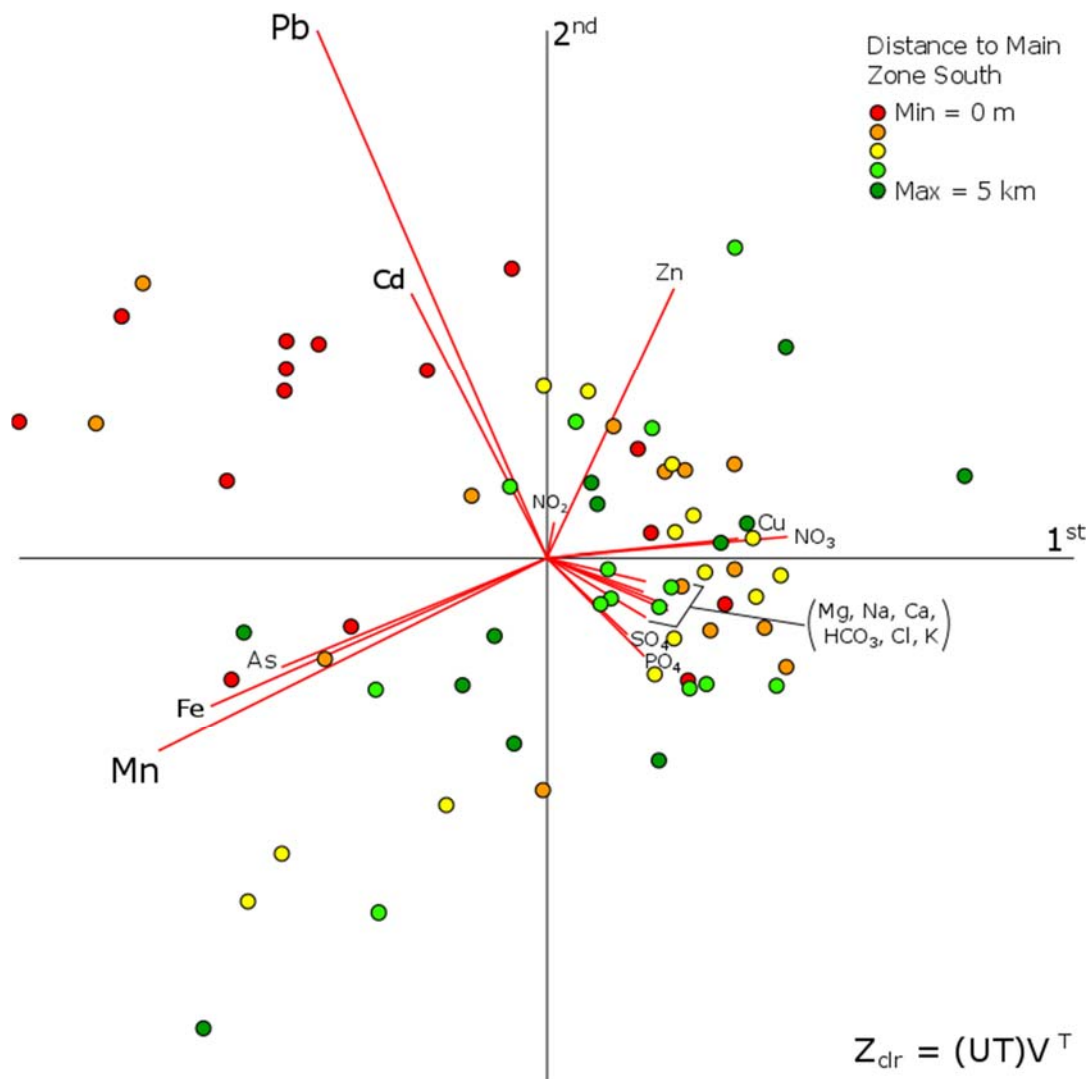
Fig. 3.5: *CoDA bi-plot (created using 'CoDA Pack' [Version 2.01]) of Pre-Mining Regional Dataset (A) from Lisheen.*
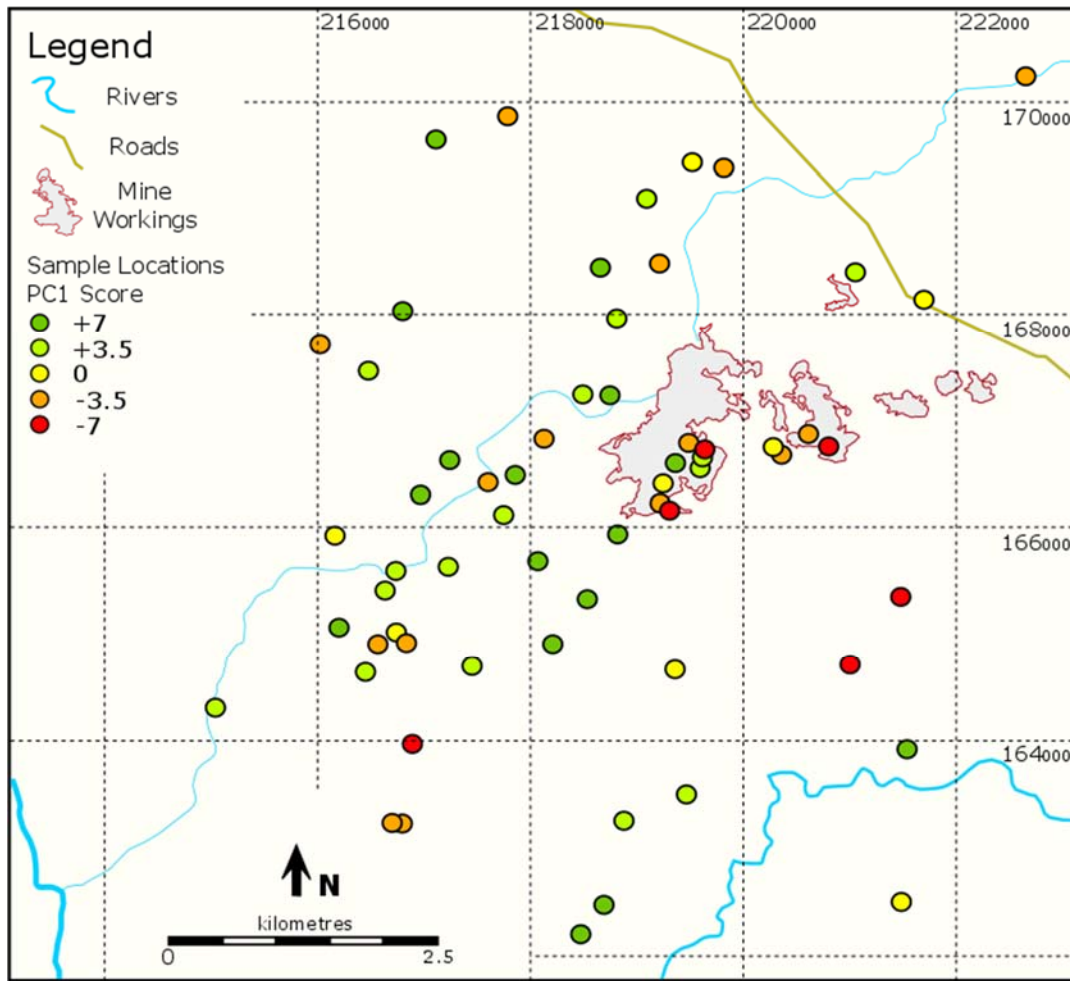
Fig. 3.6: Geographic map of the area around Lisheen showing the locations of the Pre-Mining Regional dataset sample sites, colour coded by PC1 score. See Figure 3.5 for key for colour-filled circles denoting the various sample locations.

3.3.1.6 Summary

The Pre-Mining Regional dataset (A) provides the best insight into the chemical composition of the groundwater at Lisheen prior to the discovery of the economically significant Pb/Zn deposit. With the exception of a few outliers, the groundwater at Lisheen can be broadly characterised as Ca-Mg-HCO$_3$ type. This classification is logical, and to a certain extent expected, considering the Mississippian carbonate host rocks and presence of significant dolomitisation along the Rathdowney Trend (Wilkinson and Hitzman, 2015; see Chapter 1, Figs. 1.2 and 1.8 etc.).

Taking distance to the (now known) main focal point of the ore deposit as a categorical factor for ilr-ion analysis (Fig. 3.2B), there appears to be some correlation between low Ca/Mg ratios and samples closer to the mineralisation, indicating that dolomitisation of limestone becomes

less intensive with distance from the ore deposit. It is likely that this distance measurement is acting as a proxy for distance to the geological structures related to both dolomitisation and economic mineralisation (i.e. reactivated deep-seated normal faults; e.g. see Fig. 1.11).

Spearman Rank correlative analysis highlights some elements and compounds that may be inter-related in the groundwater. In particular, there appears to be a correlation between Fe, Mn and As. This 3-part relationship is common in sub-oxic to anoxic groundwaters where redox conditions lead to the dissolution of iron, manganese and arsenic bearing minerals, such as arsenopyrite [FeAsS] or manganite [MnO(OH)]. There is also a correlation between Pb and Cd, which may be the result of the dissolution massive-sulphide minerals such as sphalerite [(Zn,Fe)S], a phenomenon commonly associated with cadmium impurities, and Galena [PbS] (Tauson *et al.*, 2005).

Hierarchical cluster analysis shows similar variable groupings to the Spearman Rank correlation (i.e. Fe-Mn-As and Pb-Cd; Fig. 3.4). It also highlights a connection between Zn, Cu and K which is fainter in the Spearman method. This grouping is possibly due to propensity of the cations of these elements to form salts through the creation of chelated and complex connections, potentially making them more mobile in groundwater than other elements.

The compositional bi-plot (Fig. 3.5), also shows similar elemental groupings, but can additionally provide an indication of the level of variation (by the length of the vectors) and which samples (observations) are influenced by a particular group. In this case, a large number of samples are characterised by low variation of many elements and compounds, indicating background groundwater geochemistry. Samples closer to the deposit are most commonly related with the Pb-Cd grouping, which suggests that these elements are the most effective vectors to mineralisation at Lisheen. However, both Pb and Cd variation is not spatially extensive and is only common in wells directly above the deposit or down hydraulic gradient (to the south; see Fig. 3.6). If an additional objective was to identify which wells had groundwater that was influenced by sub-oxic to anoxic conditions, it would be possible to do this. These are the samples close to the Fe, Mn and As vectors on the lower-right of the bi-plot (Fig. 3.5).

3.3.2 Early-Mining Regional Dataset (B)

3.3.2.1 Overview

The groundwater sampling locations for the Early-Mining Regional dataset (March to June 1999) is shown in Figure 3.7. Key compounds missing from this particular dataset are carbonate and bicarbonate. This limits the level of geochemical analysis possible, considering bicarbonate is a major anion in groundwater that has had significant contact with carbonate bedrock (e.g. at Lisheen). However, this dataset still affords an opportunity to observe the condition of the groundwater in the Lisheen region during the early phases of mineral extraction. It should also be noted that there is no information on what this water was being used for (e.g. drinking or agricultural applications) and samples were taken directly from the groundwater well and therefore might enter filtration systems in many cases.
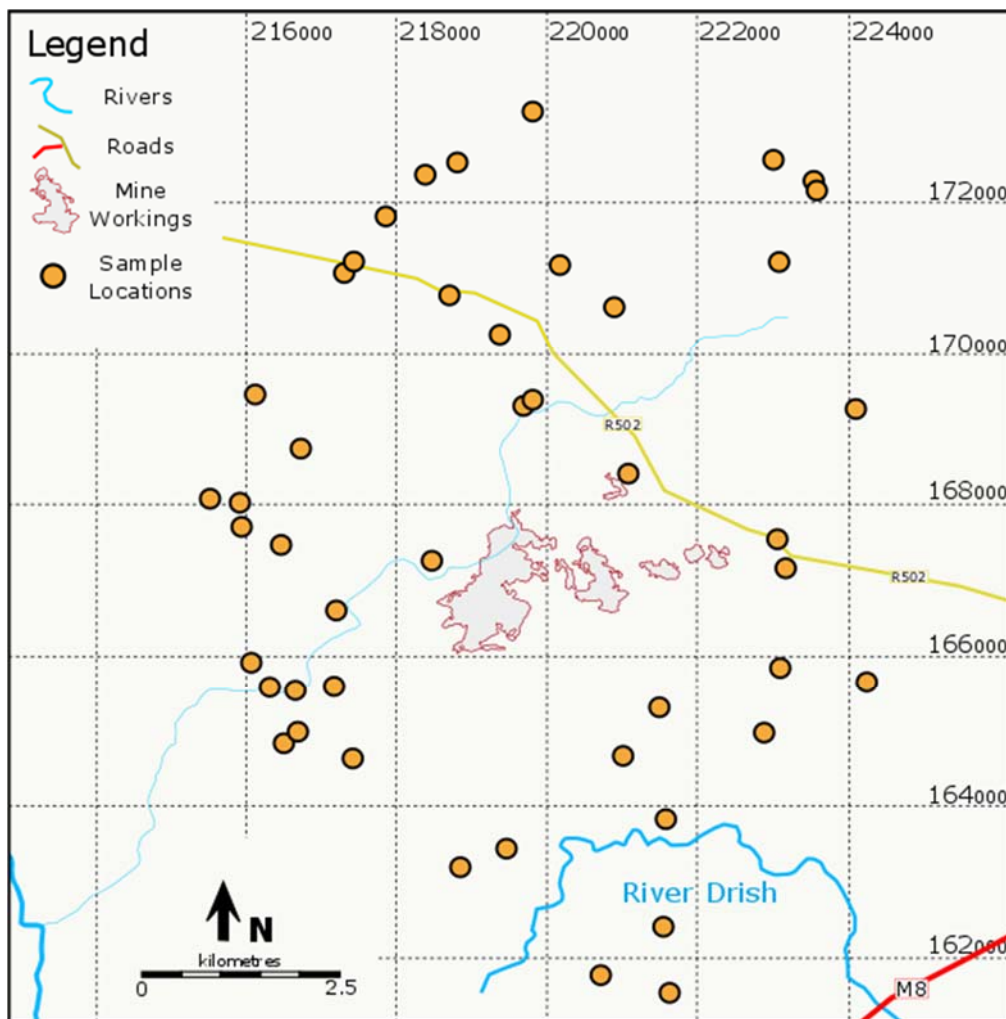

Fig. 3.7: Geographic map of the Lisheen area showing the location of sampling sites (orange filled circles) for the Early-Mining Regional dataset (B).

3.3.2.2 Parameters

The summary statistics table (Table 3.2) provides a general overview of the available data for the Early-Mining Regional Dataset (B). General parameters (e.g. pH, electrical conductivity, temperature) and bicarbonate (HCO_3) values are not available for this dataset. Chemical analytes are again compared to Irish/EU groundwater quality threshold values (S.I. 9 of 2010)[10] and the number of samples that exceed these limits (out of a total of 51) are noted (Table 3.2). As mentioned previously (Section 3.3.1.2), samples with variables in excess of the threshold values do not necessarily indicate that groundwater at that location is an unsuitable source of drinking water. All of the samples within the Early-Mining Regional Dataset (B) were recovered from privately owned domestic and agricultural wells. Therefore, the chemical signatures of deep groundwater are not well reflected within the data.

Anions

Other datasets from Lisheen (e.g. datasets A, C and D) show that bicarbonate (HCO_3^-) is the dominant anion in all samples. Therefore, despite the absence of HCO_3^- concentration data, it is reasonable to assume that this is also the case for the Early-Mining Regional Dataset (B). Chloride (Cl^-) and Sulphate (SO_4^{2-}) have the highest values from the available anion data and fall within similar ranges for most samples (means of 29.7 and 22.7 mg/l, respectively). Nitrite (NO_2^-) concentrations exceed the groundwater threshold values in 4 of the 51 samples. This may be due to groundwater contamination from agricultural practices such as the spreading of fertiliser (e.g. Brink, 1975; Parris, 2011).

Cations

The dominant cation in this dataset is calcium (Ca^{2+}) with a mean concentration value of 59.65 mg/l (Table 3.2), followed by magnesium (Mg^{2+}) and sodium (Na^+) which have mean values of 12.55 and 12.42 mg/l, respectively. As discussed in relation to the previous Lisheen dataset (A), the dominance of calcium and the influence of magnesium on groundwater in Lisheen is expected for groundwater that is sourced from

---

[10] http://www.irishstatutebook.ie/eli/2010/si/9/made/en/pdf

limestone-dolostone aquifers (see previous Section 1.3.5). Some sample sites contain groundwater with elevated concentrations of iron (Fe^{2+}) and manganese (Mn^{2+}), highlighting the role of sulphide oxidation at these locations. This is discussed further in Section 3.5.2.5 below. 31 of the 51 samples analysed have arsenic (As^{3+}) concentrations above groundwater threshold values (Table 3.2). The dissolution of arsenopyrite [FeAsS] which is prevalent within the massive sulphides associated with the Lisheen deposit (e.g. Hitzman *et al*., 2002; Torremans *et al*., 2018), is the most likely cause of elevated arsenic levels in these particular samples. Nickel bearing pyrites may also be the source of high nickel (Ni^{2+}) values in 5 of the samples (Table 3.2).

Variable	Unit	Detection Limit	Max	Mean (arithmetic)	IQR	Standard deviation	EU Limit (ground-water)	No. of samples above threshold
SO_4	mg/l		220.80	22.70	12.70	29.19	187.5	1
Cl	mg/l		99.20	29.70	15.20	22.45	187.5	0
NO_3	mg/l		73.70	7.23	5.80	10.04	37.5	1
NO_2	mg/l	0.01	2.60	0.64	0.48	0.81	0.375	4
NH_4	mg/l	0.01	1.96	0.18	0.08	0.41	0.18	4
F	mg/l	0.01	0.97	0.13	0.07	0.13		
P	mg/l	0.01	0.35	0.08	0.06	0.10	0.04	6
Ca	mg/l		221.80	59.65	95.91	58.10		
K	mg/l	0.01	0.18	0.087	0.1	0.06		
Na	mg/l		104.50	12.42	6.69	14.60		
Mg	mg/l	0.01	34.90	12.55	20.51	11.90		
Fe	mg/l	0.0002	4.76	0.44	0.15	1.01		
Ba	mg/l	0.001	1.26	0.24	0.15	0.24		
Mn	mg/l	0.00004	1.05	0.09	0.03	0.21		
Zn	mg/l	0.0002	0.76	0.06	0.03	0.14		
Cu	mg/l	0.0005	0.67	0.04	0.02	0.10	1.5	0
Al	mg/l	0.0007	0.18	0.02	0.02	0.04	0.15	1
Ni	mg/l	0.001	0.16	0.02	0.01	0.03	0.02	5
Li	mg/l	0.01	0.07	0.05	0.02	0.01		
Co	mg/l	0.001	0.04	0.00	0.00	0.01		
As	mg/l	0.0065	0.03	0.02	0.01	0.01	0.0075	31
Pb	mg/l	0.002	0.008	0.004	0.001	0.001	0.01875	0
Cr	mg/l	0.0003	0.0019	0.0010	0.0005	0.0004	0.0375	0
Cd	mg/l	0.0003	0.0009	0.0004	0.0001	0.0002	0.00375	0

Table 3.2: Data summary table showing the maximum, mean, interquartile range and standard deviation of each analyte for water samples in the Early-Mining Regional Dataset (B) at Lisheen. European Communities Environmental Objectives (Groundwater) Regulations 2010 Threshold limits (mg/l) are also provided for comparison.

3.3.2.3 Simplified Ilr-ion Analysis

Due to the lack of carbonate concentration data, a simplified version of the CoDA Ilr-ion plot that is described and used in the previous section (e.g. see Fig. 3.2B), is employed here for Lisheen dataset B (Fig. 3.8). From this plot, it is clear that samples can be divided into two broad groupings based on the ratios of major cations (Ca^{2+}, Mg^{2+}, Na^+ and K^+). When these groups are spatially mapped (Fig. 3.9), a possible relationship between the proportion of major cations and regional dolomitisation becomes apparent, considering regional groundwater flow is broadly north-west to south-east directed. The presence of a more distinct group (circled in red in Fig. 3.8) are as a consequence of much lower Ca/Mg ratios, where magnesium exceeds calcium concentrations. It is unclear whether this is the result of significant groundwater contact with dolomitised zones along NE-SW trending structures. Elevated sodium and potassium values with respect to the rest of the dataset may suggest groundwater at these sampling points has mixed with water sourced from a lithologically distinct aquifer.

Although CoDA methods used with the Early-Mining Regional dataset (B) show interesting relationships between major cation ratios and the presence of secondary mineralised limestones (Figs. 3.8-3.9), it does not offer any additional information from an environmental monitoring perspective. The statistically unprocessed raw concentration data (Table 3.1) indicates that the early phase of mining at Lisheen did not immediately affect the regional groundwater chemistry.
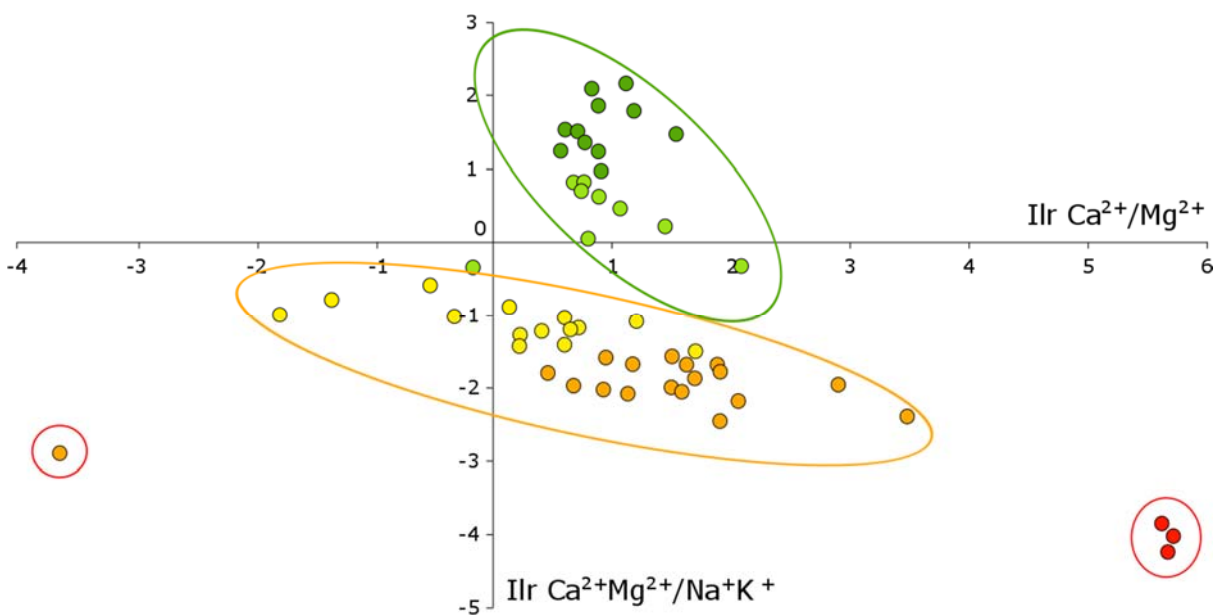

Fig. 3.8: *Simplified Ilr-ion plot of Early-Mining Regional Dataset (B) from Lisheen with points coloured based on y-value. Two distinct groupings are circled in green and orange and a Ca/Mg cluster in red.*
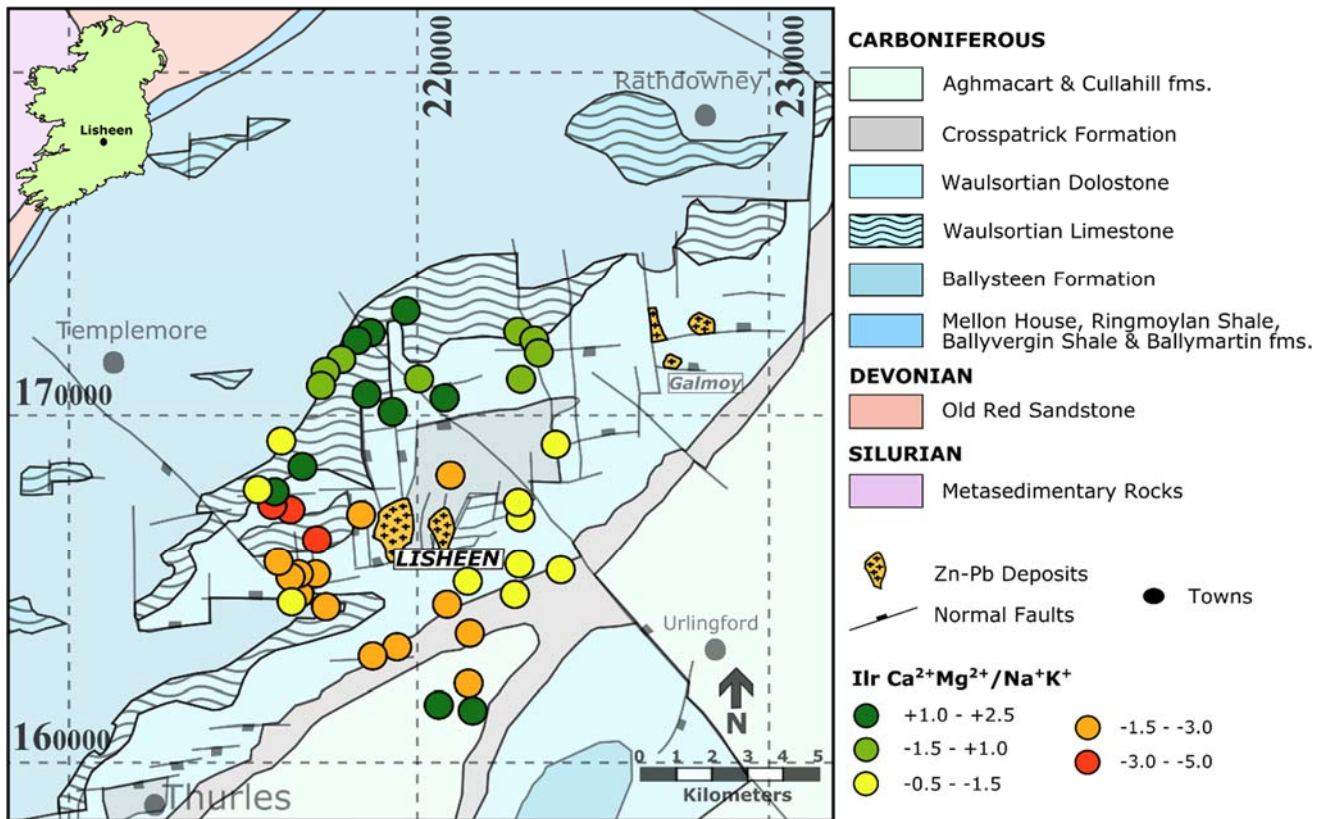
Fig. 3.9: *General geological map of the Lisheen region showing the sampling points for the Early-Mining Regional Dataset (B). The sample locations shown here are colour coded similar to Figure 3.8*

3.3.2.4 CoDA Bi-plot

As demonstrated in the previous section (Pre-Mining Regional Dataset A), the CoDA bi-plot is a powerful tool for the analysis of aqueous geochemistry data in the Early-Mining Regional Dataset. The bi-plot method is used again here (Fig. 3.10) to facilitate a better understanding of geochemical variation within the groundwater of the area. Sample wells are, again, characterised (coloured) based on their distance to the geographic point (219353166593) directly above the southern margin of the main ore zone. The 1st (x-axis) and 2nd (y-axis) principal component represent 31% and 17% of the total variance, respectively. However, interpreting this graphical representation of the data is more complex than analysing how the vectors and observations are related to each particular axis.

Small variations of a large number of elements and compounds are present in the top-right sector of the bi-plot (Fig. 3.10). As noted previously, this can be generally interpreted as representing the background chemistry of the groundwater samples. Positive values on the second principal component (y-axis, a.k.a. PC2) are primarily defined by large relative variations of NO_2, K, NH_4 and Al. Therefore, observations with high positive values of PC2

relative to the others may contain groundwater that has been influenced by agricultural contamination, as these elements are common ingredients in, or bi-products of, many fertilisers (Brink, 1975; Parris, 2011). Negative values of PC1 in the extreme left of the bi-plot (Fig. 3.10) are defined more by variations of Fe and Mn. As discussed in the previous section these wells may contain groundwater that has experienced sub-oxic to anoxic conditions that stimulate redox reactions. The bottom right sector of the bi-plot shows the vectors SO_4, Cu, F, Ca, Zn and particularly Mg. High relative Mg is more than likely accounted for by the presence of highly dolomitised limestone, while SO_4 and Zn are from groundwater potentially in direct contact with the main mineral deposit.
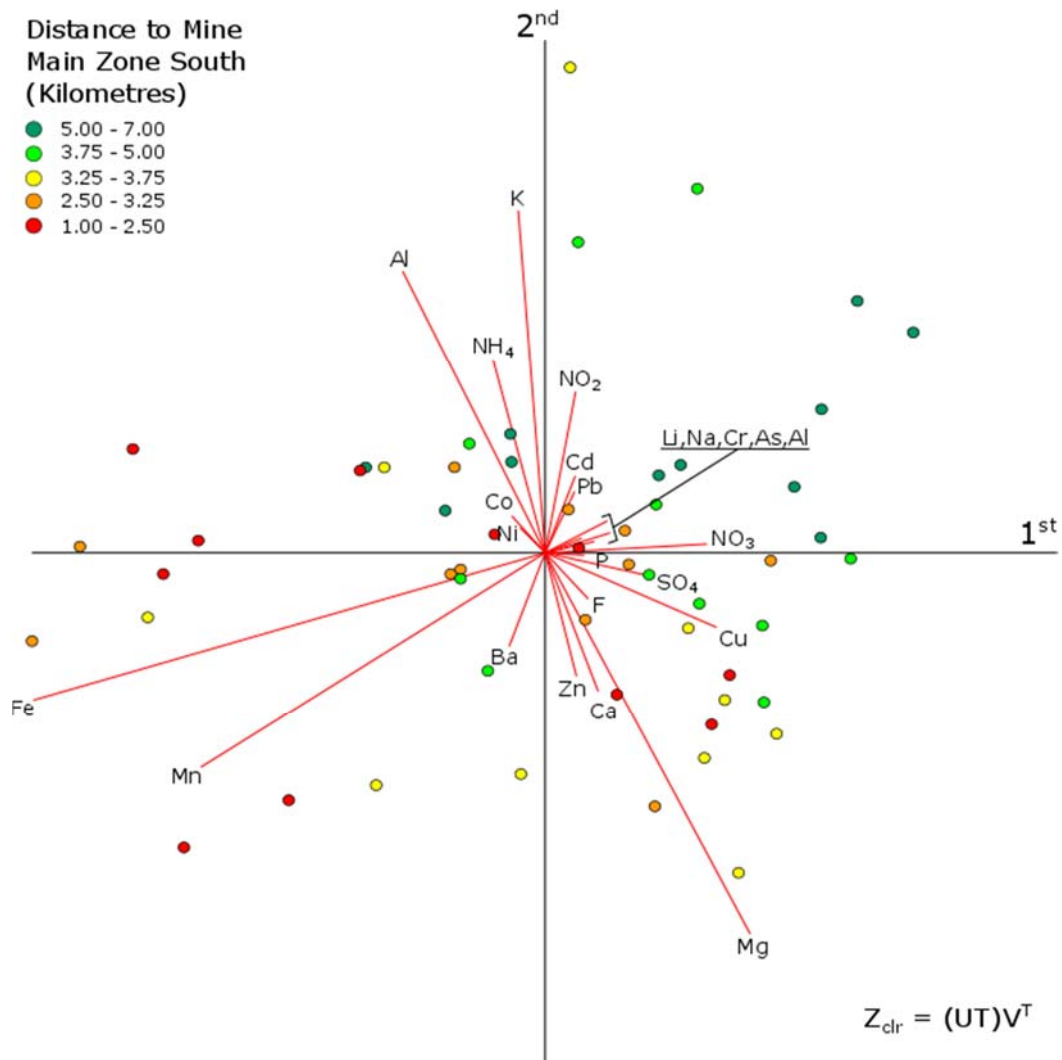

Fig. 3.10: *CoDA bi-plot of the Early-Mining Regional Dataset (B), colour coded by distance to the known ore deposit at Lisheen (created using CoDA Pack [Version 2.01])*

3.3.2.5 Summary

The Early-Mining Regional dataset (B) provides an interesting insight into the groundwater geochemistry conditions in the Lisheen area during the earliest phases of mining. By looking at the statistically unprocessed raw data (Table 3.1), it is clear that at least some of the groundwater samples exceed the European Communities Environmental Objectives (Groundwater) Regulations 2010 (S.I. No. 9/2010) threshold values in respect to NO_3, Fe, Mn and As. However, these elevated levels are unlikely to be a direct consequence of mining; instead they indicate the occurrence of redox reactions in some sub-oxic to anoxic groundwater. In comparison to dataset A, it is possible that the samples here are too spatially distributed to identify the chemical signal of the ore deposit. The lack of carbonate and bicarbonate data limits the investigation of major anion and cation compositions. However, a simplified version of the CoDA Ilr-ion plot (Fig. 3.8) shows that cation ratios (e.g. CaMg/NaK) can distinguish two broad groups of samples. Mapping the Ilr-ion data demonstrates that calcium/magnesium ratios may act as a proxy for dolomitisation of limestone regionally.

The CoDA bi-plot adds to the interpretation of the Early-Mining Regional Dataset by indicating which samples are being affected by different geochemical processes (Fig. 3.10). Samples in the top-right sector of the bi-plot represent a regional geochemical baseline, whereas samples in the top-left have been most likely influenced by contamination associated with local land-use practices (elevated NO_2, NH_4 and K associated with agriculture). The area to the far-left and lower-left of the bi-plot (Fig. 3.10) are more dominated by redox influenced groundwater and samples to the bottom-right may be showing some signal related to the presence of massive-sulphides in the area.

By examining the characterisation (colouration) of samples based on their relative distance to the main zone south (Figs. 3.9-3.10), there appears to be some level of correlation between short distances and redox influenced samples. It may be the case that the redox wells would also show a massive-sulphide signature, but it is being masked by strong iron and manganese variation. This is logical considering the red and orange groups have an average groundwater sample depth of 26 and 14m respectively, whereas the yellow, light green and dark green groups have much shallower average sample depths of 4, 6 and 2m respectively.

3.3.3 Mine Workings Dataset (**C**)

3.3.3.1 Overview

Groundwater flowing through a variety of structures (e.g. those mentioned in Section 1.3.5.2) was sampled directly, throughout a large portion of the underground mining and ore extraction phase at Lisheen (January 2004 to September 2009). These samples were then analysed for geochemistry and the results have been made available for this research project. In total, the concentration (mg/l) of 25 elements and compounds were measured (HCO_3, F, Cl, NO_2, NO_3, P, SO_4, NH_4, Li, Na, Ca, Mg, K, Al, As, Ba, Cd, Co, Cr, Cu, Fe, Mn, Ni, Pb, Zn) in 883 samples. For reliable comparison and simplified graphical data representation, only locations with 20 or more samples taken over the complete sampling period were retained for data analysis. Additionally, samples which had a significant portion of missing data were removed. This reduced the dataset to 8 distinct locations (Fig. 3.11) and 387 individual samples. Following the data replacement procedures described above (Section 2.5.1), the variables were reduced from 25 to 18 (HCO_3, F, Cl, NO_3, SO_4, NH_4, Na, Ca, Mg, Al, As, Ba, Co, Fe, Mn, Ni, Pb, Zn).
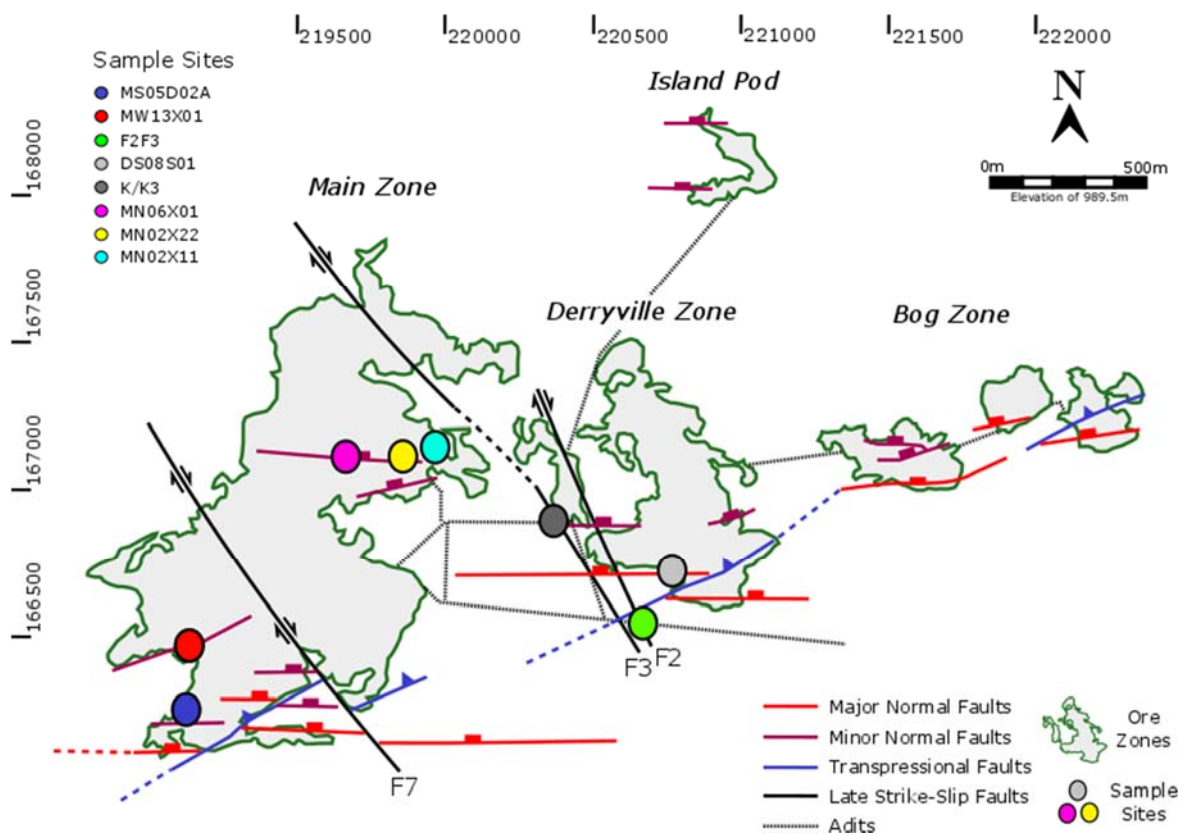

Fig. 3.11: *Geographic map of Lisheen mine workings with main structural geology features shown (modified after Torremans et al., 2018). Mine Workings Dataset (C) sample sites are overprinted (colour-filled circles).*

3.3.3.2 Parameters

The summary statistics table (Table 3.3) provides a general overview of all of the available data for the Mine Workings Dataset (C) which includes 883 samples. A reduced dataset of 315 samples is used for the later data analysis sections (Section 3.3.3.3 and 3.3.3.4). As with the previous two Lisheen datasets (A and B above), the concentrations of each relevant parameter are compared to Irish/EU groundwater quality threshold values (S.I. 9 of 2010)[11]. However, the samples in this case were collected within the workings of an underground mine and therefore a large proportion of them expectedly exceed the threshold limits for various analytes (Table 3.3). Although groundwater threshold values are not particularly relevant to the Mine Workings Dataset (C), the significant number of cases where they are exceeded for a number of analytes, provides an indication of effect of various complex geochemical interactions. A proportion of the samples within the full dataset (prior to be reduced to 387 samples), may have been contaminated through contact with walls and floors of the working mine.

pH

The pH values for Lisheen dataset C range from a minimum of 3.45 to a maximum of 9.92. Only 6 samples have a pH of less than 6 and the mean 7.42 indicating that there are very few acidic samples and the majority of groundwater is alkaline. This highlights the effect of the limestone bedrock in buffering the system and reducing the potential for acid mine drainage as a result of sulphide dissolution.

Electrical Conductivity (EC)

Electrical conductivity (EC) measurements generally range from 210 to 2179 µS/cm. However, dataset C includes three outliers of 7, 8 and 7750µS/cm that could possibly be explained by inaccurate recording or malfunctioning equipment. The average EC measurement is relatively high at 693µS/cm indicating the presence of a large proportions of dissolved material.

---

[11] http://www.irishstatutebook.ie/eli/2010/si/9/made/en/pdf

Variable	Unit	Detection Limit	Max	Mean (arithmetic)	IQR	Stanard deviation	EU Limit (ground-water)	No. of samples above threshold
pH			9.92	7.42	0.38	0.39		
EC	(µS/cm)		7750.00	693.49	191.50	282.89	1875	2
COD	(mg/l)	1	55.00	4.64	5.00	6.21		
Turbidity	(NTU)		1241.00	22.65	21.00	49.99		
HCO$_3$	(mg/l CaCO3)		560.58	337.76	92.49	57.69		
F	(mg/l)		1.78	0.11	0.06	0.09		
Cl	(mg/l)		40.60	17.71	2.93	2.63	187.5	0
NO$_2$	(mg/l)	0.001	10.31	0.59	0.18	1.61	0.375	76
NO$_3$	(mg/l)	0.001	485.86	3.49	2.72	18.02	37.5	5
P	(mg/l)	0.001	0.13	0.03	0.02	0.04	0.035	8
SO$_4$	(mg/l)		1129.57	46.88	30.14	82.55	187.5	33
Li	(mg/l)	0.001	8.60	0.13	0.00	1.03		
Na	(mg/l)		26.38	9.62	1.19	2.80	150	0
NH$_4$	(mg/l)	0.001	11.82	2.01	2.59	1.60	0.175	654
Ca	(mg/l)		710.34	91.89	35.96	50.48		
Mg	(mg/l)		246.28	31.61	10.02	16.34		
K	(mg/l)	0.001	15.91	3.68	3.60	3.15		
Al	(mg/l)	0.001	0.69	0.08	0.08	0.07	0.15	68
As	(mg/l)	0.001	0.54	0.07	0.08	0.07	0.0075	705
Ba	(mg/l)	0.001	8.79	0.83	1.14	0.72		
Cd	(mg/l)	0.001	0.07	0.00	0.00	0.00	0.00375	99
Co	(mg/l)	0.001	0.67	0.02	0.01	0.07		
Cr	(mg/l)	0.001	0.01	0.00	0.00	0.00	0.0375	0
Cu	(mg/l)	0.001	0.03	0.00	0.00	0.00	1.5	0
Fe	(mg/l)	0.001	25.14	1.57	1.92	2.15		
Mn	(mg/l)	0.001	4.48	0.16	0.21	0.22		
Ni	(mg/l)	0.001	3.98	0.05	0.03	0.18	0.015	422
Pb	(mg/l)	0.001	0.97	0.03	0.03	0.07	0.01875	277
Zn	(mg/l)	0.001	37.20	0.90	0.37	2.48		

Table 3.3: Data summary table showing the maximum, mean, interquartile range and standard deviation of each analyte for 883 water samples in the Mine Workings Dataset (C) at Lisheen. European Communities Environmental Objectives (Groundwater) Regulations 2010 Threshold limits (mg/l) are also given for comparison

Chemical Oxygen Demand

Chemical Oxygen Demand (COD) is used to quantify the amount of oxidisable organic material found in water. A strong oxidising agent, usually potassium dichromate ($K_2Cr_2O_7$), is added to a sample under acidic conditions. Following oxidation, the remaining agent is measured by titration. This value provides an indication of the chemical oxygen demand. However, dichromates do not oxidise ammonia into nitrate,

therefore nitrification is excluded from the COD test. The higher the COD value (measured in mg/l), the more organic matter is present. In the Lisheen Mine Workings Dataset (C), COD values range from 1 to a maximum of 55. However, the mean value is 4.64 indicating oxygen demand is low for most samples.

Turbidity

Turbidity is a measure of water clarity and therefore indicates the amount of suspended material. It is measured in nephelometric turbidity units (NTU) using a turbidimeter. This instrument shines a beam of light at a water sample and measures the amount of light that passes through the water compared to the amount of light that reflects off particles in the water. In this dataset 628 samples (71%) are recorded above 5 NTU indicating that the water is visibly cloudy. Additionally, 230 samples (26%) have NTU values above 25 suggesting the water is technically murky.

Anions

As mentioned in previously (Section 3.3.1.2), the dominant anion within the groundwater at Lisheen is bicarbonate (HCO_3^-). However, given the proximity to the massive sulphide deposits within the mine workings, many of the samples in this dataset have high sulphate (SO_4^{2-}) values, even exceeding HCO_3^- in 18 cases (2%). Mean HCO_3^- and SO_4^{2+} values are 338 and 47 mg/l, respectively (Table 3.3). Chloride (Cl^-) also makes up a significant proportion of anion concentrations with a mean of 18 mg/l. Although not entirely relevant given the groundwater is contained and treated prior to release, 76 samples show levels of nitrite above threshold values suggesting a redox reactions may be influencing some waters (e.g. Torrentó *et al*., 2011; Margalef-Marti *et al*., 2020).

Cations

As a result of limestone and dolostone dissolution, the most dominant cations in the groundwater samples are calcium (Ca^{2+}) and magnesium (Mg^{2+}) with means of 92 and 32 mg/l, respectively. When compared against groundwater threshold values it is clear

that a number of cations have relatively high concentrations due to sulphide mineral dissolution (e.g. aluminium (Al^{3+}), cadmium (Cd^{2+}), lead (Pb^{2+}), nickel (Ni^{2+}) and particularly arsenic (As^{3+}); Table 3.3).

3.3.3.3 Pearson Correlation

The robust Pearson correlation diagram of the Lisheen Mine Workings Dataset (Fig. 3.12) offers insight into which elements and compounds are interrelated. As seen previously (Sections 3.3.1 and 3.3.2) Ca and Mg are strongly associated again here, indicating groundwater which has been in contact with dolomitised limestone. Additionally Mn appears to have an association with Zn, perhaps as Mn is often a secondary element in sphalerite. Pb and Fe also have high Pearson correlation values, possibly due to the presence of significant pyrite close to areas of galena mineralisation. HCO_3, Cl and SO_4 appear to also have some relationship with each other. This may be as a result of the dissolution of a greater amount of minerals underground, leading to ionic imbalance which is then be filled by various readily available anions.
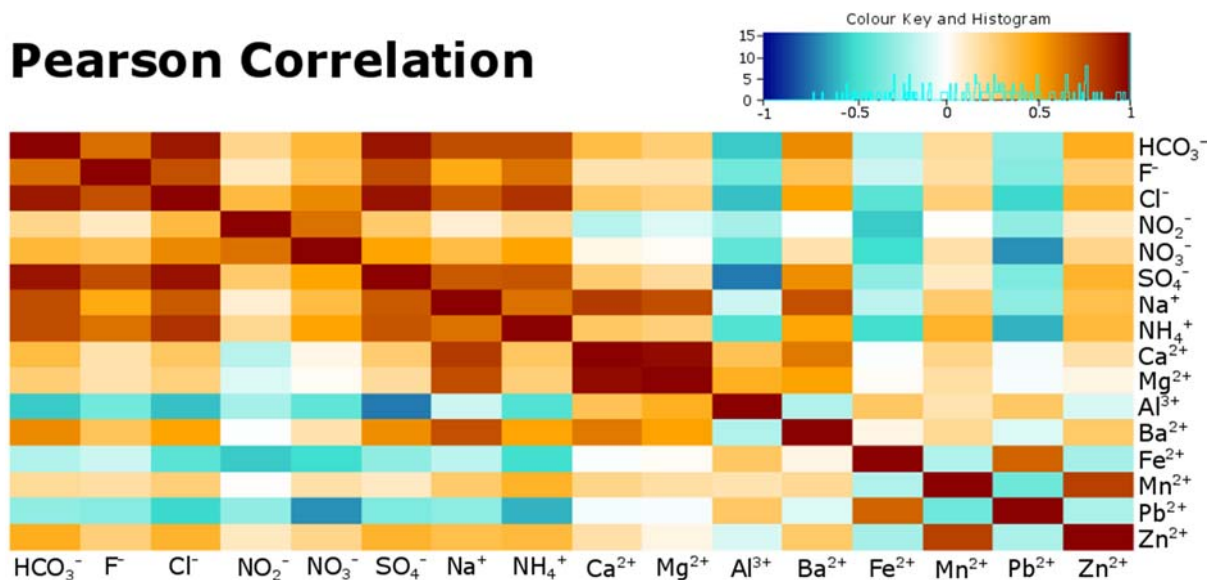

Fig. 3.12: *Graphical representation of the results of a Pearson Correlation of the Mine Workings Dataset (C) from Lisheen, showing analytes with strong inter-relationships in orange and red.*

3.3.3.4 CoDA Bi-plot

The CoDA bi-plot (Fig. 3.13) is employed as the primary tool of geochemical analysis of the Lisheen Mine Workings Dataset (C). As a number of samples (+20) are available for each discrete sampling location (Fig. 3.11), clustering on the bi-plot is apparent. This highlights one of the strengths of the CoDA bi-plot, that was not apparent in either the Pre-Mining Regional Dataset (A) or the Early-Mining Regional Dataset (B), which both admittedly had a more limited number of available samples.

The geochemistry data from the F2/F3 fault (light green filled circles) feature in the bedrock are of particular interest as the groundwater was intercepted before entering the underground mine workings, thereby lessening the potential for contamination as a direct consequence of mining activity, in comparison to other samples recovered during the period of active operation. As described previously in section 1.3.5.4, this groundwater is unique among the samples recovered, as it is sourced from the Lisduff Oolite Member (of the Ballysteen Limestone Formation), whereas other samples are generally from the stratigraphically younger Waulsortian Limestone Formation.

In the CoDA bi-plot (Fig. 3.13) the majority of F2/F3 samples (light green filled circles) are clearly located in the bottom right section. Observations relatively close to the origin of the bi-plot have low variation of the principal components plotted. Additionally the F2/F3 samples are associated with low levels of variation within a large amount variables (Ca, HCO_3, Mg, Na, Cl, F). As stated previously (Sections 3.3.1-2), this indicates that these samples are sourced from groundwater that is more representative of regional background (i.e. 'cleaner' water relative to the other samples). This is perhaps unsurprising given that this particular groundwater is sourced from a different aquifer (Lisduff Oolite Member) that is only in contact with the mineral deposits due to the localised faulting at the mine site (see Fig. 1.11).

Samples sourced from another significant fracture feature in the limestone bedrock (termed the K2/K3 fissure – shown as dark grey filled circles) together with the majority of samples from MN02X22 (yellow filled circles) have a strong association with NO_3 (Fig. 3.13). This may be attributed to these locations having a greater hydraulic connection with areas of peat bog to the north and east of the mine. The other primary nitrogen source is NH_3 (left hand side of the bi-plot, Fig. 3.13). Samples that show a strong association with ammonium may be related to contamination from agricultural activity such as the spreading of slurry. Alternatively, these two nitrogen compounds may be interrelated as nitrate can reduce to ammonium by:

$$2H^+ + NO_3^- + 2CH_2O \leftrightarrow NH_4^+ + 2CO_2 + H_2O \text{ [Equation 3.3]}$$
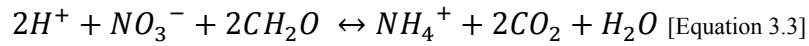
The potential for redox reactions to be a factor is further evidenced by higher variations of Fe and Mn in samples on the left of the bi-plot. These metals can more readily dissolve into groundwater in reducing conditions. It appears that the 1st principal component (x-axis) in this case broadly represents redox conditions and separates samples (left and right of the bi-plot) based on this important geochemical determinant. The availability of electron donors (sulphide minerals) in the mine setting provides a method by which oxygen may be removed from groundwater. Microbial activity might also be playing a role in oxygen reduction.
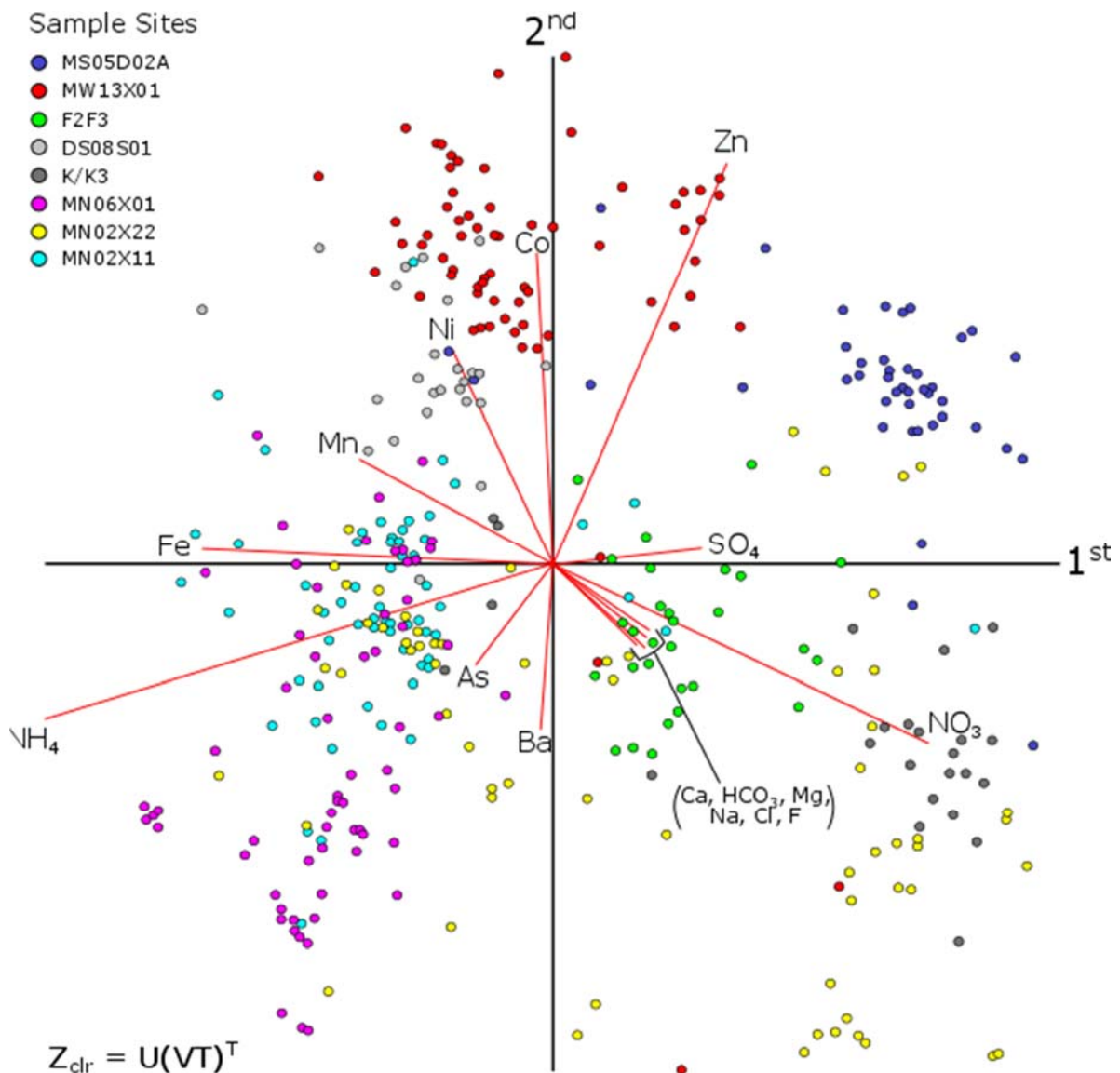
Fig. 3.13: *CoDA bi-plot of Mine Workings Dataset (C) from Lisheen mine (created using CoDA Pack [Version 2.01]).*

Samples from MS05D02A and MW13X01 (blue and red filled circles, respectively) in the south of the main zone (see map in Fig. 3.11) and closest to the feeder zones of massive-sulphide mineralisation, show strong apparent relationships with Zn, Co and Ni in the CoDA bi-plot (Fig. 3.13). These metals are known to have strong associations with the mineralisation at Lisheen (Torremans *et al*., 2018) indicating some connection between these discrete sample locations and mineralised zones. It is possible that groundwater here is sourced from fracture flow along discrete mineralised structures. Despite these locations being less than 200m apart, the individual groundwater geochemistry of each is well-defined by the bi-plot. The most notable distinguishing factor is on their x-axis values. As discussed above the 1st principal component is likely a representation of varying redox conditions and therefore it appears that groundwater at location MW13X01 is more reduced than at MS05D02A.

Sample sites MN06X01 and MN02X11 (pink and cyan filled circles, respectively) are reasonably well clustered on the left side of the bi-plot (Fig. 3.13). MN02X22 (yellow filled circles) has significantly greater geochemical variation, despite being located close to the two samples mentioned above. This may indicate that as mining continued, a variety of structures were intercepted and penetrated, facilitating the mixing of groundwater before reaching this location. Sample site DS08S01 (light grey filled circles) appears to have a very similar chemistry to MW13X01 (red filled circles) with relative high variations of Zn, Co, and Ni. Given the location of these sample sites, close to the feeder zones in the south of the Derryville and Main Zone respectively (Fig. 3.11), it is likely that groundwater at these locations is sourced from the same structures responsible for the original mineralisation.

3.3.3.5 Summary

The groundwater geochemistry of the Mine Workings Dataset (C) affords a unique and detailed insight into the chemical composition of water entering underground mine sites prior to potentially becoming contaminated as a result of mineral extraction activity at Lisheen. In particular this dataset illustrates how specific bedrock structural (fault and fracture) features can have distinctive geochemical signatures in terms of the groundwater permeating through them. At the depths that extraction (and groundwater sampling) was occurring at Lisheen, fracture/conduit flow is the primary method of water transport, particularly as the Mississippian limestone matrix is relatively impermeable and tight, in particular the massive carbonate

(calcilutite) mudbank facies of the Waulsortian Limestone Formation (e.g. Murray and Henry, 2018), which is an extremely important target facies for mineral exploration. The host rocks also provide an alkaline buffer that effectively reduces the potential for acid-base reactions that would have inevitably lead to acid mine drainage.

One of the first structures to be intercepted by mining operations at Lisheen was the F2/F3 feature in the main decline (e.g. Quaid and Wheston, 2017). This structural feature is part of a set of NNW-SSE trending strike-slip faults that are considered to be late in terms of the structural geological evolution at Lisheen as they cross-cuts many other structures (Fig. 3.11; e.g. Kyne *et al.*, 2019). Crucially, in terms of groundwater geochemistry at Lisheen, the F2/F3 structure provides a conduit to connect the permeable Lisduff Oolite Member with the stratigraphically higher Waulsortian Limestone Formation aquifer. The CoDA plot (Fig. 3.13) differentiates F2/F3 samples (green filled circles) from the remaining samples reasonably well as they are clustered together in the lower-right part of the bi-plot. These points are defined by low variations of a large number of chemical elements and compounds and are orthogonal to the vector for zinc, suggesting that the Lisduff Oolite Member contains groundwater that has not been in direct contact with significant mineralisation.

The 1st principal component (x-axis in the CoDA bi-plot) appears to represent the extent to which water samples have experienced sub-oxic to anoxic conditions, with oxygen availability interpreted to increase from left to right (Fig. 3.13). Samples on the left of the plot, such as MN06X01 and MN02X11 (pink and cyan filled circles, respectively), show variation of manganese, iron and ammonia, suggesting redox is an important geochemical process influencing the geochemical composition of groundwater at these sites. The 2nd principal component (y-axis on the bi-plot) on the other hand, represents proximity to the feeder zones of mineralisation. In particular, at the top of the bi-plot, samples MS05D02A, MW13X01 and DS08S01 (blue, red and light grey filled circles, respectively) are sites located closest to the feeder zones in the south of the Main Zone and Derryville Zone. These wells are defined by variations of zinc, nickel and cobalt.

3.4 Conclusion

The three Lisheen datasets (A-C) examined here, afford a comprehensive insight into the nature of groundwater geochemistry prior to, and during, mining operations. The majority of shallow groundwater flows from north-north-west to south-south-east through the upper 30-50m of epikarst. Deeper groundwater relies on fracture and conduit flow within the Mississippian limestone bedrock, which is significantly enhanced near to major geological structures particularly those closest to the economic grade Pb/Zn massive-sulphide mineral deposit. Groundwater hosted within the Waulsortian Limestone Formation, for example, is connected to shallower groundwater via extensive normal faulting along the Rathdowney Trend (e.g. Shearley *et al.*, 1996). A combination of normal, reverse and strike-slip faulting at the Lisheen ore deposit connects the relatively more permeable Lisduff Oolite Member with the stratigraphically younger Waulsortian Limestone Formation (Fig. 1.9; see Kyne *et al.*, 2019). This results in three recognisable groundwater signatures at Lisheen:

1. Shallow epikarst groundwater,

2. Waulsortian Limestone Formation groundwater, *and*

3. Lisduff Oolite Member groundwater

All of the groundwater sampled at Lisheen can be characterised as Ca-HCO$_3$ or Ca-Mg-HCO$_3$ type. This highlights both the dominance of limestone and diagenetically dolomitised limestone as the host rocks for the aquifers and the effect of carbonate buffering, limiting the potential for acid-base reactions to alter the primary chemistry. This is particularly noteworthy, given the presence of a former large massive-sulphide mining operation.

Shallow groundwater is characterised by relatively minor variations in the majority elements and compounds (e.g. Figs. 3.5, 3.10, 3.13). Some exceptions to this are nitrate, ammonium and potassium which can be higher either as a result of increased nitrogen beneath areas of peat bog or sourced from local agricultural practices such as the seasonal spreading of fertiliser (e.g. Fig. 3.10). Mixing with deeper groundwater can be identified where there are relatively higher concentrations of iron, manganese and sometimes arsenic. These elements have dissolved in groundwater from source minerals in redox reducing conditions as a result of lower oxygen.

Variations of iron and manganese is a common signature of the Waulsortian Limestone Formation groundwater, which at some locations closer to the deposit also contains higher

concentrations of zinc, lead and cadmium from the dissolution of minerals associated with the massive sulphides (e.g. sphalerite $[(Zn,Fe)S]$ and galena $[PbS]$). Although some mixing has occurred with shallow groundwater, the concentration levels measured remain below Irish/EU groundwater quality threshold values (Irish Statutory Instrument 9 of 2010 - European Communities Environmental Objectives (Groundwater) Regulations 2010)[12].

Groundwater that is believed to be sourced from the Lisduff Oolite Member is geochemically highlighted in the Lisheen Mine Workings dataset C (e.g. Figs. 3.11, 3.13). The so called F-structures, particularly F2/F3, evidently created a hydraulic connection between the Lisduff Oolite Member and the mine workings. Samples captured from these NNW-SSE structures in the main decline reveal that this groundwater has a unique chemical signature among the other samples recovered from underground. It is primarily characterised by having relatively low variations and low concentrations of all of the analytes (e.g. Fig. 3.13). This suggests that groundwater within the Lisduff Oolite Member is well connected to the surface, allowing for high recharge and high transmissivity.

As discussed in the introduction, CoDA is the correct mathematical framework for the analysis of compositional data. CoDA also has additional advantages as demonstrated with the Lisheen geochemistry datasets. The ilr-ion plot for example, offers a more detailed model for chemical characterisation of water-type than the traditional Piper diagram. Methods of cluster and correlation analysis (e.g. hierarchical cluster analysis, spearman rank etc.) can be completed via log-ratio transformation CoDA methods which provide a more accurate result than traditional means (e.g. Filzmoser *et al*., 2018). The benefits of these methods for gaining a better understanding of the geochemical processes active in the area, is clear from the ilr-ion plots (Figs. 3.2 and 3.8), correlation and cluster analyses (Figs. 3.3, 3.4 and 3.12) and the CoDA bi-plots (Figs. 3.5, 3.10, 3.13).

Following the closure of Lisheen Mine in 2015, regional groundwater monitoring remained active to ensure there were no adverse geochemical effects as a consequence of the rebounding water table and to identify any potential groundwater pollution from the surface site or tailings management facility (TMF). Data from the first year of this continued sampling programme in addition to a single further round of sampling in 2019 are discussed in the following chapter.

---

[12] http://www.irishstatutebook.ie/eli/2010/si/9/made/en/pdf

Chapter Four: *Groundwater Geochemistry at Lisheen B*

[Post underground Pb/Zn mining phase]

4.1 Introduction

The previous chapter discussed groundwater geochemistry in the area of Lisheen mine prior to, and during the active phase of mining for Pb/Zn. Through analysis of a combination of two regional and one within-mine geochemical datasets using CoDA methods, three distinct groundwater signatures were identified:

  i) Shallow epikarst groundwater,

  ii) Waulsortian Limestone Formation groundwater, *and*

  iii) Lisduff Oolite Member groundwater

Although mixing may occur, facilitated primarily through a variety of geological structures outlined in Section 1.3.5.2, the shallow groundwater (i), in the upper 30m of epikarst, is generally geochemically isolated from the other two groups [(ii) and (iii)].

As this shallow water (i) is utilised locally for a variety of purposes (e.g. domestic or agricultural), it was necessary to ensure that it remained uncontaminated by mining operations following the closure of Lisheen Mine in late 2015. As a result, a network of regional wells are presently sampled regularly for geochemistry to ascertain whether the groundwater has been effected by either:

  i) The rapid hydrological rebound of the water table (~12 months) transporting toxic metals upwards from the underground mine workings,

  ii) Leakage from the on-site tailings management facility (TMF), *or*

  iii) Contaminated rainwater runoff on the surface operations site

No evidence of contamination from any source has been recorded to date (2021) and the first year (December 2015 to November 2016) of geochemical data has been made available for further analysis here. This dataset offers a unique insight into the geochemical characterisation groundwater from various locations in the Lisheen area and provides an opportunity to analyse the chemical variation temporally. The primary focus of this chapter is what has been termed *'the early post-mining regional dataset'* (see below), the analysis of which is published in

Wheeler *et al.* (2021) (Appendix A). A further follow-up sampling round of wells at Lisheen completed in January 2019 is also examined.

4.2 Data Overview

As mentioned in the introduction above, this chapter will focus on two datasets that are composed of samples taken after mine closure in late 2015. Groundwater continues to be monitored in the area on a bi-annual basis; however, data beyond 2016 is held by the remediation team at the mine and is unavailable at the present time of writing (2021), with the exception of one sampling round of 10 sites from January 2019. Following on from the previous chapter (datasets A-C), the final two Lisheen groundwater geochemistry datasets (D and E) are discussed here.

D. Early Post-Mining Regional

Immediately following the closure of Lisheen Mine in December 2015, eight groundwater wells surrounding the site were sampled on a monthly basis. Eleven months of data up to November 2016 for these locations are discussed here. This dataset includes measures for the following analytes: depth, temperature, pH, electrical conductivity, dissolved oxygen, total organic carbon, turbidity, total hardness, alkalinity, SO_4, Cl, NO_3, F, NH_4, NO_2, P, Ca, Na, K, Mg, Fe, Mn, Cu, Zn, Pb, Al, Ni, Ba, As, Hg, B, Cr, Cd, Mo, Ag, Co, Sr, Be, Sb, U.

E. Recent Post-Mining Regional

In January 2019, ten wells in the Lisheen area were again sampled for groundwater geochemical analysis. As part of this one-off sampling round, triplicate samples were taken from each location. Values of the unstable parameters of temperature, electrical conductivity, dissolved oxygen, total dissolved solids, pH, ORP were recorded in the field using a YSI Multiparameter probe. The samples were then taken to NUI Galway to determine the concentration of: Cl, F, NO_3, NO_2, P, SO_4, Ca, Mg, Na, K, Fe, Mn, Ni, Zn, Pb, U, As, Al, Cu, Si, Sr, B, Se, Ba, Tl, Sn.

4.3 Results and Discussion

4.3.1 Early Post-Mining Regional Dataset (D)

4.3.1.1 Overview

As noted in the introduction, the application of CoDA methods to the Early Post-Mining Regional dataset (D), discussed in this particular section, is part of a published work (see Appendix A; Wheeler *et al.*, 2021). Under the Lisheen Mine Closure, Restoration and Aftercare Management Plan (CRAMP), six regional privately-owned groundwater wells were sampled monthly, in addition to a number of onsite monitoring wells. For the purposes of this investigation, data from these regional wells, together with two onsite monitoring wells (Fig. 4.1), recorded during the first year post-closure (December 2015-October 2016) were made available. These samples were collected and analysed by an Irish National Accreditation Board-certified company (IAS Laboratories).
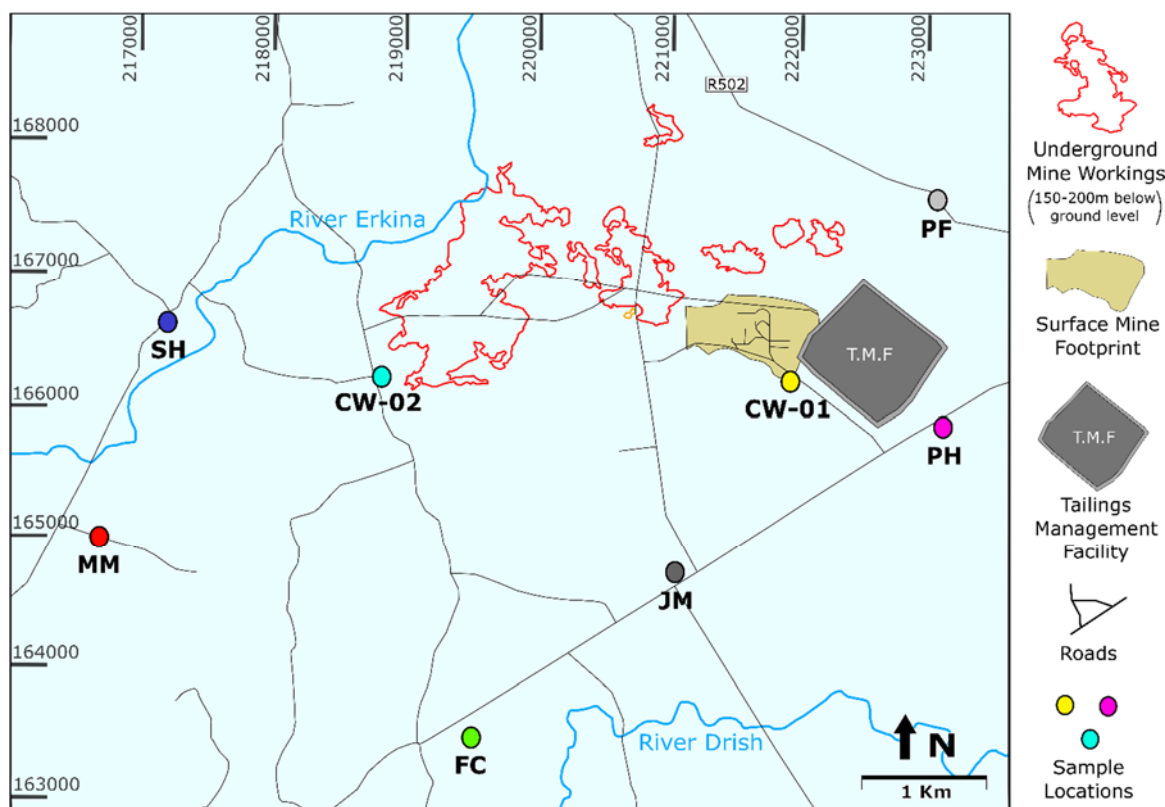
Fig. 4.1: *General geographic map of the Lisheen area showing the location of Early Post-Mining Regional dataset (D) sample points. Adapted from Wheeler et al., (2021, fig. 2).*

4.3.1.2 Parameters

The summary statistics table (Table 4.1) provides a general overview of all of the available data for the Early Post-Mining Regional Dataset (D), which includes 144 samples. As with the previous three datasets (A-C, discussed in Chapter Three), the concentrations of each relevant parameter are compared to Irish/EU groundwater quality threshold values (S.I. 9 of 2010)[13]. In cases where the threshold has been exceeded, it should be noted that the sampling location typically have a wide range of specific purposes, including domestic supply, agricultural uses and mine water monitoring. Samples are also recovered prior to entering filtration systems that may be present at some of the locations. A variety of parameters are discussed further here and graphs of variability over time are provided in Appendix B.

Depth

The depths at which the groundwater was sampled is recorded in dataset D. However, the relative elevation of each sample location is not provided. The maximum sample depth is 30.44m, whereas the average sample depth is just 7m (Table 4.1) - indicating that all samples are recovered from shallow groundwater, most likely within epikarst (type (i); see Section 1.3.5.1).

Temperature (Temp)

As mentioned previously (Section 3.3.1.2), the average groundwater temperature in Ireland ranges from 9.5 to 10.5°C (Aldwell and Burdon, 1980). The average water temperature within dataset D is 12.6°C, indicating at least some of the groundwater at Lisheen is thermal in origin, or is mixing with thermal water. The maximum value of 20.3°C recorded for well CW-01 on the 15th of August 2016 in particular, is very interesting and requires careful further study to locate the source/cause of elevated temperatures within these wells. The source may indeed be thermal or, alternatively, it may simply be a potential artefact of an inaccurate measuring procedure.

---

[13] http://www.irishstatutebook.ie/eli/2010/si/9/made/en/pdf

pH

pH values in dataset D range from a minimum of 6.58 to a maximum of 7.73 and an arithmetic mean of 7.07, suggesting all of the water samples within this dataset are essentially neutral (neither acidic, nor alkaline).

Electrical Conductivity

Electrical conductivity (EC) values range from 623 to 1129µS/cm, all of which fall below the threshold values for groundwater (Table 4.1).

Dissolved Oxygen

Dissolved oxygen (DO) provides an indication of how well-connected the groundwater is to the atmosphere. Lower levels of DO suggest that the water is sourced from confined or deeper aquifers. DO concentration within dataset D range from 0.41 to 11.43mg/l, with a mean of 4.23 mg/l. Many of the samples analysed had DO values less than 3mg/l indicating sub-oxic groundwater (see Section 4.3.1.5).

Total Organic Carbon

Total organic carbon (TOC), as the name suggests, is a measure of the amount of organic carbon within a given sample. Samples are acidified to a pH of 2 or less causing the release of inorganic carbon dioxide [CO_2] gas. The remaining non-purgeable CO_2 gas (NPOC) contained in the liquid aliquot is then oxidised releasing the gas. These gases are then sent to the detector for measurement (Bisutti *et al*., 2004).

Turbidity

Turbidity values in dataset D range from 0.5 to 10423 NTU with an average of 149 NTU (Table 4.1). However, these values are highly skewed depending on the sample location. The geometric mean of 8.7 NTU is more reflective of the majority of samples. Turbidity values are significantly higher in wells CW01 and JM (Fig. 4.1), suggesting the groundwater at these locations contains larger amounts of suspended solids.

Anions

The dominant anion within all of the samples in dataset D is bicarbonate (HCO_3^-). However, certain samples also contain relatively high concentrations of sulphate (SO_4^{2-}), chloride (Cl^-) and nitrate (NO_3^-) with arithmetic means of 52, 26 and 16mg/l, respectively (Table 4.1). Nitrate (NO_3^-) and phosphate (PO_4^{3-}) exceed groundwater threshold values in 18 and 25 cases, respectively, suggesting contamination from agricultural activity at some locations.

Cations

The dominant cation in the groundwater is calcium (Ca^{2+}) with an arithmetic mean of 156mg/l (Table 4.1). Magnesium (Mg^{2+}) is also a significant component of the water with an arithmetic mean of 30mg/l. As previously discussed (datasets A-C), the combination of high Ca^{2+} and Mg^{2+} concentrations highlights the influence of dolomitised limestone dissolution at Lisheen. Ammonium (NH_4^+) exceeds groundwater threshold values in 42 of the 144 samples, indicating either a strong redox component to the groundwater geochemistry or agricultural contamination as mentioned previously. Concentration levels of nickel (Ni^{2+}), arsenic (As^{3+}) and mercury (Hg^{2+}) also exceed groundwater threshold values in 41, 14 and 9 samples, respectively. This can most likely be attributed to the dissolution of minerals associated with the massive-sulphide ore deposit at Lisheen (Rytuba *et al.,* 2003; Hitzman *et al.,* 2002; Torremans *et al.,* 2018).

Variable	Unit	Detection Limit	Max	Mean (arithmetic)	IQR	Standard deviation	EU Limit (ground-water)	No. of samples above threshold
Depth	m		30.44	7.043916	1.798438	6.241942		
Temp	°C		20.3	12.60448	1.5	3.215856		
pH			7.73	7.069444	0.16	0.252948		
EC	μS/cm		1279	927.2222	156.25	147.0374	1875	0
DO	mg/l		11.43	4.234183	0.9525	2.659883		
TOC	Mg/l		14.83	1.641725	0.4735	2.008644		
Turbidity	NTU		10423	149.2517	2.5	901.0689		
HCO₃	mg/l		540	418.4482	60	74.61225		
SO₄	mg/l		177.99	52.14382	10.406	58.3761	187.5	0
Cl	mg/l		94.42	26.24854	3.927	11.98516	187.5	0
NO₃	mg/l	0.23	51.86	16.27661	7.9325	15.0543	37.5	18
F	mg/l	0.0049	0.153	0.04798	0.012	0.029299		
NH₄	mg/l	0.008	3.292	0.328833	0.062	0.630712	0.175	42
NO₂	mg/l	0.0056	0.388	0.05075	0.01	0.065618	0.375	1
PO₄	mg/l	0.0053	0.525	0.052622	0	0.107821	0.035	25
Ca	mg/l		223.608	155.9308	22.685	34.56596		
Na	mg/l		33.33	13.00415	4.573225	4.788336	150	0
K	mg/l		37.55	11.54783	9.055	9.965509		
Mg	mg/l		48.6628	30.15109	3.5112	7.605749		
Fe	mg/l	0.0013	16.91	0.820165	0.0005	2.897689		
Mn	mg/l	0.0004	1.49	0.372429	0.02095	0.54706		
Cu	mg/l	0.0002	0.1978	0.003664	0.0001	0.017318	1.5	0
Zn	mg/l	0.014	0.0498	0.011635	0.00285	0.004293		
Pb	mg/l	0.0009	0.0042	0.001047	0	0.000484	0.01875	0
Al	mg/l	0.0021	0.0304	0.004567	0.0011	0.003924	0.15	0
Ni	mg/l	0.0003	0.0426	0.01068	0.00532	0.012422	0.015	41
Ba	mg/l		0.3926	0.19233	0.035505	0.1027		
As	mg/l	0.001	0.013	0.003804	0.00095	0.002582	0.0075	14
Hg	mg/l	0.00028	0.0151	0.000608	0.00005	0.001507	0.00075	9
B	mg/l	0.0006	0.0988	0.017221	0.0123	0.01819	0.75	0
Cr	mg/l	0.0001	0.0006	0.000111	0	6.16E-05	0.0375	0
Cd	mg/l	0.0001	0.0016	0.000157	0	0.000164	0.00375	0
Mo	mg/l	0.0002	0.0015	0.000332	0	0.000248		
Ag	mg/l	0.0001	0.00055	9.91E-05	0	6.7E-05		
Co	mg/l	0.0053	0.0065	0.001846	0.000578	0.001762		
Sr	mg/l		0.2105	0.121871	0.0395	0.037748		
Be	mg/l	0.00002	0.0002	3.91E-05	0	4.81E-05		
Sb	mg/l	0.0008	0.0319	0.003181	0.0011	0.003053		
U	mg/l	0.0007	0.0562	0.018548	0.0051	0.011556		

Table 4.1: *Data summary table showing the maximum, mean, interquartile range and standard deviation of each analyte for 144 water samples in the Early Post-Mining Dataset (D) at Lisheen. European Communities Environmental Objectives (Groundwater) Regulations 2010 Threshold limits (mg/l) are also provided for comparison.*

4.3.1.3 Piper and ilr-ion Plots

Piper and ilr-ion plots for the Early Post-Mining groundwater geochemistry dataset (D) at Lisheen are both shown in Figure 4.2. A number of preliminary interpretations can be drawn from these more traditional methods of visualising statistical data. It is clear from the Piper diagram (Fig. 4.2A) that all water from each of the eight wells sampled at Lisheen may be classified as bicarbonate (Ca-HCO$_3^-$) type, with a slight influence of magnesium. Water samples from well CW-01 are quite conspicuously distinguishable from the other sample locations due to their relatively higher sulphate levels. The more recently devised compositional isometric log-ratio (ilr) plot of Shelton *et al*. (2018) allows for greater geochemical distinction between the groundwater wells at Lisheen (Fig. 4.2B).

As with the Piper diagram (Fig. 4.2A) the boxes on the right side of the ilr-ion plot (Fig. 4.2B) highlight the dominance of carbonate and bicarbonate in all wells in terms of the relative importance of anions (negative values indicate denominator dominance). The upper two boxes of the ilr-ion plot show that the second most dominant anion is chloride for the majority of regional well samples (SH, MM, FC, PF, JM, PH), whereas the second most dominant anion in all compliance well samples (CW-01 and CW-02) is sulphate (particularly in CW-01). Additionally the boxes on the left of the plot show that well SH is quite distinct from the rest in terms of calcium/magnesium ratio (conspicuously lower levels of magnesium).
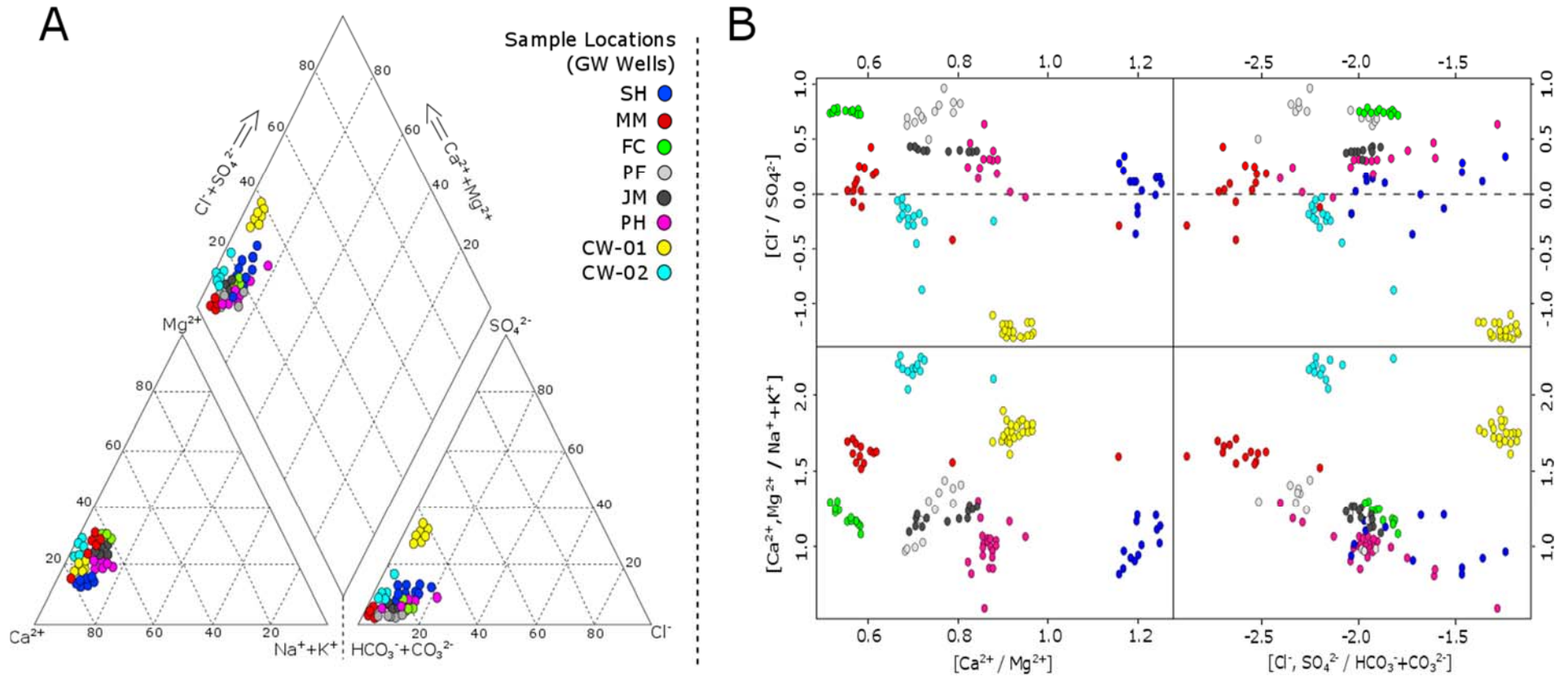
Fig. 4.2: A) *Piper diagram of the Early Post-Mining Regional Dataset (D) from Lisheen,* *B)* *Ilr-ion plot of the same data in A (created using the methods described by Shelton et al., 2018). For visual consistency, colour coding for groundwater wells sampled is the same in both A and B, and it is also the same as in Figure 4.1, which shows the geographic location of each of the various sample sites. Adapted from Wheeler et al. (2021, fig. 3)*

4.3.1.4 CoDA Bi-plot

The output data from the data preparation stage (see Section 2.5.1) was imported to the software 'CoDA Pack' (Version 2.02.21) for statistical analysis. The first output of CoDA is a table similar to that found with any form of PCA, which describes the proportion by which each variable is affecting each principal component. The most important controlling variables for each principal component are highlighted in this particular instance (Table 4.2). The 1st principal component, which represents 72% of the variance of the total dataset, is most strongly associated with relative variations of nitrate, manganese and nickel. The 2nd principal component, representing 10% of the variance is associated with ammonium and nickel, and the 3rd principal component, representing 6%, is associated with sulphate and potassium, and so on.

In the case of dataset D from Lisheen, the optimal approach to visualise the data is to plot 1st principal component along the X-axis of a CoDA bi-plot and 3rd principal component along the Y-axis (Fig. 4.3). These were chosen following data exploration to find the best visual representation of the data. The total variance displayed in this bi-plot is therefore 78%. The 2nd principal component is accounted for by the Z-axis (which runs in the third dimension orthogonally from the centre, both towards and away from the viewer). This plot is a multidimensional representation of the Early Post-Mining Regional Dataset (D) and it displays the information from Table 4.2 in terms of which variables are the controlling influences on each of the principal components by examining how the vectors (variables) relate to the axes (principal components). The bi-plot also illustrates how the observations (groundwater geochemistry samples) relate to each other, to the principal components and to the variables.

In the resultant bi-plot (Fig. 4.3), samples from each well (i.e. colour-coded observations on the bi-plot) are clearly clustered and distinguishable from each other for the most part. The 1st principal component has separated the wells based on variation of manganese, nickel and ammonium (towards the left side of the plot) and those controlled broadly by the variation of nitrate (towards the right of the plot). The 3rd principal component separates the samples further into two broad groupings either side of the x-axis. CW-01, CW-02 and SH lie above the x-axis and are predominantly influenced by sulphate variation, whereas the other wells are either geochemically balanced with respect to the 3rd principal component or are influenced by potassium variation.

The PF well is the least well-defined and clustered sample location when considered temporally over the 11-month sampling period. Changing the colour-coding of observations on the bi-plot (by date instead of by location) visually illustrates how the groundwater chemistry of well PF changed over the sampling interval, with samples gradually becoming more influenced by manganese, potassium and nickel (Fig. 4.4).

Additionally, in the biplot (Fig. 4.3), the observation points are subdivided into three groups (shown as different data symbols) on the basis of a Hierarchical Cluster Analysis (HCA) that was conducted independently of the PCA. For the HCA, centre log-ratio transformed data were imported to the software package SPSS (Version 23). Using the 'Wards Linkage' method, three significant clusters or 'groups' were readily distinguished:

- **G1:** represented by wells SH, PF and MM,

- **G2a:** represented by JM, PH, CW-02 and FC, *and*

- **G2b:** which effectively differentiates well CW-01 from the rest.

For the sake of visual clarity in Figure 4.3, the arithmetic mean of each variable at each location was used to for cluster analysis (the conclusions are the same if the full dataset is used).

	PC1	PC2	PC3	PC4	PC5	PC6
clr.HCO3	0.0586	-0.0036	0.0795	-0.1	0.0122	-0.0717
clr.SO4	-0.0819	-0.1752	0.4816	-0.224	-0.0203	-0.168
clr.Cl	0.0535	-0.1159	-0.0403	-0.05	0.1158	-0.278
clr.NO3	0.4453	0.0954	0.1876	0.7688	-0.0083	-0.001
clr.F	0.1955	0.0819	-0.1144	-0.1879	-0.1057	0.328
clr.NH4	-0.176	0.9048	0.0242	-0.0371	0.015	-0.0987
clr.Ca	0.0398	-0.03	0.1575	-0.1275	0.0092	-0.0885
clr.Na	0.053	-0.1249	0.0484	-0.2201	0.0896	-0.2111
clr.K	0.1635	-0.1058	-0.7618	0.058	0.0082	-0.1457
clr.Mg	0.0463	0.0545	0.0796	-0.0776	0.016	-0.0935
clr.Mn	-0.7398	-0.0576	-0.2083	0.1993	0.0254	0.1254
clr.Ni	-0.3386	-0.2628	0.1795	0.3832	-0.1514	0.0146
clr.Ba	0.015	-0.0927	-0.1357	-0.0169	0.1039	-0.2209
clr.Sr	0.1023	-0.065	-0.0105	-0.1371	0.0281	-0.1526
clr.Sb	0.0922	-0.0393	-0.0209	-0.1552	-0.7476	0.3927
clr.U	0.071	-0.0638	0.0541	-0.0759	0.61	0.669
Prop. Var. Ex.	0.7236	0.0963	0.0586	0.0367	0.0287	0.0232
Cum. Prop. Ex.	0.7236	0.8199	0.8785	0.9152	0.9439	0.9671
% Var. Ex.	72	10	6	4	3	2

Table 4.2: *Tabulated results of principal component analysis of the Early Post-Mining Regional Dataset (D) from Lisheen, showing which analytes have exerted the most influence on a given component. The data for the 1st and 3rd principal component is presented graphically in the CoDA bi-plot in Figure 4.3.*

= *high negative PC1*
= *high positive PC1*
= *high negative PC3*
= *high positive PC3*
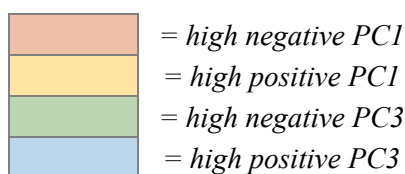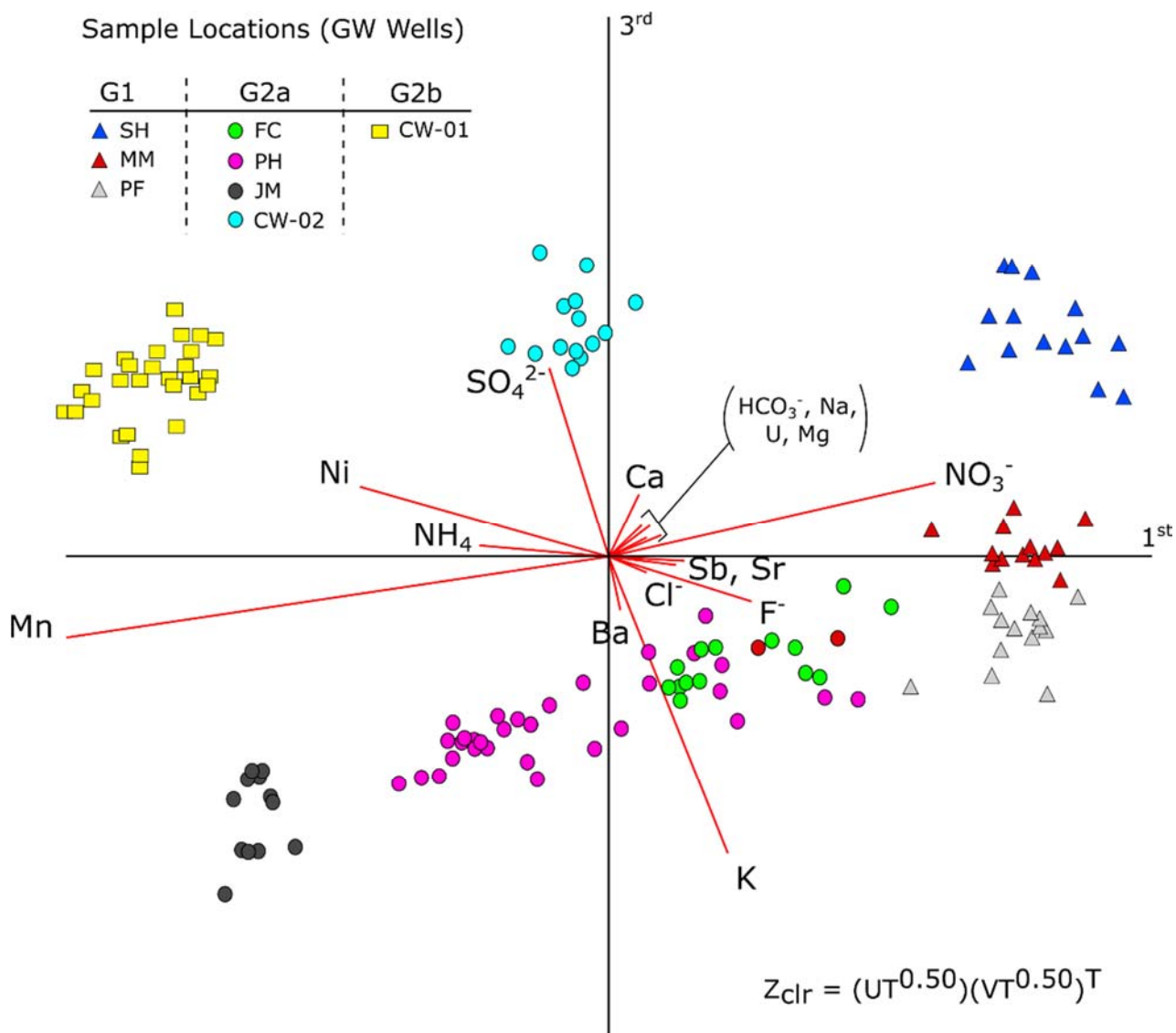
Fig. 4.3: *CoDA bi-plot of the Early Post-Mining Regional Dataset (D) from Lisheen, with different sample point shapes (filled triangles, circles and squares) indicating discrete groupings that resulted from hierarchical cluster analysis. Adapted from Wheeler et al. (2021, fig. 4).*
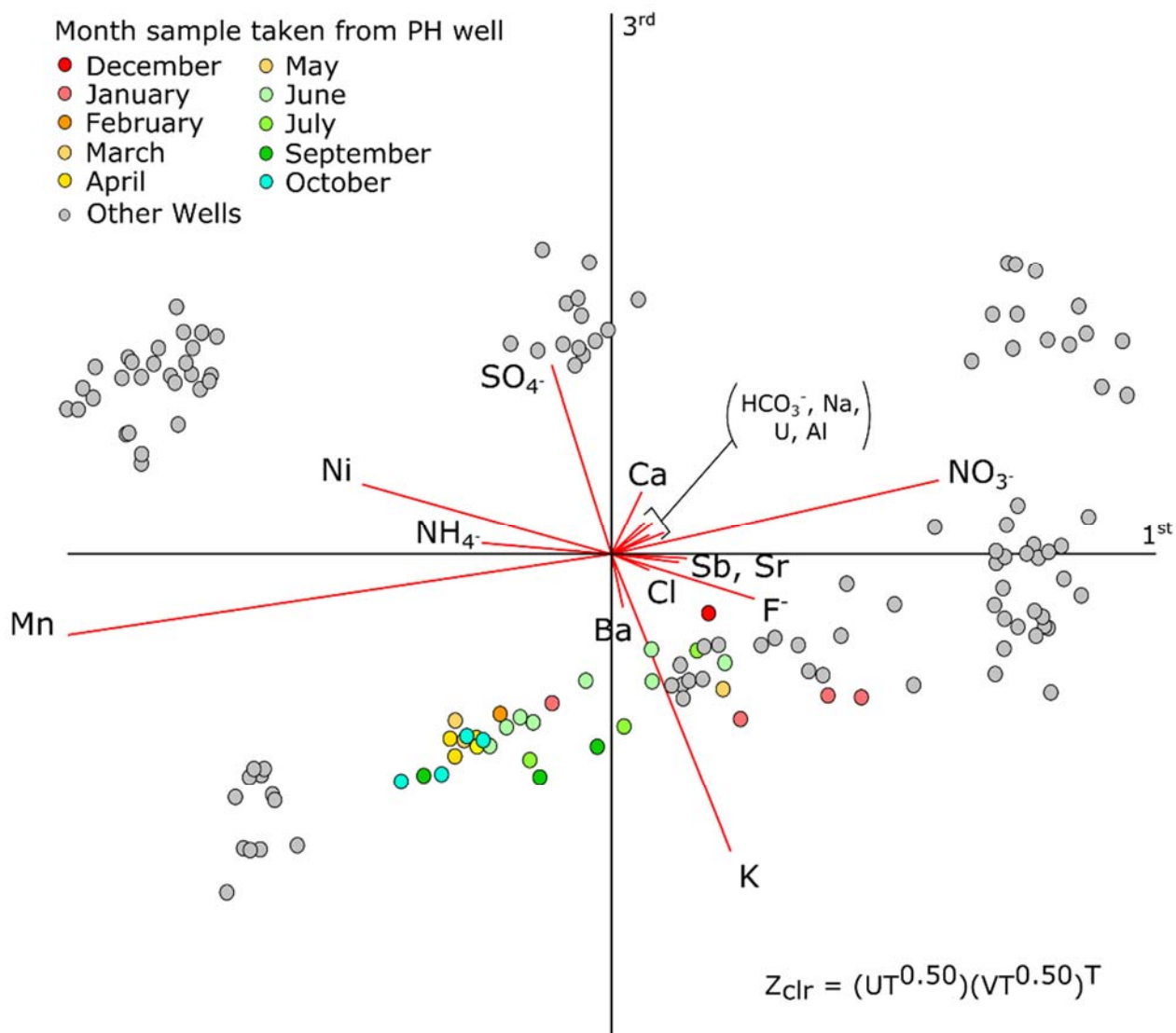
Fig. 4.4: Replicate CoDA bi-plot of Early Post-Mining Regional Dataset (D) from Lisheen, colour-coded based on sampling month for well PH (compare with Fig. 4.3). Adapted from Wheeler et al. (2021, fig. 5).

4.3.1.5 Additional Data Analysis

A portion of data collected from the groundwater monitoring wells in the Lisheen area could not be included in the CoDA analysis for dataset D because a high proportion of samples registered below the detection limit for a number of parameters (e.g. phosphate) and some are not part of the 'composition' (e.g. dissolved oxygen). However, these data, when compared against dissolved oxygen concentration (Fig. 4.5), can provide additional information that can augment the interpretation of the geochemical processes operating at various sampling wells. For example, the combined cluster analysis and bi-plot (Fig. 4.3) appears to show a strong relationship between wells SH, MM and PF, which is based primarily on relative levels of nitrate (Fig. 4.5A).

However, incorporating dissolved oxygen and phosphate data indicates the geochemical processes at sample sites SH and PF differ from those at MM – groundwater at location MM is less oxygenated and has elevated levels of phosphate relative to SH and PF (Fig. 4.5B). Manganese also has a strong influence on the characterisation of some groundwaters in the Lisheen area (Table 4.2 and Fig. 4.5C). Sample sites PH, JM and CW-01 have elevated levels of manganese and iron (Fig. 4.5D) and may be sourced from sub-oxic groundwater.
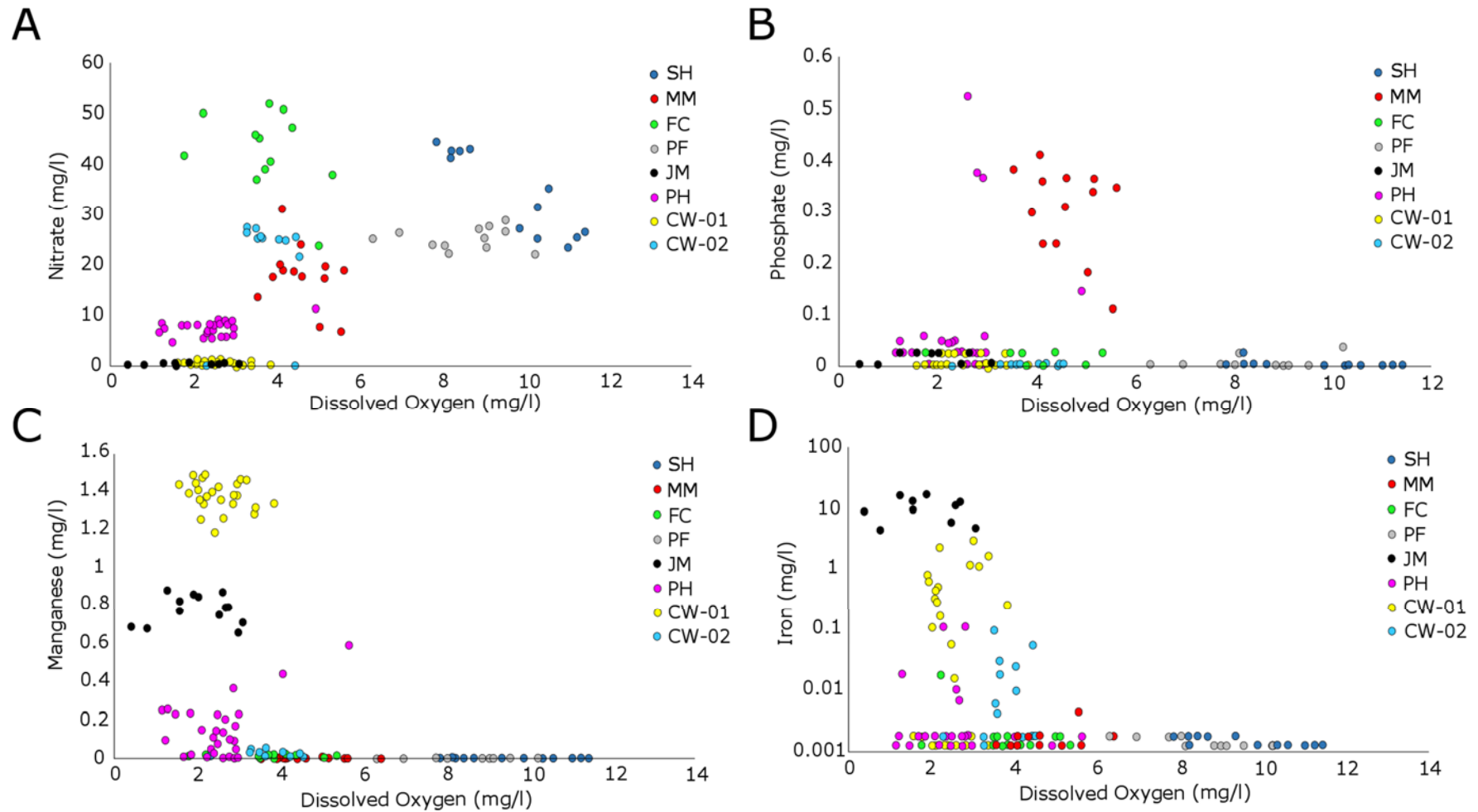
Fig. 4.5 *Additional data bi-plots from the Early Post-Mining Regional Dataset(D) at Lisheen, that compare dissolved oxygen concentrations (x-axis) to selected variables (y-axis) that may indicate varying redox conditions: A = nitrate, B = phosphate, C = manganese, D = iron. Adapted from Wheeler et al. (2021, fig. 6).*

4.3.1.6 Summary

In the context of the local and regional geological setting, the results from the Piper diagram (Fig. 4.2A) for the Early Post-Mining Regional Dataset (D) are largely unsurprising. As this area is dominated by Carboniferous (Mississippian) limestone, including the very pure mudbank carbonate facies belonging to the Waulsortian Limestone Formation, the Ca-HCO$_3$ water type observed in all eight wells is entirely expected. The minor influence of magnesium across all of the samples can be attributed to extensive regional-scale dolomitsation of carbonate bedrock along the Rathdowney Trend (Figs. 1.2 and 1.8; see also Wilkinson and Hitzman, 2015). The higher levels of sulphate seen in CW-01 are likely due to the relative proximity of this particular well to the Lisheen ore deposit (e.g. Toran, 1987; Leybourne *et al.,* 2002; Caritat *et al.,* 2005), and possibly also to the tailings management facility on the surface (Fig. 4.1). Additionally, as the regional groundwater flow direction is broadly from NNW to SSE, CW-01 is positioned directly and quite proximally downstream from the mine.

Using the CoDA ilr-ion approach (Shelton *et al.,* 2018), the sample locations can be further discriminated (Fig. 4.2B). In particular this plot indicates the secondary anion of importance in wells CW-01 and CW-02 is sulphate, highlighting the increasing influence of sulphide dissolution with greater proximity to the ore deposit. Additionally, the plot strongly discriminates well SH from the rest in terms of calcium/magnesium ratio. It is likely that the groundwater at this particular location was not in contact with as much dolomitised limestone as groundwater in the other wells. This is intuitive given the location of the well (Fig. 4.1) relative to the bedrock geology (see Fig. 1.8) and also considering the direction of groundwater flow (broadly NNW to SSE).

The influence of the regional-scale groundwater flow at Lisheen becomes more apparent when considering the three groupings resolved by the HCA (Fig. 4.3). Cluster **G1** includes the wells either peripherally located outside of the 'ore shadow' (SH and MM) or slightly upstream (in groundwater terms) from the mine itself (Fig. 4.1). This grouping thus most likely represents a best approximation for a regional baseline groundwater chemistry signal. Clusters **G2a** and **G2b** consist of all wells located downstream from the main ore deposit (Fig. 4.1), and may be geochemically influenced by the mineralisation or associated lithology and geological structures at Lisheen. Subgrouping **G2b** reflects how chemically distinguishable CW-01 is from the wells in cluster **G2a**. CW-01 is distinguished by elevated sulphate concentrations,

interpreted as a product of sulphide oxidation reactions at this location, immediately adjacent to the Lisheen ore deposit.

CoDA analysis provided significantly more detail in terms of recognising important variations in the overall geochemistry of groundwater in the Lisheen area, in addition to assessing how each sample location and particular samples vary over time (Figs. 4.3 and 4.4). It is worth noting that the variations seen from the results of CoDA may not represent any significant change in the absolute measured values for the elements and compounds in question, but rather their relative change with respect to the entire dataset. Although CoDA is a powerful data exploration tool for identifying important elements and compounds controlling variation, the interpretation of geochemical processes should be carried out in combination with additional data for dissolved species that are particularly sensitive to some geochemical processes, such as redox changes (e.g. Fig. 4.5).

The CoDA PCA output (Table 4.2) shows the most important variables (the 1st principal component, representing 72% of variance) to be the anti-correlated nitrate (positive) and manganese (negative). Both of these parameters are generally highly sensitive to redox controls (nitrate survives only in relatively oxygenated waters and manganese is soluble in sub-oxic to anoxic waters - e.g. McMahon *et al.,* 2019).

Dissolved oxygen data plotted against nitrate and manganese (Fig. 4.5A and 4.5C, respectively) shows that redox is most likely an important overall control on groundwater chemistry at Lisheen. Specifically, wells SH and PF contain oxygenated water that represents a high level of surface interaction and rapid recharge; thus retaining nitrate (e.g. Burow *et al.,* 2010). Wells CW-01, JM and PH, by contrast, have sub-oxic to anoxic groundwater with higher concentrations of manganese. The likely explanation for these reducing conditions is the oxidation of electron acceptors such as sulphide minerals associated with ore (e.g. sphalerite and galena).

The 2nd principal component (10% of variance) is primarily controlled by ammonium. Again, redox reactions may be the most important controlling factor here, as nitrogen is generally present as the ammonium ion in less oxic groundwater (e.g. Schullehner *et al.,* 2017). Wells JM and CW-02 for example have the highest concentrations of ammonium (0.14 – 0.33mg/l) and relatively low concentrations of dissolved oxygen (0.4 – 4.5mg/l).

The 3rd principal component (6% of variance) is defined primarily by apparently anti-correlated sulphate and potassium. The sources of sulphate are likely to be geogenic in nature and

associated with mineralising structures around the Lisheen ore deposit (e.g. Wilkinson *et al.,* 2005). Despite being found at low concentrations, the relative differences in potassium between the wells identified by CoDA may be attributed to leaching from fertilised soils (e.g. Alfaro *et al.,* 2004).

Visual representation of this data in the form of a CoDA bi-plot (Figs. 4.3 and 4.4) allows for further interpretation of the Lisheen data by incorporating each sample as an observation point with vectors (red lines) as variables (elements and compounds) and axes as principal components. With the exception of well PH, the discrete clustering of samples from the same wells indicates that the groundwater chemistry is unique at each location and has not changed appreciably over the sampling and monitoring period.

Broadly speaking, samples to the left of the y-axis (particularly above the x-axis) in Figure 4.3 (i.e. CW-01 and CW-02) have a chemistry that is, to a certain extent, influenced by the presence of a significant base-metal mineral deposit close by. Samples to the right of the y-axis and particularly below the x-axis (e.g. MM, PF, FC and PH), are more likely influenced by a higher level of surface interaction, particularly with fertilised soils. In the case samples from well FC, high nitrate levels occur despite relatively low levels of dissolved oxygen (Fig. 4.5A), perhaps indicating recent local inputs of fertiliser-derived nitrate that has not yet undergone denitrification.

The three sample wells clustered as **G1** using HCA, and considered as potentially reflecting a 'background' groundwater chemistry signal, all plot on the far right of the bi-plot (Fig. 4.3). Groundwater wells can, of course, be affected by both proximity to a mineral deposit and also selected land-use practices (e.g. Selck *et al.,* 2018); however, the bi-plot can indicate which influence is the more dominant. It is clear that regardless of the source of chemical elements and compounds, much of the groundwater at Lisheen has been affected by redox reactions.

A closer time-lapse analysis of sample location PH shows how the chemistry of this particular well has gradually become slightly more influenced by mineral deposit-related geochemistry throughout the 11-month sampling period (Fig. 4.4). This well is located on the eastern margin of the 'ore shadow', based on regional groundwater flow and it is interesting that it provides perhaps the only evidence of a chemical response from the rebounding groundwater levels following mine closure (Section 1.3.2).

As the cone of depression from pumping shallows, there may be a change in the source of groundwater to location SH, which is then reflected in the temporal variability of the geochemistry. This is particularly true given the rapid rate of the rebound. Another possibility is that the variation is a reflection of changes in recharge across the seasons. However, this is less likely given that similar changes are not seen in any of the other wells.

Relatively oxygenated groundwater from wells SH and PF are likely high in nitrates due to interaction with surface drainage and rapid recharge through the subsurface (Fig. 4.5A), whereas the presence of phosphate in well MM (Fig. 4.5B) may indicate that the nitrogen there is related to some artificial or anthropogenic input such as fertilizer (e.g. Alfaro *et al.,* 2004). This may also explain the variation within some of the PH samples, as four of these have elevated phosphate. Other groundwater wells with sub-oxic conditions further demonstrate the importance of redox reactions in defining water chemistry in the Lisheen study area. Manganese and iron are both sensitive to the availability of dissolved oxygen (e.g. Sundby *et al.,* 1986), and at Lisheen this is evident with elevated concentrations of these elements in wells that are anoxic to sub-oxic such as CW-01, JM and to a lesser extent, PH and CW-02 (Fig. 4.5C and 4.5D).

4.3.2 Recent Post-Mining Regional Dataset (**E**)

4.3.2.1 Overview

An additional ten samples were taken at various groundwater wells in the Lisheen area (Fig. 4.6) between the 14th and 17th of January 2019 (photographs of the sample sites are available in Appendix C). Some of the sample sites correspond to wells that are referenced in the previous section (i.e. LS01 = PH, LS02 = PF, LS03 = MM, LS04 = FC and LS06 = CW01). The remaining locations (LS05, LS07-LS10) are groundwater wells that were originally used to dewater the underground mine and therefore have a direct connection to the mine workings 150-200m below ground level. However, due to the limitations of the peristaltic pump method, groundwater was only sampled from upper 10m in each of these wells with the exception of LS09, where an additional deeper sample was taken using a bailer method to assess the level of hydraulic connection between the deep mine water and shallow groundwater. Unlike other datasets, a breakdown of the parameters and descriptive statistics is not given here as the full dataset is available (Table 4.3).
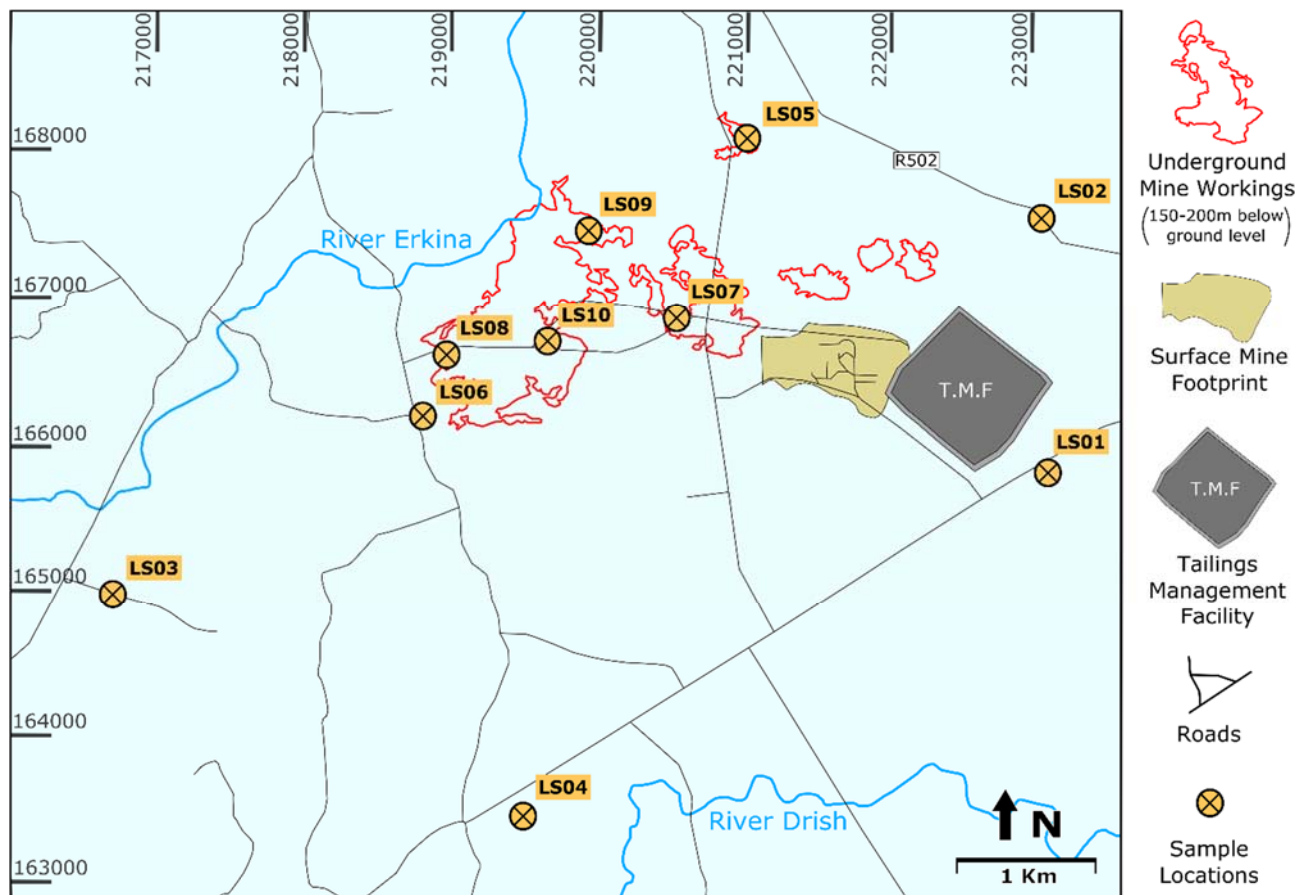
Fig. 4.6: *Geographic map of the Lisheen area showing the location of sample sites for the Recent Post-Mining Regional dataset (E)*

4.3.2.2 Sampling and Analysis

The majority of the Recent Post-Mining Regional dataset (E) samples were recovered using a peristaltic pump and fresh tubing at each location to avoid cross-contamination (see Fig. 2.1). Basic parameters were measured regularly using a YSI probe (YSI Professional Pro Plus Multiparameter Meter) until the readings (e.g. electrical conductivity) stabilised. The clean-hand/dirty-hand technique (Section 2.2.5.2) was then used to recover the samples, further mitigating against potential contamination. The groundwater was collected in pre-washed (e.g. Section 2.2.5.1) low density polyethylene (LDPE) bottles which were sealed and stored in separate plastic zip-lock bags.

The following samples were taken at each sample site;

- Three x 60ml LDPE bottles for cation analysis (filtered with a 45µm filter)

- Three x 60ml LDPE bottles for cation analysis (unfiltered)

- Three x 60ml LDPE bottles for anion analysis (unfiltered)

- One x 1L LDPE bottle for alkalinity analysis

The cation samples (six per location) were carefully acidified in the field to 1% trace metal grade nitric acid (i.e. 0.6ml nitric acid was added). Additionally, five blank samples (containing mili-Q deionised water) from randomly selected sample sites were retained for analysis. All samples were then transported to NUI Galway, where they were stored in a refrigerator (4-6°C) for two weeks until laboratory analysis could take place. The ICP-MS method was used for cation analysis and Ion Chromatography was used for anion analysis. Due to a time delay and an unforeseen lack of access to equipment, the samples were not analysed for the presence/concentration of alkalinity.

Analysis of blanks and spikes show that the data for most analytes is well within the expected range of accuracy and precision. A notable exception was aluminium, which was recorded in a number of blank samples at levels that are, in some cases, more than 50% of the value of the real sample. For this reason, caution is taken when making interpretations that include aluminium. For all analytes, the arithmetic mean of the triplicate samples are recorded as the final values (Table 4.3).

Many of the CoDA methods discussed previously require a significant amount of samples in order to make reasonable assumptions about relationships between analytes and/or sample locations. As the Recent Post-Mining Regional Dataset (E) consists of only ten samples, many of these methods are unavailable. However, traditional comparison of analyte concentrations and various other parameter values (e.g. pH, electrical conductivity etc.) still provide significant and useful information about the geochemical conditions of the groundwater in the vicinity of Lisheen Mine.

ID	X	Y	Date	Time	Method	Depth	Temp	Cond	D.O.	TDS:	pH	ORP	Cl	F	NO₃	NO₂	P	SO₄
						(m)	(°C)	(μS/cm)	(mg/l)	(mg/l)		(mV)	(mg/l)	(mg/l)	(mg/l)	(mg/l)	(mg/l)	(mg/l)
LS01	223095	165715	14/01/2019	12:15	PP	5.51	10.5	625	0.4	559	7.26	58.4	10.702	0	3.59	0	0	13.924
LS02	222926	167559	14/01/2019	14:21	B	8.3	9.7	1250	1.3	1157	7.58	229.4	23.611	0	33.991	0	0	13.762
LS03	216658	165035	15/01/2019	09:40	PP	1.03	10.6	1187	1.1	1066	7.22	244.5	14.697	0	22.757	0	4.237	10.62
LS04	219418	163503	15/01/2019	12:00	PP	4.68	10.7	2274	0.9	2034	7.09	244.9	78.164	0	99.749	0	0	35.274
LS05	221003	168094	15/01/2019	14:50	PP	7	10.3	1147	1.2	1033	7.35	270.6	18.936	0	29.914	0	0	17.822
LS06	218761	166238	16/01/2019	12:15	PP	3	10.4	1339	1.3	1209	7.3	230	8.029	0	10.961	3.082	0	45.531
LS07	220526	166851	16/01/2019	14:30	PP	6.3	10.7	1462	0.7	1306	7.4	227	11.513	0	19.598	3.055	0	43.465
LS08	218963	166636	17/01/2019	10:17	PP	1.84	10.5	2055	0.9	1833	7.25	193.3	17.097	0	3.501	0	0	223.117
LS09	219887	167487	17/01/2019	11:21	PP	1.79	9.8	1942	0.5	1781	7.2	-147	17.199	0	2.845	3.287	0	183.787
LS10	219648	166742	17/01/2019	15:13	PP	4.56	10.2	683	1.3	617	8.7	164	10.066	0	3.813	0	0	70.397

ID	Ca	Mg	Na	K	Fe	Mn	Ni	Zn	Pb	U	As	Al	Cu	Si	Sr	B	Se
	(mg/l)	(mg/l)	(mg/l)	(mg/l)	(mg/l)	(mg/l)	(mg/l)	(mg/l)	(mg/l)	(mg/l)	(mg/l)	(mg/l)	(mg/l)	(mg/l)	(mg/l)	(mg/l)	(mg/l)
LS01	124.69	33.95	6.5020	4.0197	2.0344	0.3810	0.0086	0.0026	0.0000	0.0005	0.0010	0.0019	0.0000	2.2650	0.1607	0.0350	0.0002
LS02	114.85	24.04	9.3157	16.598	0.2668	0.0330	0.0030	0.0084	0.0019	0.0005	0.0007	0.0093	0.0015	2.7333	0.1513	0.0372	0.0012
LS03	99.30	26.24	5.4330	4.9977	0.0868	0.0041	0.0027	0.0017	0.0000	0.0005	0.0018	0.0019	0.0010	2.6523	0.0953	0.0366	0.0008
LS04	143.1	32.76	22.025	65.054	0.1312	0.1162	0.0080	0.0007	0.0000	0.0012	0.0004	0.0026	0.0012	3.8050	0.1917	0.0438	0.0005
LS05	97.80	13.59	6.4137	1.1400	0.0924	0.0001	0.0165	0.0109	0.0006	0.0037	0.0009	0.0039	0.0040	1.6383	0.0933	0.0087	0.0026
LS06	105.76	27.57	7.9823	1.2233	0.0962	0.0001	0.0037	0.0046	0.0000	0.0010	0.0001	0.0041	0.0005	2.3087	0.0960	0.0286	0.0016
LS07	118.14	28.03	5.3000	1.8340	0.1286	0.2818	0.0167	0.0260	0.0003	0.0020	0.0005	0.0055	0.0020	2.4947	0.1657	0.0112	0.0009
LS08	160.36	69.9	8.3993	1.8453	0.1668	0.0790	0.0558	0.2070	0.0001	0.0201	0.0014	0.0053	0.0001	1.7070	0.2870	0.0174	0.0008
LS09	152.58	60.89	13.986	5.7800	0.8961	0.3057	0.0045	0.0069	0.0002	0.0067	0.0042	0.0112	0.0000	5.9200	0.2873	0.0302	0.0002
LS10	5.4063	45.762	6.9393	4.2077	0.0026	0.0003	0.0003	0.0015	0.0000	0.0000	0.0006	0.0100	0.0000	0.1467	0.0090	0.0210	0.0001

Table 4.3 *Recent Post-Mining Regional dataset (E) for groundwater samples from the Lisheen area.*

4.3.2.3 Data Analysis

The wells that were sampled in January 2019 can be broadly divided into two groupings:

1) The first group **[G1]** are privately owned groundwater wells (LS01 – LS04), two of which are used primarily to draw water for agricultural purposes (LS02 and LS04), with the remaining two wells used for a domestic water supply (LS01 and LS03), although LS01 has not been in used since the implementation of a Group Water Scheme in the late 1990s.

2) The second group **[G2]** are wells that were originally used for dewatering the underground mine and therefore have a direct connection to the mine workings (LS05 – LS10). Although LS06 was not used for dewatering, but rather drilled prior to mine closure to monitor the effects of the rebounding water table.

G1 wells are dominated by varying proportions of major anions such as: chloride (Cl^-), sulphate (SO_4^{2-}) and nitrate (NO_3^-; see Fig. 4.7). Well LS03 has significantly higher concentrations of chloride and nitrate. This can be attributed to the location of this well, within a working farmyard where contamination from slurry is likely. The presence of a significant concentration of phosphate in LS03 may also be attributed to agricultural contamination, in this case surface water run-off into local aquifers. Sulphate is clearly the most dominant anion in the **G2** wells (Fig. 4.7), highlighting the fact that these wells directly intercept the underground mine workings at depth.

The major cation concentrations are similar across all ten of the wells (Fig. 4.8). Calcium (Ca^{2+}) and magnesium (Mg^{2+}) are dominant, demonstrating the contact of groundwater with carbonate lithologies, some of which are dolomitised. Elevated levels of potassium (K^+) in wells LS02 and LS04 may again be attributed to agricultural contamination as potassium is a common ingredient of many fertilisers (e.g. Akiyama and Yao, 2001; da Costa Mello *et al*., 2018). Interestingly, low calcium concentrations are seen in well LS10. This may be attributed to a difference in elevation and/or soil composition whereby there is reduced groundwater contact with limestone aquifers. However, this explanation would most likely result in a corresponding reduction in magnesium, which is not observed here. Further study is required to definitively account for the chemical concentrations of groundwater at well LS10. However, given the relatively low sulphate concentration, and low concentrations of all measured cations (Table 4.3), the LS10 well would appear to offer a good source of drinking water provided there is no presence of hazardous bacteria.

Proportion of Major Anions
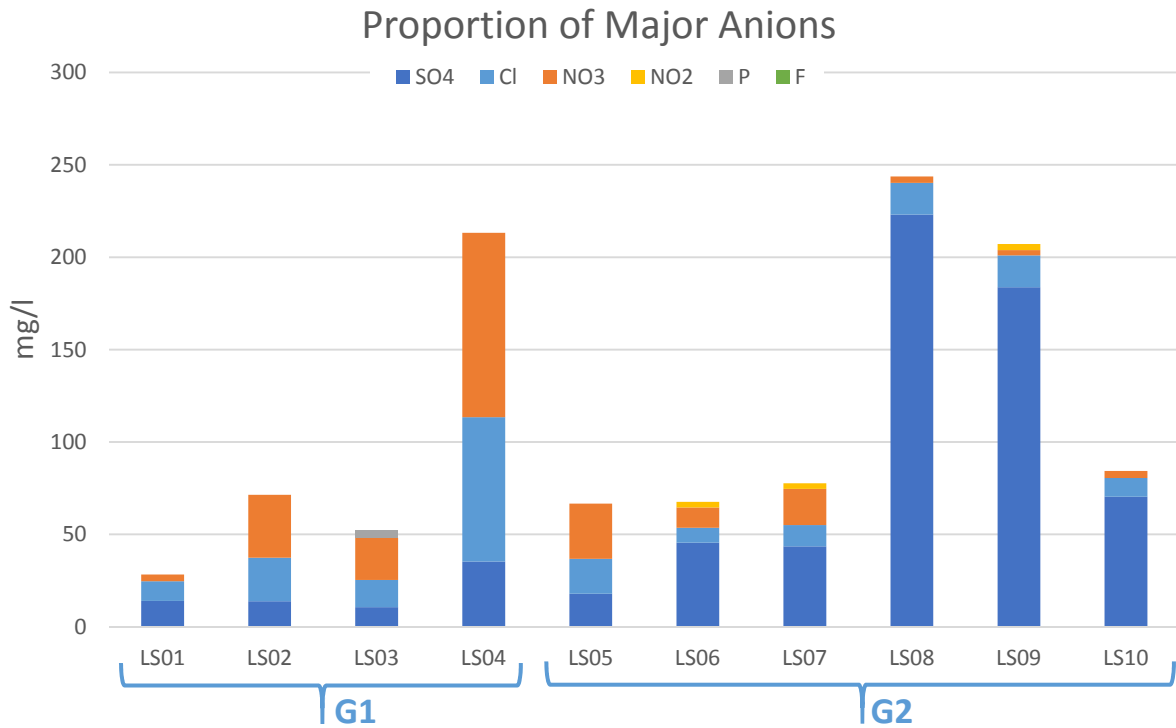
Fig. 4.7: *Stacked bar-chart of Recent Post-Mining Regional Dataset (E) from Lisheen showing the concentrations of major anions in each well.*
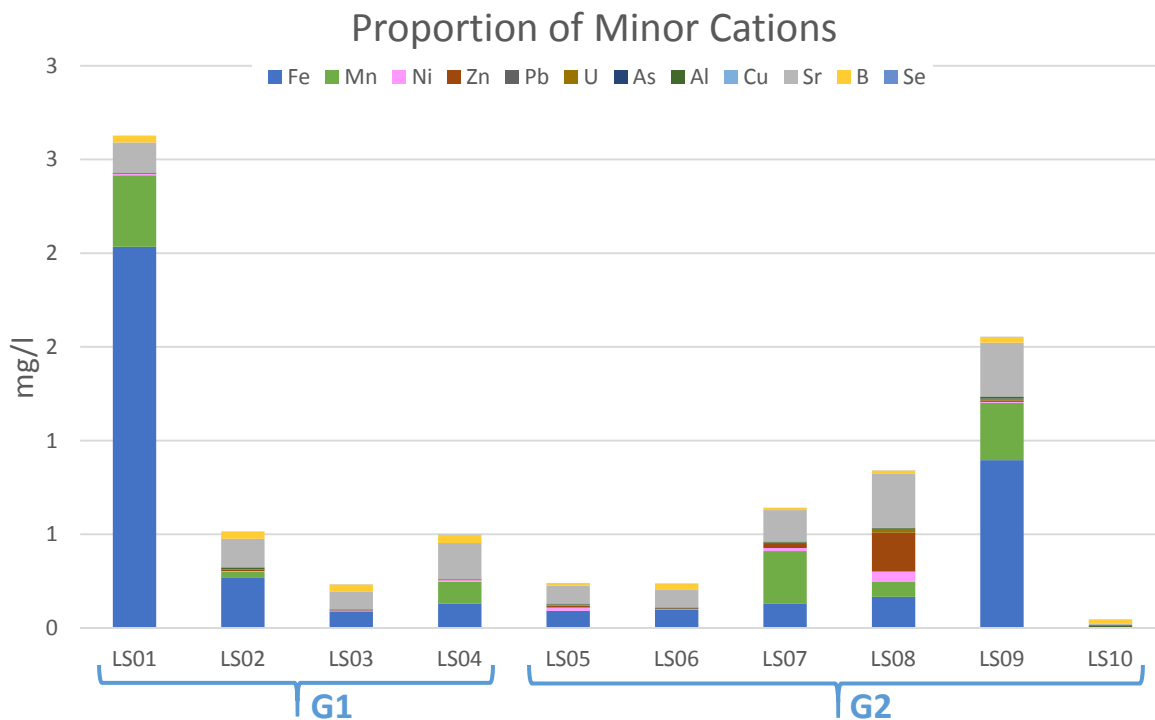
Proportion of Major Cations
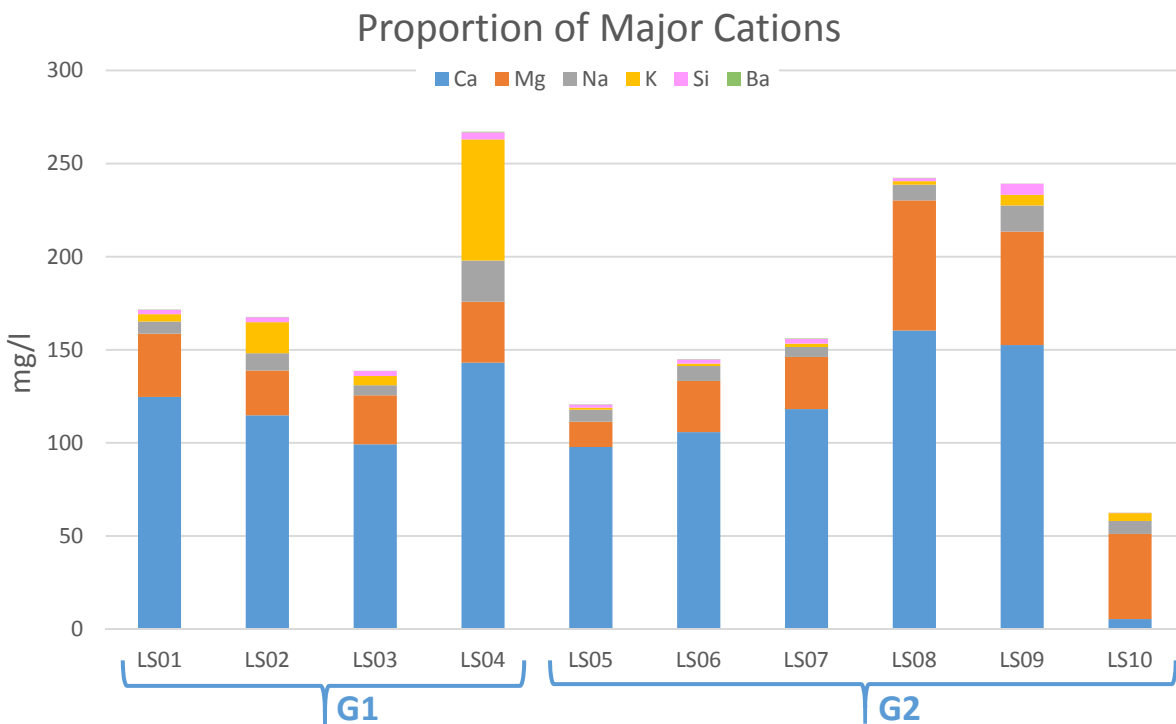
Fig. 4.8: *Stacked bar-chart of Recent Post-Mining Regional dataset (E) from Lisheen showing the concentrations of major cations for each well.*

124

Levels of minor cations (Fig. 4.9) vary across the ten wells sampled. Manganese (Mn^{2+}) concentrations exceed the EU limits for safe consumption in five of the wells (LS01, LS04, LS07, LS08, LS09) and iron ($Fe^{2+/3+}$) concentrations exceed limits in three of the wells (LS01, LS02, LS09). In particular, wells LS01 and LS09 show concentrations of iron and manganese that are indicative of a reducing groundwater environment where Fe/Mn bearing minerals are dissolved.

This is further confirmed by low concentrations of dissolved oxygen (Fig. 4.10) observed in the samples. Levels of zinc (Zn^{2+}) are significant in LS08 which also has the highest calcium and magnesium concentrations suggesting that the groundwater at this location has been in contact with mineralised rock for a relatively longer period of time. None of the analytes measured have high enough values to suggest that any significant contamination has occurred as a result of mine flooding and regional water table restoration since December 2015. This is particularly interesting for the **G2** wells which have a direct connection to the workings below, and suggests that the density model employed at Lisheen for mine water remediation is working effectively.

Proportion of Minor Cations

Fig. 4.9: *Stacked bar-chart of Recent Post-Mining Regional dataset (E) from Lisheen showing the concentrations of minor cations for each well.*

D.O. (mg/l)
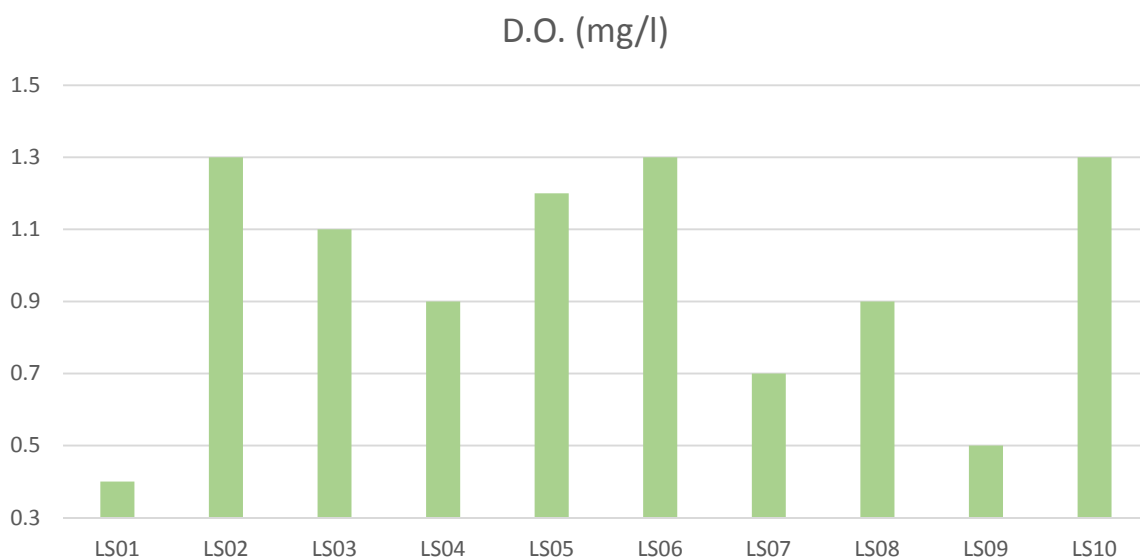
Fig. 4.10: *Dissolved oxygen concentration bar-chart for of Recent Post-Mining Regional dataset (E) sample wells from Lisheen.*

A depth comparison of major cations in well LS09 (Fig. 4.11) shows that overall concentrations of metals decrease with depth, suggesting that mixing between shallow epikarst groundwater [type (i)] and deep mine water [types (ii) and (iii)] is minimised even where there is a direct connection between the waters via the drilled borehole. This is most likely achieved through density and temperature differences in-effect creating vertical stratification that prevents mixing.
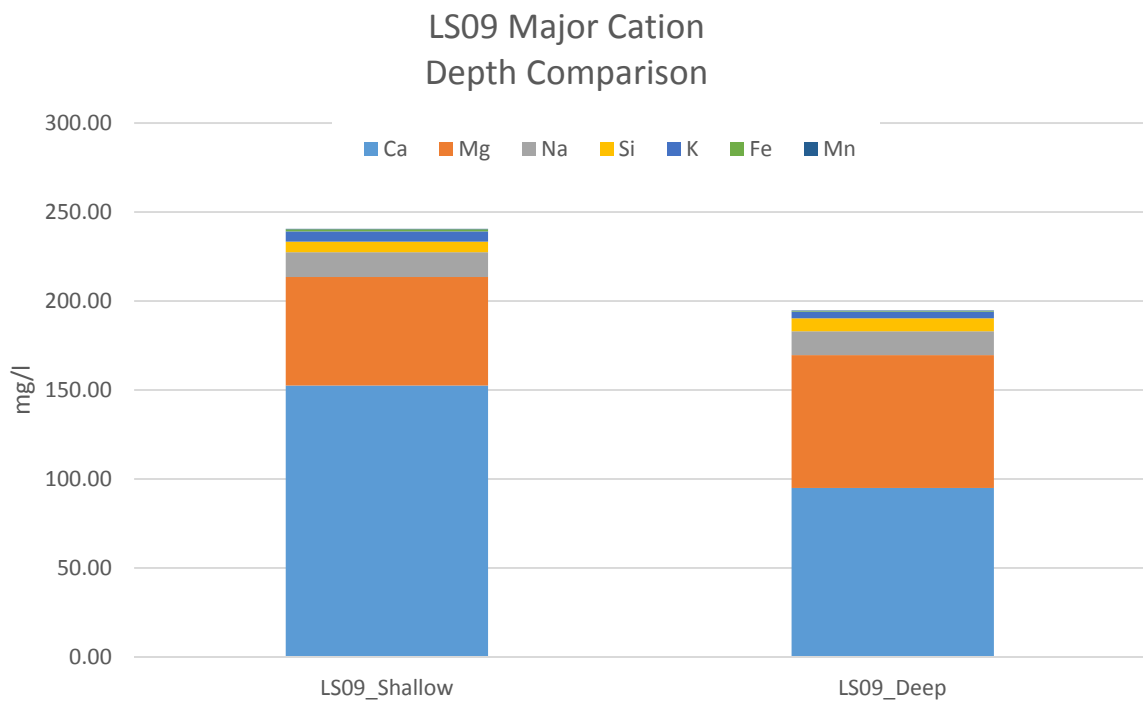
Fig. 4.11: *Stacked bar-chart showing the concentrations of major cations in well LS09 at two different depths (Shallow = 1.8m and Deep = 20m).*

4.3.2.4 CoDA Bi-plot

In the CoDA bi-plot (Fig. 4.12) the 1st principal component on the x-axis and 2nd principal component on the y-axis, represent 43% and 21% of the total variation within the Recent Post-Mining Regional Dataset (E), respectively. As with some of the data analysed previously, variation of iron and manganese appears to be an important control on geochemical variation. Sample sites LS01, LS09 and LS07 are most associated with these elements, which as previously noted in previous sections, likely represents contact with sub-oxic to anoxic groundwater. The lower-right section of the bi-plot is defined by minor variations of many elements. Again this has been interpreted to indicate baseline groundwater geochemistry. Wells LS02, LS03 and LS10 are therefore understood to have relatively 'clean' groundwater. Sample sites with positive 2nd principal component values (e.g. LS09, LS07, LS06, LS05 and particularly LS08) appear to contain groundwater that has been in some contact with the local mineral deposits as they are associated with variation of Zn, U, Ni and SO_4.
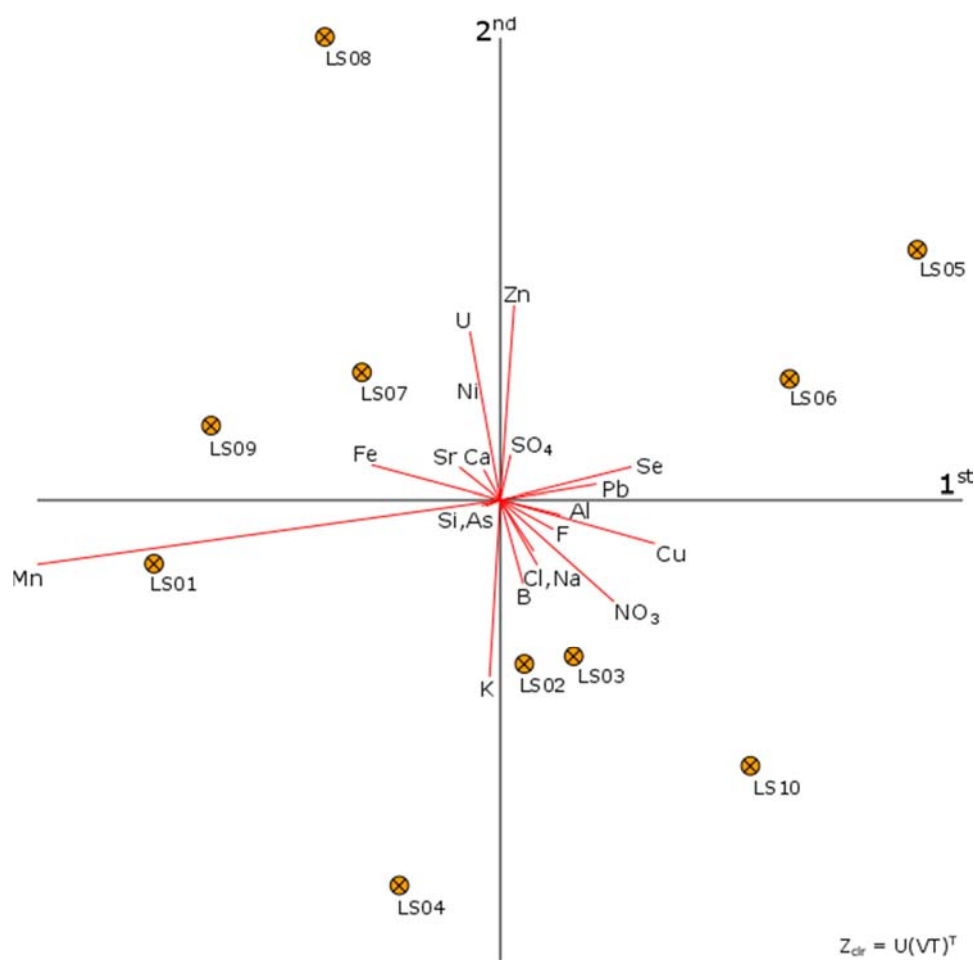
Fig. 4.12: *CoDA bi-plot of the Recent Post-Mining Regional dataset (E) from Lisheen (created using CoDA Pack [Version 2.01])*

4.3.2.5 Summary

The Recent Post-Mining Regional dataset (E) provides the most up-to-date 'snapshot' of the geochemical condition of groundwater in the Lisheen area. Some of the samples were taken directly above and downstream of the flooded mine workings and showed no evidence of mine-waste pollution based on concentrations of a variety of anions and cations. This would indicate that, at least up to January 2019, the remediation works implemented at the time of mine closure, and which continue the time of writing, are working satisfactorily.

A more extreme approach was taken to sampling and analysis techniques for the samples in dataset E (in comparison to datasets A-D). Prewashing LDPE bottles with acids, sampling using a peristaltic pump, implementing the clean hand/dirty hand method and analysing triplicates, were all steps taken to ensure minimal contamination of samples in order to achieve the highest possible levels of accuracy. However, these techniques were labour intensive, expensive and in one case failed to recover a sample without the aid of a bailer. The most ideal groundwater sampling procedure likely compromises one aspect of preparation and/or sampling in order to make it viable in practice.

Some information in the form of carbonate and bicarbonate concentrations were missing from the dataset, which limited the implementation of some methods of statistical analysis such as Piper and ilr-ion plots. However, based on all of the available data so far, it is unlikely that there would be any significant variation of bicarbonate in particular. A more traditional non-compositional data analysis approach was taken initially to compare a case where the CoDA method does not necessarily add greater understanding of the geochemical processes occurring in the groundwater.

In order to compare groundwater flowing directly above the mine workings and a more local baseline, the sample sites were split into two groups:

1) **G1:** a group of four privately owned wells to the east, west and south of the mine, and

2) **G2:** wells constructed as part of the mining process and are believed to be hydraulically connected to the workings below.

Anion and cation concentrations show that iron and manganese concentrations exceed EU drinking water standards in some of the wells from both of these groups. However, this is unlikely to be as a direct consequence of past mining activity, but rather as a result of a

connection with groundwater from a redox reductive state that is naturally stimulating mineral dissolution.

Relative concentration levels of SO_4 are higher in the **G2** wells, highlighting the hydraulic connection with the massive sulphides at depth. However, a sample depth comparison of major cations at location LS09 reveals an apparent reduction in concentrations with depth, suggesting mixing with contaminated mine water is minimal even where there is a direct connection. With the exception of the **G2** wells, groundwater in the Lisheen area is protected from water at depth by the upper parts of the Waulsortian Limestone Formation and the overlying Lower Viséan-aged Crosspatrick Formation (see Fig. 1.9) which are characterised by low hydraulic conductivity where fracture flow via structures is not present.

Using CoDA methods (e.g. CoDA bi-plot; Fig. 4.11) shows many of the same geochemical themes as those already discussed, but does not offer any additional information in this particular instance. However, similar conclusions to those made with a number of bar graphs can be made using a solitary CoDA bi-plot, once again highlighting the practical application of the CoDA method. Sample locations in the bottom part of the bi-plot represent shallow regional groundwater flow (LS02, LS03, LS04, LS10). Wells in the left part of the plot represent a connection with slighter deeper groundwater that may be sub-oxic to anoxic (LS01, LS07, LS09). The remaining observations at the top of the graph represent those wells that have some connection with massive-sulphide mineral dissolution (LS05, LS06, LS08).

4.4 Conclusions

Investigation and analysis of post-mining datasets (D-E) at Lisheen has revealed that relatively little modification of the regional groundwater geochemistry has taken place since the closure of the mine. Although the concentrations of some anions and cations were recorded above the groundwater threshold limits in a number of samples, it could not be conclusively proven that this was as a direct consequence of past mining activity. In fact, datasets A and B analysed in Chapter Three suggest that elemental concentrations exceeding limits are more likely to be the result of pre-existing mineral dissolution, redox reactions and agricultural practices. Nevertheless, analysis of samples from the Early Post-Mining Regional Dataset (D) reveals the strengths of compositional methods for differentiating sample locations on the basis of multivariate geochemistry (see Wheeler *et al.,* 2021).

The ilr-ion plot was again used to analyse the data in Lisheen dataset D. However, in this case, where a strong temporal dataset is available, the benefits of the method are highlighted even further. The most useful CoDA tool however, is the bi-plot. This is demonstrated best in the Early Post-Mining Regional dataset (D) bi-plots (Figs. 4.3 and 4.4) where each sample well can be characterised by a particular geochemical signature, and one well (SH) can be analysed temporally to reveal a fluctuation in chemical signature over time.

In some groundwater geochemistry studies the use of the CoDA method may not be necessary. For example, the Recent Post-Mining dataset (E) can be successfully geochemically analysed by looking at a collection of basic concentration bar-charts (Figs. 4.7-4.11), alleviating the necessity for log-ratio transformation. However, even in this case the geochemical characterisation of the sample locations is well summarised in the bi-plot which also provides an indication of how strongly or not, each location is geochemically related.

In general, CoDA has proven an effective and efficient tool for characterising spatial and temporal hydrogeochemical variation at Lisheen. The previous chapter utilised these methods to identify three distinctive groundwater signatures, one of which (shallow groundwater) was analysed further here. Samples from within even a single grouping can be further distinguished using CoDA, particularly the compositional bi-plot. This is perhaps best exemplified by Figure 4.3, wherein groundwater samples from a very similar source (upper 30m of epikarst – water type (i)) have been *geochemically fingerprinted* to the specific site from which the samples were recovered.

The spatial distribution of any of the Lisheen datasets is not sufficiently dense to map the geochemical characteristics that are identified by the CoDA method. As discussed within the context of the Pre-Mining Regional Dataset and demonstrated in Figure 3.6, the principal component scores that result from CoDA can be extrapolated and mapped. On much larger geographical scales (e.g. regional to national) variation within geochemical datasets generally represents the broad environmental factors that control the distribution of chemical elements (e.g. geology, soil type, land-use). These relationships are explored within the larger-scale GSI Tellus datasets in the following chapter.

Chapter Five: *Geochemistry of the Border Region*

[Analysis and Mapping of Geochemistry Data from the Border Region of Ireland]

5.1 Introduction

Principal component *mapping* is one particular application of Compositional Data Analysis (CoDA), which was only briefly explored in the Lisheen geochemistry datasets in chapters Three and Four. One benefit of using this approach is the capacity to map the distribution of a proxy for a particular process controlling the data (i.e. the cause), rather than showing the distribution of each variable within the dataset separately (i.e. the effect) (Buccianti *et al.*, 2015; Sahoo *et al.*, 2020). For example, in groundwater geochemistry, Principal Component Analysis (PCA) may reveal the 1st principal component of a given dataset to most accurately represent a given water type. *Spatially mapping* the 1st principal component values, rather than the elemental concentrations, provides a more holistic approach to defining the boundaries (which may be fuzzy or gradual) between discrete areas characterised by different water types (McKinley *et al.*, 2016; Kirkwood *et al.*, 2020).

Principal component mapping is regularly used in a variety of compositional studies that have an associated geographical mapping component (e.g. Loughlin, 1991; Tangestani and Moore, 2001; Abson *et al.*, 2012; Nandi *et al.*, 2016; Uddin *et al.*, 2019). However, this method first requires interpretation of what each principal component represents and it is only relatively recently that CoDA methods have been applied to this process (e.g. Buccianti *et al.*, 2015; Thiombane *et al.*, 2018; Sahoo *et al.*, 2020; Somma *et al.*, 2021). In particular, CoDA mapping methods and applications to geochemistry are extensively reviewed by McKinley *et al.* (2016).

As the Lisheen datasets (A-E) are too spatially limited to demonstrate the benefits of CoDA-PCA mapping, a number of geochemical datasets from the Tellus Border Project (described previously in Section 1.4) are used here instead. Specifically, 3467 soil, 3524 stream water and 3607 stream sediment samples (recovered at an approximate interval of one every $4km^2$) from across the border region in the Republic of Ireland (see Fig. 1.13) are analysed below. Datasets from this region were released together as part of a package by the Geological Survey of Ireland in 2013.

5.2 Data Overview

As end-user applications for the Tellus datasets may vary quite considerably (e.g. Appleton *et al.*, 2008; McKinley *et al.*, 2016; Steiner, 2018; Keshavarzi *et al.,* 2021), they are presented as complete matrices of real positive numbers, ready to be used for any designated and required purpose. Any element that cannot be measured in a given sample has already been replaced with half the limit of detection for that particular element. These *censored* values are available, so that they can be easily identified within the dataset if further replacement is necessary. The data was prepared for CoDA analysis using the methods outlined previously in Section 2.5. This section also describes the methods used to add categorical information, regarding soil type, bedrock geology and land-use at each sample location, to each of the datasets. Three geochemical datasets are analysed and mapped here using CoDA methods:

A. **Topsoil Geochemistry Dataset**

The Topsoil dataset was originally composed of 5643 samples recovered at regular intervals across the Tellus Border Region (Fig. 1.13) that were analysed using XRF and ICP-MS methods. Only elemental concentrations (mg/kg) that resulted from ICP-MS were used to avoid overlap within the composition. Following the data preparation methods described in Section 2.5, a dataset of 3467 samples remained containing concentration values for: Ba, Cr, Cu, Li, Mn, Ni, P, Sr, V, Zn, Zr, Ag, As, Be, Bi, Cd, Ce, Co, Cs, Ga, Hg, La, Lu, Mo, Nb, Pb, Rb, Sb, Sc, Sn, Tb, Th, Tl, U, Y, Yb.

B. **Stream Water Geochemistry Dataset**

The Stream Water Dataset was originally composed of 6836 samples that were collected at intervals that were spaced as evenly as possible depending on the natural drainage density and were analysed using a combination of IC and ICP-MS. Following data preparation methods, a dataset of 3510 samples remained containing elemental concentration (mg/l) for: HCO_3^-, Cl^-, SO_4^{2-}, NO_3^-, Br, NO_2^-, HPO_4^{2-}, F, Li, Be, B, Na, Mg, Al, Si, P, S, K, Ca, Ti, V, Cr, Mn, Fe, Co, Ni, Cu, Zn, Ga, As, Se, Rb, Sr, Y, Zr, Nb, Mo, Ag, Cd, Sn, Sb, Cs, Ba, La, Ce, Pr, Nd, Eu, Tb, Gd, Dy, Ho, Er, Tm, Yb, Lu, Hf, Ta, W, Tl, Pb, Bi, Th, U. A portion of this dataset that covers County Louth on the east coast, is examined in greater detail to demonstrate the CoDA process and highlight strong geochemical contrasts.

C. Stream Sediment Geochemistry Dataset

The Stream Sediment Dataset was originally composed of 8861 samples that were collected at intervals that were spaced as evenly as possible depending on the natural drainage density and were analysed primarily using XRF with ICP-MS used for Au, Pd and Pt. Following data preparation methods, a dataset of 3587 samples remained containing analyte concentrations (mg/l) for: Sc, V, Cr, Co, Ni, Cu, Z, As, Se, Br, Rb, Sr, Y, Zr, Nb, Mo, Nd, Sm, Yb, Hf, W, Pb, Bi, Th, U, Sn, Cs, Ba, La, Ce, Au, Pd, Pt.

5.3 Undertaking Compositional Data Analysis (CoDA)

A detailed critical evaluation of numerous CoDA methods for geochemical mapping is provided by McKinley *et al.* (2016). However, for simplicity of presentation to demonstrate the advantages of CoDA-PCA mapping, only the centre log-ratio (*clr*) transformation method (Aitchison, 1986) is used here (Equation 5.1):

$$clr(z) = \left(\ln \frac{z_1}{\sqrt[D]{\Pi_{j=1}^{D} z_j}}, \ldots, \ln \frac{z_D}{\sqrt[D]{\Pi_{j=1}^{D} z_j}} \right) \quad \text{[Equation 5.1]}$$

The software programme 'CoDA Pack' (version 2.01) was used to create compositional bi-plots in the following section by automatically imputing *clr* transformations and implementing PCA through the Singular Value Decomposition (SVD) method. However, for the purposes of mapping, the same computations were completed in the 'R' statistical environment (version 4.0.5) so that the outputs in terms of both scores (i.e. relating to sample points) and loadings (i.e. relating to variables) could be exported to 'ArcGIS Pro' (version 2.7.3). The CoDA bi-plots were created a number of times with different combinations of variables. Those shown and described below, together with accompanying loadings tables, are just one particular combination of variables that appear to describe variability reasonably well.

5.4 Results

5.4.1 Topsoil Geochemistry
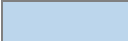
PCA of centre log-ratio (*clr*) transformed Tellus soil geochemistry data shows that almost half of the overall variance (48%) is described by the 1st principal component (Table 5.1).

- A group of elements (**G1** – highlighted yellow) with *highly positive 1st principal component* values include: Mo, Nb, Pb, Cd, and, in particular, Sr, Hg and Sb.

- A second group of elements (**G2** – highlighted orange) with *highly negative 1st principal component* values are anti-correlated to these and include: Li, Cs, Rb, Tb, and, in particular, Cr.

Plotting these data on a *clr* PCA bi-plot (Fig. 5.1A) shows an apparent correlation between **G1** (i.e. positive 1st principal component values) and locations classified as 'Blanket Peats'. Seventy-two percent (72%) of samples classified as 'Peats' (i.e. blanket peat and cut peats in this area) by Teagasc (the Irish Agriculture and Food Development Authority) have positive 1st principal component values. All other soil categories have stronger correlations with **G2** (i.e. negative 1st principal component values). A spatial variability map of the 1st principal component (Fig. 5.1B) clearly, and satisfactorily, delineates and highlights areas mapped as 'Peats' using traditional identification methods (Fig. 5.1C). The 2nd principal component accounts for 9% of the total variability within the topsoil dataset. Elements responsible for controlling variance of the 2nd principal component are: Sr, Ce, La, Nb, Th and U, with anti-correlated Cu, Li, Mn, Ni, Zn and Co. The 2nd principal component does not definitively correlate with any particular Teagasc classified soil types on the bi-plot (Fig. 5.1A).

	PC1	PC2		PC1	PC2
Ba	0.0165	-0.032	Cs	-0.184	0.0896
Cr	-0.259	-0.161	Ga	-0.086	0.0472
Cu	-0.032	-0.246	Hg	0.2864	0.0449
Li	-0.199	-0.287	La	-0.142	0.2197
Mn	-0.033	-0.223	Lu	-0.153	0.1477
Ni	-0.083	-0.276	Mo	0.1895	-0.053
P	0.1376	-0.055	Nb	0.1878	0.4013
Sr	0.2999	0.2909	Pb	0.2357	-0.111
V	-0.026	-0.027	Rb	-0.195	-0.028
Zn	0.0972	-0.217	Sb	0.3056	-0.143
Zr	0.0534	0.0667	Sc	-0.088	-0.011
Ag	0.1597	0.0755	Sn	0.1952	-0.064
As	0.063	-0.165	Tb	-0.183	0.1635
Be	-0.134	-0.012	Th	-0.19	0.2138
Bi	0.1941	0.0104	Tl	-0.049	-0.029
Cd	0.2154	-0.107	U	-0.01	0.2135
Ce	-0.157	0.1983	Y	-0.132	0.1301
Co	-0.152	-0.203	Yb	-0.15	0.138
Cumulative Proportion Explained				**0.4824**	**0.5682**

Table 5.1: CoDA PCA loadings output from Tellus Border Topsoil geochemistry database.

	= *high negative PC1*
	= *high positive PC1*
	= *high negative PC2*
	= *high positive PC2*
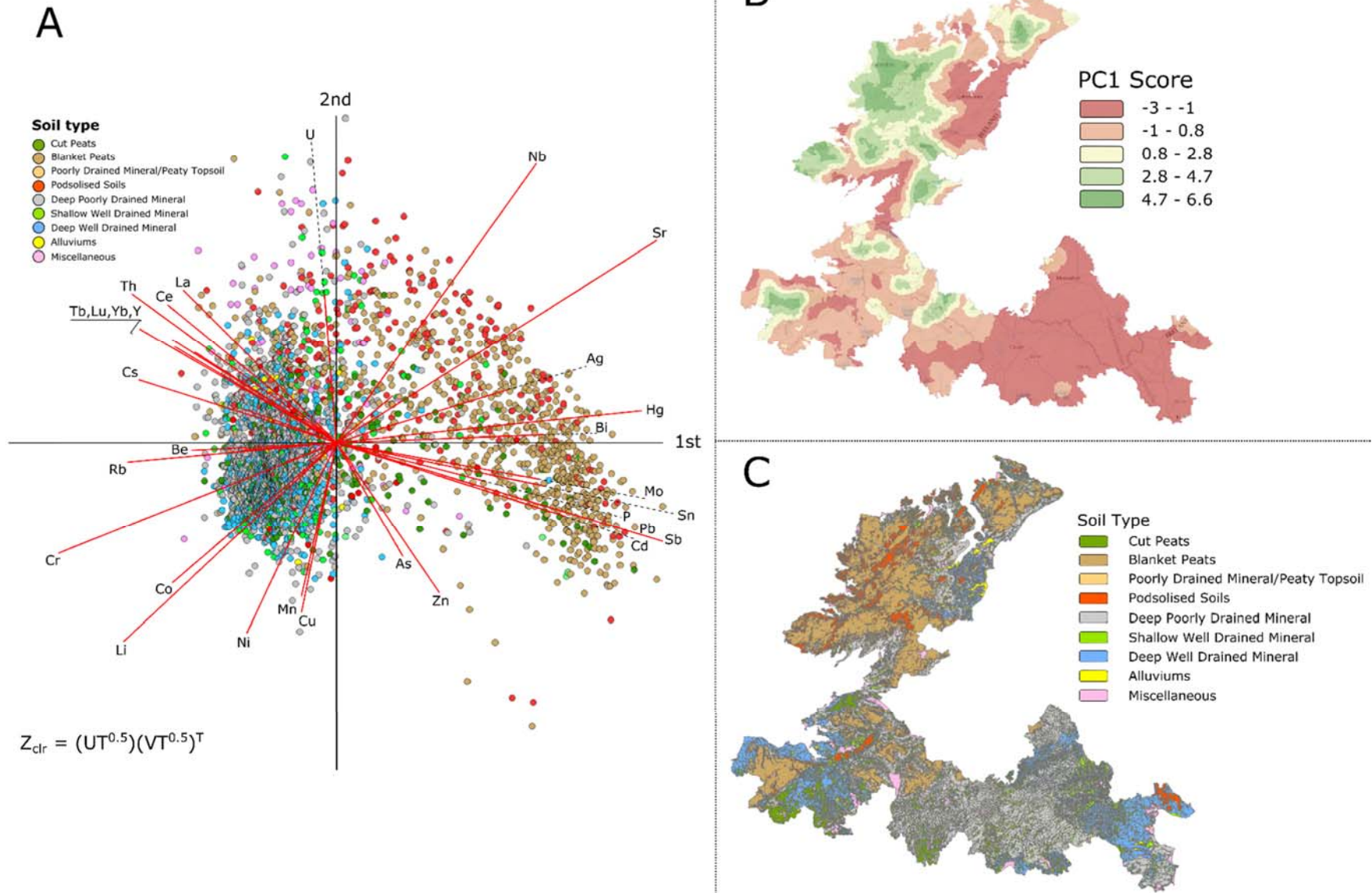
Fig. 5.1: A) *Compositional Data Analysis bi-plot of Tellus Border Topsoil geochemistry data, colour coded by soil classification at the given sampling location.* **B)** *Interpolated map of the 1st principal component (PC1) scores using kriging method.* **C)** *Teagasc Soil Type Map. Note: correlation between high PC1 scores in B and 'Blanket Peats' in C.*

5.4.2 Stream Water Geochemistry

5.4.2.1 Stream Water Geochemistry of the Tellus Border Region

Centre log-ratio PCA of the full Tellus stream water geochemistry dataset from the border region shows 49% and 8% of variability within the data is represented by 1st and 2nd principal components, respectively (Table 5.2). Strong positive associations in the 1st principal component are HCO_3^-, Ca, Sr, U and particularly NO_3^-, with apparently anti-correlated strong negative associations including Al, La, Ce, Pr, Nd and Pb. The 2nd principal component in the stream water dataset has strong positive correlation between NO_3, Ni, and Cu and negative correlations between Cl, Na, Sn, Tl and, particularly, Cs (Table 5.2).

The chemistry of stream water across the Tellus Broder Region broadly distinguishes the counties in the north and west (Donegal, Sligo and Leitrim) from those in the midlands and east (Cavan, Monaghan and Louth) (Fig. 5.2A1-A2). The former group of counties are underlain by Dalradian (largely Neoproterozoic) metamorphic rocks, Caledonian granites and Upper Paleozoic sedimentary rocks, whereas the latter group are underlain largely by Lower Paleozoic metasedimentary rocks and Upper Paleozoic sedimentary rocks (Fig. 5.2B2). Altering the display parameters of the observations (i.e. colour of sample points on the bi-plot) reveals the same chemical variation to be correlated with a number of natural environmental conditions such as bedrock geology, soil type and land-use practices (Fig. 5.2).

Extremely positive 1st principal component values appear to be correlated to a particular area of County Louth (Fig. 5.2A2) that has a land-use classification of 'non-irrigated arable land' (EEA, 2019). This category is defined as:

"Cultivated land parcels under rainfed agricultural use for annually harvested non-permanent crops, normally under a crop rotation system, including fallow lands within such crop rotation. Fields with sporadic sprinkler-irrigation with non-permanent devices to support dominant rainfed cultivation are included"

by the European Environment Agency (2019). This is significantly different from the other major land-use classifications in the Tellus Border Region study area, which largely fall under Peat, Pasture, or a Agricultural/Natural vegetation mix.

However, the strongest distinguishing factor appears to be associated with the nature of the underlying bedrock geology (Fig. 5.2B1). When classified in terms of the broadest geological groupings, the 1st principal component separates sedimentary rock lithologies on the right of

the bi-plot from everything else on the left. Additionally, the 2nd principal component segregates the igneous geology in the bottom-left of the plot from the rest. It is therefore possible to distinguish the source areas of the three major geological groupings (igneous, metamorphic and sedimentary rocks) based on the geochemistry of stream water samples. Generally, the bedrock geology of the Tellus Border Region consists of siliciclastic and carbonate sedimentary rocks in low lying areas, and more resistant felsic igneous intrusives and metamorphic rocks in areas of higher elevation (e.g. County Donegal in the north-west) (see Fig. 1.13A/B).

Categories can also be made on the basis of the broad chronostratigraphic classifications of when the rocks were formed (Fig. 5.3A):

- The sedimentary rocks that dominate most areas outside of County Donegal are generally Lower Paleozoic (Ordovician or Silurian; e.g. Hutton and Murphy, 1987; Williams and Harper, 1988) or Upper Paleozoic (predominantly Carboniferous; e.g. Sevastopulo and Wyse Jackson, 2009; Somerville and Waters, 2011a, 2011b) in terms of age, *whereas*

- Neoproterozoic metamorphic rocks underlie much of County Donegal (e.g. Daly, 2009 and references therein), and are also known from a small area immediately west of the town of Manorhamilton in County Leitrim.

- Caledonian intrusive igneous rocks occur in County Donegal (termed the Donegal Granite; e.g. Pitcher *et al.,* 1958; Hutton, 1982; Pitcher and Hutton, 2003), with a smaller intrusive occurring at Croossdoney, southwest of Cavan Town in County Cavan (Skiba, 1952; Kennan, 1979).

CoDA-PCA mapping (Fig. 5.3B-C) reveals a strong correlation between the 1st principal component and geological classification.

clr	PC1	PC2	clr	PC1	PC2
HCO$_3$	0.30	-0.01	Y	-0.10	0.09
NPOC	-0.04	-0.08	Zr	-0.03	0.15
Cl	0.05	-0.23	Nb	0.02	-0.08
SO$_4$	0.15	-0.08	Mo	0.15	0.03
NO$_3$	0.37	0.26	Cd	-0.01	0.04
Br	0.07	-0.16	Sn	0.00	-0.21
Li	0.09	-0.17	Sb	0.10	0.00
Be	-0.07	-0.07	Cs	-0.04	-0.46
Na	0.05	-0.22	Ba	0.18	0.09
Mg	0.15	-0.11	La	-0.16	0.07
Al	-0.18	-0.14	Ce	-0.20	0.05
Si	0.10	-0.06	Pr	-0.17	0.09
P	0.08	0.18	Nd	-0.19	0.12
S	0.15	-0.07	Sm	-0.14	0.10
K	0.15	0.01	Eu	-0.12	0.10
Ca	0.25	0.09	Tb	-0.12	0.11
Ti	-0.15	-0.12	Gd	-0.14	0.11
V	-0.03	-0.13	Dy	-0.12	0.10
Cr	0.00	0.01	Ho	-0.11	0.10
Mn	-0.02	0.11	Er	-0.10	0.09
Fe	-0.17	-0.01	Tm	-0.08	0.10
Co	-0.05	0.13	Yb	-0.08	0.09
Ni	0.05	0.23	Lu	-0.06	0.10
Cu	0.04	0.19	Hf	-0.01	0.00
Zn	-0.08	-0.13	Tl	-0.01	-0.22
As	0.03	0.03	Pb	-0.19	-0.10
Se	0.06	-0.09	Th	-0.12	-0.01
Rb	0.07	-0.08	U	0.22	0.00
Sr	0.21	0.05	**Cum.Prop.Exp.**	**0.49**	**0.57**

Table 5.2: *CoDA PCA loadings output from Tellus Border Stream Water geochemistry dataset:*

	= high negative PC1
	= high positive PC1
	= high negative PC2
	= high positive PC2
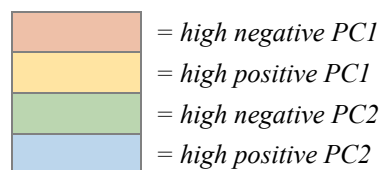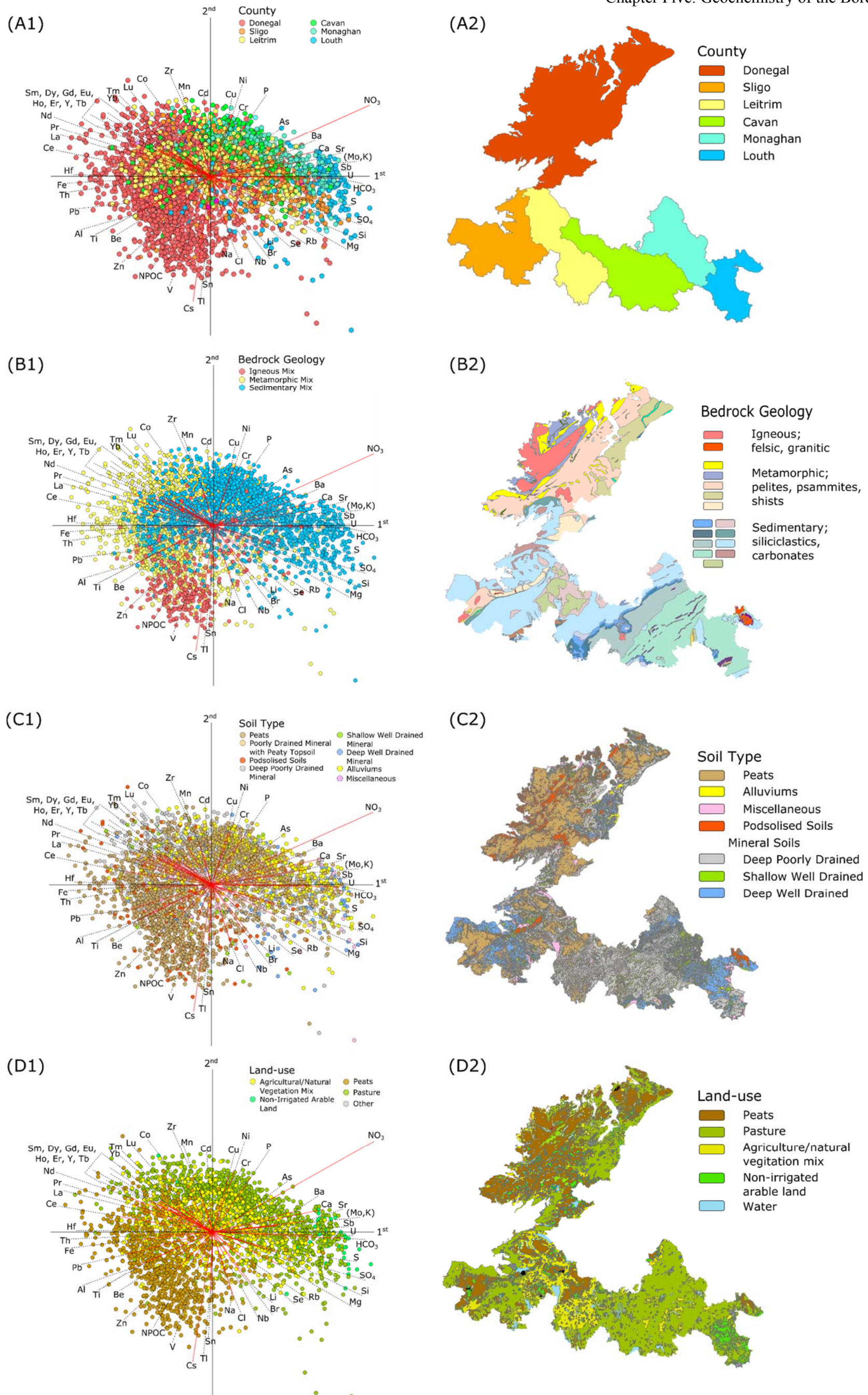
Fig. 5.2: Compositional Data Analysis bi-plots of the Tellus Border Stream Water geochemistry dataset with categorical information changed each time to reflect the varying environmental factors described by the corresponding maps for **A)** Counties, **B)** Bedrock Geology, **C)** Soil Type and **D)** Land-use. Note the gradual variation in water chemistry from left to right in the bi-plot **(A1)** and from east to west on the map **(A2)**. Igneous rocks in the north-west of Donegal **(B2)** are particularly well characterised by a specific chemistry **(B1)**. Soil types are more difficult to distinguish on the bi-plot **(C1)** but generally follow the same latitudinal trend **(C2)**. Different land-use practices also appear correspond to specific chemistries **(D1)** and extreme positive 1st principal component values relate to Non-irrigated arable land **(D2)**.

141
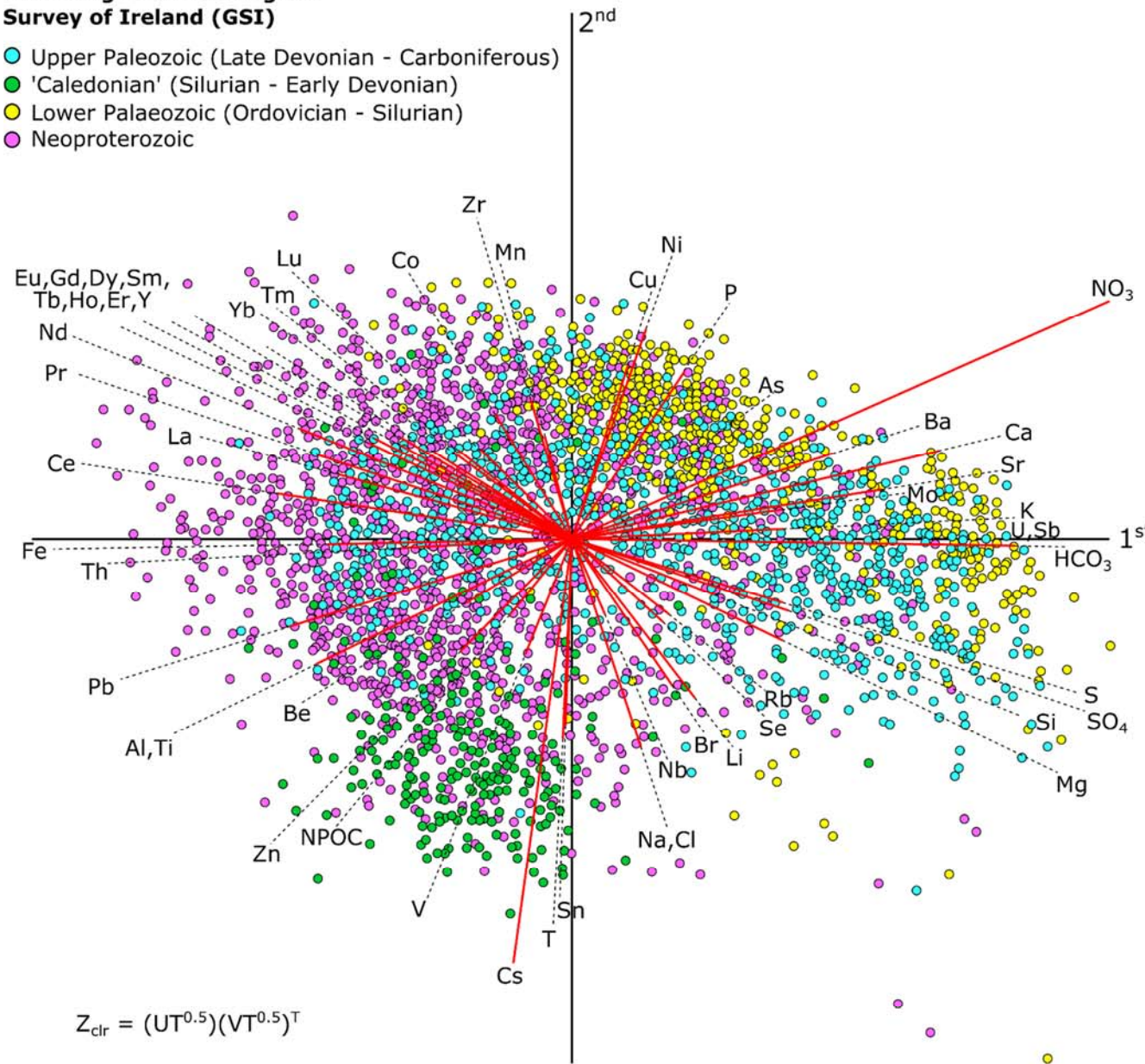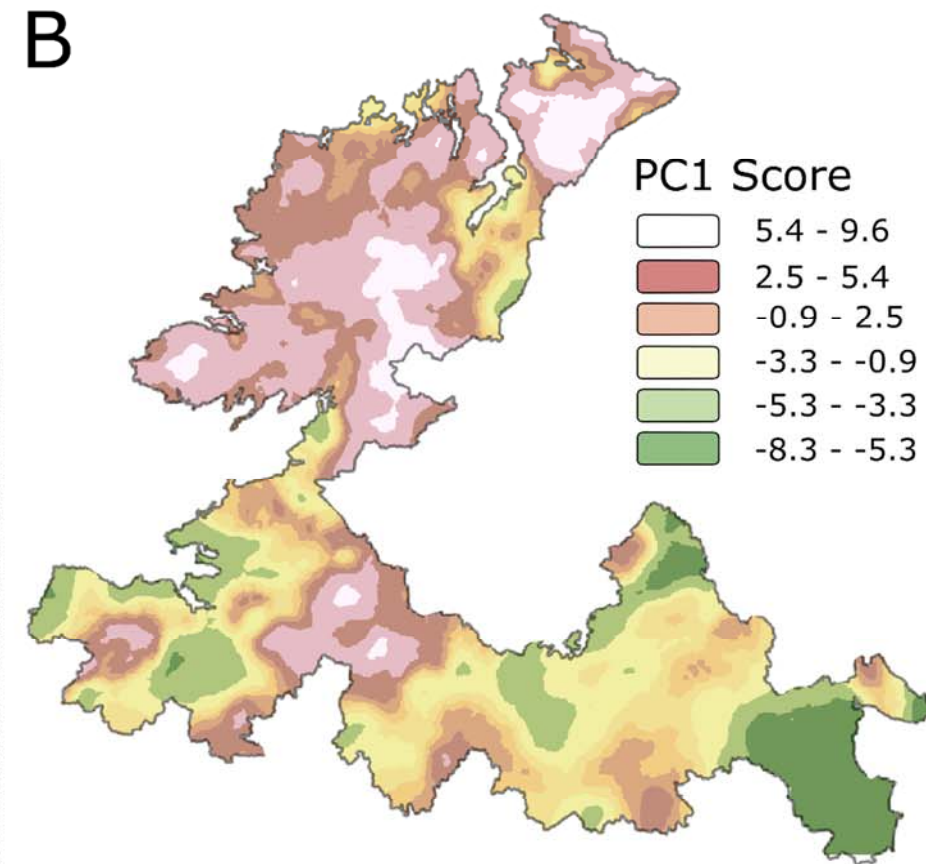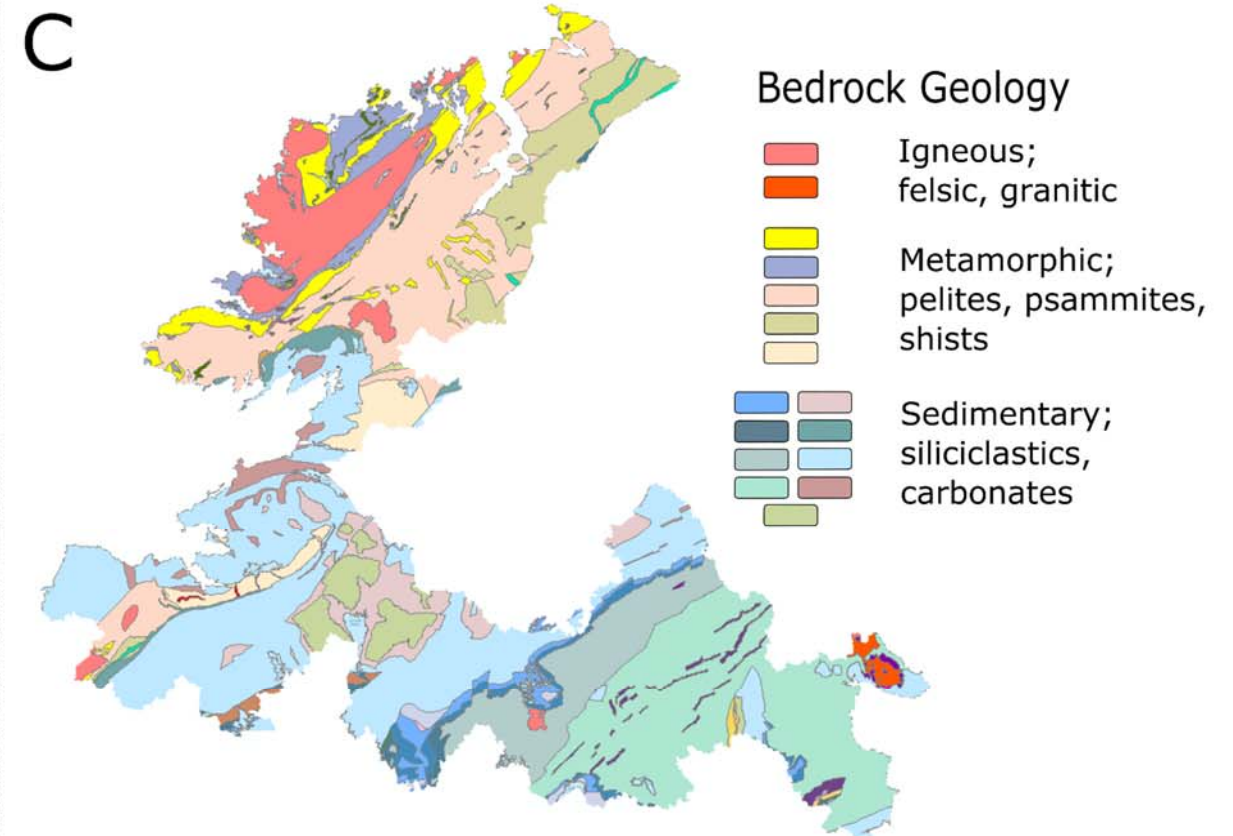
Fig. 5.3: A) Compositional Data Analysis bi-plot of Tellus Border Stream Water geochemistry data, colour coded by chronostratigraphic classification of the bedrock at the given sampling location. B) Interpolated map of PC1 scores using kriging method. C) GSI Bedrock Geology Map. Note: visual correlation between low PC1 scores in B and Paleozoic sedimentary rock lithologies in C.

5.4.2.2 Stream Water Geochemistry of County Louth

County Louth (see; Fig. 5.2A2 for general location) is positioned on the eastern margin of the GSI Tellus Border dataset and it displays particularly strong contrasts in terms of the 1st principal component scores with very high values in the far north of the county and some of the lowest scores in the border region in the rest of the county (Fig. 5.3B). For this reason, it has been chosen as a good test location to demonstrate, in greater detail, the CoDA process that culminates in the creation of a principal component map. As mentioned previously, bedrock geology is the primary control on the composition of soils which in turn is a control on land-use practices (Fig. 5.4A). In northern County Louth the geochemical variation between rock types has also been identified as an important factor for geogenic sources of arsenic in groundwater (e.g. Russell *et al.*, 2021).

The composition of the underlying bedrock also appears be the most important influence on the geochemistry of stream water. In this case, interpolated concentration maps are used to visually correlate between water geochemistry and geology (Fig. 5.4A&B). CoDA PCA considers the variation within a large number of variables simultaneously. The resulting scores can be mapped and interpolated (Fig. 5.3B and 5.4C).

This process results in a final map of the most dominant geochemical variations in the region that represents a combination of several aspects of variability. For example, the stream water geochemistry associated with the Paleogene igneous granophyre intrusion in the north of the county (e.g. McDonnell *et al.,* 2004; Troll *et al.,* 2005; Russell *et al.,* 2021) has comparatively high levels of caesium and low levels of calcium, uranium, nitrate and strontium (Fig. 5.4B). These variables, together with 61 others in this case, all contribute to showing the very pronounced stream water geochemical contrast between the two geological terrains (i.e. Paleogene igneous and Ordovician/Silurian/Carboniferous marine sedimentary rocks) (Fig. 5.4C).
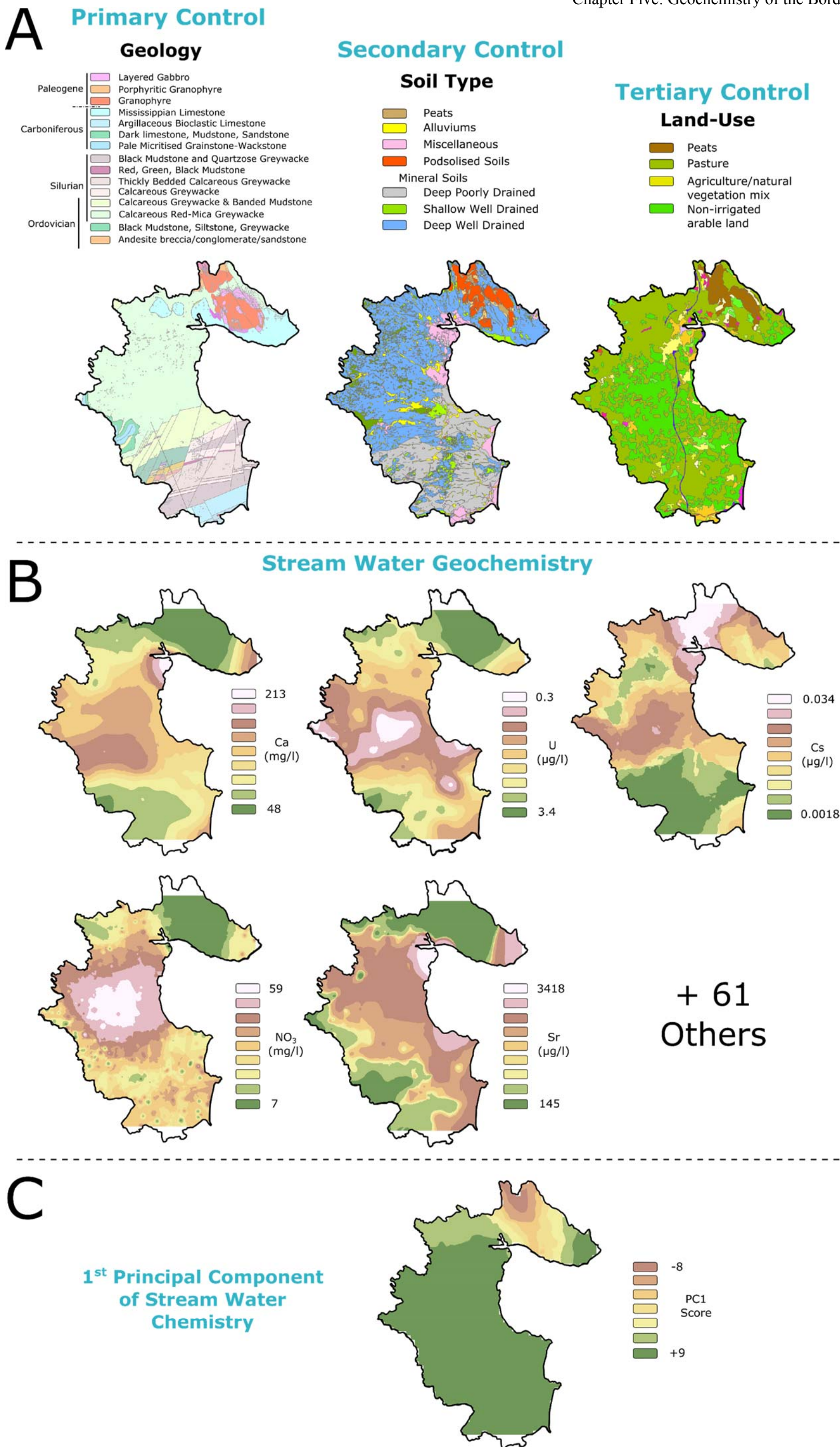
Fig. 5.4: A) Maps of County Louth showing bedrock geology (Geological Survey Ireland), soil type (Teagasc) and land-use (Environmental Protection Agency), **B)** Examples of interpolated maps of variable concentrations (Ca, U, Cs, NO_3 and Sr), **C)** Principal component map of County Louth showing the high contrast between the geochemistry in the north and the rest of the county.

5.4.3 Stream Sediment Geochemistry

When the same CoDA approach is applied to stream sediment geochemistry data from the Tellus Border Region the 1st and 2nd principal components account for just 21% and 15% of variance, respectively (Table 5.3) and significantly less correlation is evident among the variables. Important elements in terms of separating samples based on relative abundance for both main principal components are:

- **1st principal component**: Cr and Ni with anti-correlated Se, Mo and particularly I and Br.

- **2nd principal component**: well-correlated elements are; Zr and Hf, which are anti-correlated to Ni, Cu, As, Se, Mo, Au, Pd and Pt (Table 5.3).

The resultant PCA bi-plots (Fig. 5.5A1, B1, C1 and D1) indicate that the spatial distribution of stream sediment geochemistry within the Tellus Border Region is, again, largely dependent on physical characteristics, particularly the underlying bedrock geology (Fig. 5.5B1-B2).

However, any interpretation of these bi-plots is questionable given the total variance displayed is only 36% for both the 1st and 2nd principal components combined. For this reason CoDA-PCA mapping is not attempted here as the principal components are not accounted for by any known categorical factor (e.g. soil type, geology etc.) nor geochemical process worth mapping.

clr	PC1	PC2	clr	PC1	PC2
Sc	0.1227	-0.034	Sm	0.0617	0.0804
V	0.094	-0.065	Yb	0.034	0.125
Cr	0.2226	-0.08	Hf	0.0722	0.357
Co	0.0703	-0.132	W	0.0825	0.1379
Ni	0.2106	-0.262	Pb	-0.08	0.0132
Cu	0.114	-0.232	Bi	-0.005	0.1254
Zn	0.0479	-0.142	Th	0.0178	0.136
Ga	0.0943	0.0636	U	-0.14	0.0127
As	-0.035	-0.299	Sn	-0.017	0.1084
Se	-0.39	-0.203	I	-0.468	0.0506
Br	-0.574	0.1234	Cs	0.0872	-0.05
Rb	0.1075	0.1305	Ba	0.0802	0.1223
Sr	-0.062	0.0558	La	0.0465	0.0944
Y	0.0338	0.0801	Ce	0.0332	0.0992
Zr	0.0936	0.3509	Au	0.0258	-0.205
Nb	0.0841	0.1564	Pd	0.012	-0.237
Mo	-0.212	-0.239	Pt	0.1144	-0.304
Nd	0.0165	0.0587	**Cum.Prop.Exp.**	**0.2069**	**0.3576**

Table 5.3: *CoDA PCA loadings output from Tellus Border Stream Sediment geochemistry dataset:*

    ■ = *high negative PC1*
    ■ = *high positive PC1*
    ■ = *high negative PC2*
    ■ = *high positive PC2*
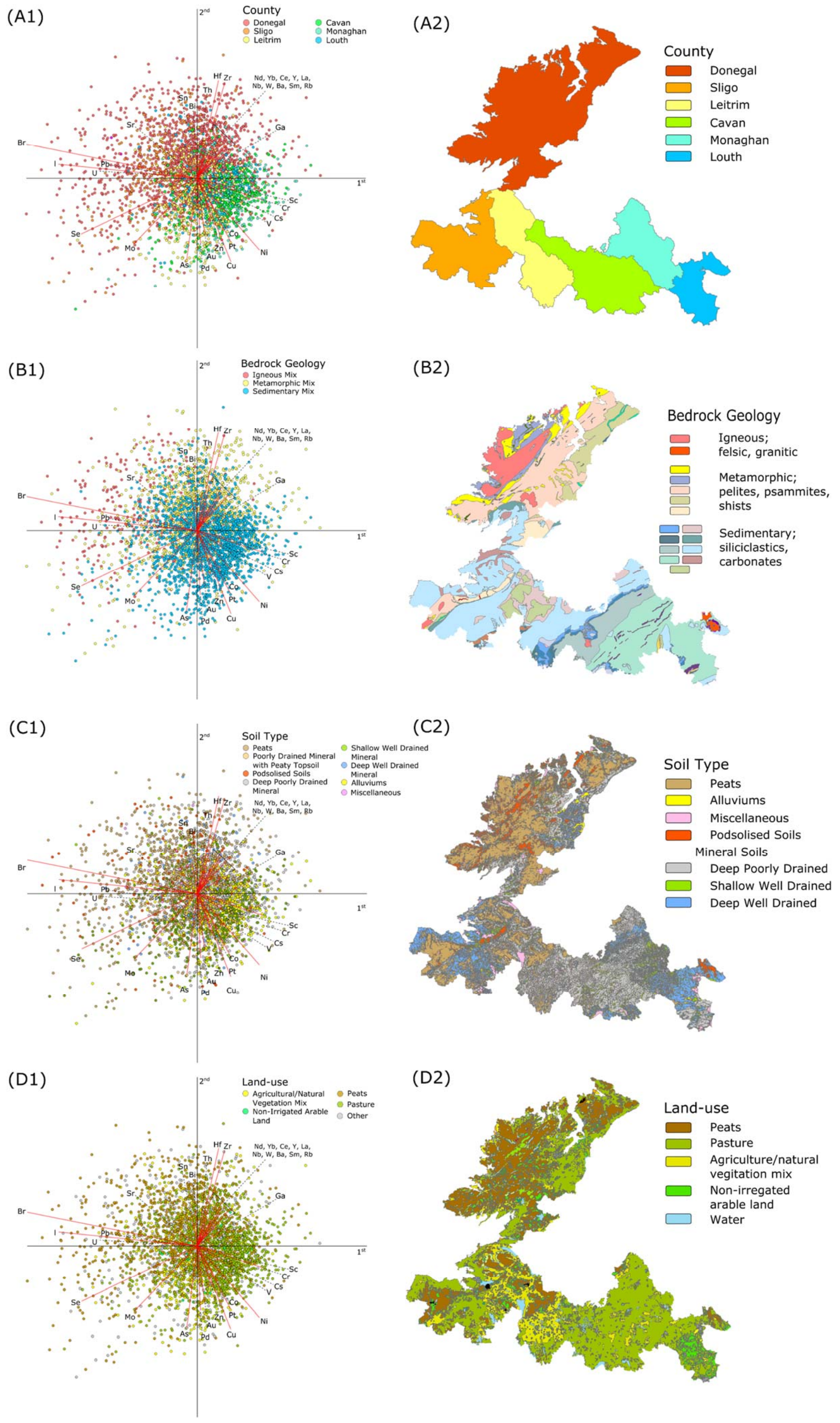
Fig. 5.5: *Compositional Data Analysis bi-plots of the Tellus Border Stream Sediment geochemistry dataset with categorical information changed each time to reflect the varying environmental factors described by the corresponding maps for **A)** Counties, **B)** Bedrock Geology, **C)** Soil Type and **D)** Land-use. Note each of the bi-plots show a similar variation from the top left of the plot to the bottom right. In particular igneous and metamorphic terrains are distinguished from sedimentary sources suggesting bedrock geology **(B2)** has an influence on stream sediment chemistry **(B1)**. Other environmental factors appear to have a weak and perhaps coincidental effect on sediment chemistry (e.g. soil type **(C1)** and land-use **(D1)**).*

5.5 Discussion

CoDA has proven reasonably effective at geochemically characterising different soil types in the Tellus Border Region of Ireland. Peaty soils appear to show a strong relationship with heavy metals, such as lead, antimony, cadmium and, particularly, mercury (Table 5.1, Fig. 5.1). This may be because peat that is rich in organic matter is known to retain more heavy metals than mineral soils (e.g. Zadrożny and Nicia, 2009, Borgulat *et al.,* 2018) due to binding and electrostatic interactions with humic acids (e.g. Sounthararajah *et al.,* 2015).

In contrast, mineral soils in the Tellus data appear to be associated with greater variations in rare earth elements (REEs), such as lanthanum, cerium, terbium, lutetium, ytterbium, scandium and yttrium (Table 5.1, Fig. 5.1). A more pronounced variation of these REEs in mineral soils can be attributed to a greater interaction with bedrock, especially in weathered zones on metamorphic lithologies together with more complex niche flora (e.g. Tyler, 2004).

It is clear that soil type is directly related to soil geochemistry. However, when analysing stream water and stream sediment geochemistry datasets (Table 5.2 and 5.3, Fig. 5.2 and 5.5), a greater number of potential physical geographical parameters may exert influence on the geochemical composition of samples. It should also be noted that categorical information (e.g. soil type, bedrock geology) was only added for the specific, particular location from which each sample was recovered and therefore, steam water geochemistry may be more characteristic of conditions upstream of the sample site in the catchment that are not represented by the assigned categories. The same is equally valid for the Stream Sediment Dataset.

The underlying bedrock geology, in particular, strongly influences the geochemistry of stream water samples (Fig. 5.2B1/B2). Areas of the Tellus Border Region that are dominated by Paleozoic sedimentary rock lithologies (in particular Carboniferous [Mississippian] carbonates) are associated with the relative abundance of calcium and bi-carbonate (Fig. 5.3A/B). The same sampling areas also show relationships with strontium, due to its chemical behaviour in the presence of abundant calcium (co-precipitation; e.g. Pingitore Jr and Eastman, 1986; Lauchnor *et al.*, 2013; AlKhatib and Eisenhauer, 2017), and uranium, which is potentially found within deep marine lithologies that are associated with the carbonates (Fig 5.3A/B; e.g. Mo *et al.*, 1973). Also in relative abundance within these samples is nitrate. This is most likely due to land-use practices in the same areas being predominantly agricultural. This is highlighted most strongly in County Louth, which has a large area classified as 'Non-

irrigated arable land' (Fig. 5.4A/B). This particular area of the border region shows the strongest geochemical contrasts (Fig. 5.4C) due to the inherent mineralogical differences between Paleogene granophyre in the north and Paleozoic marine sedimentary rocks in the rest of the county.

The capacity for CoDA to successfully delineate metamorphic areas based on stream water geochemistry data may be coincidental. The same areas (primarily in eastern Donegal) are predominantly covered with poorly drained mineral soils and therefore for the same reasons as described with soil geochemistry, show relationships with lanthanum, cerium, praseodymium, neodymium and aluminium (Fig. 5.2B1/B2). Terrains underlain by Caledonian plutonic rocks (e.g. western County Donegal), on the other hand, have a strong correlation with negative 2nd principal component values. Elements contributing to this are: sodium, chloride, tin, thallium and caesium – all of which can be attributed to relative abundances within intrusive felsic igneous rocks such as granites and pegmatites found in western County Donegal. For example, sodium is a major constituent of albite $[NaAlSi_3O_8]$, tin may be found in cassiterite $[SnO_2]$ and chloride, thallium and caesium are secondary elements within common granitic minerals such as muscovite, biotite, pegmatitic microclines, amphiboles and orthoclase (e.g. Volfinger *et al*., 1985; Smeds, 1992; Steiner, 2019).

Stream sediment geochemistry data shows similar relationships to those seen between stream water geochemistry and underlying bedrock geology (although the correlation is not as strong - compare Figs. 5.2 and 5.5). Areas underlain by sedimentary bedrock have both positive 1st principal component values and negative 2nd principal component values. These areas appear to be associated with a variety of elements including: chromium, nickel, copper, arsenic, selenium, molybdenum, gold, palladium and platinum. Although these variables appear to be related to Paleozoic sedimentary lithologies (e.g. in south Donegal), one explanation could be sediment transport from areas dominated by Neoproterozoic metasediments (e.g. eastern Donegal) which are known sources of these economically important elements (e.g. Wilkinson *et al*., 1999). However, more information would be required to delineate the geochemistry of potential parent rock lithologies further (e.g. Weltjea and von Eynatten, 2004; Blowick *et al*., 2019). Metamorphic-dominated areas appear to be associated with river sediment samples that have relative abundance of zirconium and hafnium. Zirconium is most commonly found in zircon $[ZrSiO_4]$ which is also an important source of hafnium. As zircon is resistant to many forms of weathering it may be found preferentially recycled (from primary source granites) in

sediments and metasediments (e.g. Morton and Hallsworth, 2007; Tyrrell *et al.*, 2009; Nauton-Fourteu *et al.*, 2021).

Finally the igneous areas of western County Donegal contain river sediments with abundances of selenium, molybdenum, iodine and particularly bromine. Iodine and bromine are likely sourced from abundant peats in these areas which are known sources of halogens (e.g. Biester *et al.*, 2006). However, the 1st and 2nd principal component only compose a collective 36% of the geochemical variation within the dataset. This suggests overall low levels of correlation between the variables and therefore the results of CoDA for the stream sediment geochemistry dataset should be treated with some caution. The elemental associations highlighted by CoDA have not been interpreted here for this reason.

The Tellus geochemistry datasets from the border region demonstrate the relationship between the nature of the environment (i.e. rock type, soil type, land-use practice) and the geochemical composition of soil, water and sediment samples. Geology is the dominant primary control on the geochemistry of any sample as it is the ultimate source of chemical components and also directly or indirectly influences secondary controls such as topography, ecology and soil type (purple lines in Fig. 5.6). For example, western County Donegal is dominated by extensive areas of intrusive igneous terrains (e.g. Donegal Granite) and a wet temperate climate. These primary controls influence the topography (upland areas) and the soil type (predominantly peat bogs). This then effects the geochemistry of soil samples recovered from this area (Fig. 5.1).

Together the primary and secondary controls inform how the environment is utilised. The anthropogenic impact on the chemistry of the natural environment is significant, particularly within soils and water (red lines in Fig. 5.6). This is well demonstrated in County Louth where large areas of 'non-irrigated arable land' effect the chemistry of stream waters in the area. In particular, the influence of nitrates from agricultural practices (Fig. 5.2 D1 and D2). How the land is used in the area is controlled by the soil type (Fig. 5.2 C1 and C2) which is influenced by the geology (Fig. 5.2 B1 and B2). This highlights the complex nature of the connections between the natural environment, anthropogenic effects and the geochemistry of soil, sediment and water (Fig. 5.6).
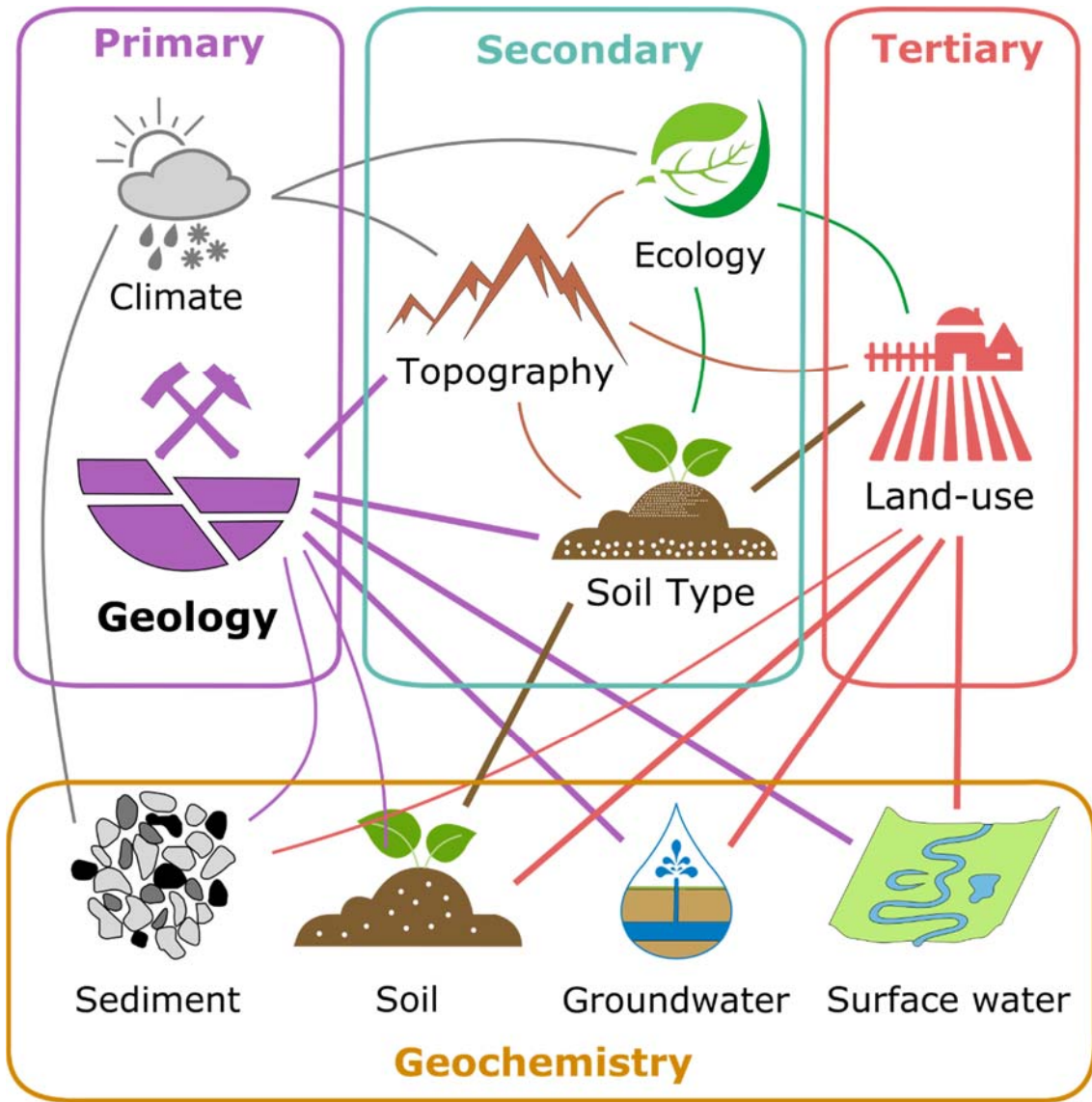
Fig. 5.6: *Pictographic web-chart showing the connections between primary, secondary and tertiary controls and their combined influence on geochemistry (heavily weighted straight lines represent strong connections and light weighted curved lined indicate weaker relationships).*

5.6 Conclusions

Soil type has, up to now, been identified on the basis of sample classification by experienced workers and designated experts. Using the CoDA method one particular group of soils ('peats') can be accurately classified using geochemistry alone (e.g. Fig. 5.1). The primary reason for this is that peat has strong geochemical contrasts to other soil types, largely due to the fact that it accumulates over relatively longer timeframes, allowing it to act as a long-term sink for many elements (e.g. mercury and lead; Bindler, 2006). Kirkwood *et al.*, 2020 demonstrated that with further refinement and additional data such as geophysical information, this delineation and

mapping process can be further refined to successfully identify and survey soil types more efficiently and accurately than more traditional soil classification mapping. This is accomplished by employing machine learning techniques to recognise patterns between geochemical and geophysical variation and then subsequently analysing the joint variability in this case using Fast Independent Component Analysis (FICA) (see Section 2.4.5).

Stream water and stream sediment geochemistry can be effected by a number of factors including: hydrological transport, anthropogenic inputs, altering redox conditions, weather and saline intrusions (closer to the coast). However, CoDA shows that the primary cause of variation within the GSI Tellus Border Region datasets is spatial differences in underlying geological composition, such as the very pronounced contrast between Paleogene granophyre and Carboniferous limestone in north County Louth being reflected in the 1st principal component (Fig. 5.4). This relationship is stronger for stream water than it is for stream sediment geochemistry (e.g. compare Fig 5.2 with Fig. 5.5). This may attributed to the recent Pleistocene glaciation varying hydrological conditions that control the deposition of stream sediments. In particular, high volumes of melt water moving vast amounts of sediment.

Another explanation may be that the chemical signature is easily picked up by dissolution, particularly of carbonates, whereas weathering that leads to sediment transport is significantly more muted especially considering the relatively low topography of the border region (see Fig. 1.13A). In fact, CoDA of the stream water geochemistry dataset from the Tellus Border Region allows for broad geological mapping on the basis of stream geochemistry alone. Further refinement of this method with additional data, such as geophysical data, could allow for the development of regional scale geology maps from Tellus geochemistry data.

This chapter has demonstrated the effectiveness of CoDA as a method for identifying the dominant relationships between variables in very large and spatially broad geochemical datasets. Following the identification of prominent correlations, the geochemical processes that relate to them can then be investigated further and in greater detail. This is a far more efficient approach than analysing and comparing numerous (separate) chemical element concentration maps. The CoDA approach can also be adapted depending on the application. For example, interrelated elements and compounds that represent a particular type of mineral deposit could be isolated for more targeted analysis, thus providing a tailored vectoring map that accounts for more than one constituent simultaneously. This would most likely occur on a spatial scale larger than Lisheen but smaller than the Tellus Border Region.

Chapter Six: *General Discussion and Concluding Summary Remarks*

6.1 Introduction

Separating the signal from the noise in datasets has never been more complicated (for examples in earth science see Clarke and Swayze, 1996; Santer *et al.,* 2011; Johnson *et al.*, 2020. In the specific context of geochemical analysis see, for example, Bailey and Krzanowski, 2000; Le Vaillant *et al.,* 2017; Esmaeiloghli and Tabatabaei, 2020). This is even more imperative today given the increasing ability to collect and compile very large datasets with relative ease, and, with respect to geochemical investigations, the instrumental advances which means the presence of elements and compounds can now be reliably detected to the parts per trillion (ppt) level. What is the most effective and appropriate way to manipulate and analyse all of these numbers and how do we extract the correct signal from these datasets?

There is no single standard or recommended methodology to do this with respect to geochemical data. Numerous single-variable statistical and multivariate statistical methods have been suggested (e.g. Gałuszka and Migaszewski, 2011; Buccianti *et al.*, 2015; Reimann *et al.*, 2018; Sahoo *et al.*, 2020); however, selecting the most suitable or appropriate method is important and will become even more so as policy and regulation continue to develop. Statistical and geostatistical techniques such as Principal Component Analysis (PCA), Hierarchical Cluster Analysis (HCA), in combination with geochemical mapping can be used to better describe the complex spatial variations of elements and identify the source and pathways of elements related to parent rock and/or soil-forming factors and anthropogenic sources.

A common problem in environmental statistics is that geochemical data are compositional (closed) data (e.g. Aitchison, 1986; Van den Boogaart and Tolosana-Delgado, 2013; Filzmoser *et al.*, 2009). Closed data cannot reliably be analysed using multivariate techniques, because they can give unrealistic and biased factors that affect the data structures (Filzmoser *et al.,* 2009). However, this can be satisfactorily addressed by transforming the data prior to analyses (or opening the closed data) and this procedure is termed Compositional Data Analysis (CoDA) (Aitchison, 1986).

Three different log-ratio transformation methods:

- the additive log-ratio (alr),

- the centred log-ratio (clr), *and*

- the isometric log-ratio (ilr)

have been proposed to both 'open' the closed compositional data, as well as to normalise the data distribution (e.g. Aitchison, 1986; Filzmoser *et al.*, 2009, 2010).

The primary over-riding objective of this thesis was to appraise the application of CoDA to geochemical datasets on different scales. To accomplish this, two groups of datasets were analysed using CoDA:

i) Lisheen groundwater geochemistry (Chapters Three and Four)

ii) GSI Tellus Border Region soil, stream water and stream sediment geochemistry (Chapter Five)

CoDA is very sensitive, so knowing and understanding how a given geochemistry dataset was created and prepared for subsequent statistical analyses is critical for determining outcomes that are meaningful and reliable. Sample material recovery, laboratory analysis and data pre-processing can all affect the outcomes of CoDA. Additionally, different CoDA methods can provide varying levels of insight into geochemical signatures within the data. The use of this method is therefore one integral part of a sequential approach that begins with sample recovery, and its use should thus be seen in that particular context. The advantages and disadvantages of CoDA are discussed below and are followed by the main learnings and outcomes from applying the various methods to each of the two groups of geochemical datasets in this study.

6.2 Advantages and Disadvantages of CoDA

CoDA is a necessity for avoiding spurious correlation (e.g. Pearson, 1897) that may result from many forms of multivariate analysis on raw data (e.g. principal component analysis, independent component analysis, cluster analysis etc.). Built upon the substantial foundational work of John Aitchison (Aitchison and Shen, 1980; Aitchison, 1982, 1983, 1985, 1986, 1992), the basis of CoDA is log-ratio transformations, which are operations completed through three methods: additive, centre and isometric (Egozcue *et al.*, 2003; Filzmoser *et al.*, 2009, 2010),

each with inherent pros and cons. Following the implementation of one or a combination of these methods, as in the case of the CoDA bi-plot, a spectrum of statistical methods can be completed without concern that artificial correlations may have been implied or made between either the variables or the samples.

In addition to the mathematical and statistical importance of CoDA, these methods also offer alternative ways of visualising multivariate data (e.g Filzmoser *et al.*, 2018). This is highlighted in both the Lisheen and Tellus Border Region geochemical datasets, where a large number of samples and variables are easily compared via the CoDA bi-plot (in addition to other forms of robust cluster analysis; e.g. see Figs. 3.13, 4.4 and 5.3). Distinctions between particular groups can be easily seen and the combinations of elements and compounds that define those groups are easily recognised, appearing as red vectors on these particular bi-plots. From this single bi-plot, inferences about the primary controls on the geochemical system can begin to be constructed. For example, Figure 3.13 shows that each groundwater type from a number of locations at Lisheen can be chemically distinguished, Figure 4.4 illustrates how the bi-plot can delineate sample chemical evolution through time (again at Lisheen), and Figure 5.3 demonstrates how CoDA can be used to relate chemistry back to the natural environment (in this case the lithostratigraphic units comprising the bedrock geology in the Tellus Border Region).

Principal Component Analysis (PCA) is used to construct the CoDA bi-plot through Singular Value Decomposition (SVD), following log-ratio transformation (Aitchison and Greenacre, 2002). The resulting values (scores and loadings) which define the coordinates of vectors and observations on the bi-plot can be extrapolated and used to explain the influence of each principal component for each sample. Mapping this data provides a stronger understanding of the spatial variability of certain geochemical process in comparison to simple element concentration mapping. This is well demonstrated by the GSI Tellus Border Region data (Chapter Five), where the combination of chemical elements that define a particular substrate (e.g. soil or rock type) can be defined by a single value (i.e. the scores from one of the principal components).

Perhaps one of the largest inherent drawbacks of CoDA is its inability to process zero values (e.g. Martín-Fernández *et al.,* 2011). In geochemistry, zeros can occur as either missing data or data that registered or measured below a defined detection limit for a given element (e.g. <0.001 mg/l Zn). For this reason a significant amount of work has concentrated on solving this

issue, as discussed in Section 2.4.2. Methods of replacing zeros with a token 'real' number above zero, must be identified as assumptions when considering implications and outputs of the resultant analysis. However, the effect of these zero replacement methods can be minimised as much as possible by reducing the amount of replacement that can be done before a variable or sample is discarded (e.g. Blake *et al*., 2016).

In addition to the zeros issue, the sensitivity of the CoDA method, which is seen as a general strength, can also be compromised, and thus considered a weakness, if any doubt about the quality and integrity of sampling and laboratory analysis methods arises. For this reason, the importance of minimising potential contamination wherever possible and inserting checks, such as triplicate and blank samples during routine laboratory analysis, is essential to ensure the subsequent data analyses are accurate and viable (see Sections 2.2 and 2.3).

6.3 Lisheen Groundwater Geochemistry

A substantial collection of groundwater geochemistry data, spanning almost three decades (1991 to 2019), from the area of Lisheen mine in south-central Ireland was analysed using CoDA methods. The use of ilr-ion plots (Shelton *et al*., 2018; see Figs. 3.2, 3.8, 4.2), robust cluster analysis (Filzmoser *et al*., 2018; see Fig. 3.3, 3.4, 3.12) and in particular compositional bi-plots (Aitchison and Greenacre, 2002; e.g. see Figs. 3.5, 3.10, 4.3, 5.1), all contributed to a greater understanding of the geochemical relationships and interactions present with the groundwater system at Lisheen.

The Pre-Mining Regional Dataset (A), offered a unique opportunity to explore the groundwater chemistry of the Lisheen area prior to the initiation of mining activity, thereby excluding direct pollution from mine water as an explanation for any observed geochemical signatures. In fact, lead (Pb^{2+}) and arsenic (As^{3+}) cation levels were found to be above Irish/EU groundwater quality threshold values in 15 and 7 samples, respectively (Table 3.1). This suggests that geogenic contamination of groundwater, due to the dissolution of minerals associated with the massive-sulphide ore (e.g. galena [PbS] and arsenopyrite [FeAsS]), was naturally occurring in the subsurface immediately prior to the discovery of the ore deposit.

The use of CoDA methods offered further insights into the groundwater chemistry prior to mining and established geochemical themes that were present across many of the temporally subsequent Lisheen datasets (B-E). For example, the strong relationship between calcium

(Ca^{2+}) and magnesium (Mg^{2+}) was highlighted by the ilr-ion plot (Fig. 3.2), indicating that the dissolution of regionally dolomitised Mississippian limestone bedrock (typical of the Rathdowney Trend in Ireland; e.g. Eyre, 1998; Hitzman *et al.*, 1998; Wilkinson *et al.*, 2005b) is a major factor controlling the concentration of major cations. Robust correlative and cluster analysis revealed that other chemical relationships also have important influences on the regional groundwater at Lisheen (Figs. 3.3 and 3.4). In particular, a strong correlation was observed between:

- lead (Pb^{2+}) and cadmium (Cd^{2+}) *and also*

- iron (Fe^{2+}), manganese (Mn^{2+}) and arsenic (As^{3+}).

Lead and cadmium levels are observed to increase in tandem at locations where groundwater comes into close contact with massive-sulphide mineralisation. Iron, manganese and arsenic variability may also be reflective of the mineral deposit; however, their inter-relationship is most likely as a result of redox reactions occurring within some sampled groundwaters.

The element group correlations mentioned above, together with additional observations, were readily determined and identified on a CoDA bi-plot (Fig. 3.5). High variability of zinc (Zn^{2+}) could be identified in a number of samples and was also attributed to massive-sulphide mineral dissolution (e.g. sphalerite $[(Zn,Fe)S]$). The reason zinc appears to display an independent signature on the bi-plot may be due to its relative capacity for mobility in groundwater. An additional important observation identified on this bi-plot was that regional background groundwater geochemistry is represented by low levels of variability within a high proportion of chemical variables. This is also the case in a number of other Lisheen bi-plots and is discussed in Wheeler *et al.* (2021). The CoDA bi-plot was also examined from a mineral exploration perspective by categorically colouring sample locations based on their distance to (what would subsequently be recognised as) the primary ore source at Lisheen. It was clear that samples in close proximity to the deposit were most related to lead and cadmium variability.

The Early-Mining Regional Dataset (B) contains the most spatially extensive geochemistry data for Lisheen. Despite missing crucial information in terms of broad chemical characterisation (i.e. bicarbonate concentration data), the geographical extent of the sample locations and the utility of CoDA methods, allowed correlations to be drawn between groundwater geochemistry and the Mississippian bedrock geology. It was demonstrated from the ilr-ion plot (Fig. 3.8) and subsequent map (Fig. 3.9) that calcium/magnesium ratios (Ca^{2+}/Mg^{2+}) are indicative of regional dolomitisation. Therefore, this particular Lisheen dataset

(B) offered the closest small-scale example of a CoDA mapping method later discussed in the context of the GSI Tellus Border Region data.

Other groundwaters in the Lisheen area were identified and differentiated within the Mine Workings Dataset (C). Water entering the underground mine workings from a variety of geological structures (principally brittle faults and fractures) was sampled and analysed by the on-site team at various stages of the mining operation (Fig 3.11). The resulting dataset afforded a unique and valuable opportunity to examine and investigate groundwater chemistry at depth (150–200m below ground level). Interconnecting geological structural features (and their influence on modifying the distribution and orientation of lithostratigraphic units; e.g. Fig. 1.10 and 1.11) at the mine site suggest that some mixing likely occurred prior to sampling. However, two distinct groundwater types could be identified:

1. Groundwater from the late Tournaisian Waulsortian Limestone Formation (Fig. 1.9) was characterised by variation of a number of elements and compounds, particularly those associated with massive-sulphide mineralisation (e.g. Fe^{2+}, Mn^{2+}, Ni^{2+}, Co^{3+}, Zn^{2+}, SO_4^{2-}). This particular formation is an important target stratigraphic level for base metal mineralisation in the southern part of the Irish ore-field (e.g. Wilkinson and Hitzman, 2015).

2. In contrast, water sampled specifically from the so called *F-structures* (e.g. F2/F3; see Fig. 1.10), which represent the youngest brittle deformation features at Lisheen (e.g. Torremans *et al.*, 2018; Kyne *et al.*, 2019), shows low levels of variability within a large number of cations/anions (e.g. Ca^{2+}, HCO_3^-, Mg^{2+}, Na^+, Cl^-, F^-). As discussed above, this indicates groundwater that is characteristic of the regional background chemistry, or 'cleaner' water. The source of this water connected to the mine workings by the F-structures is believed to be the Lisduff Oolite Member. This particular member is part of the Ballysteen Limestone Formation (occurring between the Lower and Upper calcarenite members; Fig. 1.9), which stratigraphically underlies the Waulsortian Limestone Formation (e.g. Quaid and Wheston, 2017; Torremans *et al*., 2018; Kyne *et al*., 2019).

In addition to groundwater from these two distinct sources being recognised, CoDA was also able to geochemically distinguish each of the eight sample locations analysed from the Mine Workings Dataset (C) (Fig. 3.13).

Geochemically *fingerprinting* sample sites using CoDA was an additional analytical approach employed for the Early Post-Mining Regional Dataset (D) and demonstrated in Wheeler *et al.* (2021) (Appendix A). The data analysed here was composed of samples from eight discrete locations, recovered regularly over an 11 month period (December 2015 – November 2016), immediately following the closure of Lisheen Mine. These particular samples are primarily sourced from the upper 3-5m of epikarst and are therefore representative of shallow groundwater at Lisheen.

The Early Post-Mining Regional Dataset (D), in particular, was used to demonstrate the power of CoDA methods for geochemically characterising the sample sites. Despite the source of groundwater for each sample location being quite similar (i.e. being influenced by the Mississippian carbonate bedrock at relatively shallow depths), the ilr-ion plot (Fig. 4.2) was able to chemically distinguish the various sample locations much more effectively than the traditional Piper plot. In particular, samples from the on-site compliance wells (CW-01 and CW-02) were identified by the stronger influence of sulphate (SO_4^{2-}) and all of the wells could be delineated based on relative concentrations of calcium (Ca^{2+}) and magnesium (Mg^{2+}).

The results of a hierarchical cluster analysis (HCA) were then incorporated into a CoDA bi-plot (Fig. 4.3). The HCA revealed three sample site groupings based on the geochemistry:

- **G1** (wells SH, MM and PF),

- **G2a** (wells FC, PH, JM and CW-02), *and*

- **G2b** (well CW-01)

From the bi-plot it is clear that **G1** are characterised by relatively low variability of a number of chemical components (Ca^{2+}, $HCO3^-$, Mg^{2+}, U^{6+}, Na^+, Sb^{3+}, Sr^{2+}, F^-, Cl^-) and high variability of nitrate (NO_3^-). This grouping has been interpreted to represent background groundwater geochemistry that is being influenced by contact with peat bogs or areas of intensive agriculture (e.g. De Ruijter *et al.*, 2007). **G2a** shows variability of barium (Ba^{2+}) and potassium (K^+) and **G2b** is characterised by manganese (Mn^{2+}), ammonium (NH_4^+), nickel (Ni^{2+}) and sulphate (SO_4^{2-}). These two latter groupings are more characteristic of groundwater that has been in contact with massive-sulphide mineralisation, or has mixed with deeper groundwater via brittle fault/fracture structures that act as conduits at Lisheen. Despite the three major groupings (**G1**, **G2a**, **G2b**) each of the eight sample locations were readily chemically distinguished on the resultant bi-plot.

One of the wells (PH; pink in Fig. 4.3) was also analysed from a temporal perspective as it was the only location with significant varying chemistry over time. By altering how the observations (i.e. points on the bi-plot) were characterised (by date instead of by location), it was possible to analyse how the chemistry changed through time (Fig 4.5). This demonstrates a further application of CoDA not seen in the other datasets. The temporal analysis of geochemistry data can be applied to a variety of studies. For example, analysing the accumulation effect of anthropogenic inputs to a system (e.g. discharge licences) or accounting for the hydrochemical effect of a new groundwater abstraction over time.

A final 'snapshot' round of geochemical sampling data (E) from Lisheen was recovered in January 2019 and was also analysed, primarily, by using traditional non-CoDA methods. These samples were taken from two groups of locations:

1. Privately owned wells, *and*

2. Wells that are remnants of mining activity.

Some of the samples from both groups again highlighted the important effect of redox reactions at Lisheen. Iron ($Fe^{2+/3+}$) and manganese (Mn^{2+}) in particular, are highly variable within the samples. This is further confirmed by comparative plots of various redox elements and dissolved oxygen concentrations (Figs. 4.7-10). Many of the wells connected to the underground mine show elevated concentrations of sulphate (SO_4^{2-}). However, none of the wells show any indication of mine water pollution affecting the local groundwater and therefore, at least up to January 2019, the remediation works implemented at the time of mine closure, and which continue at the time of writing, are working satisfactorily at Lisheen.

6.4 Tellus Border Region Geochemistry

Soil geochemical mapping has been widely used in mineral exploration but it is now more widely used also in broader environmental studies, such as documenting contamination, risk assessment, determining geochemical baseline/background levels of chemical contaminants, and identifying their sources linking with geogenic and human-induced factors (e.g. Garrett *et al*., 2008; Reimann *et al*., 2018; Sahoo *et al*., 2020).

The Tellus Survey is a national-scale geophysical and geochemical data collection programme by both the Geological Survey of Northern Ireland and Geological Survey Ireland (GSI). The first phase of this survey in the Republic of Ireland by the GSI covered an area known as the Border Region, which is composed of the six counties that immediately border Northern Ireland (Fig. 1.13). Soil, stream water and stream sediment geochemistry datasets from the GSI Tellus Border Survey were analysed in Chapter Five with the purpose of identifying geochemical combinations that are characteristic of particular environmental factors (e.g. soil type, bedrock geology and land-use). It was demonstrated, using CoDA methods, that soil geochemistry is representative of soil type and that stream water (and to a lesser extent, stream sediment) geochemistry is principally defined and characterised of the underlying bedrock geology.

Categorical information describing the Tellus Border Region used in the analysis was collected from the relevant sources (e.g. the GSI for bedrock geology information) and was added to the datasets using ArcGIS Pro (version 2.7.3). This meant that details pertaining to rock type, soil type and land-use practices inherited any potential inaccuracies with the original maps. It should also be noted that stream water and stream sediment samples are not necessarily representative of the conditions where they are recovered but rather they reflect more the nature of the terrain upstream of the sample sites. These are important considerations when interpreting the data produced.

The significant geochemical contrast between peaty soils and all other soils in the Tellus Border Region, allowed them to be effectively and confidently mapped using CoDA methods (Fig. 5.1). These soils, that are particularly prevalent in western County Donegal, show strong associations with selected heavy metals (e.g. $Pb^{2+/4+}$, $Sb^{+3/+5}$, Cd^{2+}, $Hg^{+/2+}$) attributed to long term storage and binding and electrostatic interaction with humic acids (e.g. Sounthararajah *et al.*, 2015). In comparison, mineral soils in the Tellus Border Region are more commonly related to variations in rare earth elements (REEs; e.g. La^{3+}, Ce^{+}, $Tb^{3+/4+}$, Lu^{3+}, $Yb^{2+/3+}$, Sc^{3+}, Y^{3+}). This has been interpreted as the result of greater interaction and exchange with the underlying bedrock, especially in weathered zones on metamorphic rocks, and the presence of more complex niche flora (e.g. Tyler, 2004). As the soil type is the primary and dominant cause of geochemical variation, the 1st principal component, which represents the contrast between peats and other soils, can be used to map peaty soils reasonably accurately.

Recognising contrasts within stream water geochemistry datasets is more complex due to the increased number of physical geographical parameters that may exert an influence on the composition of samples. However, the primary controlling factor has been identified as bedrock geology. A significant proportion of the Tellus Border Region is dominated by Upper Paleozoic (Carboniferous) carbonate sedimentary rock lithologies (Fig. 1.13). This is also reflected in the stream water geochemistry, which shows strong correlations between these areas and calcium (Ca^{2+}), bicarbonate (HCO_3^-), strontium (Sr^{2+}) and uranium (U^{6+}). Nitrate (NO_3^-) is also found in relative abundance in many of the same areas. However, this has been interpreted to represent an effect of soil type and land-use practices on the water geochemistry rather than bedrock geology.

The use of CoDA also identified metamorphic terrains, particularly in eastern County Donegal. As mentioned above in relation to soil geochemistry, samples from this area again showed variation of particular elements (e.g. La^{3+}, Ce^{4+}, Pr^{3+}, Nd^{3+}, Al^{3+}). The bedrock of western Donegal is composed primarily of Caledonian plutonic rocks (principally granites) which have been accounted for by the 2nd principal component in the CoDA bi-plot (Fig. 5.2). The stream water in these areas has relative abundances of variables associated with granites and pegmatites (e.g. Na^{2+}, Cl^-, Sn^{4+}, Tl^{3+}, Cs^+).

One particular section of the Tellus Border Region (in County Louth, in the east of the wider study area) was examined more closely in order to demonstrate the value of CoDA for delineating areas of highly-contrasting physical parameters based solely on the geochemistry of samples from that area (Fig. 5.4). More traditional methods of geochemical surveying and mapping have involved the production of concentration maps, of which more than 60 could potentially be created for County Louth stream water geochemistry. However, CoDA has extracted a combination of the primary contrasting elements and mapped them simultaneously through principal component scores. This represents a very powerful case example of CoDA being used to separate the 'signal from the noise' and rationalise a complex geochemical signature down to its essential component variables. In this case, water chemistry in the area of the Paleogene shallow intrusive igneous granophyres in the north of the county has been strongly distinguished from the Paleozoic marine sedimentary rocks prevalent throughout the rest of Louth.

The geochemical influence of underlying bedrock was also evident from the analysis of the Tellus Border Region stream sediment data (although the resultant correlations were admittedly

not as strong; e.g. Fig. 5.5). Areas dominated by sedimentary lithologies, particularly clastic rocks, were found to be related to a number of variables that may be of significant economic importance (e.g. $Cr^{3+/6+}$, Ni^{2+}, $Cu^{+/2+}$, $As^{3+/5+}$, $Se^{4+/6+}$, $Mo^{2+/6+}$, $Au^{+/3+}$, $Pd^{2+/4+}$, $Pt^{2+/4+}$). The CoDA bi-plot showed these samples to be related to Paleozoic sedimentary lithologies (Fig. 5.5). However, sediment transport from areas dominated by Neoproterozoic metasediments that are recognised sources for mineralisation of this kind (e.g. Wilkinson et al., 1999) is also a possibility. Further sampling and analysis, in particular investigation of the nature of river movement and general detrital sediment provenance in the study area, would be required to confidently identify the likely parent rock lithologies (e.g. Weltjea and von Eynatten, 2004; Blowick et al., 2019).

Areas of primarily igneous bedrock (e.g. the Caledonian granites of Donegal) showed some correlation with the variability of halogens (e.g. I and Br) in the stream sediments. This was interpreted as coincidental, due to these regions being dominated by peats which have been identified as a common source of halogens (e.g. Biester et al., 2006). The low total variability (36%) explained by the 1st and 2nd principal component and CoDA biplot meant that the stream sediment geochemistry could not be mapped in the same way as the previous soil and stream water datasets.

6.5 Conclusions

CoDA provides the correct mathematical framework for any multivariate investigation of geochemistry data. The basis of CoDA are the log-ratio transformations. These retain only the information important for subsequent analysis (the ratios between the component parts). In doing so, any spurious correlation which might arise as a result of the 'closure problem' can be avoided and the newly transformed data is free to be examined using robust multivariate methods. Traditional statistical techniques have been adapted to operate within the CoDA framework (e.g. robust hierarchical cluster analysis, Filzmoser et al., 2018) and new methods have been developed for specific types of investigation (e.g. the ilr-ion plot for groundwater geochemistry; see Shelton et al., 2018). However, the most powerful CoDA method remains the compositional bi-plot (e.g. Aitchison and Greenacre, 2002). This multi-dimensional display of singular value decomposition outcomes, allows for simultaneous interrogation of the;

i)   relationship between the variables,

ii)   chemical similarity/dissimilarity of sample locations,

iii)   geochemical interactions that define the dataset,

iv)   how those interactions relate to the natural environment, *and*

v)   how the geochemistry of each location varies over time

In combination, the application of CoDA methods leads to a considerably more comprehensive and complete understanding of geochemistry data. This is particularly well-demonstrated through the analysis of both the Lisheen and Tellus Border Region datasets.

Groundwater in the area around Lisheen is characterised as Ca-Mg-HCO$_3$-type. However, the major ions can be considered superficial in terms of the full story of this geochemically complex region. The faults that once carried mineralising hydrothermal fluids, now act as conduits for mixing between deep and shallow groundwaters. By using CoDA to analyse geochemistry data that spans almost three decades (1991 – 2019) of sample collection, it is clear that the dissolution of massive sulphide minerals, redox reactions and nitrogen contamination, have all played an important role in defining groundwater chemistry at Lisheen. Specific sample locations in the area can even be *geochemically fingerprinted* using the CoDA bi-plot.

The relationship between the geochemistry of natural materials (e.g. soils, sediments and water) and the composition of the physical environment (e.g. bedrock geology, soil type and land-use practices) is to a certain extent, inherently intuitive. However, to demonstrate and objectively analyse this connection, a significant amount of data is required over a relatively large area of variable conditions. The Tellus Border Region provides an ideal dataset for this particular purpose. CoDA has been used on this data to highlight the primary controls on the geochemistry in the border region. For soil this is soil type and for stream water and stream sediments the most important factor is the underlying bedrock geology, which essentially represents the context in which the various surface processes are operating. The outcomes of principal component analysis (which are used to construct CoDA bi-plots) can be extracted to geographically map geochemical variation in the environment. This has obvious implications for mineral exploration, environmental monitoring and land-use planning.

6.6 Recommendations for future work

a) Compositional Data Analysis (CoDA) should be used in any new and developing studies that involve geochemical analyses, as the resulting data is inherently compositional (e.g. mg/l, mg/kg, ppm, %).

b) Considerable care should always be taken in the recovery and laboratory analysis of geochemical samples, especially those that are most sensitive to alteration and contamination (e.g. water samples), as minor variations within a few variables can greatly affect the resulting overall interpretation. The effects of a variety of sampling approaches on the outcomes of CoDA could be tested and documented through controlled experimentation.

c) An important data preparation step prior to the use of CoDA is the replacement of zeros and values below the detection limit. The recommended methods of data replacement are based on the mathematical implications (e.g. Martín-Fernández *et al.*, 2011) and should also be tested in a practice depending on the specific type of data (e.g. groundwater geochemistry).

d) CoDA can be used in tandem with a number of other data analysis methods to provide a clearer understanding of geochemical processes and their spatial variability. For example Fast Independent Component Analysis has shown great promise in this particular area (e.g. Liu *et al.*, 2014; Muehlmann *et al.*, 2020). Incorporating geophysical data can also aid interpretations particularly in the context of mapping (Kirkwood *et al.*, 2020).

e) Groundwater sampling and geochemical analysis is continuing in the area around Lisheen Mine as per the Closure, Restoration and Aftercare Management Plan (CRAMP, 2016). Any new data acquired should also be analysed in a compositional context, in order to provide the most accurate and easily interpreted understanding of geochemical variation at the site.

f) Historic and recent geochemistry data from the area surrounding Galmoy Mine (approximately 7.5 kilometres northeast of Lisheen; see Fig. 1.3) could also be examined using CoDA methods and compared to the findings from Lisheen. This would provide a complete perspective of the effects of Pb/Zn mining activity on groundwater in this part of south-central Ireland.

g) The outcomes from CoDA at Lisheen in a mineral exploration context, could be applied to other mineralogically prospective areas in Ireland with similar Mississippian bedrock geology (e.g. counties Tipperary, Limerick and Clare; Ireland, 2016).

h) The CoDA method should be refined for the Tellus Border Region and the rest of Ireland as the data becomes available, so that the variability that is most reflective of environmental conditions is displayed in the resulting maps.

The outcomes of this thesis and those documented in Wheeler *et al.* (2021), should be combined with other recent and emerging research results from the Irish Centre for Research in Applied Geosciences (iCRAG) (e.g. Hitzman *et al.*, 2018; Torremans *et al.*, 2018; Walsh *et al.*, 2018; Kyne *et al.*, 2019) to provide a greater understanding of nature of mineral resources in Ireland, their importance to the Irish economy and how they can be sustainably utilised.

References

ABDI, H., & WILLIAMS, L.J. (2010). Principal component analysis. *WIREs Comp. Stat.*, **2**, 433-459. https://doi.org/10.1002/wics.101.

ABSON, D. J., DOUGILL, A. J., & STRINGER, L. C. (2012). Using principal component analysis for information-rich socio-ecological vulnerability mapping in Southern Africa. *Applied Geography*, **35**(1-2), 515-524. https://doi.org/10.1016/j.apgeog.2012.08.004.

AITCHISON, J. (1982). The statistical analysis of compositional data (with discussion). *Journal of the Royal Statistical Society, Series B (Statistical Methodology)*, **44**(2), 139-177. https://www.jstor.org/stable/2345821.

AITCHISON, J.D. (1983). Principal component analysis of compositional data. *Biometrika*, **70**, 57-65. https://doi.org/10.1093/biomet/70.1.57.

AITCHISON, J.D. (1985). A General Class of Distributions on the Simplex. *Journal of the Royal Statistical Society. Series B (Methodological)*, **47**, 136-146. https://doi.org/10.1111/j.2517-6161.1985.tb01341.x.

AITCHISON, J. (1986). The statistical analysis of compositional data. Monographs on statistics and applied probability. *Chapman and Hall Ltd. (reprinted 2003 with additional materials by The Blackburn Press), London, UK*.

AITCHISON, J. (1992). On criteria for measures of compositional difference. *Mathematical Geology*, **24**(4), 365-379. https://doi.org/10.1007/BF00891269.

AITCHISON, J., & GREENACRE, M. (2002). Biplots for compositional data. *Applied Statistics*, **51**(4), 375-392. https://www.jstor.org/stable/3592616.

AITCHISON, J., & NG, K. (2005). The role of the perturbation in compositional data analysis. *Statistical Modelling*, **5**(2), 173-185. https://doi.org/10.1191/1471082X05st091oa.

AITCHISON, J., & SHEN, S.M. (1980). Logistic-normal distributions. Some properties and uses. *Biometrika*, **67**(2), 261-272. https://doi.org/10.2307/2335470.

AITCHISON, J., BARCELÓ-VIDAL, C., MARTÍN-FERNÁNDEZ, J.A., & PAWLOWSKY-GLAHN, V. (2000). Logratio analysis and compositional distance. *Mathematical Geology*, **32**(3), 270-275. https://doi.org/10.1023/A:1007529726302.

AKCIL, A., & KOLDAS, S. (2006). Acid Mine Drainage (AMD): causes, treatment and case studies. *Journal of Cleaner Production*, **14**(12-13), 1139-1145. https://doi.org/10.1016/j.jclepro.2004.09.006.

AKIYAMA, T., & YAO, Y. M. (2001). A major compound in fused potassium silicate fertilizer. *Japanese Journal of Soil Science and Plant Nutrition (Japan)*.

ALDWELL, C. R. (1990). Some examples of mining in Ireland and its impact on the environment. *Environmental Geology and Water Sciences*, **15**(2), 145-157. https://doi.org/10.1007/BF01705103.

ALDWELL, C. R., & BURDON, D. J. (1980). Hydrogeothermal conditions in Ireland. In: *XXVI International Geological Congress. Fossil Fuels Sec, Paris* (Vol. 14, No. 14.0068, p. 21).

ALFARO, M.A., JARVIS, S.C., & GREGORY, P.J. (2004). Factors affecting potassium leaching in different soils. *Soil Use and Management*, **20**(2), 182-189. https://doi.org/10.1111/j.1475-2743.2004.tb00355.x.

ALKHATIB, M., & EISENHAUER, A. (2017). Calcium and strontium isotope fractionation during precipitation from aqueous solutions as a function of temperature and reaction rate; II. Aragonite. *Geochimica et Cosmochimica Acta*, **209**, 320-342. https://doi.org/10.1016/j.gca.2017.04.012.

AMUNDSON, R., BERHE, A.A., HOPMANS, J.W., OLSON, C., SZTEIN, A.E., & SPARKS, D.L. (2015). Soil and human security in the 21st century. *Science*, **348**(6235). https://doi.org/10.1126/science.1261071.

ANDREW, C.J. (1986). The tectono-stratigraphic controls to mineralization in the Silvermines area, County Tipperary, Ireland. In: ANDREW, C.J., CROWE, R.W.A., FINLAY, S., PENNEL, W.M., & PYNE, J.F., (Eds.),

Geology and genesis of mineral deposits in Ireland: Dublin. Irish Association for Economic Geology, 377–417.

APPLETON, J. D., MILES, J. C. H., GREEN, B. M. R., & LARMOUR, R. (2008). Pilot study of the application of Tellus airborne radiometric and soil geochemical data for radon mapping. *Journal of Environmental Radioactivity*, **99**(10), 1687-1697. https://doi.org/10.1016/j.jenvrad.2008.03.011.

ARCHER, J. B. (1981). The Lower Palaeozoic rocks of the northwestern part of the Devilsbit-Keeper Hill inlier and their implications for the postulated course of the Iapetus Suture zone in Ireland. *Journal of Earth Sciences*, 21-38. https://www.jstor.org/stable/30002459.

ARUGA, R. (1997). Treatment of responses below the detection limit: some current techniques compared by factor analysis on environmental data. *Anal. Chim. Acta,* **354**, 255– 262. https://doi.org/10.1016/S0003-2670(97)00463-7.

ASHTON, J.H., BLAKEMAN, R.J., GERAGHTY, J.F., O'DONOVAN, B., BEACH, A., COLLER, D., PHILCOX, M., BOYCE, A., & WILKINSON, J. (2016). The Giant Navan Carbonate-Hosted Zn-Pb Deposit: Exploration and Geology: 1970-2015. *Mineral Deposits Studies Group, 39th Winter Meeting 2016*.

ASLIBEKIAN, O., GRAY, N., & MOLES, R. (1999). Metal Contamination of surface water related to past mining activity in Ireland. *In: IMWA-Mine, Water & Environment Congress. Sevilla*. 535-541.

BACON, J. R., BUTLER, O. T., CAIRNS, W. R., CAVOURA, O., COOK, J. M., DAVIDSON, C. M., & MERTZ-KRAUS, R. (2021). Atomic spectrometry update–a review of advances in environmental analysis. *Journal of Analytical Atomic Spectrometry*, **36**, 10-55. https://doi.org/10.1039/D0JA90074E.

BACON-SHONE, J. (2011). A short history of compositional data analysis. In: *Pawlowsky-Glahn, V. & Buccianti, A.* (eds.), Compositional data analysis: Theory and applications. *John Wiley & Sons*.

BAILEY, T. C., & KRZANOWSKI, W. J. (2000). Extensions to spatial factor methods with an illustration in geochemistry. *Mathematical Geology*, **32**(6), 657-682. https://doi.org/10.1023/A:1007589505425.

BANKS, D., YOUNGER, P. L., ARNESEN, R. T., IVERSEN, E. R., & BANKS, S. B. (1997). Mine-water chemistry: the good, the bad and the ugly. *Environmental Geology*, **32**(3), 157-174. https://doi.org/10.1007/s002540050204.

BARHAM, M., MURRAY, J., SEVASTOPULO, G.D., & WILLIAMS, D.M. (2015). Conodonts of the genus Lochriea in Ireland and the recognition of the Viséan–Serpukhovian (Carboniferous) boundary. *Lethaia*, **48**(2), 151-171. https://doi.org/10.1111/let.12096.

BAUER, S., LIEDL, R., & SAUTER, M. (2005). Modelling the influence of epikarst evolution on karst aquifer genesis: A timevariant recharge boundary condition for joint karst-epikarst development. *Water Resources Research*, **41**, https://doi.org/10.1029/2004WR003321.

BENEDETTI, M. F., DIA, A., RIOTTE, J., CHABAUX, F., GÉRARD, M., BOULEGUE, J., FRITZ, B., CHAUVELE, C., BULOURDE, M., DÉRUELLE, B., & ILDEFONSE, P. (2003). Chemical weathering of basaltic lava flows undergoing extreme climatic conditions: the water geochemistry record. *Chemical Geology,* **201**(1-2), 1-17. https://doi.org/10.1016/S0009-2541(03)00231-6.

BHATIA, M. R. (1985). Rare earth element geochemistry of Australian Paleozoic graywackes and mudrocks: provenance and tectonic control. *Sedimentary geology*, **45**(1-2), 97-113. https://doi.org/10.1016/0037-0738(85)90025-9.

BIESTER, H., SELIMOVIĆ, D., HEMMERICH, S., & PETRI, M. (2006). Halogens in pore water of peat bogs–the role of peat decomposition and dissolved organic matter. *Biogeosciences*, **3**(1), 53-64. https://doi.org/10.5194/bg-3-53-2006.

BINDLER, R. (2006). Mired in the past—looking to the future: geochemistry of peat and the analysis of past environmental changes. *Global and Planetary change*, **53**(4), 209-221. https://doi.org/10.1016/j.gloplacha.2006.03.004.

BIRKS, S. J., FENNELL, J. W., GIBSON, J. J., YI, Y., MONCUR, M. C., & BREWSTER, M. (2019). Using regional datasets of isotope geochemistry to resolve complex groundwater flow and formation connectivity in northeastern Alberta, Canada. *Applied Geochemistry*, **101**, 140-159. https://doi.org/10.1016/j.apgeochem.2018.12.013.

BISUTTI, I., HILKE, I., & RAESSLER, M. (2004). Determination of total organic carbon–an overview of current methods. *TrAC Trends in Analytical Chemistry*, **23**(10-11), 716-726. https://doi.org/10.1016/j.trac.2004.09.003.

BLAKE, S., HENRY, T., MURRAY, J., FLOOD, R., MULLER, M.R., JONES, A.G., & RATH, V. (2016). Compositional multivariate statistical analysis of thermal groundwater provenance: A hydrogeochemical case study from Ireland. *Applied Geochemistry*. **75**, 177-188. https://doi.org/10.1016/j.apgeochem.2016.05.008.

BLOWICK, A., HAUGHTON, P., TYRRELL, S., HOLBROOK, J., CHEW, D., & SHANNON, P. (2019). All mixed up: Pb isotopic constraints on the transit of sands through the Mississippi-Missouri River drainage basin, North America. *Bulletin*, **131**(9-10), 1501-1518. https://doi.org/10.1130/B35057.

BORGULAT, J., MĘTRAK, M., STASZEWSKI, T., WIŁKOMIRSKI, B., & SUSKA-MALAWSKA, M. (2018). Heavy Metals Accumulation in Soil and Plants of Polish Peat Bogs. *Polish Journal of Environmental Studies*, **27**(2). https://doi.org/10.15244/pjoes/75823.

BOTTRELL, S., & BARTLETT, R. (2008). Stable isotope methods in groundwater engineering. *Proceedings of the Institution of Civil Engineers – Water Management*, **161**(6), 357-365. https://doi.org/10.1680/wama.2008.161.6.357.

BRAND, N. W. (1999). Element ratios in nickel sulphide exploration: vectoring towards ore environments. *Journal of Geochemical Exploration*, **67**(1-3), 145-165. https://doi.org/10.1016/S0375-6742(99)00063-1.

BRINK, N. (1975). Water pollution from agriculture. *Journal (Water Pollution Control Federation)*, 789-795. https://www.jstor.org/stable/25076345.

BRUNI, J., CANEPA, M., CHIODINI, G., CIONI, R., CIPOLLI, F., LONGINELLI, A., MARINI, L., OTTONELLO, G., & ZUCCOLINI, M. V. (2002). Irreversible water–rock mass transfer accompanying the generation of the neutral, Mg–HCO3 and high-pH, Ca–OH spring waters of the Genova province, Italy. *Applied Geochemistry*, **17**(4), 455-474. https://doi.org/10.1016/S0883-2927(01)00113-5.

BUCCIANTI, A., LIMA, A., ALBANESE, S., CANNATELLI, C., ESPOSITO, R., & DE VIVO, B. (2015). Exploring topsoil geochemistry from the CoDA (Compositional Data Analysis) perspective: The multi-element data archive of the Campania Region (Southern Italy). *Journal of Geochemical Exploration*, **159**, 302-316. https://doi.org/10.1016/j.gexplo.2015.10.006.

BUCCIANTI, A., & PAWLOWSKY-GLAHN, V. (2005). New perspectives on water chemistry and compositional data analysis. *Mathematical Geology,* **37**(7), 703-727. https://doi.org/10.1007/s11004-005-7376-6.

BUROW, K.R., NOLAN, B.T., RUPERT, M.G., & DUBROVSKY, N.M. (2010). Nitrate in Groundwater of the United States, 1991−2003. *Environmental Science and Technology*. **44**(13), 4988-4997. https://doi.org/10.1021/es100546y.

CARBONI, V., WALSH, J., STEWART, D., & GÜVEN, J. (2003). Timing and geometry of normal faults and associated structures at the Lisheen Zn/Pb deposit — investigating their role in the transport and the trapping of metals, In: ELIOPOULOS, D.G., *et al*., (Eds.), Proceedings of the Seventh Biennial SGA Meeting, Mineral Exploration and Sustainable Development: Rotterdam, *Millpress Science Publishers*, 665–668.

CARITAT, P. DE, KIRSTE, D., CARR, G., & MCCULLOCH, M. (2005). Groundwater in the Broken Hill region, Australia: recognising interaction with bedrock and mineralisation using S, Sr and Pb isotopes. *Applied Geochemistry*. **20**(4), 767-787. https://doi.org/10.1016/j.apgeochem.2004.11.003.

CARUCCI, V., PETITTA, M., & ARAVENA, R. (2012). Interaction between shallow and deep aquifers in the Tivoli Plain (Central Italy) enhanced by groundwater extraction: a multi-isotope approach and geochemical modeling. *Applied Geochemistry*, **27**(1), 266-280. https://doi.org/10.1016/j.apgeochem.2011.11.007.

CHAYES, F. (1960). On correlation between variables of constant sum. *Journal of Geophysical Research*, **65**(12), 4185-4193. https://doi.org/10.1029/JZ065i012p04185.

CHAYES, F. (1962). Numerical correlation and petrographic variation. *The Journal of Geology*, **70**, 440-452. https://doi.org/10.1086/626835.

CHAYES, F. (1971). Correlations between proportions: the closed array. In: CHAYES, F., (*Eds*.), Ratio Correlation: A Manual for Students of Petrology and Geochemistry. *The University of Chicago Press.*

CHAYES, F., & TROCHIMCZYK, J. (1978). An effect of closure on the structure of principal components. *Mathematical Geology*, **10**, 323. https://doi.org/10.1007/BF01031737.

CHEW, D.M. (2009). Grampian Orogeny. In: HOLLAND, C.H., & SANDERS, I.S. (Eds.), The geology of Ireland, Second Edition, *Dunedin Academic Press*, 69-93.

CHEW, D.M. (2012). The Grampian evolution of the Caledonides of NW Ireland. *Open University Geological Society Journal,* **33**(1), 19-25.

CHEW, D.M., & STRACHAN, R.A. (2014). The Laurentian Caledonides of Scotland and Ireland. In: CORFU, F., GASSER, D., & CHEW, D.M. (Eds.), New Perspectives on the Caledonides of Scandinavia and Related Areas. *Geological Society, London, Special Publications*. **309**, 45–91.

CHUNG, C.F. (1993). Estimation of covariance matrix from geochemical data with observations below detection limits. *Mathematical* Geology, **25**, 851– 865. https://doi.org/10.1007/BF00891047.

CLARK I. D., & FRITZ P. (1997). Environmental Isotopes in Hydrogeology, *CRC Press, Boca Raton, FL.*

CLARKE, J.U. (1998). Evaluation of censored data methods to allow statistical comparisons among very small samples with below detection limit observations. *Environmental Science Technol*ogy, **32**, 177–183. https://doi.org/10.1021/es970521v.

CLARK, R. N., & SWAYZE, G. A. (1996, March). Evolution in imaging spectroscopy analysis and sensor signal-to-noise: An examination of how far we have come. In *Proc. Summaries 6th Annu. JPL Airborne Earth Sci. Workshop* (pp. 49-53).

CLAYTON, G., GRAHAM, J.R., HIGGS, K.T., SEVASTOPULO, G.D., & WELSH, A. (1986). Late Devonian and Early Carboniferous palaeogeography of southern Ireland and southwest Britain. *Annales de la Société géologique de Belgique*. **109**, 103-111.

Closure, Restoration and Aftercare Management Plan (C.R.A.M.P), Lisheen Mine. 2016.

CLOUTIER, V., LEFEBVRE, R., THERRIEN, R., & SAVARD, M. M. (2008). Multivariate statistical analysis of geochemical data as indicative of the hydrogeochemical evolution of groundwater in a sedimentary rock aquifer system. *Journal of Hydrology*, **353**(3-4), 294-313. https://doi.org/10.1016/j.jhydrol.2008.02.015.

COLE, G.A.J. (1922). Memoir of localities of minerals of economic importance and metalliferous mines in Ireland. Memoir of the Geological Survey of Ireland (facsimile edition by Mining Heritage Society of Ireland: Dublin, 1998).

COLLER, D.W. (1984). Variscan structures in the Upper Palaeozoic rocks of west central Ireland: *Geological Society, London, Special Publications*, **14**, 185–194, https://doi.org/10.1144/GSL.SP.1984.014.01.18.

COLMER, A.R., & HINKLE, M.E. (1947). The role of Microorganisms in Acid Mine Drainage: A preliminary report. *Science*, **106**(2751). 253-256. https://www.jstor.org/stable/1675656.

CONNELLY, R., REES, B., BOWELL, R., & FARRELL, L. (2005). Rehabilitation Planning for Abandoned Mines at Silvermines, Tipperary, Ireland. *Proceedings international mine water association*.

CONTI, A., SACCHI, E., CHIARLE, M., MARTINELLI, G., & ZUPPI, G.M. (2000). Geochemistry of the formation waters in the Po plain (Northern Italy): an overview. *Applied Geochemistry*. **15**(1), 51-65. https://doi.org/10.1016/S0883-2927(99)00016-5.

COPE, R. N. (1959, January). The Silurian Rocks of the Devilsbit Mountain District, County Tipperary (With an Appendix on the Micro-Petrography by WA Cummins). In Proceedings of the Royal Irish Academy. Section B: Biological, Geological, and Chemical Science (pp. 217-242). Hodges, Figgis, & Co..

COURTNEY, R. (2018). Chapter 24 - Irish Mine Sites Rehabilitation — A Case Study. *Bio-Geotechnologies for Mine Site Rehabilitation,* 439-456. https://doi.org/10.1016/B978-0-12-812986-9.00024-5.

COWAN, M., & VERBRUGGEN, K. (2016). Directors' Foreword. In: STEWART, I., (Author) & YOUNG M. (Ed.), Unearthed: Impacts of the Tellus surveys of the north of Ireland (pp. Xi-Xii). Dublin: Royal Irish Academy. https://doi.org/10.2307/j.ctt1g69w6r.4.

CRISS R. E. (1999). Principles of Stable Isotope Distribution, *Oxford University Press, New York.*

DA COSTA MELLO, S., PIERCE, F. J., TONHATI, R., ALMEIDA, G. S., NETO, D. D., & PAVULURI, K. (2018). Potato response to polyhalite as a potassium source fertilizer in Brazil: Yield and quality. *HortScience*, **53**(3), 373-379. https://doi.org/10.21273/HORTSCI12738-17.

DALY, J.S. (2009) Precambrian. In: Holland, C.H. and Sanders, I.S. (eds) *The Geology of Ireland, 2nd Edition*, Dunedin Academic Press, Edinburgh, pp.7 - 42.

DA SILVA, Y. J. A. B., DO NASCIMENTO, C. W. A., VAN STRAATEN, P., BIONDI, C. M., DE SOUZA JÚNIOR, V. S., & DA SILVA, Y. J. A. B. (2017). Effect of I-and S-type granite parent material mineralogy and geochemistry on soil fertility: A multivariate statistical and Gis-based approach. *Catena*, **149**, 64-72. https://doi.org/10.1016/j.catena.2016.09.001.

DARROCH, J.N., & JAMES, I.R. (1974). F-Independence and Null Correlation of Continuous, Bounded-Sum, Positive Variables. *Journal of the Royal Statistical Society. Series B (Methodological)*, **36**(3), 467-483. https://doi.org/10.1111/j.2517-6161.1974.tb01023.x.

DE RUIJTER, F. J., BOUMANS, L. J. M., SMIT, A. L., & VAN DEN BERG, M. (2007). Nitrate in upper groundwater on farms under tillage as affected by fertilizer use, soil type and groundwater table. *Nutrient Cycling in Agroecosystems*, **77**(2), 155-167. https://doi.org/10.1007/s10705-006-9051-9.

DORAN, A., MENUGE, J., HOLLIS, S. P., GÜVEN, J., & DENNIS, P. (2017, August). Enhancing current understanding of Irish Zn-Pb mineralization: a closer look at the Island Pod orebody, Lisheen deposit. In: SGA Quebec 2017 14th Biennial Meeting, Quebec City, Canada, August 20-23 2017. *Society for Geology Applied to Mineral Deposits*.

DUANE, M. J., WELKE, H. J., & ALLSOPP, H. L. (1986). U-Pb age for some base-metal sulfide deposits in Ireland: Genetic implications for Mississippi Valley-type mineralization. *Geology*, **14**(6), 477-480. https://doi.org/10.1130/0091-7613(1986)14<477:UAFSBS>2.0.CO;2.

EANG, K. E., IGARASHI, T., KONDO, M., NAKATANI, T., TABELIN, C. B., & FUJINAGA, R. (2018). Groundwater monitoring of an open-pit limestone quarry: Water-rock interaction and mixing estimation within the rock layers by geochemical and statistical analyses. *International journal of mining science and technology*, **28**(6), 849-857. https://doi.org/10.1016/j.ijmst.2018.04.002.

EGOZCUE, J.J., & PAWLOWSKY-GLAHN, V. (2005). Groups of parts and their balances and compositional data analysis. *Mathematical Geology*, **37**(7), 795-828. https://doi.org/10.1007/s11004-005-7381-9.

EGOZCUE, J., & PAWLOWSKY-GLAHN, V. (2011). Basic concepts and procedures. In: PAWLOWSKY-GLAHN, V., & BUCCIANTI, A., (Eds.), Compositional Data Analysis. Theory and Applications. *John Wiley & Sons, Chichester (UK)*, 12-28.

EGOZCUE, J.J., PAWLOWSKY-GLAHN, V., MATEU-FIGUERAS, G., & BARCELÓ-VIDAL, C. (2003). Isometric logratio transformations for compositional data analysis. *Mathematical Geology*, **35**(3), 279-300. https://doi.org/10.1023/A:1023818214614.

ENGLE, M.A., & BLONDES, M.S. (2014). Linking compositional data analysis with thermodynamic geochemical modeling: Oilfield brines from the Permian Basin, USA. *Journal of Geochemical Exploration*. **141**, 61-70. https://doi.org/10.1016/j.gexplo.2014.02.025.

Environmental Protection Agency (Irish EPA), (2012). Corine Landcover Map.

ESMAEILOGHLI, S., & TABATABAEI, S. H. (2020). Comparative analysis of geochemical data processing methods for allocation of anomalies and background. *Geochemistry International*, **58**, 472-485. https://doi.org/10.1134/S0016702920040084.

European Communities (Drinking Water) (No.2) Regulations (2007) (S.I. 278 of 2007). Section 4: Guidance on Sampling. In: *A Handbook on the Implementation of the Regulations for Water Services Authorities for Public Water Supplies.*

European Environment Agency (EEA), (2019). Updated CLC illustrated nomenclature guidelines.

EVERETT, C. E., WILKINSON, J. J., & RYE, D. M. (1999). Fracture-controlled fluid flow in the Lower Palaeozoic basement rocks of Ireland: implications for the genesis of Irish-type Zn-Pb deposits. *Geological Society, London, Special Publications*, **155**(1), 247-276. https://doi.org/10.1144/GSL.SP.1999.155.01.18.

EYRE, S.L. (1998). Geochemistry of dolomitization and Zn-Pb mineralization in the Rathdowney trend, Ireland: Ph.D. thesis, London, University of London, 419.

FALLON, P., & MURRAY, J. (2015). Conodont biostratigraphy of the mid-Carboniferous boundary in Western Ireland. *Geological Magazine*, **152**(6), 1025-1042. https://doi.org/10.1017/S0016756815000072.

FARNHAM, I.M., STETZENBACH, K.J., SINGH, A.S., & JOHANNESSON, K.H. (2002). Treatment of nondetects in multivariate analysis of groundwater geochemistry data. *Chemometrics and Intelligent Laboratory Systems*, **60**, 265-281. https://doi.org/10.1016/S0169-7439(01)00201-5.

FILZMOSER, P, HRON, K., & REIMANN, C. (2009). Univariate statistical analysis of environmental (compositional) data: Problems and possibilities. *Science of the Total Environment*, **407**, 23, 6100-6108. https://doi.org/10.1016/j.scitotenv.2009.08.008.

FILZMOSER, P, HRON, K., & REIMANN, C. (2010). The bivariate statistical analysis of environmental (compositional) data. *Science of the Total Environment*, **408**, 19, 4230-4238. https://doi.org/10.1016/j.scitotenv.2010.05.011.

FILZMOSER, P., HRON, K., & TEMPL, M. (2018). Applied Compositional Data Analysis, With Worked Examples in R. *Springer Series in Statistics*. https://doi.org/10.1007/978-3-319-96422-5_6.

FIŠEROVÁ, E., & HRON, K. (2011). On the Interpretation of Orthonormal Coordinates for Compositional Data. *Mathematical Geosciences*, **43**, 455. https://doi.org/10.1007/s11004-011-9333-x.

FITCH RESOURCES (2018). Industry Trend Analysis - Global Zinc Mining Outlook. Business Monitor International Ltd and/or Fitch Solutions Group Ltd.

FLETCHER, W. K. (1986). *Exploration geochemistry: design and interpretation of soil surveys* (Vol. 3, p. 180). Society of Economic Geologists.

FORGY, E.W. (1965). Cluster analysis of multivariate data: efficiency vs interpretability of classifications. *Biometrics*, **21**, 768-769.

FORMOSO, M. L. (2006). Some topics on geochemistry of weathering: a review. *Anais da Academia Brasileira de Ciências*, **78**(4), 809-820. http://dx.doi.org/10.1590/S0001-37652006000400014.

FORTESCUE, J. A. (2012). Environmental geochemistry: A holistic approach (Vol. 35). Springer Science & Business Media.

FRALEY, C., & RAFTERY, A.E. (2002). Model-based clustering, discriminant analysis, and density estimation. *Journal of the American Statistical Association*, **97**(458), 611–631. https://doi.org/10.1198/016214502760047131.

FRALEY, C., RAFTERY, A., SCRUCCA, L., MURPHY, T.B., FOP, M., & SCRUCCA, M.L. (2012). Package 'mclust'. *The R journal*.

FRANKS, F. (1973). The solvent properties of water. In: *Water in Crystalline Hydrates Aqueous Solutions of Simple Nonelectrolytes* (pp. 1-54). Springer, Boston, MA.

FRY, J.M., FRY, T.R.L., & MCLAREN, K.R. (2000). Compositional data analysis and zeros in micro data… *Applied Economics*, **32**(8), 953-959. https://doi.org/10.1080/000368400322002.

FU, W., TUNNEY, H., & ZHANG, C. (2010). Spatial variation of soil nutrients in a dairy farm and its implications for site-specific fertilizer application. *Soil and Tillage Research*, **106**(2), 185-193. https://doi.org/10.1016/j.still.2009.12.001.

FUSCIARDI, L.P., GÜVEN, J.F., STEWART, D.R.A., CARBONI, V., & WALSH, J.J. (2004). The geology and genesis of the Lisheen Zn-Pb deposit, Co. Tipperary, Ireland, In: KELLY, J.G., ANDREW, C.J., ASHTON, J.H., BOLAND, M.B., EARLS, G., FUSCIARDI, L., & STANLEY, G., (Eds.), Europe's major base metal deposits: Special Publication of the Irish Association for Economic Geology, 455–481.

GABRIEL, K.R. (1971). The biplot – graphic display of matrices with application to principal component analysis. *Biometrika*, **58**(3), 453-467. https://doi.org/10.2307/2334381.

GALLAGHER, V., & O'CONNOR, P. (1999). The Avoca Mine Site. *Biology and Environment: Proceedings of the Royal Irish Academy,* **99B**, 43-57.

GALLO, M., & BUCCIANTI, A. (2013). Weighted principal component analysis for compositional data: application example for the water chemistry of the Arno river (Tuscany, central Italy). *Environmetrics*, **24**, 269-277. https://doi.org/10.1002/env.2214.

GAŁUSZKA, A., & MIGASZEWSKI, Z. (2011). Geochemical background-an environmental perspective. *Mineralogia*, **42**, 1, 7-17. https://doi.org/10.2478/v10002-011-0002-y.

GARRETT, R.G., REIMANN, C., SMITH, D.B., & XIE, X. (2008). From geochemical prospecting to international geochemical mapping: a historical overview. *Geochemistry: Exploration, Environment, Analysis*, **8**, 3-4, 205-217. https://doi.org/10.1144/1467-7873/08-174.

GAT, J. R., & GONFIANTINI, R. (1981). Stable isotope hydrology. Deuterium and oxygen-18 in the water cycle. *International Atomic Energy Agency (IAEA)*.

Geological Survey of Ireland (GSI), (2004). Bedrock Geology of Ireland. Simplified from the Geological Survey of Ireland 1:100,000 scale Bedrock Map Series (1993 - 2003) and the Geological Survey of Northern Ireland 1:250,000 scale Geological Map of Northern Ireland (1997).

Geological Survey of Ireland (GSI), (2018). GSI Bedrock Geology 100k Series (1:100,000). "Contains Irish Public Sector Data (Geological Survey Ireland) licensed under a Creative Commons Attribution 4.0 International (CC BY 4.0) licence".

GHASEMZADEH, S., MAGHSOUDI, A., YOUSEFI, M., & MIHALASKY, M. J. (2019). Stream sediment geochemical data analysis for district-scale mineral exploration targeting: Measuring the performance of the spatial U-statistic and CA fractal modeling. *Ore Geology Reviews*, **113**, 103115. https://doi.org/10.1016/j.oregeorev.2019.103115.

GILLMOR, D. A. (1965). The revival of base metal mining in the republic of Ireland. *Irish Geography*, **5**(2), 220-225.

GLEESON, T., & MANNING, A. H. (2008). Regional groundwater flow in mountainous terrain: Three-dimensional simulations of topographic and hydrogeologic controls. *Water Resources Research*, **44**(10). https://doi.org/10.1029/2008WR006848.

GOCHFELD, M., VOLZ, C. D., BURGER, J., JEWETT, S., POWERS, C. W., & FRIEDLANDER, B. (2006). Developing a health and safety plan for hazardous field work in remote areas. *Journal of occupational and environmental hygiene*, **3**(12), 671-683.

GOUDIE, A.S. (2018). Human impact on the natural environment. John Wiley & Sons.

Government of Ireland, (1940). *Minerals Development Act*, No 31 of 1940.

Government of Ireland, (1956). *Finance (Profits of Certain Mines) (Temporary Relief From Taxation) Act*, No 8 of 1956.

Govett, G. J. S. (Ed.). (2013). *Rock geochemistry in mineral exploration*. Elsevier.

GOZZI, C., SAURO GRAZIANO, R., FRONDINI, F., & BUCCIANTI, A. (2018). Innovative monitoring tools for the complex spatial dynamic of river chemistry: case study for the Alpine Region. *Environmental Earth Science,* **77**(16), 579, 1-11. https://doi.org/10.1007/s12665-018-7756-0.

GRAHAM, J.R. (2009). Devonian. In: HOLLAND, C.H., & SANDERS, I.S. (Eds.), The Geology of Ireland, second ed. Dunedin Academic Press Ltd, Edinburgh, 175-214.

GRAHAM, J.R., & SEVASTOPULO, G.D. (2020). The stratigraphy of latest Devonian and earliest Carboniferous rocks in Ireland. *Palaeobiodiversity and Palaeoenvironments.* https://doi.org/10.1007/s12549-020-00455-y.

GÜLER, C., THYNE, G. D., MCCRAY, J. E., & TURNER, K. A. (2002). Evaluation of graphical and multivariate statistical methods for classification of water chemistry data. *Hydrogeology journal*, **10**(4), 455-474. https://doi.org/10.1007/s10040-002-0196-6.

GÜLER, C., KURT, M.A., ALPASLAN, M., & AKBULUT, C. (2012). Assessment of the impact of anthropogenic activities on the groundwater hydrology and chemistry in Tarsus coastal plain (Mersin, SE Turkey) using fuzzy clustering, multivariate statistics and GIS techniques. *Journal of Hydrology*, 435-451. https://doi.org/10.1016/j.jhydrol.2011.11.021.

GÜLER, C., THYNE, G. D., TAĞA, H., & YILDIRIM, Ü. (2017). Processes governing alkaline groundwater chemistry within a fractured rock (ophiolitic melange) aquifer underlying a seasonally inhabited headwater area in the Aladağlar range (Adana, Turkey). *Geofluids*, 2017. https://doi.org/10.1155/2017/3153924.

GUO, W., ZHANG, J., GUO, Q., JIN, L., & HU, S. (2016). Sensitive screening of bromate in drinking water by an improved ion chromatography ICP-MS method. *Microchemical Journal*, **124**, 127-131. https://doi.org/10.1016/j.microc.2015.08.009.

HAN, G., & LIU, C. Q. (2004). Water geochemistry controlled by carbonate dissolution: a study of the river waters draining karst-dominated terrain, Guizhou Province, China. *Chemical Geology*, **204**(1-2), 1-21. https://doi.org/10.1016/j.chemgeo.2003.09.009.

HARTIGAN, J. A., & WONG, M. A. (1979). Algorithm AS 136: A K-means clustering algorithm. *Applied Statistics*, **28**, 100-108. https://doi.org/10.2307/2346830.

HAWKES, H. E., & WEBB, J. S. (1963). Geochemistry in mineral exploration. *Soil Science*, **95**(4), 283.

HELSEL, D.R. (1990). Less than obvious; Statistical treatment of data below the detection limit. *Environmental Science & Technology,* **24**, 1766–1773. https://doi.org/10.1021/es00082a001.

HENGL, T., LEENAARS, J. G., SHEPHERD, K. D., WALSH, M. G., HEUVELINK, G. B., MAMO, T., ... & KWABENA, N. A. (2017). Soil nutrient maps of Sub-Saharan Africa: assessment of soil nutrient content at 250 m spatial resolution using machine learning. *Nutrient Cycling in Agroecosystems*, **109**(1), 77-102. https://doi.org/10.1007/s10705-017-9870-x.

HENRY, T. (2011, September). Tynagh mine groundwater issues. In Mine Water-Managing the Challenges, Proceedings of the 11th Congress of the International Mine Water Association, Aachen, Germany (pp. 4-11).

HENRY, T. (2014). An Integrated Approach to Characterising the Hydrogeology of the Tynagh Mine Catchment, County Galway, Ireland. *PhD Thesis, National University of Ireland Galway*.

HERITY, M., & EOGAN, G. (1996). Ireland in Prehistory. *Routledge*.

HITZMAN, M.W. (1995). Geological setting of the Irish Zn-Pb-(Ba-Ag) orefield. *Society of Economic Geologists Guidebook Series*, 21, 3−23.

HITZMAN, M.W., (1999). Extensional faults that localize Irish syndiagenetic Zn±Pb deposits and their reactivation during Variscan compression. *In:* McCaffrey, K.J.W., Lonergan, L., Wilkinson, J.J. (Eds.), *Fractures, Fluid Flow and Mineralization*. Geological Society of London Special Publication, **151**, 233-245.

HITZMAN, M.W., ALLAN, J.R., BEATY, D.W., 1998. Regional dolomitization of the Waulsortian limestone in southeastern Ireland: Evidence of large-scale fluid flow driven by the Hercynian orogeny. *Geology*, 26(6), 547-550. https://doi.org/10.1130/0091-7613(1998)026<0547:RDOTWL>2.3.CO;2.

HITZMAN, M. W., GUVEN, J., & CRAIG, J. (2018, December). Integrated Approaches to Mineral Resource Security: A view from Ireland. In AGU Fall Meeting Abstracts (Vol. 2018, pp. V31G-0205).

HITZMAN, M.W., O'CONNOR, P.G., SHEARLEY, E., SCHAFFALITZKY, C., BEATTY, D.W., ALLAN, J.R., & THOMPSON, T. (1992). Discovery and geology of the Lisheen Zn-Pb-Ag prospect, Rathdowney trend, Ireland. In: BOWDEN, A.A., EARLS, G., O'CONNOR, P.G., PYNE, J.F. (Eds.), *The Irish Minerals Industry 1980–1990*. Irish Association for Economic Geology, Dublin, pp. 227–246.

HITZMAN, M.W., REDMOND, P.B., & BEATY, D.W. (2002). The Carbonate-Hosted Lisheen Zn-Pb-Ag Deposit, County Tipperary, Ireland. *Economic Geology*. 97, 1627-1655. https://doi.org/10.2113/gsecongeo.97.8.1627.

HÖCKER, O., BADER, T., SCHMIDT, T. C., SCHULZ, W., & NEUSÜß, C. (2020). Enrichment-free analysis of anionic micropollutants in the sub-ppb range in drinking water by capillary electrophoresis-high resolution mass spectrometry. *Analytical and bioanalytical chemistry*, 1-9. https://doi.org/10.1007/s00216-020-02525-8.

HOEFS, J. (1997) *Stable Isotope Geochemistry*. Springer-Verlag (1997) 4th completely revised, updated, and enlarged edition. 201 p.

HOLLAND, C.H. (2009). Silurian. In: Holland, C.H. & Sanders, I.D. (eds) *The Geology of Ireland*. Dunedin Academic Press, Edinburgh, 119–141.

HOSSEINI-DINANI, H., MOKHTARI, A. R., SHAHRESTANI, S., & DE VIVO, B. (2019). Sampling density in regional exploration and environmental geochemical studies: a review. *Natural Resources Research*, **28**(3), 967-994. https://doi.org/10.1007/s11053-018-9431-2.

HUTTON, D.H.W. (1982) A tectonic model for the emplacement of the Main Donegal Granite, NW Ireland. *Journal of the Geological Society*, **139**(5), 615-631. https://doi.org/10.1144/gsjgs.139.5.0615.

HUTTON, D. H. W., & MURPHY, F. C. (1987). The Silurian of the Southern Uplands and Ireland as a successor basin to the end-Ordovician closure of Iapetus. *Journal of the Geological Society*, **144**(5), 765-772. https://doi.org/10.1144/gsjgs.144.5.0765.

IRELAND, S. C. (2016). Competent Persons Report for Prospecting Licences held by IMC Exploration Group PLC in the Republic of Ireland.

ISO 18400-105:2017, Soil quality — Sampling — Part 105: Packaging, transport, storage and preservation of samples.

JACKSON, J.E. (2005). *A User's Guide to Principal Components*. John Wiley & Sons.

JACKSON, P. E. (2001). Determination of inorganic ions in drinking water by ion chromatography. *TrAC Trends in Analytical Chemistry*, **20**(6-7), 320-329. https://doi.org/10.1016/S0165-9936(01)00070-X.

JACOB, A.W.B., KAMINSKI, W., MURPHY, T., PHILLIPS, W.E.A., & PRODEHL, C. (1985). A crustal model for a northeast-southwest profile through Ireland. *Tectonophysics*. 113, 75-103. https://doi.org/10.1016/0040-1951(85)90111-8.

JANZEN, H.H. (2004). Carbon cycling in earth systems—a soil science perspective. *Agiculture, Ecosystems and Environment,* 104(3), 399-417. https://doi.org/10.1016/j.agee.2004.01.040.

JOHNSON, D.B., & HALLBERG, K.B. (2005). Acid mine drainage remediation options: a review. *Science of the Total Environment*, 338, 3-14. https://doi.org/10.1016/j.scitotenv.2004.09.002.

JOHNSTON, J.D. (1999). Regional fluid flow and the genesis of Irish Carboniferous base metal deposits. *Mineralium Deposita*, 34, pp 571-598. https://doi.org/10.1007/s001260050221.

JOHNSTON, J.D., COLLER, D., MILLAR, G., & CRITCHLEY, M.F. (1996). Basement structural controls on Carboniferous-hosted base metal mineral deposits in Ireland. In: Strogen, P., Somerville, I.D., and Jones, G.L., (Eds.), Recent Advances in Lower Carboniferous Geology: *Geological Society of London Special Publication,* 107, 2–21.

JOLLIFFE, I.T., 2002. Principal Component Analysis, Second Edition. *Springer, New York.*

JOLLIFFE, I. T., & CADIMA, J. (2016). Principal component analysis: a review and recent developments. Philosophical Transactions of the Royal Society A: Mathematical, *Physical and Engineering Sciences*, **374**(2065), 20150202. https://doi.org/10.1098/rsta.2015.0202.

KELLY, J. (2007). A History of Zn-Pb-Ag Mining at Abbeytown, Co. Sligo. *Journal of the Mining Heritage Trust of Ireland*, 7, 9-18.

KENNAN, P. S. (1979). Plutonic rocks in the Irish Caledonides. *Geological Society, London, Special Publications*, **8**(1), 705-711. https://doi.org/10.1144/GSL.SP.1979.008.01.85.

KESHAVARZI, A., KUMAR, V., ERTUNÇ, G, BREVIK, E.C. (2021). Ecological risk assessment and source apportionment of heavy metal contamination: an appraisal based on the Tellus soil survey. *Environ Geochem Health*, **43**, 2121-2142. https://doi.org/10.1007/s10653-020-00787-w.

KIRKWOOD, C., COOPER, M., FERREIRA, A., & BEAMISH, D. (2020). Unmixing and mapping components of Northern Ireland's geochemical composition using FastICA and random forests. *(Unpublished Preprint) EarthArXiv*. https://doi.org/10.31223/osf.io/8k3f7.

KRAUSMANN, F., GINGRICH, S., EISENMENGER, N., ERB, K. H., HABERL, H., & FISCHER-KOWALSKI, M. (2009). Growth in global materials use, GDP and population during the 20th century. *Ecological economics*, **68**(10), 2696-2705. https://doi.org/10.1016/j.ecolecon.2009.05.007.

KRISHNA, A. K., MURTHY, N. N., & GOVIL, P. K. (2007). Multielement analysis of soils by wavelength-dispersive X-ray fluorescence spectrometry. ATOMIC SPECTROSCOPY-NORWALK CONNECTICUT-, 28(6), 202.

KRONBERG, B. I., & NESBITT, H. W. (1981). Quantification of weathering, soil geochemistry and soil fertility. *Journal of Soil Science*, **32**(3), 453-459. https://doi.org/10.1111/j.1365-2389.1981.tb01721.x.

KRUMBEIN, W.C. (1962). Open and closed number systems in stratigraphic mapping. *AAPG Bulletin*. 46, 2229-2245. https://doi.org/10.1306/BC743963-16BE-11D7-8645000102C1865D.

KYNE, R., TORREMANS, K., GÜVEN, J., DOYLE, R., & WALSH, J. (2019). 3-D modeling of the lisheen and silvermines deposits, County Tipperary, Ireland: insights into structural controls on the formation of Irish Zn-Pb deposits. *Economic Geology*. 114(1), 93-116. https://doi.org/10.5382/econgeo.2019.4621.

KYNE R., TORREMANS K., DOYLE R., GÜVEN, J., & WALSH, J.J. (2017). Segmented fault arrays and their control on the formation of Irish-type Zn-Pb deposits: *Biennial Meeting of the Society for Geology Applied to Mineral Deposits, Quebec, Canada, August 20–23, 2017, Extended Abstracts*, 617–620.

KYSER, K., BARR, J., & IHLENFELD, C. (2015). Applied geochemistry in mineral exploration and mining. *Elements,* 11(4), 241-246. https://doi.org/10.2113/gselements.11.4.241.

LAKSHMANAN, E., KANNAN, R., & KUMAR, M. S. (2003). Major ion chemistry and identification of hydrogeochemical processes of ground water in a part of Kancheepuram district, Tamil Nadu, India. *Environmental geosciences*, **10**(4), 157-166. https://doi.org/10.1306/eg.0820303011.

LANCE, G., & WILLIAMS, W. (1966). A Generalized Sorting Strategy for Computer Classifications. *Nature*, 212, 218. https://doi.org/10.1038/212218a0.

LARGE, R. R., & MCGOLDRICK, P. J. (1998). Lithogeochemical halos and geochemical vectors to stratiform sediment hosted Zn–Pb–Ag deposits, 1. Lady Loretta Deposit, Queensland. *Journal of Geochemical Exploration*, **63**(1), 37-56. https://doi.org/10.1016/S0375-6742(98)00013-2.

LAUCHNOR, E. G., SCHULTZ, L. N., BUGNI, S., MITCHELL, A. C., CUNNINGHAM, A. B., & GERLACH, R. (2013). Bacterially induced calcium carbonate precipitation and strontium coprecipitation in a porous media flow system. *Environmental science & technology*, **47**(3), 1557-1564. https://doi.org/10.1021/es304240y.

LEEDER, M.R. (1982). Upper Palaeozoic basins of the British Isles – Caledonide inheritance versus Hercynian plate Margin processes. *Journal of the Geological Society, London*, 139, 479-491. https://doi.org/10.1144/gsjgs.139.4.0479.

LEEDER, M.R. (1987). Tectonic and palaeogeographic models for Lower Carboniferous Europe. In: Miller, J., Adams, A.E. and Wright, V.P. (Eds.), European Dinantian Environments. John Wiley, London, 1-20.

LEES, A., & MILLER, J. (1995). Waulsortian Banks. In: Monty, C.L.V., Bosence, D.W.J., Bridges, P.H., Pratt, B.R. (Eds.), Carbonate mud-mounds: their origin and evolution. Special Publication of the International Association of Sedimentologists, Blackwell Science, Oxford, 23, 191-271.

LEHURAY, A. P., CAULFIELD, J. B. D., RYE, D. M., & DIXON, P. R. (1987). Basement controls on sediment-hosted Zn-Pb deposits; a Pb isotope study of Carboniferous mineralization in central Ireland. *Economic Geology*, **82**(7), 1695-1709. https://doi.org/10.2113/gsecongeo.82.7.1695.

LE VAILLANT, M., HILL, J., & BARNES, S. J. (2017). Simplifying drill-hole domains for 3D geochemical modelling: An example from the Kevitsa Ni-Cu-(PGE) deposit. *Ore Geology Reviews*, **90**, 388-398. https://doi.org/10.1016/j.oregeorev.2017.05.020.

LEWIS, S.L. & MASLIN, M.A. (2015). Defining the anthropocene. *Nature*, **519**(7542), 171-180. https://doi.org/10.1038/nature14258.

LEYBOURNE, M.I., GOODFELLOW, W.D., & BOYLE, D.R. (2002). Sulphide oxidation and groundwater transport of base metals at the Halfmile Lake and Restigouche Zn–Pb massive sulphide deposits, Bathurst Mining Camp, New Brunswick. *Geochemistry: Exploration, Environment, Analysis*. **2**, 37-44. https://doi.org/10.1144/1467-787302-005.

LEYBOURNE, M.I., & CAMERON, E.M. (2010). Groundwater in geochemical exploration. *Geochemistry: Exploration, Environment, Analysis*. **10**, 99-118. https://doi.org/10.1144/1467-7873/09-222.

LIAO, Q. L., EVANS, L. J., GU, X., FAN, D. F., JIN, Y., & WANG, H. (2007). A regional geochemical survey of soils in Jiangsu Province, China: preliminary assessment of soil fertility and soil contamination. *Geoderma*, **142**(1-2), 18-28. https://doi.org/10.1016/j.geoderma.2007.07.008.

LIU, B., GUO, S., WEI, Y., & ZHAN, Z. (2014). A Fast Independent Component Analysis Algorithm for Geochemical Anomaly Detection and Its Application to Soil Geochemistry Data Processing. *Journal of Applied Mathematics*, 2014, https://doi.org/10.1155/2014/319314.

LOUGHLIN, W. P. (1991). Principal component analysis for alteration mapping. *Photogrammetric Engineering and Remote Sensing*, **57**(9), 1163-1169.

LUSTY, P. A. J., SCHEIB, C., GUNN, A. G., & WALKER, A. S. D. (2012). Reconnaissance-scale prospectivity analysis for gold mineralisation in the Southern Uplands-Down-Longford Terrane, Northern Ireland. *Natural Resources Research*, **21**(3), 359-382. https://doi.org/10.1007/s11053-012-9183-3.

LYONS, W. B., & HARMON, R. S. (2012). Why urban geochemistry?. *Elements*, **8**(6), 417-422. https://doi.org/10.2113/gselements.8.6.417.

MACDERMOT, C.V., & SEVASTOPULO, G.D. (1972). Upper Devonian and lower Carboniferous stratigraphical setting of Irish mineralisation. *Geol. Surv. Irel*. **1**, 267-280.

MACHIWAL, D., CLOUTIER, V., GULER, C., & KAZAKIS, N. (2018). A review of GIS-integrated statistical techniques for groundwater quality evaluation and protection. *Environmental Earth Sciences*. **77**, 681. 1-30. https://doi.org/10.1007/s12665-018-7872-x.

MACQUEEN, J. (1967). Some methods for classification and analysis of multivariate observations. In: *Proceedings of the Fifth Berkeley Symposium on Mathematical Statistics and Probability*, Le Cam, L.M., Neyman, J. (Eds.), 1, 281-297. *Berkeley, CA: University of California Press*.

MALOZEWSKI P., & ZUBER A. (1982). Determining the turnover time of groundwater systems with the aid of environmental tracers. *Journal of Hydrology*, **57**, 207–231. https://doi.org/10.1016/0022-1694(82)90147-0.

MALOZEWSKI P., RAUERT W., STICHLER W., & HERRMANN A. (1983). Application of flow models in an alpine catchment using tritium and deuterium data. *Journal of Hydrology*, **66**, 319–330. https://doi.org/10.1016/0022-1694(83)90193-2.

MARGALEF-MARTI, R., CARREY, R., BENITO, J. A., MARTI, V., SOLER, A., & OTERO, N. (2020). Nitrate and nitrite reduction by ferrous iron minerals in polluted groundwater: Isotopic characterization of batch experiments. *Chemical Geology*, **548**, 119691. https://doi.org/10.1016/j.chemgeo.2020.119691.

MARQUES, J.A., COSTA, P.G., MARANGONI, L.F., PEREIRA, C.M., ABRANTES, D.P., CALDERON, E.N., CASTRO, C.B. & BIANCHINI, A. (2019). Environmental health in southwestern Atlantic coral reefs: Geochemical, water quality and ecological indicators. *Science of The Total Environment*, **651**, 261-270. https://doi.org/10.1016/j.scitotenv.2018.09.154.

MARTÍN-FERNÁNDEZ, J.A., BARCELÓ-VIDAL, C., & PAWLOWSKY-GLAHN, V. (2003). Dealing with zeros and missing values in compositional data sets using nonparametric imputation. *Mathematical Geology*, **35**, 253-278. https://doi.org/10.1023/A:1023866030544.

MARTÍN-FERNÁNDEZ JA, PALAREA-ALBALADEJO J, & OLEA RA. (2011). Dealing with zeros. In: PAWLOWSKY-GLAHN V, BUCCIANTI A, (Eds.), *Compositional Data Analysis: Theory and Applications*, Chichester, UK: John Wiley & Sons, Ltd. pp. 43–58. https://doi.org/10.1002/9781119976462.ch4.

MASKALL, J., & STOKES, A. (2008). *Designing effective fieldwork for the environmental and natural sciences* (p. 78). Plymouth, UK: Higher Education Academy Subject Centre for Geography, Earth and Environmental Sciences.

MCGRORY, E., HOLIAN, E., ALVAREZ-IGLESIAS, A., BARGARY, N., MCGILLICUDDY, E.J., HENRY, T., DALY, E., & MORRISON, L. (2018). Arsenic in Groundwater in South West Ireland: Occurrence, Controls, and Hydrochemistry. *Frontiers in Environmental Science*. 6:154. https://doi.org/10.3389/fenvs.2018.00154.

MCKINLEY, J., TOLOSANA DELGADO, R., HRON, K., DE CARITAT, P., GRUNSKY, E., REIMANN, C., FILZMOSER P., & VAN DEN BOOGAART K.G. (2016). Single Component map: Fact or Fiction? *Journal of Geochemical Exploration*, **162**, 16-28. http://dx.doi.org/doi:10.1016/j.gexplo.2015.12.005.

MCMAHON, P.B., BELITZ, K., REDDY, J.E., & JOHNSON, T.D. (2019). Elevated Manganese Concentrations in United States Groundwater, Role of Land Surface–Soil–Aquifer Connections. *Environmental Science & Technology,* **53** (1), 29-38. https://doi.org/10.1021/acs.est.8b04055.

MEERMANN, B., & NISCHWITZ, V. (2018). ICP-MS for the analysis at the nanoscale–a tutorial review. *Journal of Analytical Atomic Spectrometry*, **33**(9), 1432-1468. https://doi.org/10.1039/C8JA00037A.

MEYER, D., DIMITRIADOU, E., HORNIK, K., WEINGESSEL, A., LEISCH, F., & CHANG, C.C. (2020). Package 'e1071'. *The R Journal*.

MIESCH, A. T., & BARNETT, P. R. (1976). *Geochemical survey of Missouri: methods of sampling, laboratory analysis, and statistical reduction of data*. US Government Printing Office.

MO, T., SUTTLE, A. D., & SACKETT, W. M. (1973). Uranium concentrations in marine sediments. *Geochimica et Cosmochimica Acta*, **37**(1), 35-51. https://doi.org/10.1016/0016-7037(73)90242-1.

MORALES, J. A., DE GRATEROL, L. S., & MESA, J. (2000). Determination of chloride, sulfate and nitrate in groundwater samples by ion chromatography. *Journal of Chromatography A*, **884**(1-2), 185-190. https://doi.org/10.1016/S0021-9673(00)00423-4.

MORRIS, J.H. (1983). The Stratigraphy of the Lower Palaeozoic Rocks in the Western End of the Longford-Down Inlier, Ireland. *Journal of Earth Sciences*. **5**, 201-218. https://www.jstor.org/stable/30002165.

MORRIS, P., & MAX, M.D. (1995). Magnetic Crustal Character in Central Ireland. *Geological Journal*. **30**.1 49-67. https://doi.org/10.1002/gj.3350300106.

MORTON, A. C., & HALLSWORTH, C. (2007). Stability of detrital heavy minerals during burial diagenesis. In M. A. MANGE, & D. T. WRIGHT (Eds.), *Heavy minerals in use, developments in sedimentology*, (Vol. 58, 215–245). Amsterdam: Elsevier.

MOSES, C., ROBINSON, D., & BARLOW, J. (2014). Methods for measuring rock surface weathering and erosion: A critical review. *Earth-Science Reviews*, **135**, 141-161. https://doi.org/10.1016/j.earscirev.2014.04.006.

MOSIMANN, J.E. (1962). On the Compound Multinomial Distribution, the Multivariate β- Distribution, and Correlations Among Proportions. *Biometrika*. 49, 65-82. https://doi.org/10.2307/2333468.

MOSIMANN, J.E. (1962). On the Compound Negative Multinomial Distribution and Correlations Among Inversely Sampled Pollen Counts. *Biometrika*. 50, 47-54. https://doi.org/10.2307/2333745.

MUEHLMANN, C., FACEVICOVÁ, K., GARDLO, A., JANECKOVÁ, H., & NORDHAUSEN, K. (2020). Independent Component Analysis for Compositional Data. (Unpublished) arXiv:2007.00456v1 [stat.ME].

MUELLER, D.K., SCHERTZ, T.L., MARTIN, J.D., & SANDSTROM, M.W. (2015). Design, analysis, and interpretation of field quality-control data for water-sampling projects: *U.S. Geological Survey Techniques and Methods, Book 4, chap. C4*, 54 p.

MURRAY, J. (2010). Mid to Upper Viséan facies and palaeoenvironments of the Shannon Basin, Western Ireland. Unpublished Ph.D. thesis, University of Dublin, Trinity College. Available online at: http://www.tara.tcd.ie/handle/2262/78115

MURRAY, J., & HENRY, T. (2018). Waulsortian Limestone: geology and hydrogeology. Paper presented at the conference 'Groundwater Matters: science and practice', Tullamore, County Offaly, Ireland, April. Available online at: http://www.iah-ireland.org/conference-proceedings/2018.pdf

NANDI, A., MANDAL, A., WILSON, M., & SMITH, D. (2016). Flood hazard mapping in Jamaica using principal component analysis and logistic regression. *Environmental Earth Sciences*, **75**(6), 465. https://doi.org/10.1007/s12665-016-5323-0.

NAUTON-FOURTEU, M., TYRRELL, S., MORTON, A., MARK, C., O'SULLIVAN, G. J., & CHEW, D. M. (2021). Constraining recycled detritus in quartz-rich sandstones: insights from a multi-proxy provenance study of the Mid-Carboniferous, Clare Basin, western Ireland. *Basin Research*, **33**(1), 342-363. https://doi.org/10.1111/bre.12469.

NEIVA, A. M. R., DE CARVALHO, P. C. S., ANTUNES, I. M. H. R., DOS SANTOS, A. C. T., & DA SILVA CABRAL-PINTO, M. M. (2015). Spatial and temporal variability of surface water and groundwater before and after the remediation of a Portuguese uranium mine area. *Geochemistry*, **75**(3), 345-356. https://doi.org/10.1016/j.chemer.2015.06.001.

NEWMAN, C. P., PASCHKE, S. S., & KEITH, G. (2021). Natural and Anthropogenic Geochemical Tracers to Investigate Residence Times and Groundwater–Surface-Water Interactions in an Urban Alluvial Aquifer. *Water*, **13**(6), 871. https://doi.org/10.3390/w13060871.

NOCKOLDS, S. R. (1954). Average chemical compositions of some igneous rocks. *Geological Society of America Bulletin*, **65**(10), 1007-1032. https://doi.org/10.1130/0016-7606(1954)65[1007:ACCOSI]2.0.CO;2.

NOLAN, P. (2008). Ensemble of regional climate model projects for Ireland. *EPA*. Report No. 159.

O'BRIEN, W. (1995). Ross Island: the beginning. *Archaeology Ireland*, 24-27.

O'BRIEN, W. (2003). Bronze age mining heritage. In: Morris, J.H., Parkes, M. (Eds.). Mine Heritage and Tourism: A Hidden Resource. Proceedings of a conference held on November 3-9, 1999, at Nenagh, Co. Tipperary, Ireland. *Mining Heritage Trust of Ireland*.

O'BRIEN, P. (2013). Bronze Age Copper Mining in Europe. In: Fokkens, H, Harding, A. (Eds.). The Oxford Handbook of the European Bronze Age. *Oxford University Press*. 443-445.

O'BRIEN, W. (1994). Mount Gabriel: bronze age mining in Ireland. Galway, Ireland: Galway University Press.

OLSEN, R. L., O'CARROLL, R., DOYLE, E., & STANLEY, G. (2012). Evaluation of rehabilitation alternatives at the abandoned Avoca mining site in Ireland. *Environmental Impact*, **162**, 375-387.

O'REILLY, B.M., READMAN, P.W., & MURPHY, T. (1999). Gravity lineaments and Carboniferous-hosted base metal deposits of the Irish Midlands, in McCaffery, K., Lonergan, L., and Wilkinson, J., (Eds*.)*, Fractures, Fluid Flow and Mineralization: *Geological Society of London Special Publication.* 155, 313–322.

OTTERSEN, G., PLANQUE, B., BELGRANO, A., POST, E., REID, P. C., & STENSETH, N. C. (2001). Ecological effects of the North Atlantic oscillation. *Oecologia*, **128**(1), 1-14.

OTTESEN, R. T., BOGEN, J., BØLVIKEN, B., & VOLDEN, T. (1989). Overbank sediment: a representative sample medium for regional geochemical mapping. *Journal of Geochemical Exploration*, **32**(1-3), 257-277. https://doi.org/10.1016/0375-6742(89)90061-7.

OWEN, D. D. R., PAWLOWSKY-GLAHN, V., EGOZCUE, J. J., BUCCIANTI, A., & BRADD, J. M. (2016). Compositional data analysis as a robust tool to delineate hydrochemical facies within and between gas-bearing aquifers. *Water Resources Research*, **52**(8), 5771-5793. https://doi.org/10.1002/2015WR018386.

PALAREA-ALBALADEJO, J., & MARTIN-FERNANDEZ, J.A. (2015). ZCompositions - R package for multivariate imputation of left-censored data under a compositional approach. *Chemometrics and Intelligent Laboratory Systems*. 143, 85-96. https://doi.org/10.1016/j.chemolab.2015.02.019.

PALAREA-ALBALADEJO, J., MARTÍN-FERNÁNDEZ, J.A., & GÓMEZ-GARCÍA, J.A. (2007). Parametric approach for dealing with compositional rounded zeros. *Mathematical Geology*, **39**(7), 625-645. https://doi.org/10.1007/s11004-007-9100-1.

PARRIS, K. (2011). Impact of agriculture on water pollution in OECD countries: recent trends and future prospects. *International journal of water resources development*, **27**(1), 33-52. https://doi.org/10.1080/07900627.2010.531898.

PARNELL, J., EARLS, G., WILKINSON, J. J., HUTTON, D. H. W., BOYCE, A. J., FALLICK, A. E., ELLAM, R. M., GLEESON, S. A., MOLES, N. R., LEGG, I., & CAREY, P. F. (2000). Regional fluid flow and gold mineralization in the Dalradian of the Sperrin Mountains, Northern Ireland. *Economic Geology*, **95**(7), 1389-1416. https://doi.org/10.2113/gsecongeo.95.7.1389.

PAWLOWSKY, V., & BURGER, H. (1992). Spatial structure analysis of regionalized compositions. *Mathematical Geology*, **24**(6), 675-691.

PAWLOWSKY, V., OLEA, R. A., & DAVIS, J. C. (1994). Additive logratio estimation of regionalized compositional data: an application to calculation of oil reserves. In: Geostatistics for the next century (pp. 371-382). Springer, Dordrecht.

PEARSON, K. (1987). Mathematical contributions to the theory of evolution. On a form of spurious correlation which may arise when indices are used in the measurement of organs. *Proceedings of the Royal Society of London LX*, 489-502. https://doi.org/10.1098/rspl.1896.0076.

PERSELLIN, C. J., GREGG, J. M., SHELTON, K. L., SOMERVILLE, I. D., & ATEKWANA, E. A. (2010). Base Metal Sulfide Mineralization in Lower Carboniferous Strata, Northwest Ireland. *Exploration and Mining Geology*, **19**(1-2), 35-54. https://doi.org/10.2113/gsemg.19.1-2.35.

PINGITORE JR, N. E., & EASTMAN, M. P. (1986). The coprecipitation of Sr2+ with calcite at 25 C and 1 atm. *Geochimica et Cosmochimica Acta*, **50**(10), 2195-2203. https://doi.org/10.1016/0016-7037(86)90074-8.

PIPER, A.M. (1944). A graphic procedure in the geochemical interpretation of water-analyses. *EOS Trans. Am. Geophys. Union*, **25**(6), 914-928, https://doi.org/10.1029/TR025i006p00914.

PITCHER, W. S., & HUTTON, D. H. (2003). A master class guide to the granites of Donegal. Geological Survey of Ireland.

PITCHER, W.S., READ, H.H., CHEESMAN, R.L., PANDE, I. C., & TOZER, C. F. (1958). The main Donegal granite. *Quarterly Journal of the Geological Society*, **114**(1-4), 259-300. https://doi.org/10.1144/gsjgs.114.1.0259.

POHORILLE, A., & PRATT, L. R. (2012). Is water the universal solvent for life?. *Origins of Life and Evolution of Biospheres*, **42**(5), 405-409. https://doi.org/10.1007/s11084-012-9301-6.

PROMMER, H., BARRY, D. A., & DAVIS, G. B. (2000). Numerical modelling for design and evaluation of groundwater remediation schemes. *Ecological Modelling*, **128**(2-3), 181-195. https://doi.org/10.1016/S0304-3800(99)00230-6.

PUNTANEN, S., STYAN, G.P.H., & ISOTALO, J. (2011). Matrix Tricks for Linear Statistical Models. *Springer, Heidelberg*. https://doi.org/10.1007/978-3-642-10473-2.

QUAID, B., & WHESTON, S. (2017). The closing of Lisheen Mine. *Boherlahan and Dualla Community Website* (https://boherlahandualla.ie/the-closing-of-lisheen-mine-by-brian-quaid-stephen-wheston/) – last accessed 13/04/2021 at 16:20.

RAIBER, M., WHITE, P. A., DAUGHNEY, C. J., TSCHRITTER, C., DAVIDSON, P., & BAINBRIDGE, S. E. (2012). Three-dimensional geological modelling and multivariate statistical analysis of water chemistry data to analyse and visualise aquifer structure and groundwater composition in the Wairau Plain, Marlborough District, New Zealand. *Journal of Hydrology*, **436**, 13-34. https://doi.org/10.1016/j.jhydrol.2012.01.045.

READMAN, P.W., O'REILLY, B.M., & MURPHY, T. (1997). Gravity gradients and upper-crustal tectonic fabrics, Ireland. *Journal of the Geological Society*. 154, 817-828. https://doi.org/10.1144/gsjgs.154.5.0817.

REHDER, S., & ZIER, U. (2001). Letter to the editor: Comment on 'Logratio analysis and compositional distance' by Aitchison, J., Barceló-Vidal, C., Martín-Fernández, J.A., Pawlowsky-Glahn, V., *Mathematical Geology*, **33**(7), 845-848. https://doi.org/10.1023/A:1010902931554.

REIMANN, C., FILZMOSER, P., HRON, K., KYNČLOVÁ, P., & GARRETT, R.G. (2017). A new method for correlation analysis of compositional (environmental) data – a worked example. *Science of the Total Environment*, **607-608**, 965-971. https://doi.org/10.1016/j.scitotenv.2017.06.063.

REIMANN, C., FABIAN, K, BIRKE, M., FILZMOSER, P., DEMETRIADES, A., NÉGREL, P, OORTS, K, MATSCHULLAT, J., & DE CARITAT, P. (2018). GEMAS: Establishing geochemical background and threshold for 53 chemical elements in European agricultural soil. *Applied Geochemistry*, **88B**, 302-318. https://doi.org/10.1016/j.apgeochem.2017.01.021.

RINGWOOD, A.E. (1966). Chemical evolution of the terrestrial planets. *Geochimica et Cosmochimica Acta*, **30**(1), 41-104. https://doi.org/10.1016/0016-7037(66)90090-1.

RODRIGUEZ-GALIANO, V., SANCHEZ-CASTILLO, M., CHICA-OLMO, M., & CHICA-RIVAS, M. J. O. G. R. (2015). Machine learning predictive models for mineral prospectivity: An evaluation of neural networks, random forest, regression trees and support vector machines. *Ore Geology Reviews*, **71**, 804-818. https://doi.org/10.1016/j.oregeorev.2015.01.001.

ROHAN, P. K. (1975). The Climate of Ireland. *Dublin, Ireland: Stationery Office*.

ROSE, A.W., & GUNDLACH, H. (1981). Geochemical Exploration 1980. *Developments in Economic Geology,* **15**, 1-698.

RUSSELL, A., MCDERMOTT, F., MCGRORY, E., COOPER, M., HENRY, T., & MORRISON, L. (2021). As–Co–Ni sulfarsenides in Palaeogene basaltic cone sheets as sources of groundwater arsenic contamination in co. Louth, Ireland. *Applied Geochemistry*, **127**, 104914. https://doi.org/10.1016/j.apgeochem.2021.104914.

RYTUBA, J. J. (2003). Mercury from mineral deposits and potential environmental impact. *Environmental Geology*, **43**(3), 326-338. https://doi.org/10.1007/s00254-002-0629-5.

SAHOO, P. K., DALL'AGNOL, R., SALOMÃO, G. N., JUNIOR, J. D. S. F., SILVA, M. S., E SOUZA FILHO, P. W. M., & SIQUEIRA, J. O. (2020). Regional-scale mapping for determining geochemical background values in soils of the Itacaiúnas River Basin, Brazil: The use of compositional data analysis (CoDA). *Geoderma*, **376**, 114504. https://doi.org/10.1016/j.geoderma.2020.114504.

SAHOO, P.K., DALL'AGNOL, R., SALOMÃO, G.N., DA SILVA FERREIRA JUNIOR, J., DA SILVA, M.S., MARTINS, G.C., E SOUZA FILHO, P.W.M., POWELL, M.A., MAURITY, C.W., ANGELICA, R.S., DA COSTA, M.F., SIQUEIRA, J.O. (2020). Source and background threshold values of potentially toxic elements in soils by multivariate statistics and GIS-based mapping: a high density sampling survey in the Parauapebas basin, Brazilian Amazon. *Environmental Geochemistry and Health*, **42**, 255-282. https://doi.org/10.1007/s10653-019-00345-z.

SANTER, B. D., MEARS, C., DOUTRIAUX, C., CALDWELL, P., GLECKLER, P. J., WIGLEY, T. M. L., ... & WENTZ, F. J. (2011). Separating signal and noise in atmospheric temperature changes: The importance of timescale. *Journal of Geophysical Research: Atmospheres*, **116**(D22). https://doi.org/10.1029/2011JD016263.

SAPORTA, G., & NIANG N. (2009). Principal component analysis: application to statistical process control. In: Govaert G, (Ed.), Data Analysis. *London: John Wiley & Sons*; 1–23.

SAURO GRAZIANO, R., GOZZI, C., BUCCIANTI, A. (2020). Is Compositional Data Analysis a theory able to discover complex dynamics in aqueous geochemical systems? *Journal of Geochemical Exploration*, 211, 106465. https://doi.org/10.1016/j.gexplo.2020.106465.

SCHAEFER, L., & FEGLEY JR, B. (2010). Chemistry of atmospheres formed during accretion of the Earth and other terrestrial planets. *Icarus*, **208**(1), 438-448. https://doi.org/10.1016/j.icarus.2010.01.026.

SCHULLEHNER, J., STAYNER, L., & HANSEN, B. (2017). Nitrate, Nitrite, and Ammonium Variability in Drinking Water Distribution Systems. *International Journal of Environmental Research and Public Health*. **14**(3), 267. https://doi.org/10.3390/ijerph14030276.

SELCK, B.J., CARLING, G.T., KIRBY, S.M., HANSEN, N.C., BRICKMORE, B.R., TINGEY, D.G., REY, K., WALLACE, J., & JORDAN, J.L. (2018). Investigating Anthropogenic and Geogenic Sources of Groundwater Contamination in a Semi-Arid Alluvial Basin, Goshen Valley, UT, USA. *Water, Air & Soil Pollution*. **186**. https://doi.org/10.1007/s11270-018-3839-5.

SEVASTOPULO, G.D. (2009). Carboniferous: Mississippian (Serpukhovian) and Pennsylvanian. In: Holland, C.H. and Sanders, I.S. (Eds.), The Geology of Ireland, Second Edition. Dunedin Academic Press, Edinburgh, 269-294.

SEVASTOPULO, G.D., & REDMOND, P. (1999). Age of mineralization of carbonate-hosted, base metal deposits in the Rathdowney trend, Ireland. *Geological Society, London, Special Publications*, **155**, 303–311. https://doi.org/10.1144/GSL.SP.1999.155.01.20.

SEVASTOPULO, G.D., & WYSE JACKSON, P.N. (2009). Carboniferous: Mississippian (Tournaisian and Viséan). In: Holland, C.H., Sanders, I.S. (Eds.), The Geology of Ireland, second edition. Dunedin Academic Press Ltd, Edinburgh, 215-268.

SHEARLEY, E., REDMOND, P.B., KING, M., & GOODMAN, R. (1996). Geological controls on mineralization and dolomitization of the Lisheen Zn-Pb-Ag deposit, Co. Tipperary, Ireland. *Geological Society, London, Special Publications*, **107**, 23–33. https://doi.org/10.1144/GSL.SP.1996.107.01.03.

SHELTON, J.L., ENGLE, M.A., BUCCIANTI, A., & BLONDES, M.S. (2018). The isometric log-ratio (ilr)-ion plot: A proposed alternative to the Piper diagram. *Journal of Geochemical Exploration*, **190**, 130-141. https://doi.org/10.1016/j.gexplo.2018.03.003.

SLIVER, N. (2012). The Signal & The Noise: the art of science and prediction. Penguin, London.

SIMATE, G.S., & NDLOVU, S. (2014). Acid mine drainage: Challenges and opportunities. *Journal of Environmental Chemical Engineering*, **2**(3), 1785-1803. https://doi.org/10.1016/j.jece.2014.07.021.

SKIBA, W. (1952). The contact phenomena on the north-west of the Crossdoney Complex, Co. Cavan. *Transactions of the Edinburgh Geological Society*, **15**(1), 322-345. https://doi.org/10.1144/transed.15.1.322.

SMART, D., CALLERY, S., & COURTNEY, R. (2016). The potential for waste-derived materials to form soil covers for the restoration of mine tailings in Ireland. *Land Degradation & Development*, **27**(3), 542-549. https://doi.org/10.1002/ldr.2465.

SMEDS, S. A. (1992). Trace elements in potassium-feldspar and muscovite as a guide in the prospecting for lithium-and tin-bearing pegmatites in Sweden. *Journal of Geochemical Exploration*, **42**(2-3), 351-369. https://doi.org/10.1016/0375-6742(92)90032-4.

SOMERVILLE, I.D., & WATERS, C.N., (2011a), Chapter 19. NW Ireland. In: WATERS, C.N. *et al.* (eds) A Revised Correlation of Carboniferous Rocks in the British Isles: Geological Society of London, Special Report 26, p. 128–132.

SOMERVILLE, I.D., & WATERS, C.N. (2011b), Chapter 21. Dublin Basin. In: WATERS, C.N. *et al.* (eds) A Revised Correlation of Carboniferous Rocks in the British Isles: Geological Society of London, Special Report 26, p. 138–143132.

SOMMA, R., EBRAHIMI, P., TROISE, C., DE NATALE, G., GUARINO, A., CICCHELLA, D., & ALBANESE, S. (2021). The first application of compositional data analysis (CoDA) in a multivariate perspective for detection of pollution source in sea sediments: The Pozzuoli Bay (Italy) case study. *Chemosphere*, **274**, 129955. https://doi.org/10.1016/j.chemosphere.2021.129955.

SOUNTHARARAJAH, D. P., LOGANATHAN, P., KANDASAMY, J., & VIGNESWARAN, S. (2015). Effects of humic acid and suspended solids on the removal of heavy metals from water by adsorption onto granular activated carbon. *International Journal of Environmental Research and Public Health*, **12**(9), 10475-10489. https://doi.org/10.3390/ijerph120910475.

SRINIVASAN, K. (2017). Chapter Nine - Ion Chromatography Instrumentation for Water Analysis. In: Ahuja, S. (Eds.), Chemistry and Water; The Science Behind Sustaining the World's Most Crucial Resource. *Elsevier*. https://doi.org/10.1016/B978-0-12-809330-6.00009-X.

STANLEY, G., GALLAGHER, V., NÍMHAIRTÍN, F., BROGAN, J., LALLY, P., DOYLE, E. & FARRELL, L. (2010). Historic Mine Sites – Inventory and Risk Classification, Volume 1: Geochemical Characterisation and Environmental Matters, A joint study carried out by the Environmental Protection Agency and the Geological Survey of Ireland. Environmental Protection Agency, Dublin.

Statistical Analysis of Ground-Water Monitoring Data at RCRA Facilities, (1989). *US Environmental Protection Agency Technical Report*, EPA530-SW-89-026, Washington, DC.

STEINER, B. (2018). Using Tellus stream sediment geochemistry to fingerprint regional geology and mineralisation systems in southeast Ireland. *Irish Journal of Earth Sciences*, **36**, 45-61.

STEINER, B. M. (2019). Tools and Workflows for Grassroots Li–Cs–Ta (LCT) Pegmatite Exploration. *Minerals*, **9**(8), 499. https://doi.org/10.3390/min9080499.

Stuermer, M. (2017). Industrialization and the demand for mineral commodities. *Journal of International Money and Finance*, **76**, 16-27. https://doi.org/10.1016/j.jimonfin.2017.04.006.

SUNDBY, B., ANDERSON, L.G., HALL, P.O.J., IVERFELDT, A., RUTGERS VAN DER LOEFF, M.M., & WESTERLUND, S.F.G. (1986). The effect of oxygen on release and uptake of cobalt, manganese, iron and phosphate at the sediment-water interface. *Geochimica et Cosmochimica Acta.* **50**(6), 1281-1288. https://doi.org/10.1016/0016-7037(86)90411-4.

SWEENEY, J. (2014). Regional weather and climates of the British Isles – Part 6: Ireland. *Weather*, **69**(1), 20-27.

SZMAGARA, A., & KRZYSZCZAK, A. (2019). Monitoring of fluoride content in bottled mineral and spring waters by ion chromatography. *Journal of Geochemical Exploration*, **202**, 27-34. https://doi.org/10.1016/j.gexplo.2019.03.008.

TABELIN, C.B., CORPUZ, R.D., IGARASHI, T., VILLACORTE-TABELIN, M., DIAZ ALORRO, R., YOO, K., RAVAL, S., ITO, M., & HIROYOSHI, N. (2020). Acid mine drainage formation and arsenic mobility under strongly acidic conditions: Importance of soluble phases, iron oxyhydroxides/oxides and nature of oxidation layer on pyrite. Journal of Hazardous Materials, **399**, 122824. https://doi.org/10.1016/j.jhazmat.2020.122844.

TANGESTANI, M. H., & MOORE, F. (2001). Comparison of three principal component analysis techniques to porphyry copper alteration mapping: a case study, Meiduk area, Kerman, Iran. *Canadian journal of remote sensing*, **27**(2), 176-182. https://doi.org/10.1080/07038992.2001.10854931.

TAUFEN, P.M. (1997). Groundwaters and Surface Waters in Exploration Geochemical Surveys. *Exploration Geochemistry*. **34**, 271-284.

TAUSON, V. L., PARKHOMENKO, I. Y., BABKIN, D. N., MEN'SHIKOV, V. I., & LUSTENBERG, E. E. (2005). Cadmium and mercury uptake by galena crystals under hydrothermal growth: A spectroscopic and element thermo-release atomic absorption study. *European Journal of Mineralogy*, **17**(4), 599-610.

TEAGASC, (2014). Irish National Soils Map, 1:250,000k, V1b.Teagasc, Cranfield University. Jointly funded by the EPA STRIVE Research Programme 2007-2013 and Teagasc.

TEMPL, M., HRON, K., & FILZMOSER, P. (2011). robCompositions: an R-package for robust statistical analysis of compositional data.

THIÓ-HENESTROSA, S., EGOZCUE, J.J., PAWLOWSKY-GLAHN, V., KOVÁCS, L.O., & KOVÁCS, G. (2008). Balance-dendrogram, a new routine in codapack. *Computer and Geoscience*, **34**(12), 1682-1696. https://doi.org/10.1016/j.cageo.2007.06.011.

THIOMBANE, M., MARTÍN-FERNÁNDEZ, J. A., ALBANESE, S., LIMA, A., DOHERTY, A., & DE VIVO, B. (2018). Exploratory analysis of multi-element geochemical patterns in soil from the Sarno River Basin (Campania region, southern Italy) through compositional data analysis (CODA). *Journal of Geochemical Exploration*, 195, 110-120. https://doi.org/10.1016/j.gexplo.2018.03.010.

THOMSON, S., FOUNTAIN, D., & WATTS, T. (2007, September). Airborne geophysics–evolution and revolution. In *Proceedings of Exploration* (Vol. **7**, No. 56, pp. 19-37).

TOLONEN, H. (2016). EHES Manual: Part B. Fieldwork procedures.

TOLOSANA-DELGADO, R., & VAN DEN BOOGAART, K.G. (2011). Linear models with compositions in R. In: Pawlowsky-Glahn, V., Buccianti, A., (Eds.), Compositional Data Analysis. Theory and Applications. John Wiley & Sons, Chichester (UK), pp. 356-371.

TORAN, L. (1987). Sulfate contamination in groundwater from a carbonate-hosted mine. *Journal of Contaminant Hydrology*. 2(1), 1-29. https://doi.org/10.1016/0169-7722(87)90002-7.

TORREMANS, K., KYNE, R., DOYLE, R., GÜVEN, J.F., & WALSH, J.J. (2018). Controls on Metal Distributions at the Lisheen and Silvermines Deposits: Insights into Fluid Flow Pathways in Irish-Type Zn-Pb Deposits. *Economic Geology*, **113**(7), 1455-1477. https://doi.org/10.5382/econgeo.2018.4598.

TORRENTÓ, C., URMENETA, J., OTERO, N., SOLER, A., VIÑAS, M., & CAMA, J. (2011). Enhanced denitrification in groundwater and sediments from a nitrate-contaminated aquifer after addition of pyrite. *Chemical Geology*, **287**(1-2), 90-101.

TROLL, V. R., CHADWICK, J. P., ELLAM, R. M., MCDONNEL, S. U. S. A. N., EMELEUS, C. H., & MEIGHAN, I. G. (2005). Sr and Nd isotope evidence for successive crustal contamination of Slieve Gullion ring-dyke

magmas, Co. Armagh, Ireland. *Geological Magazine*, **142**(6), 659-668. https://doi.org/10.1017/S0016756805001068.

TYLER, G. (2004). Rare earth elements in soil and plant systems-A review. *Plant and soil*, **267**(1), 191-206. https://doi.org/10.1007/s11104-005-4888-2.

TYRRELL, S., LELEU, S., SOUDERS, A. K., HAUGHTON, P. D., & DALY, J. S. (2009). K-feldspar sand-grain provenance in the Triassic, west of Shetland: distinguishing first-cycle and recycled sediment sources?. *Geological Journal*, **44**(6), 692-710. https://doi.org/10.1002/gj.1185.

UDDIN, M. N., ISLAM, A. S., BALA, S. K., ISLAM, G. T., ADHIKARY, S., SAHA, D., & AKTER, R. (2019). Mapping of climate vulnerability of the coastal region of Bangladesh using principal component analysis. *Applied geography*, **102**, 47-57. https://doi.org/10.1016/j.apgeog.2018.12.011.

ÚJVÁRI, G., VARGA, A., & BALOGH-BRUNSTAD, Z. (2008). Origin, weathering, and geochemical composition of loess in southwestern Hungary. *Quaternary Research*, **69**(3), 421-437. https://doi.org/10.1016/j.yqres.2008.02.001.

US EPA, (2020a). LSASDPROC-300-R4, Soil Sampling Operating Procedure.

US EPA, (2020b). LSASDPROC-205-R4, Field Equipment Cleaning and Decontamination Operating Procedure.

US EPA, (1996). Method 1669; Sampling Ambient Water for Trace Metals at EPA Water Quality Criteria Levels.

US EPA, (1994). "Method 200.8: Determination of Trace Elements in Waters and Wastes by Inductively Coupled Plasma-Mass Spectrometry," Revision 5.4. Cincinnati, OH.

US EPA, (1996). "Low Stress (low-flow) purging and sampling procedure for the collection of groundwater samples from monitoring wells". (Revised 2017). Quality Assurance Unit, U.S. Environmental Protection Agency – Region 1, 11 Technology Drive, North Chelmsford, MA.

US EPA, (2017). Operating Procedure: SESDPROC-301-R4. Groundwater Sampling. Region 4.

VAN DEN BOOGAART, K.G., TOLOSANA-DELGADO, R. (2013). Analyzing compositional data with R. Springer, Heidelberg.

VAN DEN BRINK, C., FRAPPORTI, G., GRIFFIOEN, J., & ZAADNOORDIJK, W. J. (2007). Statistical analysis of anthropogenic versus geochemical-controlled differences in groundwater composition in The Netherlands. *Journal of Hydrology*, **336**(3-4), 470-480. https://doi.org/10.1016/j.jhydrol.2007.01.024.

VOLFINGER, M., ROBERT, J. L., VIELZEUF, D., & NEIVA, A. M. R. (1985). Structural control of the chlorine content of OH-bearing silicates (micas and amphiboles). *Geochimica et Cosmochimica Acta*, **49**(1), 37-48. https://doi.org/10.1016/0016-7037(85)90189-9.

WALSH, J.J., TORREMANS, K., GÜVEN, J., KYNE, R., CONNEALLY, J., & BONSON, C. (2018). Fault-controlled fluid flow within extensional basins and its implications for sedimentary rock-hosted mineral deposits. *Society of Economic Geologists Special Publications,* **21**, 237-269. http://doi.org/10.5382/sp.21.11.

WALVOORT, D. J., & DE GRUIJTER, J. J. (2001). Compositional kriging: a spatial interpolation method for compositional data. *Mathematical Geology*, **33**(8), 951-966. https://doi.org/10.1023/A:1012250107121.

WATER MANAGEMENT CONSULTANTS (WMS), (2009). Lisheen Mine – Preliminary hydrogeological study of the Tailings Management Facility under closure conditions.

WELTJE, G. J., & VON EYNATTEN, H. (2004). Quantitative provenance analysis of sediments: review and outlook. *Sedimentary Geology*, **171**(1-4), 1-11. https://doi.org/10.1016/j.sedgeo.2004.05.007.

WETHERILL, G. W. (1990). Formation of the Earth. *Annual Review of Earth and Planetary Sciences*, **18**(1), 205-256. https://doi.org/10.1146/annurev.ea.18.050190.001225.

[dataset] WHEELER, S. (2020). Utilising CoDA methods for the spatio-temporal geochemical characterisation of groundwater; a case study from Lisheen Mine, south central Ireland (Datasets and Supplementary Materials). *Mendeley Data, v1,* http://dx.doi.org/10.17632/9hmz589r7g.1.

[datasets] WHEELER, S. (2021). Characterising the geochemistry of the natural environment using Compositional Data Analysis. *Mendeley Data*, v1, https://www.gsi.ie/en-ie/data-and-maps/Pages/Geochemistry.aspx.

WHEELER, S., HENRY, T., MURRAY, J., MCDERMOTT, F., & MORRISON, L. (2021). Utilising CoDA methods for the spatio-temporal geochemical characterisation of groundwater; a case study from Lisheen Mine, south central Ireland. *Applied Geochemistry*, **127**. https://doi.org/10.1016/j.apgeochem.2021.104912.

WHITE, J. G., & ZASOSKI, R. J. (1999). Mapping soil micronutrients. *Field crops research*, **60**(1-2), 11-26. https://doi.org/10.1016/S0378-4290(98)00130-0.

WILKINSON, J. J., BOYCE, A. J., EARLS, G., & FALLICK, A. E. (1999). Gold remobilization by low-temperature brines; evidence from the Curraghinalt gold deposit, Northern Ireland. *Economic Geology*, **94**(2), 289-296. https://doi.org/10.2113/gsecongeo.94.2.289.

WILKINSON, J.J., & HITZMAN, M.W. (2015). The Irish Zn-Pb orefield: The view from 2014. *In* Archibald, S.M., PIERCEY, S.J. (Eds.), *Current perspectives in zinc deposits.* Irish Association of Economic Geology, Dublin, 59–72.

WILKINSON, J.J., EVERETT, C.E., BOYCE, A.J., GLEESON, S.A., & RYE, D.M. (2005a). Intracratonic crustal seawater circulation and the genesis of subseafloor zinc-lead mineralization in the Irish orefield. *Geology*, 33, 805–808. https://doi.org/10.1130/G21740.1.

WILKINSON, J.J., EYRE, S.L., & BOYCE, A.J. (2005b). Ore-Forming Processes in Irish-Type Carbonate-hosted Zn-Pb Deposits: Evidence from Mineralogy, Chemistry, and Isotopic Composition of Sulfides at the Lisheen Mine. *Economic Geology*. 100, 63-86. https://doi.org/10.2113/100.1.0063.

WILKINSON, J.J., CROWTHER, H.L., & COLES, B.J. (2011). Chemical mass transfer during hydrothermal alteration of carbonates: Controls of seafloor subsidence, sedimentation, and Zn–Pb mineralization in the Irish Carboniferous. *Chemical Geology*, **289**, 55–75, https://doi.org/10.1016/j.chemgeo.2011.07.008.

WILLIAMS, D. M., & HARPER, D. A. T. (1988). A basin model for the Silurian of the Midland Valley of Scotland and Ireland. *Journal of the Geological Society*, **145**(5), 741-748. https://doi.org/10.1144/gsjgs.145.5.0741.

WILLIAMS, P. W. (1983). The role of the subcutaneous zone in karst hydrology, *Journal of Hydrology*, **61**, 45 – 67. https://doi.org/10.1016/0022-1694(83)90234-2.

WORDEN, R.H. (2005). Analytical Methods, Geochemical Analysis (including X-ray). In (Eds.): SHELLEY, R.C., COCKS, R.M., PLIMER, I.R., Encyclopedia of Geology. Elsevier, 54-76. https://doi.org/10.1016/B0-12-369396-9/00096-4.

WOUTERS, S., HADDAD, P. R., & EELTINK, S. (2017). System design and emerging hardware technology for ion chromatography. *Chromatographia*, **80**(5), 689-704. https://doi.org/10.1007/s10337-016-3184-z.

YANG, J., & CHENG, Q. (2015). A comparative study of independent component analysis with principal component analysis in geological objects identification, Part I: Simulations. *Journal of Geochemical Exploration*, **149**, 127-135. https://doi.org/10.1016/j.gexplo.2014.11.013.

YOUNG, M. (2016). The Tellus geoscience surveys of the north of Ireland: Context, delivery and impacts. In Stewart, I., (Author) & Young, M. (Ed.), *Unearthed: Impacts of the Tellus surveys of the north of Ireland* (pp. 3-10). Dublin: Royal Irish Academy. https://doi.org/10.2307/j.ctt1g69w6r.6.

YOUNG, M., KNIGHTS, K., SMYTH, D., GLENNON, M., SCANLON, R., & GALLAGHER, V. (2016). 3. The Tellus geochemical surveys, results and applications. *Unearthed: Impacts of the Tellus Surveys of the North of Ireland*. Royal Irish Academy, 33-52.

YOUNGER, P.L. (2000). Nature and practical implications of heterogeneities in the geochemistry of zinc-rich, alkaline mine waters in an underground F–Pb mine in the UK. *Applied Geochemistry*. 15(9), 1383-1397. https://doi.org/10.1016/S0883-2927(00)00010-X.

ZADROŻNY, P., & NICIA, P. (2009). Heavy Metals in the Peat Soils of the Konecki County. *Ecological Chemistry and Engineering. A*, **16**(9), 1205-1208.

ZENG, B., ZHANG, Z., & YANG, M. (2018). Risk assessment of groundwater with multi-source pollution by a long-term monitoring programme for a large mining area. *International Biodeterioration & Biodegradation*, **128**, 100-108. https://doi.org/10.1016/j.ibiod.2017.01.002.

ZHAN, N., HUANG, Y., RAO, Z., & ZHAO, X. (2016). Fast Detection of Carbonate and Bicarbonate in Groundwater and Lake Water by Coupled Ion Selective Electrode. *Chinese Journal of Analytical Chemistry,* 44(3), 355-360. https://doi.org/10.1016/S1872-2040(16)60913-1.

ZHANG, C., MANHEIM, F. T., HINDE, J., & GROSSMAN, J. N. (2005). Statistical characterization of a large geochemical database and effect of sample size. *Applied Geochemistry*, **20**(10), 1857-1874. https://doi.org/10.1016/j.apgeochem.2005.06.006.

ZHI, C., CAO, W., ZHANG, Z., LI, Z., & REN, Y. (2021). Hydrogeochemical Characteristics and Processes of Shallow Groundwater in the Yellow River Delta, China. *Water* 2021, **13**, 534. https://doi.org/10.3390/w13040534.

ZUO, R. (2017). Machine learning of mineralization-related geochemical anomalies: A review of potential methods. *Natural Resources Research*, **26**(4), 457-464. https://doi.org/10.1007/s11053-017-9345-4.

Appendix A

[Wheeler *et al.*, (2021)]

Utilising CoDA methods for the spatio-temporal geochemical characterisation of groundwater; a case study from Lisheen Mine, south central Ireland

Seán Wheeler [a,b,*], Tiernan Henry [a,b], John Murray [a,b], Frank McDermott [b,c], Liam Morrison [a,b]

[a] Earth and Ocean Sciences, School of Natural Sciences, National University of Ireland Galway, University Road, Galway, Ireland
[b] Irish Centre for Research in Applied Geosciences (iCRAG), Ireland
[c] School of Earth Sciences, University College Dublin, Ireland

ARTICLE INFO

ABSTRACT

Lisheen Mine in County Tipperary, Ireland exploited an underground Pb/Zn massive sulphide deposit hosted in Carboniferous (Mississippian) carbonates. During the extraction phase, the mine workings (located at an average depth of 170 m below ground level), were continuously pumped to lower the groundwater level. Following mine closure in 2015, pumping ceased and eight groundwater wells in the surrounding area were sampled monthly over an 11-month period to monitor the effects of groundwater rebound. These wells draw water from the upper 30 m of a limestone/dolostone aquifer and the monthly samples were analysed for the concentration of 31 elements and compounds (SO_4, Cl, NO_3, F, NH_4, NO_2, P, Ca, Na, K, Mg, Fe, Mn, Cu, Zn, Pb, Al, Ni, Ba, As, Hg, B, Cr, Cd, Mo, Ag, Co, Sr, Be, Sb and U). All of the water can be described as Ca–HCO_3 type as expected. Standard methods for analysing groundwater geochemistry data (e.g. piper diagrams etc.) are useful, differentiating groundwaters with first-order contrasting chemical signatures, for example, distinguishing Ca–HCO_3-type from Na–HCO_3-type water. Samples from the 8 monitoring wells appear to be broadly similar, using this approach. However, these major ion methods fail to further distinguish between different groundwaters. The use of multivariate statistical analytical techniques has become more common in groundwater studies in recent years, allowing the interaction of all the elements and compounds to be considered simultaneously. Compositional Data Analysis (CoDA) was used on the Lisheen dataset to gain a better understanding of the spatial and temporal variation in groundwater geochemistry. Ilr-ion plotting, Hierarchical Cluster Analysis (HCA) and Principal Component Analysis (PCA) through CoDA highlights the elements and compounds that account for the majority of the variance and at Lisheen these are nitrate, manganese, ammonium, sulphate and potassium. By displaying these data visually in a CoDA bi-plot, each location can be reliably 'geochemically fingerprinted' despite similar concentrations of major ions within a relatively small geographical area (<30 km^2). Relabeling the bi-plot observations by date of recovery reveals how one particular groundwater well (PH) subtly varies over time, most likely as a result of seasonal land-use changes (input of compounds associated with fertiliser). This type of statistical analysis has broad applications in hydrology and hydrogeology including contaminant tracing and interaction, environmental studies, land-use planning and mineral exploration.

1. Introduction

Groundwater monitoring is a major component of environmental remediation following mine closure, particularly in areas where potable water could be compromised. Lisheen Mine, located in County Tipperary, Ireland, is a case in point: whilst operational it was necessary to pump water continuously from the underground mine workings. However, following closure, and groundwater rebound, the impact of local groundwater interaction with the flooded working is of particular concern. Typically, a number of regular sampling locations are established surrounding underground mines to determine if changes are occurring as a result of this rebound. Geochemical groundwater sampling focuses heavily on ascertaining whether the concentration of particular elements and compounds exceed drinking water standards.

More subtle changes in minor element composition or relative concentrations of a number of elements and compounds, may, however, provide early indications of changing chemistry, before the established standards are exceeded.

The chemistry of a point sample of groundwater reflects the time the water has spent in and on the ground, the pathways it has taken, and the materials it has interacted with. Improvements in analytical technologies in geochemistry (including inductively coupled plasma mass spectrometry: ICP-MS) have allowed for routine measurement of a wide range of elements with greater accuracy. Elements that were not traditionally considered as important for groundwater characterisation studies (e.g. Conti et al., 2000; Younger, 2000 etc.) may indeed be valuable for evaluating the primary controls on water chemistry. Relatively newer methods of statistical analysis (e.g. Principal Component Analysis and Compositional Data Analysis) can be used to assess which elemental relationships are important in defining the chemistry of groundwater (e.g. Gallo and Buccianti, 2013; Engle and Blondes, 2014; Blake et al., 2016), at specific locations within relatively uniform or homogenous geological contexts, and also within relatively small areas (e.g. Lisheen <30 km^2). These methods of data analysis offer an efficient way to explore the variance in large datasets and unlike some conventional approaches to geochemical data (e.g. Piper diagrams, Harker diagrams), do not rely on *a-priori* expectations about inter-element behaviour.

Appropriate datasets for Principal Component Analysis (PCA) are generally in the form of a data table consisting of variables (e.g. chemical parameters) and observations (e.g. a particular sample for which that variable was measured) that are in some way inter-correlated. PCA works by extracting the important and pertinent information and expressing it as new set of orthogonal variables called principal components (Machiwal et al., 2018). Displaying the resulting data as points on maps provides a representation of the pattern of similarity between observations and variables (Jolliffe, 2002; Jackson, 2005; Saporta and Niang, 2009; Abdi and Williams; 2010). However, using any correlative technique (e.g. ternary diagram, PCA, cluster analysis) on raw compositional data can lead to spurious correlations as a result of the 'closure problem' (e.g. Chayes and Trochimczyk, 1978) or the 'negative bias problem' (see below).

'Standard' multivariate analysis methods do not account for the relative nature of compositional datasets and may lead to spurious and inaccurate results. The reason for this is described as the 'negative bias problem' and has been alluded to by Chayes (1960, 1962, 1971), Krumbein (1962) and Mosimann (1962, 1963). The problem can be described as follows: for a D-part composition $[X_1,\dots, X_D]$ with the component sum $X_1 + \dots + X_D = 1$, since;

$$cov(X_1, X_1 + \dots + X_D) = 0 \quad (1)]$$

we have;

$$cov(X_1, X_2) + \dots + cov(X_1, X_D) = -var(X_1) \quad (2)$$

The right hand side of Equation (2) is negative, implying that at least one of the covariances on the left must be negative and therefore the correlations are not free to range over the usual $(-1, 1)$ interval.

Early attempts to solve this problem focused on corrective treatments to 'standard' methods (e.g. Darroch and James, 1974; Chayes and Trochimezyk, 1978). The necessity for a method that takes into account the special nature of the compositional sample space was first recognised and developed by Aitchison and Shen (1980), and subsequently by Aitchison (1982, 1983, 1985, 1986). Key to this new approach was the recognition that compositional data provide information only about the relative magnitudes of the parts, and not their absolute values.

Therefore, this information essentially concerns ratios of the components. In general, ratios do not show exact relationships in terms of variation (e.g. no exact relationship between $var(X_i/X_j)$ and $var(X_j/X_i)$). However, log ratios are different;

$$var\{log(X_i/X_j)\} = var\{log(X_j/X_i)\} \quad (3)$$

There is also a one-to-one correspondence between compositions and a full set of log ratios;

$$[Y_1\dots, Y_{D-1}] = [log(X_1/X_D)\dots log(X_{D-1}/X_D)] \quad (4)$$

with inverse;

$$[X_1, X_2\dots, X_D] = [exp(Y_1)\dots exp(Y_{D-1})1]/\{exp(Y_1) + \dots + exp(Y_{D-1}) + 1\} \quad (5)$$

Therefore, any problem or hypothesis concerning compositions can be fully expressed in terms of log ratios and vice versa. Because log-ratio transformation takes the log-ratio vector onto the whole of the real space, it is possible to then use all methods of unconstrained multivariate analyses on the result (with caution). Recently, significant advancements have been made in Compositional Data Analysis (CoDA) theory and its applications (e.g. Egozcue and Pawlowsky-Glahn, 2011; Pawlowsky-Glahn and Buccianti, 2011; Tolosana-Delgado and van den Boogaart, 2011; van den Boogaart and Tolosana-Delgado, 2013; McKinley et al., 2016).

CoDA can use multivariate principal component analysis to 'geochemically fingerprint' groundwater sampling locations. As this process is highly sensitive to any changes in geochemistry, it facilitates reliable and robust groundwater monitoring. By analysing a number of elements and compounds simultaneously, it is also possible to identify potential sources of contamination. The CoDA process has been successfully used to gain a better understanding of the nature of groundwater in previous studies (e.g. Buccianti and Pawlowsky-Glahn, 2005; Gallo and Buccianti, 2013; Engle and Blondes, 2014; Gozzi et al., 2015; Blake et al., 2016; Sauro Graziano et al., 2020), each with a specific purpose in mind (e.g. investigating the environmental and ecological characteristics of a river basin, modelling thermodynamic geochemical variations within oilfield brines and identifying the geochemical variation of thermal waters). Here, the process is used in a broader sense to geochemically distinguish sampling locations in a relatively small area (~30 km^2), and to evaluate temporal changes over a defined period of 11 months.

The primary objective is to assess the application of CoDA to groundwater geochemistry research. In the specific case of the area around Lisheen Mine, this method of statistical analysis will be used to characterise the chemistry of groundwater recovered from eight monitoring wells and evaluate the hydrogeochemical changes over time. This research using CoDA statistics and visualisation methods to evaluate these temporal changes in the context of environmental monitoring is an advancement on previous research.

2. Materials and methods

2.1. Study area – geological/hydrogeological context

Lisheen was the most significant of a number of base-metal (Zn–Pb) ore deposits that lie along the NE-SW Rathdowney Trend in south-central Ireland (Fig. 1; Hitzman et al., 2002; Hitzman 1995; Wilkinson and Hitzman, 2015). These mineral deposits are believed to have developed in this part of Ireland as a result of extensive Carboniferous deep-seated normal faulting that provided conduits for mineral-rich ore forming hydrothermal fluids (e.g. Johnston et al., 1996; O'Reilly et al.,
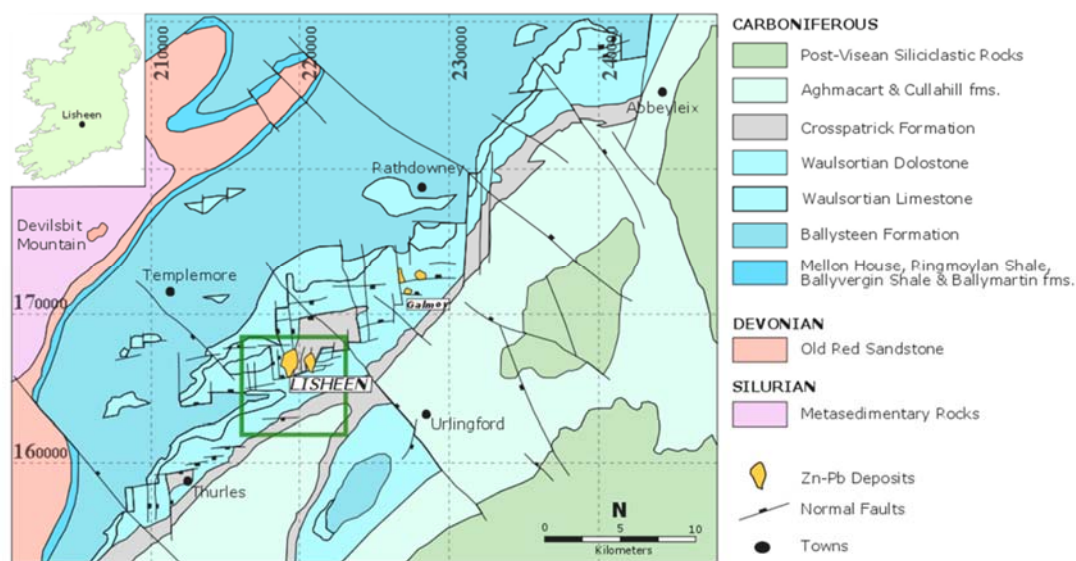
Appendix A

S. Wheeler et al.   Applied Geochemistry 127 (2021) 104912

Fig. 1. Summary Paleozoic bedrock geology in the area of the Rathdowney Trend in south central Ireland. The locations of the mines at Lisheen and Galmoy are shown and coordinates are in Irish Grid 1965) (modif ed from Hitzman et al., 2002). Location of sample location map in Fig. 2 is highlighted with a green box. Inset map (top left) shows the general location of the area of the main map compilation in Ireland. In lithostratigraphic key (on right) fms. = formations. (For interpretation of the references to colour in this f gure legend, the reader is referred to the Web version of this article.)

1999; Hitzman et al., 1998; Hitzman, 1999; Wilkinson et al., 2005; Kyne et al., 2019).

The structural trend at Lisheen is broadly ENE-NE trending, which mirrors underlying reactivated Lower Paleozoic (Caledonian) structures (Kyne et al., 2019). This broad trend ref ects proximity to the Iapetus Suture Zone, which represents the area of convergence between the continents of Laurentia and Avalonia during the latter stages of the Caledonian Orogenic Cycle (e.g., Chew, 2009; 2012; Chew and Strachan, 2014). The Lower Paleozoic basement rocks are rarely intercepted by modern exportation as they lie at signif cant depth. They are believed to consist primarily of low-grade metasedimentary rocks (Morris, 1983); but the presence of major buried intrusive bodies across the Irish midlands has also been implied by geophysical surveys (e.g. Jacob et al., 1985; Morris and Max, 1995; Readman et al., 1997).

In Ireland, the Lower Paleozoic basement is unconformably overlain by a late Devonian to Carboniferous (Mississippian) transgressive sequence, initially beginning in terrestrial (red-bed) siliciclastic facies and progressing stratigraphically upwards into marine carbonates (e.g., MacDermot and Sevastopulo, 1972; Clayton et al., 1986; Graham, 2009; Graham and Sevastopulo, 2020). During the Tournaisian, these carbonate sediments were produced largely in ramp environments; however, later during the Viséan, extensional re-activation of faults led to a more complex palaeogeography, with the formation of several intracratonic basins and adjacent carbonate platform highs (e.g. Leeder, 1982; 1987; Somerville, 2008; Sevastopulo and Wyse Jackson, 2009; Murray, 2010). Later, during the Serpukhovian and Bashkirian, carbonate production ceased and was replaced by non-calcareous facies (Sevastopulo, 2009; Barham et al., 2014; Fallon and Murray, 2015).

The Mississippian stratigraphy of the Lisheen mine area is described by Hitzman et al. (2002) and is summarised in Fig. 1. The Ballymartin and Ballysteen formations are predominantly composed of argillaceous limestones and shales, ref ecting the initial ramp phase of sedimentation. Subsequently, in late Tournaisian times, a regionally widespread series of carbonate mudbanks developed, termed Waulsortian Limestone (Lees and Miller, 1995). Base-metal mineralisation is associated primarily with the base of this relatively pure carbonate facies, particularly where it has been regionally dolomitized along the Rathdowney Trend (Wilkinson and Hitzman, 2015). The ore deposits at Lisheen occurred at

an average depth of c. 170m (Torremans et al., 2018). The generally low permeability of the bedrock (Murray and Henry, 2018), together with signif cant faulting along the Rathdowney Trend and karstif cation of the upper 30m of the bedrock, means that regional groundwater f ow is primarily propagated through fractures, and is broadly directed from NNW towards SSE (Lisheen mine closure plan, 2016). Most groundwater f ow at the mine site, and in the broader east Thurles region, occurs in the upper 30–50m of epi-karst. The bulk of the bedrock in the region is classed as Locally Important aquifers by the Geological Survey of Ireland (GSI), while the Waulsortian (WA) limestone is classed as Regionally Important (karstif ed – diffuse). The bedrock sequence is overlain by low permeability glacial till and peaty soils.

2.2. Geochemical data acquisition

Under the Lisheen Mine Closure, Restoration and Aftercare Management Plan (CRAMP), six regional privately owned groundwater wells were sampled monthly, in addition to a number of onsite monitoring wells. For the purposes of this research, data from these regional wells, together with two onsite monitoring wells (Fig. 2), recorded during the f rst year post-closure (December 2015–October 2016) were made available. These samples were collected and analysed by an Irish National Accreditation Board-certif ed company (IAS Laboratories) for the presence of SO_4, Cl, NO_3, F, NH_4, NO_2, P, Ca, Na, K, Mg, Fe, Mn, Cu, Zn, Pb, Al, Ni, Ba, As, Hg, B, Cr, Cd, Mo, Ag, Co, Sr, Be, Sb, and U as well as a number of other parameters (e.g. alkalinity, pH, temperature, dissolved oxygen etc.). Geochemical parameters were also analysed at the ISO accredited IAS Laboratories in County Carlow, Ireland using a combination of ICP-OES (for cations) and ion-chromatography (for anions). The limit of detection (LOD) value for a given element or compound was used as a replacement for any parameter that could not be measured in a given sample. The raw dataset has recently been made available ([dataset] Wheeler, 2020). Electro-neutrality was calculated using Aquachem (Version, 2014.2) and all samples that exhibited greater than 10% variation from neutral were disregarded.
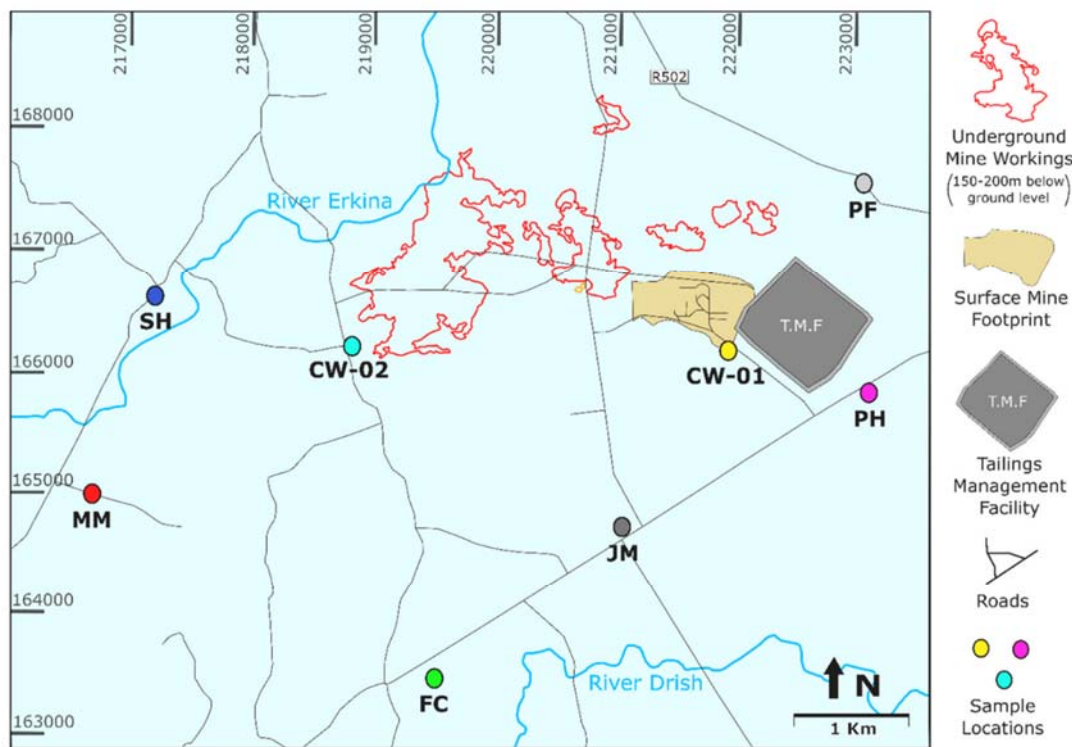
Fig. 2. Map of groundwater sampling locations in the vicinity of Lisheen Mine, County Tipperary, Ireland. CW-01 and CW-02 are both on-site compliance wells and the surrounding sample points are all private wells. The colours used for the sample locations are replicated for visual consistency in the various plots in Figs. 3, 4 and 6 herein. (For interpretation of the references to colour in this f gure legend, the reader is referred to the Web version of this article.)

2.3. Data preparation

Many forms of statistical analysis, including PCA, require a dataset complete with real numbers in order to generate calculations and identify trends. This has led to signif cant research in how best to deal with values below detection limits (DL) and also zeros (e.g. Chung, 1993; Helsel, 1990; Clarke, 1998; Aruga, 1997; Farnham et al., 2002; Güler et al., 2012). Replacing these values with a constant (e.g. DL/2, DL, 0) is generally acceptable when they only represent a relatively small proportion of the overall dataset (US EPA, 1989). However, if the dataset is suff ciently large and the proportion of data below the DL is between 5% and 30%, distributional methods such as maximum likelihood estimation may be more appropriate.

For the Lisheen data, values below the detection limit were recorded and returned at the point of the detection limit and missing data were left blank. The blank cells (2% of the total dataset) were replaced with the mean value of that element at that location over the 11 month period of monitoring. The values recorded as the detection limit were replaced in the statistical environment R (Version 3.5.2) using expectation maximisation algorithms (Palarea-Albaladejo and Martin-Fernandez, 2015).

2.4. Undertaking Compositional Data Analysis (CoDA)

The centred log-ratio (clr) transformation approach of Aitchison (1986) and the isometric log-ratio approach of Egozcue et al. (2003) was used on the Lisheen dataset, following appropriate replacement of non-detect and zero values. Clr coordinates are def ned as;

$$clr(z) = \left(\ln \frac{z_1}{\sqrt[D]{\prod_{j=1}^{D} z_j}}, \ldots, \ln \frac{z_D}{\sqrt[D]{\prod_{j=1}^{D} z_j}} \right) \quad (6)$$

Data transformed by the isometric log-ratio (ilr) approach f rst requires a sequential binary partition (SBP) matrix to be def ned. For a

given SBP whereby the numerator is denoted (+) and the denominator is denoted (−), the ilr coordinates (D-1) of a data matrix are given by;

$$z_k = \sqrt{\frac{r_k s_k}{r_k + s_k}} \ln \frac{(x_{i_1}, x_{i_1} \ldots x_{i_{r_k}})^{\frac{1}{r_k}}}{(x_{j_1}, x_{j_1} \ldots x_{j_{s_k}})^{\frac{1}{s_k}}}, \text{ for } k = 1, \ldots, D-1 \quad (7)$$

where x_i and x_j are constituents coded as + and − and r_i and s_i are the number of constituents coded as + and −, respectively (e.g. Fišerová and Hron, 2011; Shelton et al., 2018). This process was completed a number of times, varying the SBP used each time depending on the objective (e. g. strategic elemental grouping based on known geochemical identif ers).

3. Results

3.1. Piper plot and ilr-ion plot

A Piper plot and an isometric log-ratio (ilr)-ion plot for the Lisheen groundwater geochemistry dataset are shown in Fig. 3. A number of preliminary interpretations can be drawn from these traditional methods of visualising statistical data. It is clear from the Piper diagram (Fig. 3a) that all water from each of the eight wells sampled at Lisheen may be classif ed as bicarbonate (Ca–HCO$_3$) type, with a slight inf uence of magnesium. Water samples from well CW-01 are quite conspicuously distinguishable from the other sample locations due to their relatively higher sulphate levels. Building upon the analytical strengths of the original Piper diagram (Piper, 1944), a new compositional isometric log-ratio (ilr) ion plot has been devised (Shelton et al., 2018), which allows for greater geochemical distinction between the groundwater wells at Lisheen (Fig. 3B). As with the Piper diagram (Fig. 3A) the boxes on the right side of the ilr-ion plot (Fig. 3B) highlight the dominance of carbonate and bicarbonate in all wells in terms of the relative

Appendix A

S. Wheeler et al.   Applied Geochemistry 127 (2021) 104912
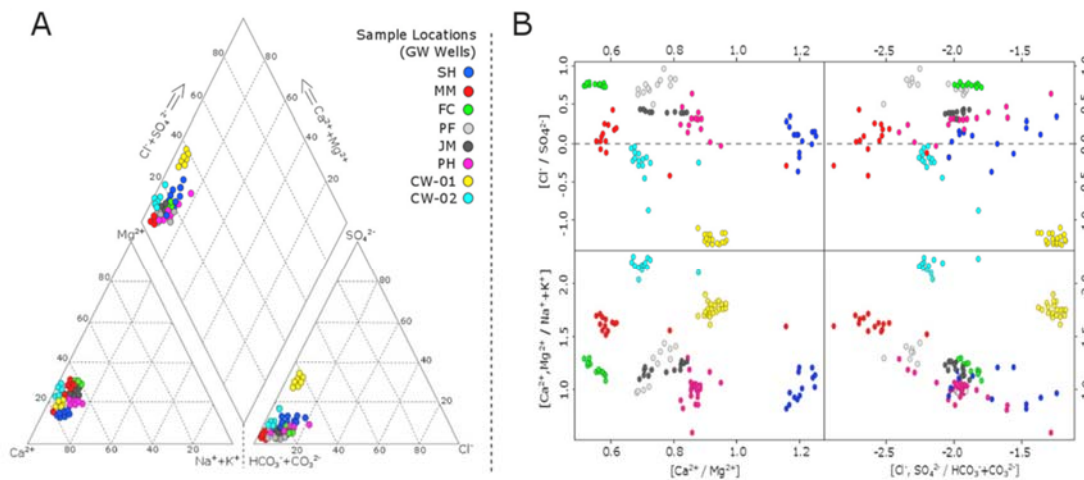
Fig. 3. (A) Traditional Piper diagram of dataset and (B) ilr-ion plot of ilr-transformed data based on the intuitive SBP described by Shelton et al. (2018). The upper right and lower left panels of (B) represent the anion and cation trilinear diagrams (respectively) of the Piper plot (A). The lower right panel of (B) represents the diamond diagram of the Piper plot (A) and the upper left panel of (B) describes additional data not plotted in (A). The dashed line, where y = 0, represents a change in dominance from the denominator of the ilr coordinates (y < 0) to the numerator of the plotted ilr coordinates (Y > 0).

importance of anions (negative values indicate denominator dominance). The upper two boxes of the ilr-ion plot show that the second most dominant anion is chlorine for the majority of regional well samples (SH, MM, FC, PF, JM, PH) whereas the second most dominant anion in all compliance well samples (CW-01 and CW-02) is sulphate (particularly in CW-01). Additionally the boxes on the left of the plot show that well SH is quite distinct from the rest in terms of calcium/magnesium ratio (conspicuously lower levels of magnesium).

3.2. CoDA clr-biplot

The output data from the data preparation stage (Section 3.1) was imported to the software 'CoDA Pack' (Version 2.02.21) for statistical analysis. The first output of CoDA is a table similar to that found with any form of PCA, which describes the proportion by which each variable is affecting each principal component (PC). The most important

controlling variables for each PC are highlighted in this particular instance (Table 1). The first PC, which represents 72% of the variance of the total dataset, is most strongly associated with relative variations of nitrate, manganese and nickel. PC2, representing 10% of the variance is associated with ammonium and nickel, PC3, representing 6%, is associated with sulphate and potassium, and so on.

In the case of this particular dataset, the best approach to visualise the data is to plot PC1 along the X-axis of a CoDA bi-plot and PC3 along the Y-axis (Fig. 4). The total variance displayed in this bi-plot is therefore 78%. PC2 is accounted for by the Z-axis (which runs in the third dimension orthogonally from the centre, both towards and away from the reader). This plot is a multidimensional representation of the data and it shows the information in Table 1 in terms of which variables are the controlling influences on each of the principal components by examining how the vectors (variables) relate to the axes (PC's). The bi-plot also illustrates how the observations (groundwater geochemistry

Table 1
CoDA PCA results for Lisheen groundwater data using centre log-ratio transformation (clr) method. Note; most influential elements for each PC are highlighted in yellow.

	PC1	PC2	PC3	PC4	PC5	PC6
clr.HCO3	0.0586	-0.0036	0.0795	-0.1	0.0122	-0.0717
clr.SO4	-0.0819	-0.1752	0.4816	-0.224	-0.0203	-0.168
clr.Cl	0.0535	-0.1159	-0.0403	-0.05	0.1158	-0.278
clr.NO3	0.4453	0.0954	0.1876	0.7688	-0.0083	-0.001
clr.F	0.1955	0.0819	-0.1144	-0.1879	-0.1057	0.328
clr.NH4	-0.176	0.9048	0.0242	-0.0371	0.015	-0.0987
clr.Ca	0.0398	-0.03	0.1575	-0.1275	0.0092	-0.0885
clr.Na	0.053	-0.1249	0.0484	-0.2201	0.0896	-0.2111
clr.K	0.1635	-0.1058	-0.7618	0.058	0.0082	-0.1457
clr.Mg	0.0463	0.0545	0.0796	-0.0776	0.016	-0.0935
clr.Mn	-0.7398	-0.0576	-0.2083	0.1993	0.0254	0.1254
clr.Ni	-0.3386	-0.2628	0.1795	0.3832	-0.1514	0.0146
clr.Ba	0.015	-0.0927	-0.1357	-0.0169	0.1039	-0.2209
clr.Sr	0.1023	-0.065	-0.0105	-0.1371	0.0281	-0.1526
clr.Sb	0.0922	-0.0393	-0.0209	-0.1552	-0.7476	0.3927
clr.U	0.071	-0.0638	0.0541	-0.0759	0.61	0.669
Prop. Var. Ex.	0.7236	0.0963	0.0586	0.0367	0.0287	0.0232
Cum. Prop. Ex.	0.7236	0.8199	0.8785	0.9152	0.9439	0.9671
% Var. Ex.	72	10	6	4	3	2

Fig. 4. Compositional PCA bi-plot of Lisheen geochemistry data colour-coded by groundwater well (see Fig. 2 for reference). The primary (first) Principal Component (PC) accounts for 72% of variation along the x-axis, the second PC accounts for 10% of variation (z-axis) and third PC accounts for 6% of variation (y-axis). Groupings (G1, G2a and G2b) were determined on the basis of an independent hierarchical cluster analysis. . (For interpretation of the references to colour in this figure legend, the reader is referred to the Web version of this article.)
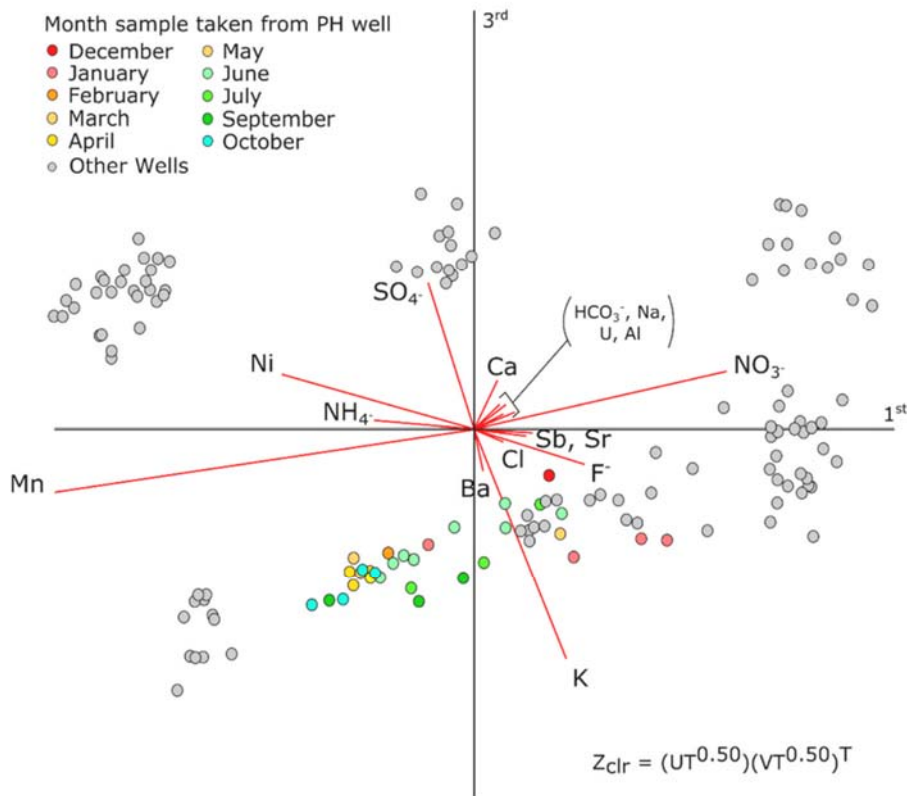
Fig. 5. Compositional PCA bi-plot of sample well PH from Lisheen geochemistry data, recoded (coloured) by month of sample taken (2015/16). Data from other sample sites are greyed and remain for general reference.

samples) relate to each other, to the principal components and to the variables.

In the bi-plot (Fig. 4), samples from each well (i.e. colour-coded observations on the bi-plot) are very clearly clustered and distinguishable from each other for the most part. PC1 has separated the wells based on variation of manganese, nickel and ammonium (towards the left side of the plot) and those controlled broadly by the variation of nitrate (towards the right of the plot). PC3 separates the samples further into two broad groups either side of the x-axis. CW-01, CW-02 and SH lie above the x-axis and are predominantly influenced by sulphate variation, whereas the other wells are either geochemically balanced with respect to the third principal component or are influenced by potassium variation. The PF well is the least well-defined and clustered sample location when considered temporally over the 11 month sampling period. Changing the colour-coding of observations on the bi-plot (by date instead of by location) visually illustrates how the groundwater chemistry of well PF changed over the sampling period, with samples gradually becoming more influenced by manganese, potassium and nickel (Fig. 5).

In addition, in the biplot (Fig. 4), the observation points are sub-divided into three groups (shown as different data symbols) on the basis of a Hierarchical Cluster Analysis (HCA) that was conducted independently of the PCA. For the HCA, centre log-ratio transformed data were imported to the software package SPSS (Version 23). Using the 'Wards Linkage' method, three significant clusters or 'groups' were readily distinguished: **G1**) represented by wells SH, PF and MM, **G2a**) represented by JM, PH, CW-02 and FC and **G2b**) which effectively differentiates well CW-01 from the rest. For the sake of visual clarity in Fig. 4, the arithmetic mean was used for each location (the conclusions are the same if the full dataset is used).

3.3. Additional data

A portion of data collected from the groundwater monitoring wells in the Lisheen area could not be included in the CoDA analysis because a high proportion of samples registered below the detection limit for a number of parameters (e.g. phosphate) and some are not part of the 'composition' (e.g. dissolved oxygen). However, these data can add additional information that can augment the interpretation of the geochemical processes operating at various sampling wells. For

example, the cluster analysis and bi-plot (Figs. 3B and 4 respectively) appear to show a strong relationship between wells SH, MM and PF, which is based primarily on relative levels of nitrate. However, incorporating dissolved oxygen and phosphate data indicates the geochemical processes at sample sites SH and PF differ from those at MM – groundwater at location MM is less oxygenated and has elevated levels of phosphate relative to SH and PF (Fig. 6A and B). Manganese also has a strong influence on the characterisation of some groundwaters in the Lisheen area (Table 1 and Fig. 5). Sample sites PH, JM and CW-01 have elevated levels of manganese and iron (Fig. 6C and D) and are sub-oxic.

4. Discussion

In the context of the local and regional geological setting, the results from the Piper diagram (Fig. 3) are unsurprising. As this area is dominated by Carboniferous (Mississippian) limestone, including the very pure Waulsortian bank carbonates, the Ca–HCO$_3$ water type observed in all eight wells is expected. The minor influence of magnesium across all of the samples can be attributed to extensive regional-scale dolomitsation of carbonate bedrock along the Rathdowney Trend (Fig. 1; see Wilkinson and Hitzman, 2015). The higher levels of sulphate seen in CW-01 are likely due to the relative proximity of this particular well to the Lisheen ore deposit (e.g. Toran, 1987; Leybourne et al., 2002; Caritat et al., 2005), and possibly also to the tailings management facility on the surface (Fig. 2). Additionally, as the regional groundwater flow direction is broadly from NNE to SSW, CW-01 is positioned directly and quite proximally downstream from the mine.

Using the CoDA ilr-ion approach (asas), the sample locations can be further discriminated. In particular this plot indicates the secondary anion of importance in wells CW-01 and CW-02 is sulphate, highlighting the increasing influence of sulphide dissolution with greater proximity to the ore deposit. Additionally, the plot strongly discriminates well SH from the rest in terms of calcium/magnesium ratio. It is likely that the groundwater at this location was not in contact with as much dolomitised limestone as groundwater in the other wells. This is intuitive given the location of the well (Fig. 2) relative to the bedrock geology (Fig. 1) and also considering the direction of groundwater flow (broadly north-west to south-east).

The influence of the regional-scale groundwater flow at Lisheen becomes more apparent when considering the three groupings resolved
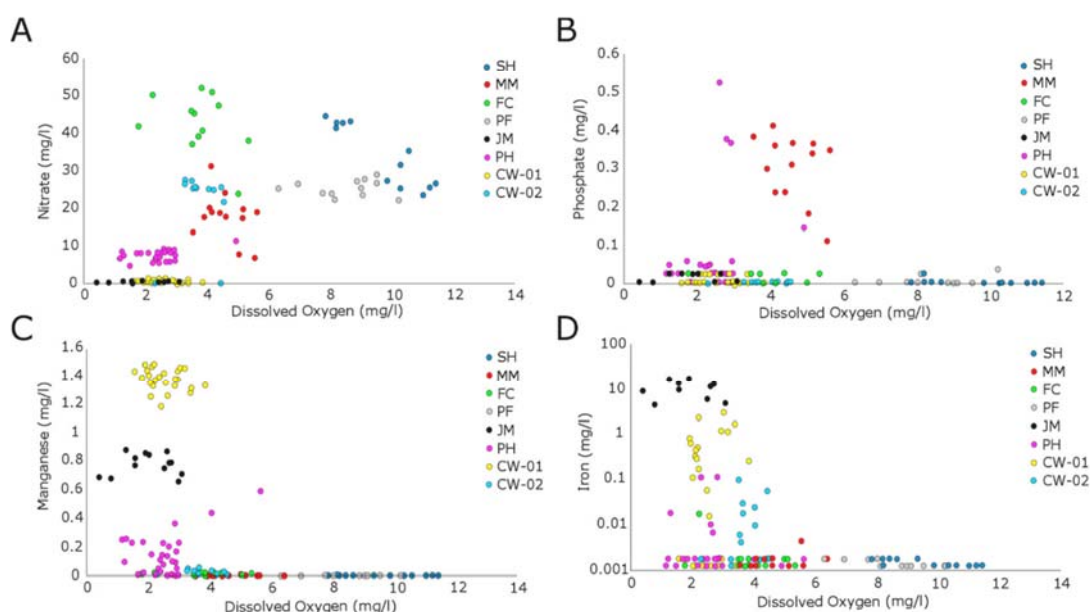
Fig. 6. Traditional bi-plots of Lisheen geochemical data showing the concentration of dissolved oxygen (x-axis) against; (A) nitrate, (B) phosphate, (C) magnesium and (D) iron.

by the HCA (Fig. 3B). Cluster **G1** includes the wells either peripherally located outside of the 'ore shadow' (SH and MM) or slightly upstream (in groundwater terms) from the mine itself (Fig. 2). This grouping thus most likely represents a best approximation for a regional baseline groundwater chemistry signal. Clusters **G2a** and **G2b** consist of all wells located downstream from the main ore deposit (Fig. 2), and may be geochemically influenced by the mineralisation or associated lithology and structures at Lisheen. Subgrouping **G2b** reflects how chemically distinguishable CW-01 is from the wells in cluster **G2a**. CW-01 is distinguished by elevated sulphate concentrations, interpreted as a product of sulphide oxidation reactions at this location, immediately adjacent to the Lisheen deposit.

CoDA analysis provided significantly more detail in terms of recognising important variations in the overall geochemistry of groundwater in the Lisheen area, in addition to assessing how each sample location and particular samples vary over time (Figs. 4 and 5). It is worth noting that the variations seen from the results of CoDA may not represent any significant change in the absolute measured values for the elements and compounds in question, but rather their relative change with respect to the entire dataset. Although CoDA is an excellent data exploration tool for identifying important elements and compounds controlling variation, the interpretation of geochemical processes should be carried out in combination with additional data for dissolved species that are particularly sensitive to some geochemical processes, such as redox changes (e.g. Fig. 6).

The CoDA PCA output (Table 1) shows the most important variables (PC1, representing 72% of variance) to be the anti-correlated nitrate (positive) and manganese (negative). Both of these parameters are generally highly sensitive to redox controls (nitrate survives only in relatively oxygenated waters and manganese is soluble in sub-oxic to anoxic waters - e.g. McMahon et al., 2019). Dissolved oxygen data plotted against nitrate and manganese (Fig. 6A and C respectively) shows that redox is most likely an important overall control on groundwater chemistry at Lisheen. Specifically, wells SH and PF contain oxygenated water that represents a high level of surface interaction and rapid recharge; thus retaining nitrate (e.g. Burow et al., 2010). Wells CW-01, JM and PH, by contrast, have sub-oxic to anoxic groundwater with higher concentrations of manganese.

PC2 (10% of variance) is primarily controlled by ammonium. Again, redox reactions may be the most important controlling factor here, as nitrogen is generally present as the ammonium ion in less oxic groundwater (e.g. Schullehner et al., 2017). Wells JM and CW-02 for example have the highest concentrations of ammonium (0.14–0.33 mg/l) and relatively low concentrations of dissolved oxygen (0.4–4.5 mg/l).

PC3 (6% of variance) is defined primarily by apparently anti-correlated sulphate and potassium. The sources of sulphate are likely to be geogenic in nature and associated with mineralising structures around the Lisheen deposit (e.g. Wilkinson et al., 2005). Despite being found at low concentrations, the relative differences in potassium between the wells identified by CoDA may be attributed to leaching from fertilised soils (e.g. Alfaro et al., 2004).

Visual representation of this data in the form of a CoDA bi-plot (Figs. 4 and 5) allows for further interpretation of the Lisheen data by incorporating each sample as an observation point with vectors (red lines) as variables (elements and compounds) and axes as principal components. With the exception of well PH, the discrete clustering of samples from the same wells indicates that the groundwater chemistry is unique at each location and has not changed appreciably over the sampling and monitoring period.

Broadly speaking, samples to the left of the Y-axis (particularly above the X-axis) in Fig. 4 (i.e. CW-01 and CW-02) have a chemistry that is, to a certain extent, influenced by the presence of a significant mineral deposit close by. Samples to the right of the Y-axis and particularly below the X-axis (e.g. MM, PF, FC and PH), are more likely influenced by a higher level of surface interaction particularly with fertilised soils. In the

case samples from well FC, high nitrate levels occur despite relatively low levels of dissolved oxygen (Fig. 6A), perhaps indicating recent local inputs of fertiliser-derived nitrate that has not yet undergone denitrification.

The three sample wells clustered as **G1** using HCA and considered as potentially reflecting a background groundwater chemistry signal all plot on the far right of the bi-plot (Fig. 4). Groundwater wells can, of course, be affected by both proximity to a mineral deposit and also land-use (e.g. Selck et al., 2018); however, the bi-plot can indicate which influence is the more dominant. It is clear that regardless of the source of chemical elements and compounds, much of the groundwater at Lisheen has been affected by redox reactions.

A closer analysis of sample location PH shows how the chemistry of this particular well has gradually become slightly more influenced by mineral deposit-related geochemistry throughout the 11-month sampling period (Fig. 5). This well is located on the eastern margin of the 'ore shadow', based on regional groundwater flow and it is interesting that it provides perhaps the only evidence of a chemical response from the rebounding groundwater levels following mine closure.

Relatively oxygenated groundwater from wells SH and PF are likely high in nitrates due to interaction with surface drainage and rapid recharge through the subsurface (Fig. 6A), whereas the presence of phosphate in well MM (Fig. 6B) perhaps indicates that the nitrogen there is related to some artificial or anthropogenic input such as fertiliser (e.g. Alfaro et al., 2004). This may also explain the variation within some of the PH samples, as four of these have elevated phosphate. Other groundwater wells with sub-oxic conditions further demonstrate the importance of redox reactions in defining water chemistry in the area. Manganese and iron are both sensitive to the availability of dissolved oxygen (e.g. Sundby et al., 1986), and at Lisheen this is evident with elevated concentrations of these elements in wells that are anoxic to sub-oxic such as CW-01, JM and to a lesser extent, PH and CW-02 (Fig. 6C and D).

5. Conclusions

Relatively new, efficient and cost-effective methods of geochemical analysis (e.g. ICPMS) allow for groundwater to be analysed for a broader range of trace elements with better accuracy than ever before. These additional data may initially seem unimportant as most elements and compounds are present at very low concentrations (μgL^{-1} level); however, they are often indicative of inherent heterogeneity within a particular hydrogeological system that would not otherwise be recognised. Statistical methods for utilising this additional information are well established (e.g. PCA), but they are largely inappropriate for use with raw compositional data (e.g. groundwater geochemistry data) due to the potential for spurious correlations. CoDA involves the log-ratio transformation of raw data in order to avoid this specific problem; however, it is more than simply a necessity for data of this nature. It also facilitates efficient and straightforward exploratory analysis of large datasets in a way that is not possible with more traditional methods. A principal component bi-plot visually illustrates the primary controls on variation within the data. This allows for the identification of the elements or compounds that are responsible for variation and which samples they are influencing. From this, over a regular sampling period, groundwater wells can be geochemically distinguished. This is well demonstrated by the samples taken from Lisheen over an 11-month monitoring period in 2015 and 2016 (Figs. 2–5).

Using the CoDA method, each well, and individual sample, can be geochemically characterised. For relatively small study areas (e.g. Lisheen) this method is more appropriate than traditional groundwater characterisation methods (e.g. Piper diagrams), because by incorporating both the major and a range of minor constituents it can successfully differentiate sample sites that previously would have been difficult to distinguish from each other. For example, all of the Lisheen samples would simply be considered Ca–HCO$_3$ water type (Fig. 3A) in

conventional Piper plots, whereas the CoDA method can further differentiate each sample location by specif c geochemistry, in a reliable way (i.e. the samples are reasonably well clustered by individual sample location; Fig. 4). The Lisheen data primarily ref ects a complex interplay between geogenic factors (carbonate bedrock geology, regional mineralisation) and more localised agricultural land use practices, which, to a certain extent, are inf uenced by geographic position relative to the mine site (Fig. 4; see also Fig. 2) and varying redox conditions (Fig. 6). This approach also makes it possible to discern temporal changes in the Lisheen data, a good example being the subtle geochemical variation seen in samples from well 'PH', most likely as a result of seasonal changes in land-use practices (Fig. 5). As a consequence, CoDA clearly provides an effective and eff cient method of statistically analysing groundwater chemistry data from Lisheen.

Generally for geochemistry studies, CoDA can be seen primarily as an exploratory method of statistical data analysis that can inform and guide further investigative methods by identifying the important controls on chemical variation within the given dataset. One limitation of the CoDA method is the inability to incorporate data which has a signif cant portion either missing or below prescribed detection limits. This leads to some variables being removed entirely. The 'removed' data requires independent study as it may contain important information about geochemical processes in a given area. For example, with the Lisheen dataset, phosphate was removed from CoDA as it was missing or below the detection limit for more than 66% of samples, and therefore could not be appropriately statistically analysed. However, the minority of samples that did measure phosphate concentrations contribute an important part of the geochemical interpretation for the area (Fig. 6).

Application of CoDA to groundwater geochemistry data has the potential to facilitate and support mineral exploration. Solid sample (soil and rock) geochemical vectoring is a common tool in this industry; however, it is costly as it relies on high-resolution sampling to identify trends and often in the case of rock sampling, requires drilling. Groundwater, on the other hand, is representative of a larger sampling area as the water permeates through the subsurface and therefore requires a lower-resolution sampling and additionally the infrastructure is already in place (e.g. private water wells; Taufen, 1997; Leybourne and Cameron, 2010; McGrory et al., 2018). CoDA may also provide a useful tool for identifying geochemical relationships and spatial trends in environmental studies (e.g. contaminant tracing) and land-use planning (e.g. appropriate management of farming practices).

Data availability

Datasets related to this article can be found at https://doi.org/10.17632/9hmz589r7g.1, an open-source online data repository hosted at Mendeley Data (Wheeler, 2020).

Declaration of competing interest

The authors declare that they have no known competing f nancial interests or personal relationships that could have appeared to inf uence the work reported in this paper.

Acknowledgements

References

Abdi, H., Williams, L.J., 2010. Principal component analysis. WIREs Comp Stat 2, 433–459. https://doi.org/10.1002/wics.101.

Aitchison, J.D., 1982. The statistical analysis of compositional data. Journal of the royal statistical society. Ser. Bibliogr. 44, 139–177. https://doi.org/10.1111/j.2517-6161.1982.tb01195.x.

Aitchison, J.D., 1983. Principal component analysis of compositional data. Biometrika 70, 57–65. https://doi.org/10.1093/biomet/70.1.57.

Aitchison, J.D., 1985. A general class of distributions on the simplex. Journal of the royal statistical society. Ser. Bibliogr. 47, 136–146. https://doi.org/10.1111/j.2517-6161.1985.tb01341.x.

Aitchison, J.D., 1986. The Statistical Analysis of Compositional Data. Chapman and Hall, London.

Aitchison, J.D., Shen, S.M., 1980. Logistic-normal distributions: some properties and uses. Biometrika 67, 261–272. https://doi.org/10.1093/biomet/67.2.261.

Alfaro, M.A., Jarvis, S.C., Gregory, P.J., 2004. Factors affecting potassium leaching in different soils. Soil Use Manag. 20 (2), 182–189.

Aruga, R., 1997. Treatment of responses below the detection limit: some current techniques compared by factor analysis on environmental data. Anal. Chim. Acta 354, 255–262. https://doi.org/10.1016/S0003-2670(97)00463-7.

Barham, M., Murray, J., Sevastopulo, G.D., Williams, D.M., 2015. Conodonts of the genus lochriea in Ireland and the recognition of the viséan–serpukhovian (carboniferous) boundary. Lethaia 48 (2), 151–171. https://doi.org/10.1111/let.12096.

Blake, S., Henry, T., Murray, J., Flood, R., Muller, M.R., Jones, A.G., Rath, V., 2016. Compositional multivariate statistical analysis of thermal groundwater provenance: a hydrogeochemical case study from Ireland. Appl. Geochem. 75, 177–188. https://doi.org/10.1016/j.apgeochem.2016.05.008.

Buccianti, A., Pawlowsky-Glahn, V., 2005. New perspectives on water chemistry and compositional data analysis. Math. Geol. 37 (7), 703–727. https://doi.org/10.1007/s11004-005-7376-6.

Burow, K.R., Nolan, B.T., Rupert, M.G., Dubrovsky, N.M., 2010. Nitrate in groundwater of the United States, 1991−2003. Environ. Sci. Technol. 44 (13), 4988–4997. https://doi.org/10.1021/es100546y.

Caritat, P.de, Kirste, D., Carr, G., McCulloch, M., 2005. Groundwater in the Broken Hill region, Australia: recognising interaction with bedrock and mineralisation using S, Sr and Pb isotopes. Appl. Geochem. 20 (4), 767–787. https://doi.org/10.1016/j.apgeochem.2004.11.003.

Chayes, F., 1960. On correlation between variables of constant sum. J. Geophys. Res. 65, 4185–4193. https://doi.org/10.1029/JZ065i012p04185.

Chayes, F., 1962. Numerical correlation and petrographic variation. J. Geol. 70, 440–452. https://doi.org/10.1086/626835.

Chayes, F., 1971. Correlations between proportions: the closed array. In: Chayes, F. (Ed.), Ratio Correlation: A Manual for Students of Petrology and Geochemistry. The University of Chicago Press.

Chayes, F., Trochimczyk, J., 1978. An effect of closure on the structure of principal components. Math. Geol. 10 (323) https://doi.org/10.1007/BF01031737.

Chew, D.M., 2009. Grampian orogeny. In: Holland, C.H., Sanders, I.S. (Eds.), The Geology of Ireland, Second Edition. Dunedin Academic Press, pp. 69–93.

Chew, D.M., 2012. The grampian evolution of the caledonides of NW Ireland. Open Univ. Geol. Soc. J 33 (1), 19e25.

Chew, D.M., Strachan, R.A., 2014. The laurentian caledonides of scotland and Ireland. In: Corfu, F., Gasser, D., Chew, D.M. (Eds.), New Perspectives on the Caledonides of Scandinavia and Related Areas, vol. 309. Geological Society, London, Special Publications, pp. 45–91.

Chung, C.F., 1993. Estimation of covariance matrix from geochemical data with observations below detection limits. Math. Geol. 25, 851–865. https://doi.org/10.1007/BF00891047.

Clarke, J.U., 1998. Evaluation of censored data methods to allow statistical comparisons among very small samples with below detection limit observations. Environ. Sci. Technol. 32, 177–183. https://doi.org/10.1021/es970521v.

Clayton, G., Graham, J.R., Higgs, K.T., Sevastopulo, G.D., Welsh, A., 1986. Late devonian and early carboniferous palaeogeography of southern Ireland and southwest britain. Ann. Soc. Geol. Belg. 109, 103–111.

Conti, A., Sacchi, E., Chiarle, M., Martinelli, G., Zuppi, G.M., 2000. Geochemistry of the formation waters in the Po plain (Northern Italy): an overview. Appl. Geochem. 15 (1), 51–65. https://doi.org/10.1016/S0883-2927(99)00016-5.

Darroch, J.N., James, I.R., 1974. F-independence and null correlation of continuous, bounded-sum, positive variables. Journal of the royal statistical society. Ser. Bibliogr. 36 (3), 467–483. https://doi.org/10.1111/j.2517-6161.1974.tb01023.x.

Egozcue, J., Pawlowsky-Glahn, V., 2011. Basic concepts and procedures. In: Pawlowsky-Glahn, V., Buccianti, A. (Eds.), Compositional Data Analysis. Theory and Applications. John Wiley & Sons, Chichester (UK), pp. 12–28.

Egozcue, J.J., Pawlowsky-Glahn, V., Mateu-Figueras, G., Barceló-Vidal, C., 2003. Isometric Logratio Transformations for Compositional Data Analysis. Mathematical Geology 35, 279–300. https://doi.org/10.1023/A:1023818214614.

Engle, M.A., Blondes, M.S., 2014. Linking compositional data analysis with thermodynamic geochemical modeling: oilf eld brines from the Permian Basin, USA. J. Geochem. Explor. 141, 61–70. https://doi.org/10.1016/j.gexplo.2014.02.025.

Fallon, P., Murray, J., 2015. Conodont biostratigraphy of the mid-Carboniferous boundary in Western Ireland. Geol. Mag. 152 (6), 1025–1042. https://doi.org/10.1017/S0016756815000072.

Farnham, I.M., Stetzenbach, K.J., Singh, A.S., Johannesson, K.H., 2002. Treatment of nondetects in multivariate analysis of groundwater geochemistry data. Chemometr. Intell. Lab. Syst. 60, 265–281. https://doi.org/10.1016/S0169-7439(01)00201-5.

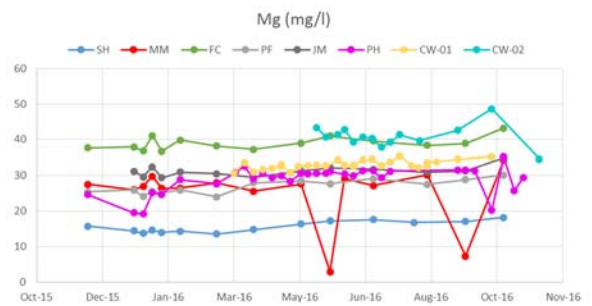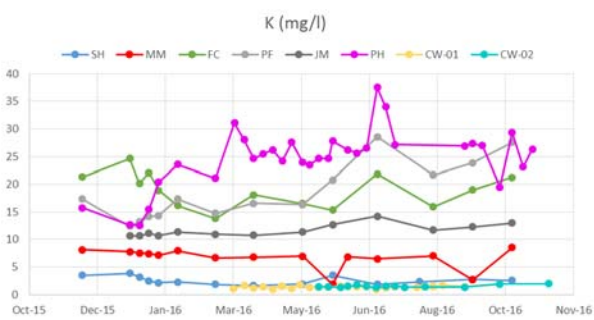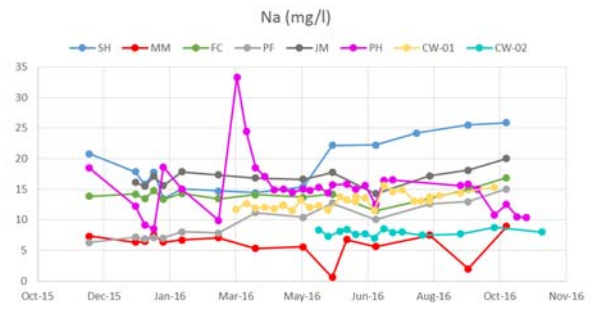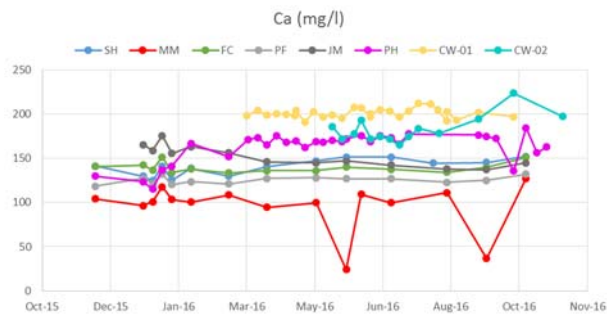Fišerová, E., Hron, K., 2011. On the Interpretation of Orthonormal Coordinates for Compositional Data. Mathematical Geosciences 43, 455. https://doi.org/10.1007/s11004-011-9333-x.

Gallo, M., Buccianti, A., 2013. Weighted principal component analysis for compositional data: application example for the water chemistry of the Arno river (Tuscany, central Italy). Environmetrics 24, 269–277. https://doi.org/10.1002/env.2214.

Gozzi, C., Sauro Graziano, R., Frondini, F., Buccianti, A., 2018. Innovative monitoring tools for the complex spatial dynamic of river chemistry: case study for the Alpine Region. Environ Earth Sci. 77, 1–11. https://doi.org/10.1007/s12665-018-7756-0 (16), 579.

Graham, J.R., 2009. Devonian. In: Holland, C.H., Sanders, I.S. (Eds.), The Geology of Ireland, second ed. Dunedin Academic Press Ltd, Edinburgh, pp. 175–214.

Graham, J.R., Sevastopulo, G.D., 2020. The stratigraphy of latest Devonian and earliest Carboniferous rocks in Ireland. Palaeobiodiversity and Palaeoenvironments. https://doi.org/10.1007/s12549-020-00455-y.

Güler, C., Kurt, M.A., Alpaslan, M., Akbulut, A., 2012. Assessment of the impact of anthropogenic activities on the groundwater hydrology and chemistry in Tarsus coastal plain (Mersin, SE Turkey) using fuzzy clustering, multivariate statistics and GIS techniques. J. Hydrol. 414–415. https://doi.org/10.1016/j.jhydrol.2011.11.021, pp. 435–451.

Helsel, D.R., 1990. Less than obvious; Statistical treatment of data below the detection limit. Environ. Sci. Technol. 24, 1766–1773. https://doi.org/10.1021/es00082a001.

Hitzman, M.W., 1995. Geological setting of the Irish Zn-Pb-(Ba-Ag) orefield. Society of Economic Geologists Guidebook Series 21, 3–23.

Hitzman, M.W., 1999. Extensional faults that localize Irish syndiagenetic Zn± Pb deposits and their reactivation during Variscan compression. In: McCaffrey, K.J.W., Lonergan, L., Wilkinson, J.J. (Eds.), Fractures, Fluid Flow and Mineralization, vol. 151. Geological Society of London Special Publication, pp. 233–245.

Hitzman, M.W., Allan, J.R., Beaty, D.W., 1998. Regional dolomitization of the Waulsortian limestone in southeastern Ireland: evidence of large-scale fluid flow driven by the Hercynian orogeny. Geology 26 (6), 547–550. https://doi.org/10.1130/0091-7613(1998)026<0547:RDOTWL>2.3.CO;2.

Hitzman, M.W., Redmond, P.B., Beaty, D.W., 2002. The carbonate-hosted lisheen Zn-Pb-Ag deposit, county tipperary, Ireland. Econ. Geol. 97, 1627–1655. https://doi.org/10.2113/gsecongeo.97.8.1627.

Jackson, J.E., 2005. A User's Guide to Principal Components. John Wiley & Sons.

Jacob, A.W.B., Kaminski, W., Murphy, T., Phillips, W.E.A., Prodehl, C., 1985. A crustal model for a northeast-southwest profile through Ireland. Tectonophysics 113, 75–103. https://doi.org/10.1016/0040-1951(85)90111-8.

Johnston, J.D., Coller, D., Millar, G., Critchley, M.F., 1996. Basement structural controls on Carboniferous-hosted base metal mineral deposits in Ireland. In: Strogen, P., Somerville, I.D., Jones, G.L. (Eds.), Recent Advances in Lower Carboniferous Geology: Geological Society of London Special Publication, vol. 107, pp. 2–21.

Jolliffe, I.T., 2002. Principal Component Analysis, second ed. Springer, New York.

Krumbein, W.C., 1962. Open and closed number systems in stratigraphic mapping. AAPG (Am. Assoc. Pet. Geol.) Bull. 46, 2229–2245.

Kyne, R., Torremans, K., Güven, J., Doyle, R., Walsh, J., 2019. 3-D modeling of the lisheen and silvermines deposits, County Tipperary, Ireland: insights into structural controls on the formation of Irish Zn-Pb deposits. Econ. Geol. 114 (1), 93–116. https://doi.org/10.5382/econgeo.2019.4621.

Leeder, M.R., 1982. Upper palaeozoic basins of the British isles – caledonide inheritance versus hercynian plate margin processes. J. Geol. Soc. 139, 479–491. https://doi.org/10.1144/gsjgs.139.4.0479. London.

Leeder, M.R., 1987. Tectonic and Palaeogeographic Models for Lower Carboniferous Europe. In: Miller, J., Adams, A.E., Wright, V.P. (Eds.), European Dinantian Environments. John Wiley, London, pp. 1–20.

Lees, A., Miller, J., 1995. Waulsortian Banks. In: Monty, C.L.V., Bosence, D.W.J., Bridges, P.H., Pratt, B.R. (Eds.), Carbonate Mud-Mounds: Their Origin and Evolution. Special Publication of the International Association of Sedimentologists, vol. 23. Blackwell Science, Oxford, pp. 191–271.

Leybourne, M.I., Cameron, E.M., 2010. Groundwater in geochemical exploration. Geochemistry: Exploration. Environment, Analysis 10, 99–118. https://doi.org/10.1144/1467-7873/09-222.

Leybourne, M.I., Goodfellow, W.D., Boyle, D.R., 2002. Sulphide oxidation and groundwater transport of base metals at the halfmile lake and restigouche Zn–Pb massive sulphide deposits, bathurst mining camp, new brunswick. Geochemistry: exploration. Environment, Analysis 2, 37–44. https://doi.org/10.1144/1467-787302-005.

MacDermot, C.V., Sevastopulo, G.D., 1972. Upper Devonian and lower Carboniferous stratigraphical setting of Irish mineralisation. Geol. Surv. Irel 1, 267–280.

Machiwal, D., Cloutier, V., Guler, C., Kazakis, N., 2018. A review of GIS-integrated statistical techniques for groundwater quality evaluation and protection. Environmental Earth Sciences 77 (681), 1–30. https://doi.org/10.1007/s12665-018-7872-x.

McGrory, E., Holian, E., Alvarez-Iglesias, A., Bargary, N., McGillicuddy, E.J., Henry, T., Daly, E., Morrison, L., 2018. Arsenic in groundwater in south west Ireland: occurrence, controls, and hydrochemistry. Frontiers in Environmental Science 6 (154). https://doi.org/10.3389/fenvs.2018.00154.

McKinley, J., Tolosana Delgado, R., Hron, K., de Caritat, P., Grunsky, E., Reimann, C., Filzmoser, P., van den Boogaart, K.G., 2016. Single component map: fact or fiction? J. Geochem. Explor. 162, 16–28. https://doi.org/10.1016/j.gexplo.2015.12.005.

McMahon, P.B., Belitz, K., Reddy, J.E., Johnson, T.D., 2019. Elevated manganese concentrations in United States groundwater, role of land surface–soil–aquifer connections. Environmental Science & Technology 53 (1), 29–38. https://doi.org/10.1021/acs.est.8b04055.

Morris, J.H., 1983. The stratigraphy of the lower palaeozoic rocks in the western end of the longford-down inlier, Ireland. J. Earth Sci. 5, 201–218.

Morris, P., Max, M.D., 1995. Magnetic crustal character in Central Ireland. Geol. J. 30 (1), 49–67. https://doi.org/10.1002/gj.3350300106.

Mosimann, J.E., 1962. On the compound multinomial distribution, the multivariate β-distribution, and correlations among proportions. Biometrika 49, 65–82. https://doi.org/10.2307/2333468.

Mosimann, J.E., 1963. On the compound negative multinomial distribution and correlations among inversely sampled pollen counts. Biometrika 50, 47–54. https://doi.org/10.2307/2333745.

Murray, J., 2010. Mid to Upper Viséan Facies and Palaeoenvironments of the Shannon Basin, Western Ireland. Unpublished Ph.D. thesis. University of Dublin, Trinity College. http://www.tara.tcd.ie/handle/2262/78115.

Murray, J., Henry, T., 2018. Waulsortian limestone: geology and hydrogeology. Paper presented at the conference 'groundwater matters: science and practice', tullamore, county offaly, Ireland, april. Available online at. In: http://www.iah-ireland.org/conference-proceedings/2018.pdf.

O'Reilly, B.M., Readman, P.W., Murphy, T., 1999. Gravity lineaments and Carboniferous-hosted base metal deposits of the Irish Midlands. In: McCaffery, K., Lonergan, L., Wilkinson, J. (Eds.), Fractures, Fluid Flow and Mineralization: Geological Society of London Special Publication, vol. 155, pp. 313–322.

Palarea-Albaladejo, J., Martin-Fernandez, J.A., 2015. ZCompositions - R package for multivariate imputation of left-censored data under a compositional approach. Chemometr. Intell. Lab. Syst. 143, 85–96. https://doi.org/10.1016/j.chemolab.2015.02.019.

Pawlowsky-Glahn, V., Buccianti, A., 2011. In: Pawlowsky-Glahn, V., Buccianti, A. (Eds.), Compositional Data Analysis: Theory and Applications. Wiley, p. 400.

Piper, A.M., 1944. A graphic procedure in the geochemical interpretation of water-analyses. Eos Trans. Am. Geophys. Union 25 (6), 914–928. https://doi.org/10.1029/TR025i006p00914.

Readman, P.W., O'Reilly, B.M., Murphy, T., 1997. Gravity gradients and upper-crustal tectonic fabrics, Ireland. J. Geol. Soc. 154, 817–828. https://doi.org/10.1144/gsjgs.154.5.0817.

Saporta, G., Niang, N., 2009. Principal component analysis: application to statistical process control. In: Govaert, G. (Ed.), Data Analysis. John Wiley & Sons, London, pp. 1–23.

Sauro Graziano, R., Gozzi, C., Buccianti, A., 2020. Is Compositional Data Analysis a theory able to discover complex dynamics in aqueous geochemical systems? J. Geochem. Explor. 211, 106465. https://doi.org/10.1016/j.gexplo.2020.106465.

Schullehner, J., Stayner, L., Hansen, B., 2017. Nitrate, nitrite, and ammonium variability in drinking water distribution systems. Int. J. Environ. Res. Publ. Health 14 (3), 267. https://doi.org/10.3390/ijerph14030276.

Selck, B.J., Carling, G.T., Kirby, S.M., Hansen, N.C., Brickmore, B.R., Tingey, D.G., Rey, K., Wallace, J., Jordan, J.L., 2018. Investigating anthropogenic and geogenic sources of groundwater contamination in a semi-arid alluvial basin, goshen valley, UT, USA. Water, Air & Soil Pollution 186. https://doi.org/10.1007/s11270-018-3839-5.

Sevastopulo, G.D., 2009. Carboniferous: mississippian (serpukhovian) and pennsylvanian. In: Holland, C.H., Sanders, I.S. (Eds.), The Geology of Ireland, second ed. Dunedin Academic Press, Edinburgh, pp. 269–294.

Sevastopulo, G.D., Wyse Jackson, P.N., 2009. Carboniferous: mississippian (tournaisian and viséan). In: Holland, C.H., Sanders, I.S. (Eds.), The Geology of Ireland, second ed. Dunedin Academic Press Ltd, Edinburgh, pp. 215–268.

Shelton, J.L., Engle, M.A., Buccianti, A., Blondes, A., 2018. The isometric log-ratio (ilr)-ion plot: A proposed alternative to the Piper diagram. J. Geochem. Explor. 190, 130–141. https://doi.org/10.1016/j.gexplo.2018.03.003.

Somerville, I.D., 2008. Biostratigraphic zonation and correlation of Mississippian rocks in Western Europe: some case studies in the late Viséan/Serpukhovian. Geol. J. 43 (2–3), 209–240. https://doi.org/10.1002/gj.1097.

Statistical Analysis of Ground-Water Monitoring Data at Rcra Facilities, 1989. US Environmental Protection Agency Technical Report. EPA530-SW-89-026, Washington, DC.

Sundby, B., Anderson, L.G., Hall, P.O.J., Iverfeldt, A., Rutgers van der Loeff, M.M., Westerlund, S.F.G., 1986. The effect of oxygen on release and uptake of cobalt, manganese, iron and phosphate at the sediment-water interface. Geochem. Cosmochim. Acta 50 (6), 1281–1288. https://doi.org/10.1016/0016-7037(86)90411-4.

Taufen, P.M., 1997. Groundwaters and surface waters in exploration geochemical surveys. Exploration Geochemistry 34, 271–284.

Tolosana-Delgado, R., van den Boogaart, K.G., 2011. Linear models with compositions in R. In: Pawlowsky-Glahn, V., Buccianti, A. (Eds.), Compositional Data Analysis. Theory and Applications. John Wiley & Sons, Chichester (UK), pp. 356–371.

Toran, L., 1987. Sulfate contamination in groundwater from a carbonate-hosted mine. J. Contam. Hydrol. 2 (1), 1–29. https://doi.org/10.1016/0169-7722(87)90002-7.

Torremans, K., Kyne, R., Doyle, R., Güven, J.F., Walsh, J.J., 2018. Controls on Metal Distributions at the Lisheen and Silvermines Deposits: Insights into Fluid Flow Pathways in Irish-Type Zn-Pb Deposits. Econ. Geol. 113 (7), 1455–1477. https://doi.org/10.5382/econgeo.2018.4598.

van den Boogaart, K.G., Tolosana-Delgado, R., 2013. Analyzing Compositional Data with R. Springer, Heidelberg.

Wheeler, S., 2020. Utilising CoDA methods for the spatio-temporal geochemical characterisation of groundwater; a case study from Lisheen Mine, south central Ireland (Datasets and Supplementary Materials). set Mendeley Data v1. https://doi.org/10.17632/9hmz589r7g.1.data.
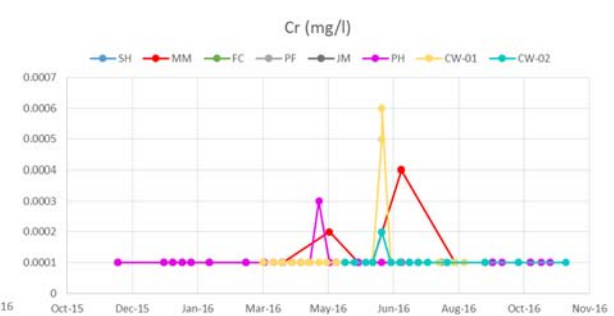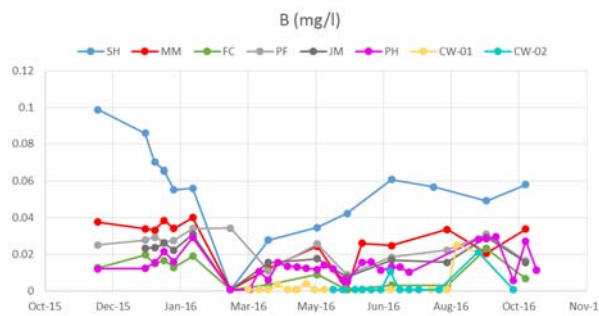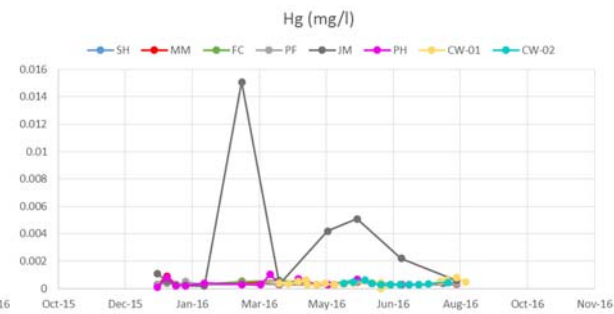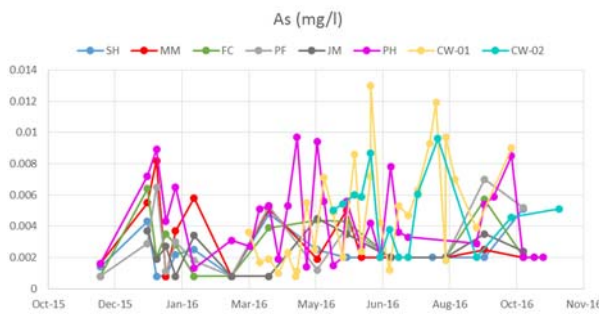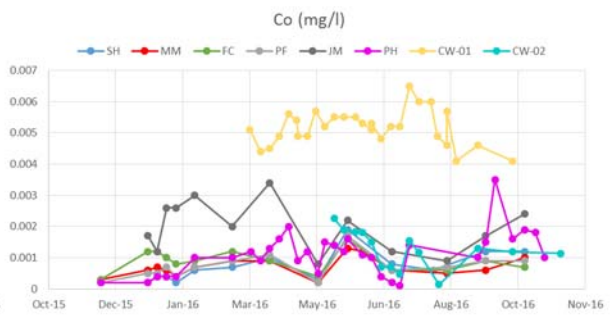
Appendix B

[Lisheen Early Post-Mining Regional Dataset – Additional Graphs]

Groundwater Depth (m)

Temperature (°C)

pH

Electrical Conductivity (Sm-1)

Dissolved Oxygen (mg/l)

Total Organic Carbon (mg/l)

Turbidity (NTU)

Total Hardness (mg/l)

Alkalinity (mg/l)

SO4 (mg/l)

Cl (mg/l)

NO3 (mg/l)

F (mg/l)

NH4 (mg/l)

NO2 (mg/l)

P (mg/l)

Ca (mg/l)

Na (mg/l)

K (mg/l)

Mg (mg/l)

Fe (mg/l)

Mn (mg/l)

Cu (mg/l)

Zn (mg/l)

Pb (mg/l)

Al (mg/l)

Ni (mg/l)

Ba (mg/l)

As (mg/l)

Hg (mg/l)

B (mg/l)

Cr (mg/l)

Cd (mg/l)

Mo (mg/l)

Ag (mg/l)

Co (mg/l)

Sr (mg/l)

Be (mg/l)

Sb (mg/l)

U (mg/l)
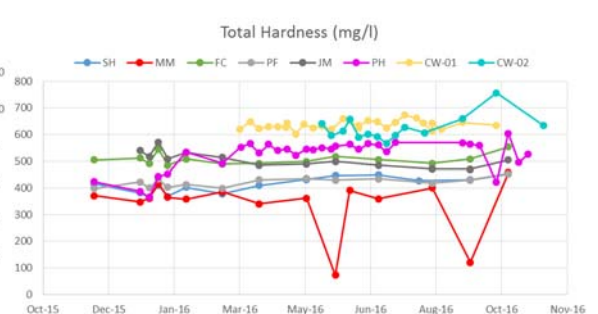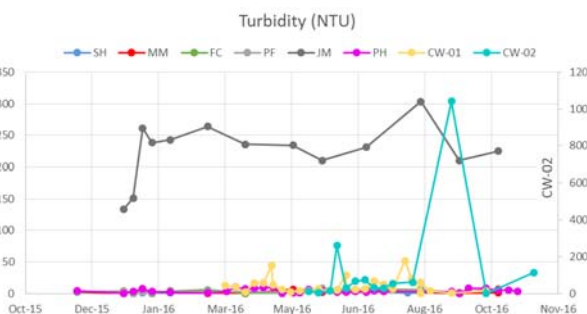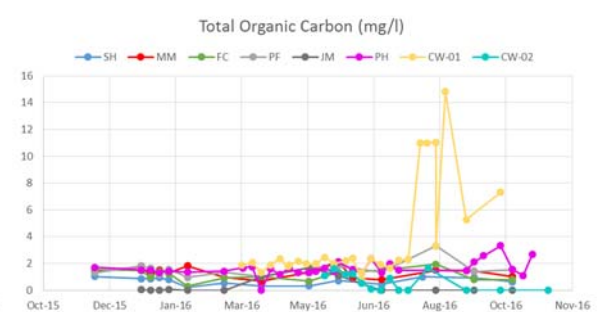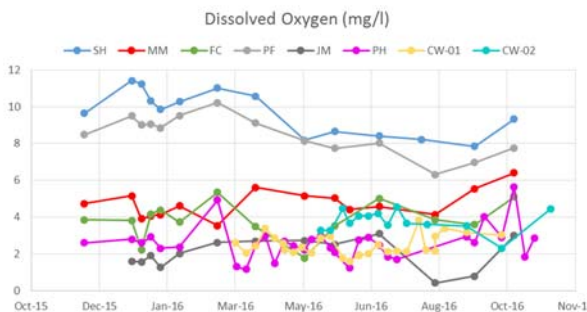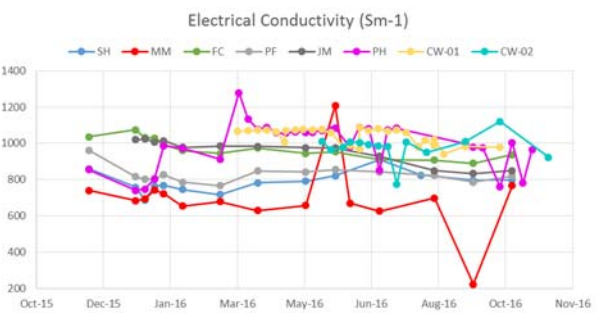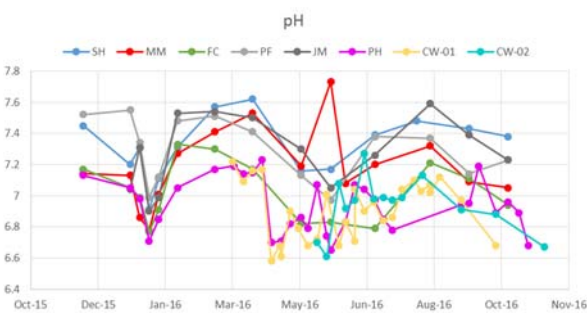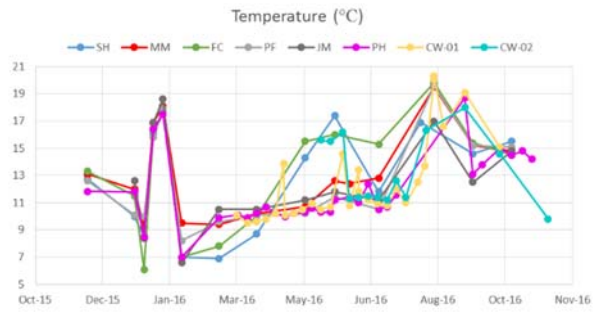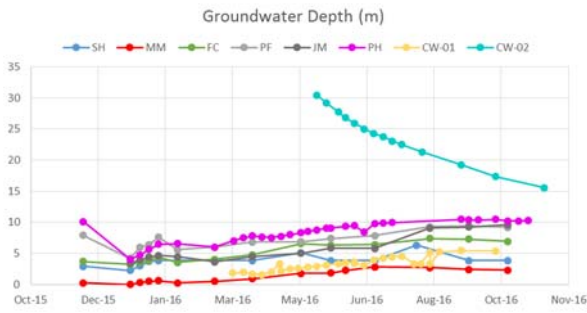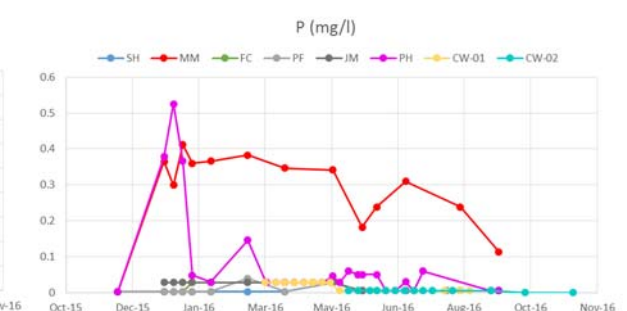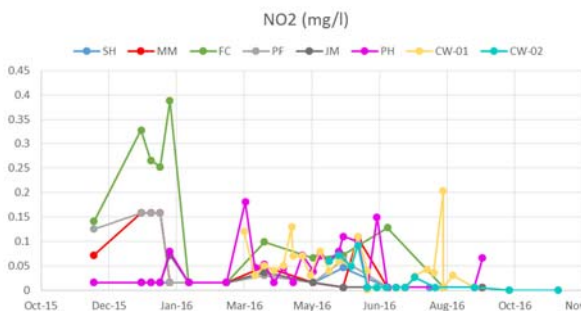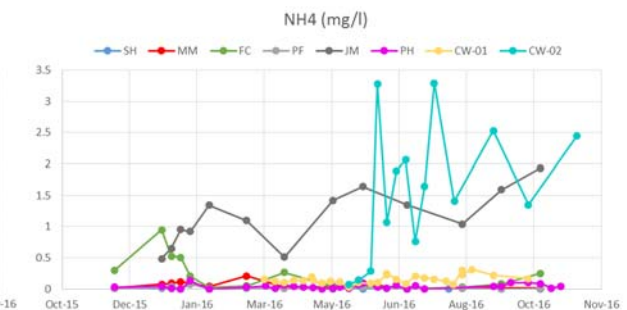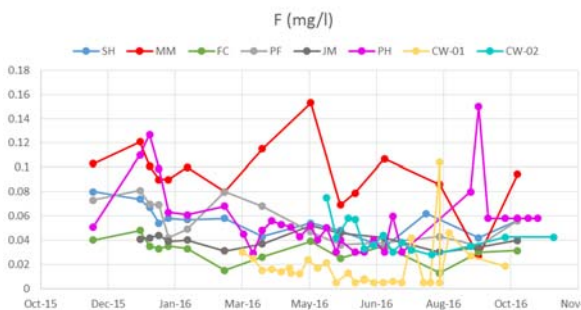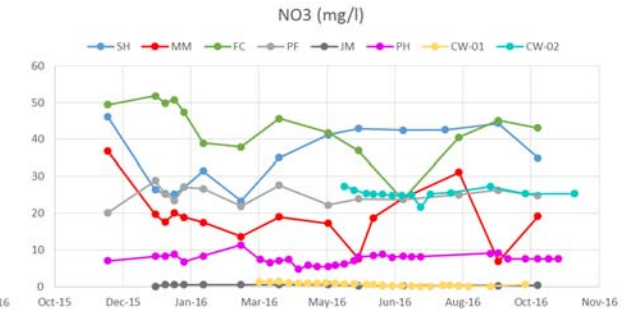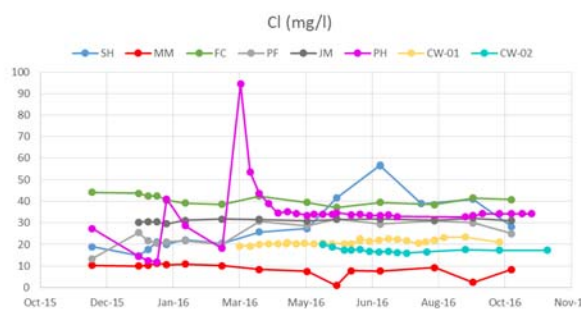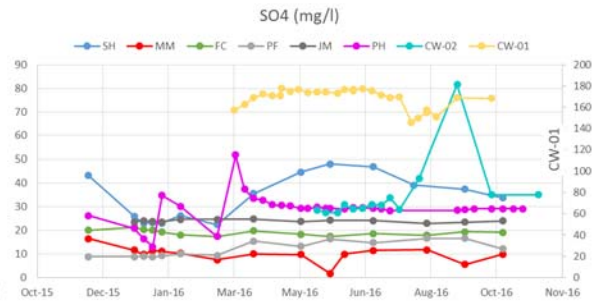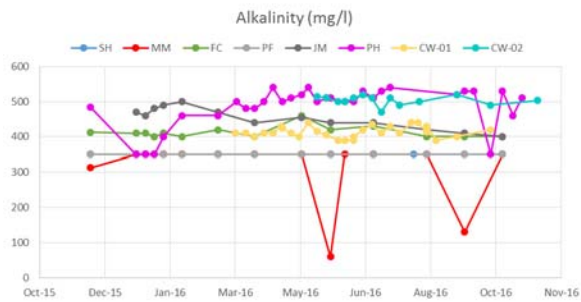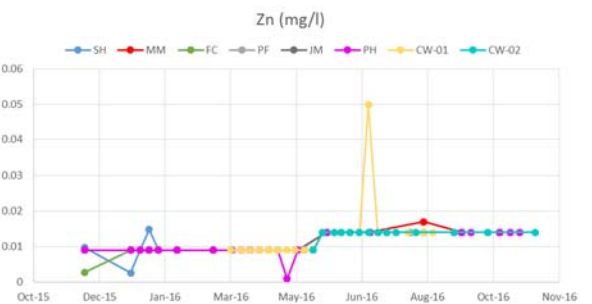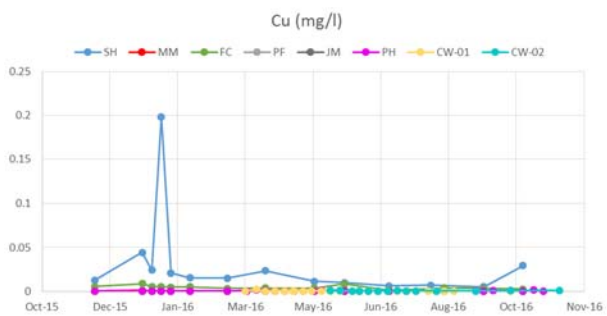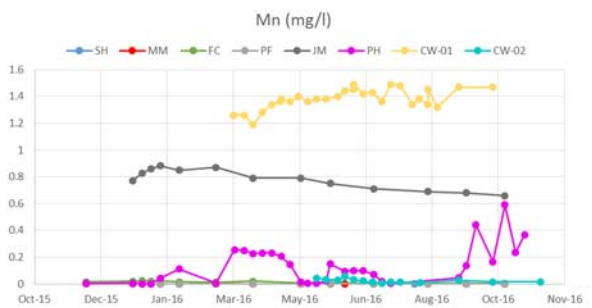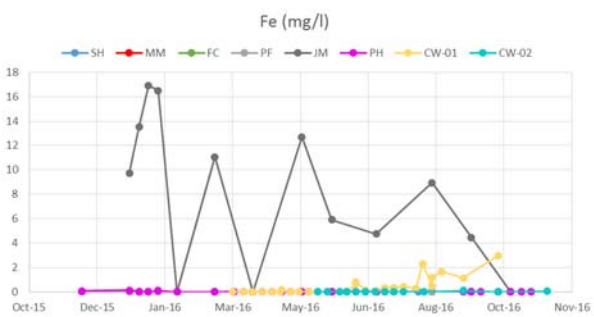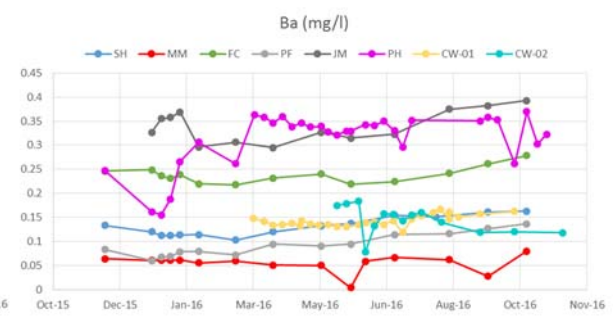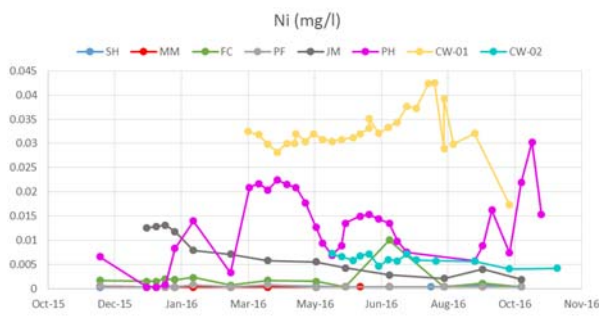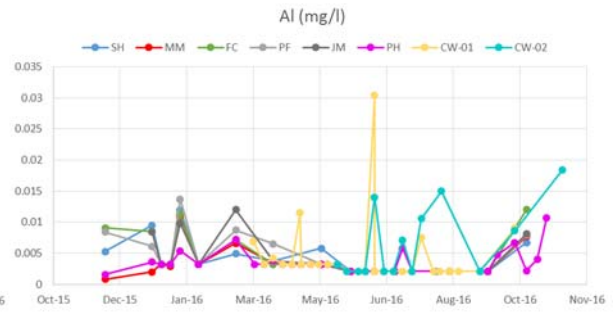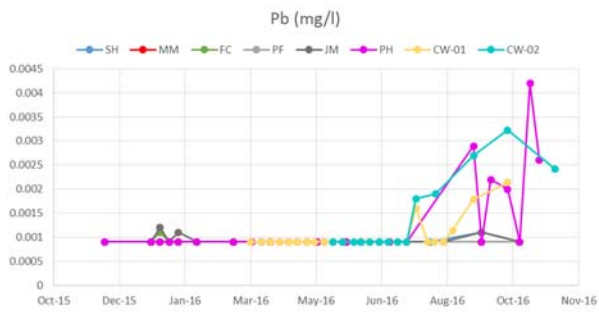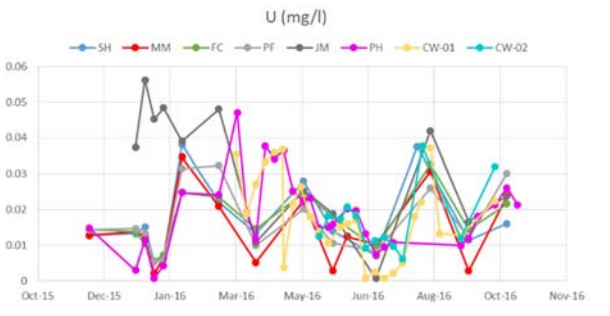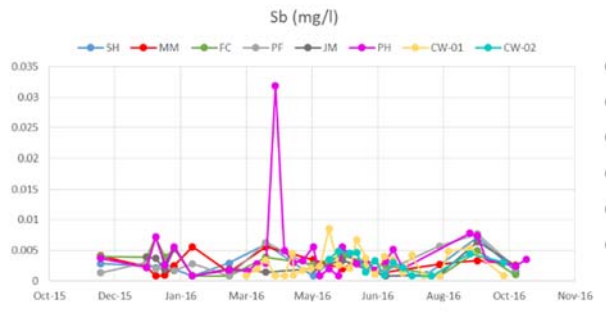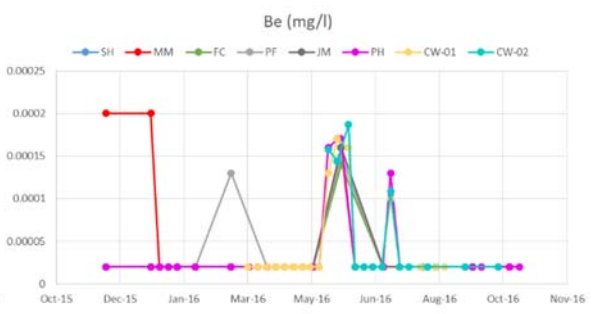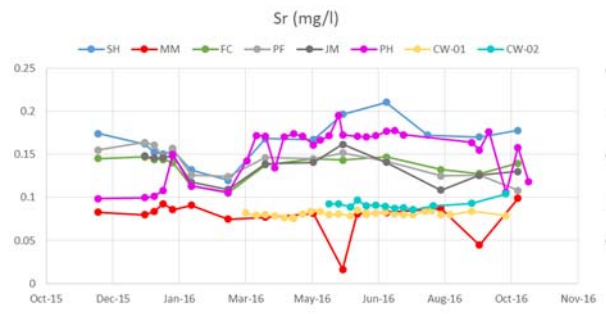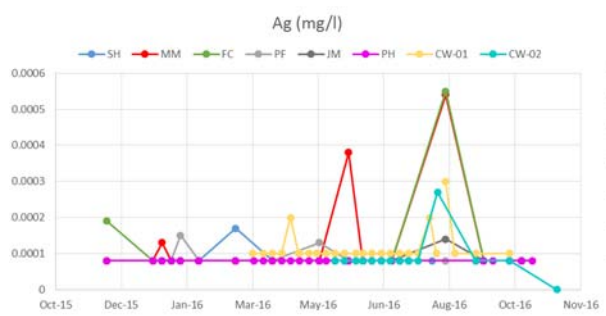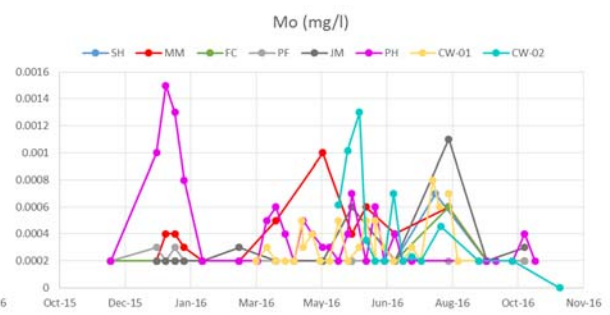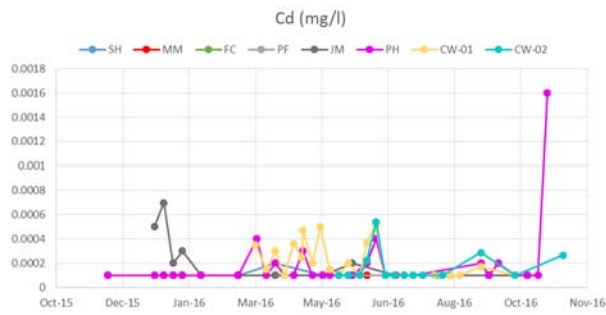
Appendix C

[Lisheen Recent Post Mining Regional Dataset – Sampling Photographs]

LS01

LS02

LS03

LS04

LS05

LS06

LS07

LS08

LS09

LS10

Appendix D

[Data Availability]

Data Repository

All of the data and code used in this thesis has been uploaded to Mendeley Data at Wheeler (2021); https://doi.org/10.17632/b6kk6dj73v.1.

The following are included:

Lisheen Groundwater Geochemistry

1. Pre-Mining Regional (A)
2. Early-Mining Regional (B)
3. Mine Workings (C)
4. Early Post-Mining Regional (D)
5. Recent Post-Mining Regional (E)

Tellus Border Region Geochemistry

6. Topsoil
7. Stream Water
8. Stream Sediment

R Code

9. R Code for Data Preparation and Analysis

The Lisheen datasets A to D were gathered from the remediation team at Lisheen Mine in partnership with the Irish Centre for Research in Applied Geosciences (iCRAG). Sampling for dataset E was completed by the author in January 2019 and subsequent analysis was done at the NUI Galway ICP-MS laboratory (class 6 and 7 clean room facility). Tellus geochemistry datasets (which have been added here for consistency) are available to download from the Geological Survey of Ireland (GSI) online at;

https://www.gsi.ie/en-ie/data-and-maps/Pages/Geochemistry.aspx.

The R code used in this thesis was generated by the author with the assistance of Dr. Sarah Blake and Dr. Juan Jose Egozcue. R packages used are 'zCompositions' (Palarea-Albaladejo and Martin Fernandez, 2015), 'compositions' (van den Boogaart and Tolosana-Delgado, 2013) and robCompositions (Templ *et al.*, 2011). Code from Shelton *et al.* (2018) for producing ilr-ion plots is also included.